Investigating and exploiting the interaction

of Multimerin-2 and its receptors CLEC14A

and CD93

by

Marco Mambretti

A thesis submitted to the University of Birmingham for the

degree DOCTOR OF PHILOSOPHY

School of Cardiovascular Sciences

College of Medical and Dental Sciences

The University of Birmingham

August 2018

UNIVERSITY OF
BIRMINGHAM

University of Birmingham Research Archive

e-theses repository

Abstract

Multimerin-2 is an endothelial specific extracellular matrix protein, which has been found to play a role in angiogenesis and tumour progression. MMRN2 is a ligand for the C-type lectin domain family proteins CLEC14A, CD93 and CD248. CLEC14A and CD93 bind to MMRN2 in the same mapped region MMRN2$^{495\text{-}674}$. CLEC14A is expressed in the vessel of a number of tumour types as tumour endothelial marker (TEM) and like CD93 is involved in angiogenesis. Single or double siRNA-mediated knockdown of CLEC14A, CD93 and MMRN2 confirmed an important role of CD93 in sprouting angiogenesis that is CLEC14A and MMRN2 independent. Furthermore, due to the high affinity of the binding of MMRN2$^{495\text{-}674}$ to the TEM CLEC14A, it has been exploited to target tumour endothelium. The fragment has been employed in the generation of a Chimeric Antigen Receptor (CAR) and other applications. T cells transduced with this receptor were activated on stimulation with both purified antigens and antigens expressed on the cell surface. The activation of T cells was measured as levels of IFNγ released in ELISA assays. Overall, this work sheds light on the interactions of MMRN2 and two of its receptors in *in vitro* models of angiogenesis.

Al mio grande amico Francesco Manzoni

Acknowledgements

CONTENTS

List of Figures

List of Tables

List of abbreviations

Aa – amino acids

AP- Alkaline Phosphatase

APC – Antigen presenting cell

bp – Base pairs

BSA – bovine serum albumin

CAR – Chimeric Antigen Receptor

CD – cluster of differentiation

cDNA – complementary DNA

CFA – Complete Freund's Adjuvant

CTLD – C-type lectin domain

DAPI – (4', 6-diamidino-2-phenylindole)

dNTP -deoxynucleotide triphosphate

DTT – Dithiothreitol

E. coli – Escherichia coli

ECD – extracellular domain

ED – embryonic day

EDTA – Ethylene-diamine-tetra-acetic acid

ELISA - enzyme-linked immunosorbent assay

F- Forward (oligonucleotide primer)

Fab – Fragment antigen-binding

FACS – Fluorescence activated cell sorting

Fc – Fragment crystallisable

FCS – Fetal calf serum

FITC – Fluorescein-5-isothiocyanate

His – Polyhistidine tag

HRP – Horse Radish Peroxidase

HUVEC – Human umbilical vein endothelial cell

IF – Immunofluorescence

IFA – Incomplete Freund's Adjuvant

IgG – immunoglobulin G

IHC – immunohistochemistry

IP – Intraperitoneal

Kan – Kanamycin

kDa – Kilo Dalton

KO – Knockout

MMP – Matrix metalloproteinase

NaCl – Sodium Chloride

PBS- Phosphate buffered saline

PCR – Polymerase chain reaction

PEG - Polyethylene glycol

PEI - Polyethilenimine

PMSF - phenylmethylsulfonyl fluoride

PMSF – Phenylmethanesulfonyl fluoride

R – Reverse (oligonucleotide primer)

rpm – Revolutions per minute

ScFv – Single chain variable fragment

SDS – sodium dodecyl sulphate

siRNA – Small interfering ribonucleic acid

TCR – T cell receptor

Th – T helper

TNFα - Tumour necrosis factor-α

v/v – volume per volume

VEGF – Vascular endothelial growth factor

w/v – weight per volume

WT – Wild type

CHAPTER 1: Introduction

1. Introduction

1.1 Angiogenesis

Angiogenesis describes the growth of new vessels from pre-existing vessels. The term angiogenesis is derived from the Greek *angeîon* and *genesis*. *Angeîon* stands for vessel and *genesis* for birth. Angiogenesis occurs in both physiological and pathological conditions. For example, in physiology angiogenesis is essential for the development of the *corpus luteum* formation in the ovary and the endometrial regeneration during the menstrual cycle. Dysregulated angiogenesis contributes to various pathologies including cancer (Carmeliet, 2003).

The result of physiological angiogenesis is a well-structured and functional vasculature. It is strictly controlled by gradients of stimulatory and inhibitory factors and the coordination of several independent but related processes. Although the main steps of neovascularization are similar both in healthy tissues and in pathology (e.g. tumours), the resulting vasculature differs greatly. In fact, the pathological angiogenic process is driven by an aberrantly high concentration of growth factors such as VEGF and the vessels generated are usually extremely unorganised, misshaped, tortuous and not very functional (leaky) (Papetti and Herman, 2002). The differences are clearly visible as shown in figure 1.1.

The study in physiology and pathology of the mechanisms that regulate angiogenesis is important to improve the current therapeutic approaches to either stop or
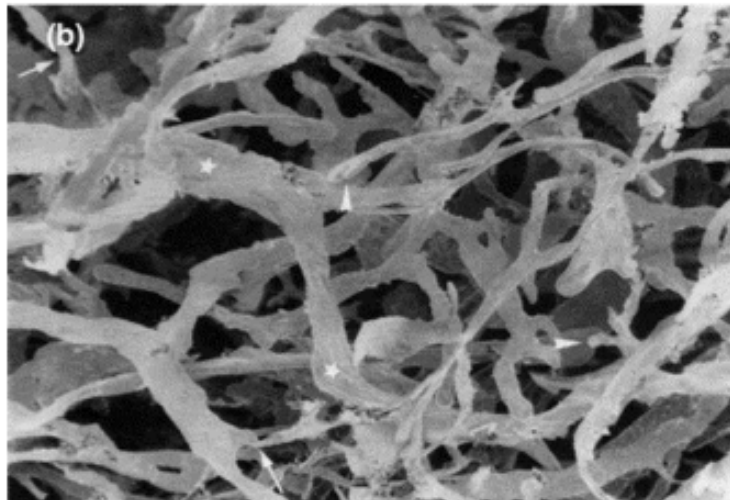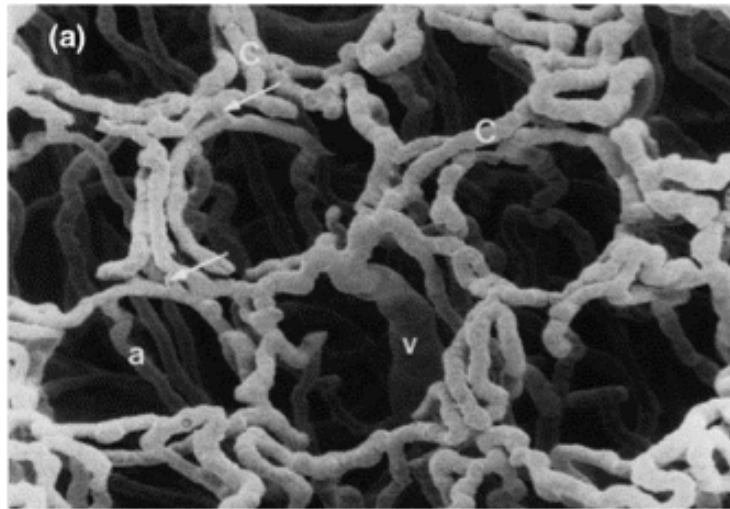
Figure 1.1 Comparison between the vasculature in the tumour and its healthy counterpart

Scanning electro micrographs of corrosion casts of the vasculature of colorectal normal mucosa (a) and colorectal carcinoma (b). It is possible to visibly appreciate the clear differences in organisation, shape and tortuosity. Within the normal mucosa the vasculature is very well organised, vessels are functional and well-shaped. This is completely lost in the vasculature of the tumour counterpart (Konerding, Fait and Gaumann, 2001)

promote angiogenesis. Whilst in tumours the angiogenic switch is something that should be prevented, many efforts to promote this process are being undertaken in regenerative medicine (e.g. in post-ischemic tissues) (Aday *et al.*, 2017).

It is well documented that tumours can grow to 1-2 mm^3 of size and then not develop further. The lack of further growth is thought to be due to the absence of perfusion and limited supply of oxygen and nutrients (Holmgren, O'reilly and Folkman, 1995; Parangi *et al.*, 1996). Folkman observed that tumours produce chemical signals that induce angiogenesis, later known as the angiogenic switch. Once perfused, tumour growth and metastasis accelerates (Folkman, 1971; Hanahan and Weinberg, 2011).

Tumour angiogenesis has been described in five stages. Initially, quiescent endothelial cells are activated by the angiogenic stimulus, for example the vascular endothelial growth factor (VEGF).
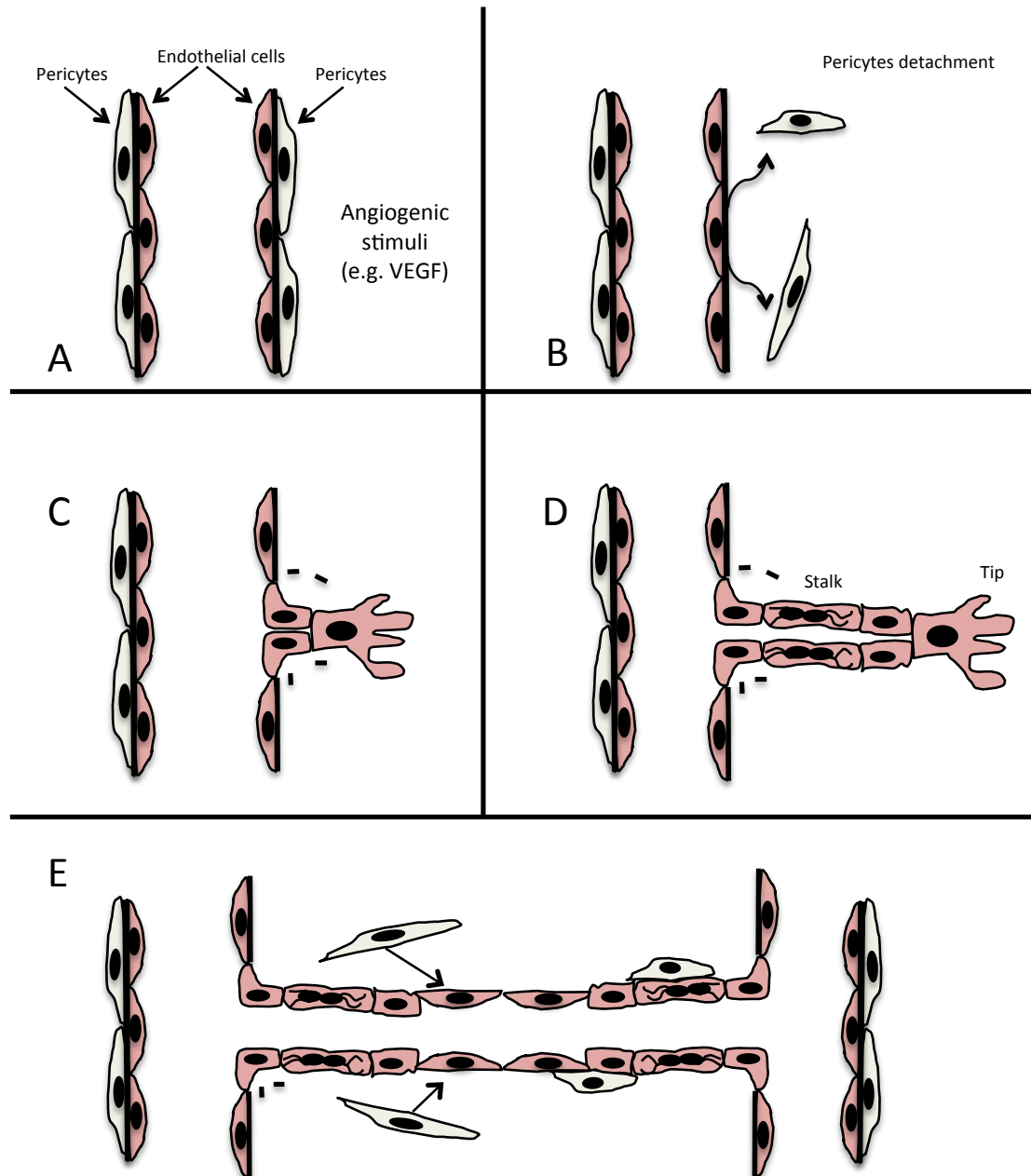
Figure 1.2 Schematic representation of the main steps in sprouting angiogenesis

A. The angiogenic stimuli activate the endothelial cells (red). B. In consequence of the stimulus, pericytes (in white) start detaching, while the basement membrane and extra cellular are gradually degraded. C. This allows endothelial cells to migrate through the perivascular region. D Stalk cells start proliferating following the migrating tip cells. E The sprout is drawn to the proximity of another sprout. The fusion of the sprouts leads to the formation of new vessels. Following, the perivascular cells are recruited to shape and stabilize the newly formed vessel.

Secondly, the structure of the existing vessels starts to disassemble and the endothelial cell-cell contacts are destabilised as a result of detachment of the perivascular cells and degradation of basement membrane and the extracellular matrix (ECM) by matrix metalloproteinases (MMPs). Thirdly, endothelial tip cells migrate to the angiogenic stimulus. Fourthly, the proliferation of stalk cells behind the tip cells extends the sprout while migrating. Endothelial cells change morphology and adhere to each other to form a lumen. Finally, new vessel networks are generated by contact and fusion of angiogenic sprouts via anastomosis. Lastly, the secretion of platelet derived growth factor-B (PDGFB) by endothelial cells leads to the recruitment of perivascular cells and to the maturation of the vessels (Bjarnegard, 2004) (Figure 1.2).

In angiogenesis, tip cells follow a VEGF concentration gradient. Thus, blocking VEGF-A signalling stopped tip cell migration and sprouting (Gerhardt *et al.*, 2003). More recent findings also showed that VEGF-A is stimulating properly spaced branching and sprouting due to the activity of Dll4/Notch signalling. Downstream signalling of the VEGF-A/VEGFR2 pathway means that tip cells express elevated levels of Delta like ligand 4 (Dll4). This prevents adjacent cells to becoming tip cells (Hellström *et al.*, 2007). Dll4 is not the only notch ligand to play a role in the balance between tip and stalk cells. In fact, branching and sprouting is an extremely dynamic process and endothelial cells constantly compete for the tip cell position (Jakobsson *et al.*, 2010). It is known that additional mechanisms to sprouting exist by which new blood vessels are formed. For example, blood vessels are able to split giving rise to daughter vessels in a process called intussusception.
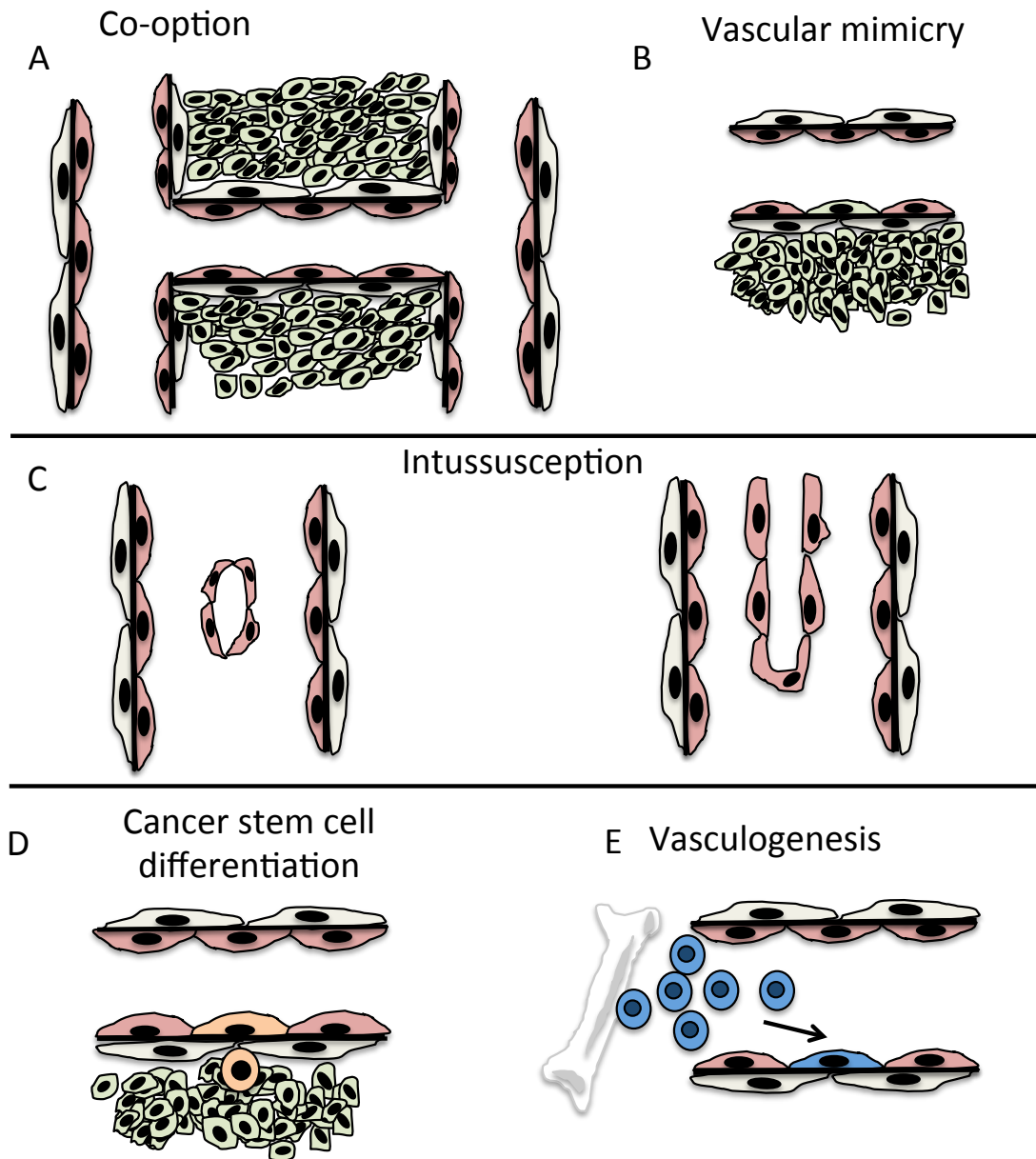
Figure 1.3 Alternative processes to form vessels

There are various known methods of blood vessel formation both in healthy tissues and in tumours. A. Cancer cells (green cells) can hijack the existing vasculature in a process called vessel co-option. B. Tumour cells can exert endothelial like functions in a process called vascular mimicry. C. Existing healthy or tumoral vessels can split (intussusception) generating new vessels. D. Cancer stem cell (orange cells) can differentiate in endothelial-like cells. E. Recruitment and differentiation of endothelial cell progenitors (blue cells) into endothelial cells (Post-natal vasculogenesis). (Adapted from Carmeliet and Jain, 2011). Endothelial cells are represented in red and pericytes in white.

Tumours have been shown to hijack the existing vasculature in a process called vessel co-option. In the same context, tumours cells are able to acquire endothelial-like properties and to form vascular-patterned networks. This process is named vascular mimicry. Finally, cancer stem cells can differentiate to tumour endothelium. Unlike normal tissues, in which vasculature can be formed by vasculogenesis, sprouting or intussusception, tumours can generate new blood vessels using any of the methods described and reviewed in (Carmeliet and Jain, 2011) (Figure 1.3).

1.2 Anti-angiogenic therapy

Tumour angiogenesis and its role in tumour progression and metastasis led to its inclusion as one of the hallmarks of cancer by Hanahan and Weinberg (Hanahan and Weinberg, 2000). A major effort has been made to understand angiogenesis at the molecular level, trying to dissect the pathways involved and design possible therapeutic strategies in order to block tumour growth and metastasis.

Most ant-angiogenic strategies have focused on blocking the VEGF/VEGFR signalling pathway. These studies led to the generation of a monoclonal antibody to vascular endothelial growth factor (VEGF), named Bevacizumab. Bevacizumab in combination with chemotherapy gave 5 months increased survival in metastatic colorectal cancer (Hurwitz *et al.*, 2004). Following the approval of Avastin (the commercial name of Bevacizumab), Sunitinib, a VEGFR2 kinase inhibitor was approved for metastatic renal and gastrointestinal stromal cancer (Roskoski, 2007). The multikinase inhibitor

Sorafenib, originally discovered for its inhibition of the Raf kinase was also shown to be anti-angiogenic (Wilhelm *et al.*, 2008).

Blockade of VEGF presents various obstacles of which the main one is acquired resistance. It was observed that tumours are able to adapt upon treatment with VEGF blockers and switch to other pro-angiogenic growth factors such as fibroblast growth factor-2 (FGF2) or angiopoietin-2 (Ang2) (Casanovas *et al.*, 2005; Rigamonti *et al.*, 2014). Another important aspect of prolonged VEGF blockade that has been elucidated in different tumour models is the promotion of invasive and metastatic cancer phenotypes (Ebos *et al.*, 2009; Pàez-Ribes *et al.*, 2009; Wragg, Heath and Bicknell, 2017). It has also been observed in a preclinical study in glioblastoma that systemic anti-VEGF therapy results in prolonged survival due to increased vascular co-option (Rubenstein *et al.*, 2000). VEGF was reported to inhibit invasion and mesenchymal transition in glioblastoma cells. This effect is achieved by recruiting at the newly described heterodimer VEGFR2/MET the tyrosine protein phosphatase B1 (PTP1B), resulting in the reduction of MET phosphorylation and cell migration. Consequently, upon VEGF-blockage the activity of MET was increased independently from the oxygen levels. In the frame of the same study, it was also shown the beneficial effects of the concomitant blockage of MET together with VEGF. This approach was able to prevent the mesenchymal transition as well as invasion prompted by anti-VEGF treatment, leading to an increased survival (Lu *et al.*, 2012).

1.2.1 Evaluation of preclinical models for anti-angiogenic therapy

Considering the exciting results that pre-clinical studies had shown regarding anti-angiogenic therapies, it was surprising that this translated poorly in the clinic. Over the years, it became clear that many of the preclinical models studied were inadequate. In fact, most of the reports showed efficacy of different angiogenic drugs in subcutaneous tumour models (Kerbel et al., 2013). These models are fairly easy to set up and fairly consistent, nevertheless, there are problems associated with such models. The cell lines employed in these models are characterised by a rapid growth, which does not recapitulate the much slower growth of human cancers. This makes them much more sensitive to chemotherapies. Another characteristic that should be considered when evaluating anti-angiogenic agents, as well as chemotherapeutic drugs, in these models is that it is still unclear whether the response of ectopic tumours is comparable to tumours growing orthotopically. For example, tumours growing subcutaneously are highly angiogenic and efficacies seen with anti-angiogenic agents may be exaggerated (Kerbel et al., 2013). One important consideration is the finding that tumour cells can grow by non-angiogenic growth and in fact can hijack normal blood vessels in highly vascularised organs such as the lung and liver amongst others (Donnem *et al.*, 2018). Importantly, it has been shown that when the anti-angiogenic drug sorafenib is used on orthotopic models of liver cancer in mice, the tumours initially respond but then become resistant (Kuczynski and Kerbel, 2016). This resistance mechanism was due to the tumour cells co-opting the normal liver vasculature and is likely a contributing factor in both intrinsic and acquired resistance to anti-angiogenic drugs in the clinic. Furthermore, a

fundamental difference between these preclinical models and the clinical testing is that, usually patients have undergone and progressed under one or more therapies to which their tumours have become resistant. Finally, Phase III clinical trial patients usually present advanced metastatic disease in multiple organ sites and these simple subcutaneous implantation models fail to recapitulate metastatic disease (Francia *et al.*, 2011). Due to these considerations, it has become more common to employ subcutaneous tumour models as first indication of activity of a specific drug, but more advanced models, which include orthotopic and genetically engineered mouse models, to evaluate the efficacy in a more reliable way are necessary. Furthermore, models in which primary subcutaneous tumours are resected were found to develop advanced multiple metastases. This can give an indication of the efficacy of the drugs in a metastatic model. It has been demonstrated that previously pre-clinically successful drugs that failed to improve standard care in clinical trial were not effective on early or late stage breast cancer metastasis (Francia *et al.*, 2011).

1.2.2 Targeting pro-angiogenic protein-protein interactions

Existing anti-angiogenesis therapies have been less successful than expected and have promoted the search for alternatives due to acquired resistance and cases of increased metastasis in different pre-clinical tumour models (Casanovas *et al.*, 2005; Ebos *et al.*, 2009; Pàez-Ribes *et al.*, 2009). One alternative is to block other pro-angiogenic protein-protein interactions that are known to be critical. To effectively block the interaction between two proteins different means can be employed.

Anti-angiogenic agents include those that block FGF2-FGFR interaction. For example, an FGF trap comprising the extracellular domain (ECD) of FGFR2 fused to an Fc-tag sequesters the growth factor preventing binding to the receptor. This reduced the formation of pancreatic tumours in a spontaneous tumour model (Compagni *et al.*, 2000). Another attempt to disrupt this interaction was the generation of a monoclonal antibody specific for FGF2, which has shown efficacy alone or in combination with anti-VEGF therapy in preclinical studies (Wang *et al.*, 2012). A different approach was taken for the inhibition of the interaction between Ang1 and Ang2 with the Tie2 receptor. Trebananib is a peptide that prevents the binding of the two ligands to the receptor and retarded tumour growth in colorectal xenografts in mice (Oliner *et al.*, 2004).

1.2.3 Vessel normalization

Blood vessels usually form a very organised, hierarchical and functional network supported by the presence of perivascular cells such as pericytes. The malfunctioning of this network might be detrimental for all the tissues, which strictly depend on the oxygen and nutrients provided. For this reason, the generation of new blood vessels plays an important role in healthy human development. In a number of human diseases, the angiogenic process happens in a dysregulated way and solid tumours represent a perfect example. As already mentioned, tumour vessels are abnormal and chaotic, leading to aberrations in the local blood flow and oxygenation (Carmeliet, 2003). It is known that hypoxia in tumours is able to reduce the tumour cell sensitivity to radiation and chemotherapy (Teicher, 1996) and that

due to the leaky nature of these vessels, chemotherapeutic agents struggle to reach the target. This contributes to tumour growth and the metastatic potential but reduces the response to cytotoxic therapies. As anti-angiogenic therapy so far has not proven to be as effective as preclinical studies suggested, Jain and colleagues proposed a different approach, which requires the normalisation of the tumour vessels. According to this hypothesis, instead of attempting to obliterate the aberrant vessels, the use of anti-angiogenic therapy should be aimed to reverting the abnormal structure and function of the vessels, re-establishing a more normal state. The vascular normalisation hypothesis entails that direct or indirect antiangiogenic therapy tips the ratio between pro- and antiangiogenic factors back to a more equilibrated state.

Preclinical studies shed light on possible flaws of this hypothesis. Many genetics studies have shown quite a rather stable normalisation of the vessels and an improvement in the efficacy of chemo and radiotherapy (Mazzone *et al.*, 2009; Leite de Oliveira *et al.*, 2012), on the other hand studies testing the effects of drugs have shown the presence of a "normalisation window". In these latter studies, it has been shown that the normalisation of the vessels lasts about 1-2 days but, eventually, the features of the normalisation are lost (Goel, Wong and Jain, 2012). This effect might be due to an excessive or prolonged dosage of the anti-angiogenic agents, resulting in the skew of the balance towards the anti-angiogenic factors and hence towards vascular regression. It is still unclear if it is possible to replicate the phenotype observed in the genetic studies with pharmacological agents and considerable optimisation is needed to implement this type of approach in the clinic.

1.3 Tumour endothelial markers

It is known that tumour vasculature differs from healthy vasculature due to the different environment (Neri and Bicknell, 2010). The acidic and hypoxic environment in combination with the poor blood flow and the lack of nutrients imprint in the tumour blood vessels a different gene expression pattern, this is unique and differs from the one that is observed in healthy tissues. Moreover, the organisational and structural changes of the two types of vasculatures can be visually depicted as shown by Konerding and colleagues when comparing normal and tumour vascular of the colon (Konerding, Fait and Gaumann, 2001). For these reasons, vascular biology has focused on the identification of these genetic differences. The clarification of these differences opens up the possibility to develop more selective anti-cancer drugs. Various studies have been published exploiting different approaches to identify which genes are differentially expressed in health and disease. The investigation on tumour endothelial markers (TEMs) started by employing subtractive cDNA analysis methodologies (Wyder *et al.*, 2000). One of the main and most important contributions to this type of investigation has been a study using a serial analysis of gene expression (SAGE) to determine which genes were differentially expressed in vessels of colorectal cancer compared with the healthy colon (St Croix *et al.*, 2000). Alternatively, a bioinformatics approach was used with the aim to discover TEMs exploiting the availability of an increasing number of transcriptomes of solid tumours. Indeed, a subtractive algorithm was applied to the sequence tag expression data to identify new tumour endothelial markers (Huminiecki and Bicknell, 2000). Later attempts used microarray platforms,

comparing tumour endothelial cells with healthy tissue counterparts including various cancer types, e.g. lung, colorectal and renal cell carcinoma (Zhuang *et al.*, 2015; Ferguson *et al.*, 2016; Wragg *et al.*, 2016). These latter studies identified and validated GRIN2D in colorectal cancer and MCAM and LAMA4 in renal cell carcinoma as new tumour endothelial markers. Furthermore proteomics studies were able to classify Annexin A1 and CD276 as novel TEMs (Oh *et al.*, 2004; Mesri *et al.*, 2013).

Altogether the output of these studies is a list of genes preferentially or uniquely expressed by tumour endothelium (a so-called signature). An experimental validation is needed to confirm the expression at the protein level of the potential TEM and also its absence in tissues other than tumour endothelium. Finally, for a tumour endothelial marker to be exploited as target, the protein should have a targetable extracellular portion (Neri and Bicknell, 2010).

So far these and other studies have led to the conclusion that it is possible to clearly determine the differences between the healthy and tumour endothelium (St Croix *et al.*, 2000; Mura *et al.*, 2012; X. Zhuang *et al.*, 2015; Ferguson *et al.*, 2016; Wragg *et al.*, 2016). In addition, it has become clear that there is not a global pattern of markers for all the tumours. In other words, the targeting of TEMs against solid tumours should be evaluated and design for each specific tumour setting and a generic approach against all the tumour types is unlikely to be possible.

1.3.1 Vascular targeting

It has become increasingly clear that tumour endothelium plays a key role in tumour development and anti-angiogenic therapy has not been the only attempt to exploit this tumour compartment. In fact, the discovery of the first tumour endothelial markers prompted a new line of research that aimed to develop potential therapeutic tools in order to target not the tumour, but its blood supply. This approach is, in theory, a better strategy than inhibiting angiogenesis, because it does not rely on blocking a specific pathway. In fact, it effectively targets and kill tumour endothelial cells expressing a specific marker, so avoiding the acquired resistance that targeting tumour endothelium showed in clinical testing, due to alternative pathways.

As previously explained, anti-angiogenic therapy prevents the formation of new blood vessels blocking angiogenesis. In contrast, vascular targeting aims to deliver therapeutics and kill existing tumour vessels with the aim of starving the tumour to death. Furthermore, targeting the endothelium is considered a particularly appealing strategy against cancer, due to its high genetic stability and the fact that tumours rely on new blood vessels to sustain growth and invasion. However, with the advent of single-cell genetic analysis the paradigm of the genetic stability of the endothelium may need to be reconsidered (Carmeliet, Gordon Angiogenesis Conference 2017). Various strategies have been used to target TEMs. Antibodies conjugated with radionuclide or drugs/toxins and vaccination are the main approaches. Nevertheless, the application of alternative strategies has become more

common. Among others one of the most notable is the engineering of T cells with a Chimeric Antigen Receptor (CAR).

1.3.1.1 Antibody radionuclide and drug conjugates

Monoclonal antibodies are a class of molecule, which can be raised quickly and potentially against any type of antigen. This makes them particularly interesting in order to target specific antigens, which are expressed on the surface of the cell. Although the intact form of the antibodies, IgG format, is the most commonly employed, many other smaller versions of antibodies, such as Fab or ScFv, are increasingly considered for applications in pharmacodelivery (Neri and Bicknell, 2010). They are a versatile tool used for delivery strategies and can easily be conjugated to either radionuclides or cytotoxic drugs (Carter and Senter, 2008; Sharkey and Goldenberg, 2008).

There are a number of TEMs, which have been extensively studied so far and have been used as targets exploiting different approaches. One the most studied TEMs is an alternatively spliced variant of fibronectin, the extra-domain B (EDB) that can be found abundant in tumour neo-vascular structures and it is usually absent from adult tissues (Neri and Bicknell, 2010). Various types of antibodies have been developed against this domain, such as a full immunoglobulin G (IgG), a single chain antibody (ScFv) and small immunoprotein (SIP). The comparison among those led to the conclusion that the SIP version was preferred for conjugation with iodine (^{131}I) and the result was named radretumab. This antibody has shown to be well tolerated and

positive results were obtained in treating patients with lymphoma and brain metastasis of different types of cancers (Poli *et al.*, 2013). Another example is one using the antibody A8 conjugated with ^{131}I (^{131}I-A8) against the neo angiogenic marker endoglin that showed activity on hepatocellular carcinoma allowing also non-invasive fluorescence imaging (Duan *et al.*, 2014).

Alternatively, antibodies can be conjugated to a cytotoxic drug instead of a radionuclide. Antibody Drug Conjugates (ADCs) to be effective need to be released for their activation, which commonly happens after internalisation into the target cells. For this reason, only specific targets that are internalised upon binding of the antibody are eligible for developing this type of therapeutic approach. There is an increasing amount of data to date regarding ADCs, even though few have developed into the clinic (Gerber, Senter and Grewal, 2009). Other important aspects, which are fundamental for this therapeutic approach, are the target expression, the linker used and the type of drug chosen. Indeed, ADCs are ideally used when the target is expressed at high level and does not present great heterogeneity. Moreover, the shedding of the target should be limited in order to avoid the binding of the antibody in the circulation. Finally, the linker and the drug should be designed to promote the action on site of the ADCs. It was also observed that the bystander effect can influence the off-target systemic toxicity of the ADCs and it should be taken into account when evaluating the efficacy of the newly designed drugs (Diamantis and Banerji, 2016). Various already approved monoclonal antibodies are now under study as ADCs. Interestingly, it is possible to identify a few attempts of ADCs targeting the endothelium or the tumour stroma. For example, a pre-clinical

study showed the efficacy of delivering TNFα to the alternatively spliced variant EDB or EDA of fibronectin in combination with doxorubicin (Hemmerle *et al.*, 2013). This was achieved by conjugating TNFα with either L19 or L8 antibodies creating an immunecytokine; complete eradication and vaccination against the sarcomas were obtained in almost all the mice treated (Hemmerle *et al.*, 2013). Another study showed the increased efficacy and the reduced toxicity of a targeted delivery of arsenic-trioxide As203 with an antibody against VEGFR2 compared to the drug alone in hepatocellular carcinoma (Xiangbao *et al.*, 2014). A more recent study showed promising results in a variety of preclinical tumour models targeting CD276, which is both expressed in cancer cells and tumour-associated endothelial cells, with monomethyl auristatin E (MMAE)- and pyrrolobenzodiazepine (PBD)-linked ADCs (Seaman *et al.*, 2017).

So far, three ADCs have been licenced for cancer treatment, but after a decade from approval one of those, Mylotarg1, gemtuzumab ozogamicin was withdrawn from the market due to a lack of effect on the overall survival (Diamantis and Banerji, 2016). Two other ADCs have been recently licensed and are currently in use for cancer treatment. One is ado-trastuzumab-emtansine (T-DM1 Kadcyla) for the treatment of breast cancer in HER2-positive patients and Brentuximab vedotin for Hodgkin's Lymphoma (Diamantis and Banerji, 2016). Only ADC's against cancer cells have been approved so far and they showed improvement in overall survival and had a positive impact in cancer treatment. Nevertheless, it has been observed resistance in the treatment of breast cancer with T-DM1 and a recent study showed the possible mechanism *in vitro* (Li *et al.*, 2018).

1.3.1.2 Vaccines and the tumour vasculature

Anti-angiogenic therapy and anti-vascular therapy are not the only two approaches, which have been used in an attempt to intervene with the endothelium to stop tumour growth. In fact, examples of vaccination against the tumour vasculature and the up-regulated markers of angiogenesis are progressively increasing. The main aim of this approach is to raise the immune system against the unique markers of tumour endothelium, avoiding the cross-reaction with the healthy endothelium to exclude any possible autoimmune reaction. One of the advantages of vaccination in comparison with the other strategies is that, hypothetically, it should overcome the above-described side effects and the resistance. Moreover, the vaccination will raise a polyclonal antibody response, which display a wider neutralising action of the antigen when compared with the monoclonal counterpart. On the other hand, a possible relevant obstacle to a cancer vaccine is to raise an efficient response in cancer patients entering phase I clinical trials, whose immune system is impaired from chemo and radiotherapy. Additionally, the tolerance for self-antigens constitutes a major problem to overcome in order to stimulate an effective immune response (Wagner *et al.*, 2016).

To date the vaccines developed are either against a specific tumour-endothelium-associated antigen or polyvalent, generated using the whole endothelial cells or isolated proteins from endothelial cell membranes. Based on the knowledge of the differences between healthy and tumour endothelium, a variety of vaccines against the most known proteins involved in angiogenesis or Tumour Endothelial Markers

(TEMs) have been developed. The vaccine CIGB-247 designed to raise immunity against a human VEGF variant molecule represents an example of the efficacy of this approach. The employment of CIGB-247 in a phase I clinical study showed promising immunogenicity and also no abnormality in hematopoiesis, in which VEGF is critical. From this study it is possible to conclude that immunity against self-antigens is achievable without triggering an autoimmune response (Gavilondo *et al.*, 2014).

More recently, other studies have described the possibility of raising the immune system against tumour endothelial markers with vaccines composed by the extracellular domain (ECD) of the transmembrane proteins studied fused with an hFc-tag in mice. Both of the studies have shown an effective humoral response upon immunisation with Robo4 or GRIN2D and the subsequent reduction in tumour growth (Zhuang *et al.*, 2015; Ferguson *et al.*, 2016). Finally, a technique has been developed and studied in the preclinical setting of a vaccine consisting of placenta-derived endothelial cells (ValloVax^TM). The results of the study showed inhibition of tumour growth in different tumour models *in vivo* and also an effect on lung metastasis (Ichim *et al.*, 2015).

From these studies and others in the literature, it is possible to conclude that vaccines constitute a promising tool for cancer treatment.

1.4. The adaptive immune system and immune evasion in cancer

T lymphocytes, along with B lymphocytes, are a part of the adaptive immune response and are able to respond to stimuli with great specificity. In fact, these cells are able to recognize a vast repertoire of ligands through unique T cell receptors (TCR), which are generated by a process of somatic recombination, called V(D)J recombination. Theoretically the outcomes of this process can reach a number of different TCR sequence combinations in the order of 10^{15} (Vrisekoop *et al.*, 2014). Hence, considering that in the human body the T cell repertoire is in the order of 10^{11}, it is clear that each individual carries only a subset of all possible TCRs. Nevertheless, the mechanism by which the T cells are selected is clearly not random and only an effective repertoire is formed to prevent pathogen persistence and spread. So far, various models of selection have been proposed but the full mechanism is not yet completely understood (Vrisekoop *et al.*, 2014).

Generally speaking, T cell lymphocytes are an extremely important asset in various processes such as inflammation or cancer. T lymphocytes are responsible for the recognition and direct CD8$^+$ mediated cytotoxic activity of cellular pathogens. Moreover, regulatory CD4$^+$ T cells are also involved in orchestrating other cell types of the immune system, such as B cells or macrophages, as well as various different processes. As for most of the immune cells, T lymphocytes display an incredible plasticity and their phenotype can vary greatly according to the stimuli and the microenvironment. Indeed, during cancer progression, CD4$^+$ T cells can display various different phenotypes and were originally divided in two subgroups, Th1 and

Th2. From the original dichotomy described, many others T helper (Th) subsets were described (Raphael *et al.*, 2015). Each subset of T cells expresses different cytokines and receptor patterns, based on a specific genetic program. These subsets are shown to be flexible and can change their functional phenotypes in response to the environment. Clearly, this plasticity functions at different stages of pathological processes, such as cancer and autoimmune diseases, and thus it is extremely important.

During cancer progression a Th1/Th17 response is elicited and a tumour is actively recognised as non-self. This pro-inflammatory response is mediated by the presence of T regulatory cells within the tumour mass, which allows the tumour to grow. At latter stages the hypoxic and acidic tumour microenvironment as well as Th2 and T regulatory cells contribute to tune the immune system down at the local and global level, which also favours the spreading of metastasis. Th2 mediated IL-4 production influences macrophages to display a more pro-angiogenic and pro-tumoral phenotype (Dunn *et al.*, 2002). Formally, the dynamic interaction between the immune system and the tumour has been associated with a concept called "cancer immunoediting", which can be divided in three phases, also known as the three E's (Kim, 2007) (Figure 1.4). During the first phase, known as elimination, innate and adaptive immune cells are able to obliterate the tumour cells, keeping the organism clear. In this phase the main players are natural killer cells and the IFN-γ released by the innate immune cells. This phase ends when an immune-resistant population of the tumour appears. Within this population the cells represent tumour variants with decreased immunogenicity, becoming resistant to the immune effector cells; this
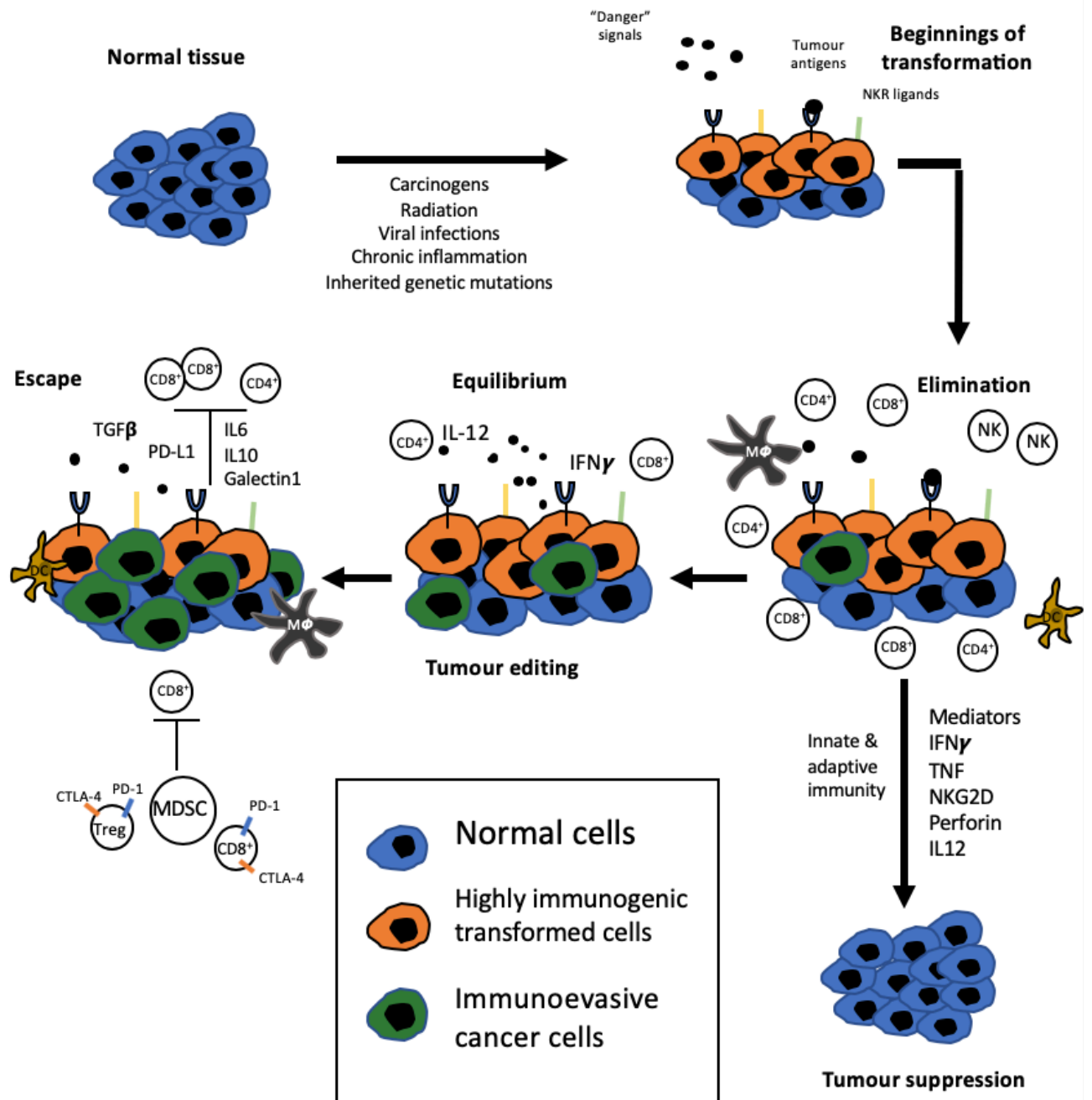
Figure 1.4 Tumour immunoediting

The figure represents the most important steps in tumour immunoediting: elimination, equilibrium and escape. Transformed cells becomes immunogenic and are actively recognised by the immune system. The activation of the immune system can lead to the total elimination of the transformed cells (Elimination). The action of the immune system can lead to the selection of less immunogenic cells, which start expanding (Equilibrium). The combination between the low immunogenicity of the new clones and the strongly immunosuppressive microenvironment allow the tumour to escape the immune system and develop (Escape) adapted from (Schreiber, Old and Smyth, 2011).

24

new phase is called equilibrium. The equilibrium phase can last for years. Eventually, when the tumour has developed the proper mechanisms to dodge the action of the immune system, the escape phase starts. During this last phase, the tumour is able to evade immune detection or destruction by loss of tumour antigens, downregulating MHC class I molecules, and by the secretion of inhibitory cytokines among others. The microenvironment is able to produce a variety of stimuli, which result in the final effect of suppressing the immune system altogether. Moreover, some cell types end up being more pro-angiogenic and favour the tumour growth and the spread of metastasis. The outcome of this last phase is the suppression of the immune system and tumour progression. It has been shown that the reactivation of the immune system and stimulation of a Th1 type response, combined with an M1 type response in macrophages, showed a positive effect in retarding tumour growth and, in some cases, eradication of the tumour (Kim, 2007). A feasible approach to reactivate the immune system against cancer would be to manipulate the regulatory T cells to differentiate in Th17. Nevertheless, this approach could be associated with autoimmune disorders.

1.4.1 Chimeric antigen receptor (CAR) modified T cells

Conventional therapies are targeting highly proliferating cells and are not able to distinguish between highly replicating malignant cells and highly replicating healthy tissues, such as the haematopoietic cells and the epidermis that have high turnover. As result, various side effects are connected with standard therapy (Pettitt *et al.*, 2018). The recent application of monoclonal antibody in cancer therapy was an

attempt to selectively target the tumour without affecting healthy tissues and reducing side effects (Coulson *et al.*, 2014).

One of the most promising advances regarding highly targeted therapy is immunotherapy. As previously mentioned, adaptive immunity is able to recognise newly encountered antigens of bacteria, viruses, parasites, and malignant cells. The capacity of the immune system to adapt and selectively target specific antigens is unique and unparalleled. Moreover, over the years various techniques have been developed to be able to reprogram these cells, in order to display a particular specificity. Considering the number of possible variants of the TCR, T cells could be reprogrammed against virtually any type of target (Pettitt *et al.*, 2018).

With this aim, in 1989 Gross and colleagues attempted to manipulate T cells with chimeric receptors (Gross, Waks and Eshhar, 1989). Over time, the limitations of this technique, such as poor *in vivo* expansion or persistence after post-infusion, were overcome. Indeed, recent reports both from pre-clinical and clinical studies showed the potential of this approach for cancer treatment.

Chimeric Antigen Receptors are synthetic receptors, which originally comprised a single-chain variable fragment (scFv) to direct the specificity and a CD3ζ domain to allow the intracellular signalling of T cells for activation upon antigen binding. Other generations of CAR T cells included an additional domain to mimic the co-stimulation, such as CD28, 4-1BB or OX40 (Maher *et al.*, 2002; Imai *et al.*, 2004; Pulè

et al., 2005) (Figure 1.5). Co-stimulation is also present during a physiological TCR recognition by antigen presenting cells, in order to fully activate the T cells.

In 1970 it was hypothesised that a T cell requires not only the TCR signalling pathway but also another signal from Antigen Presenting Cells (APCs), providing costimulatory signals, in order to fully activate. This model was suggested as a possible mechanism by which T cells discriminate self/non self peptide presentation (Bretscher and Cohn, 1970). In the following years the discovery and characterisation of the CD28 pathway, supported this theory. In fact, according to this model it is not only the binding between the T cell receptor (TCR) with the peptide presented by APCs, but also the activation of a costimulatory domain such as CD28 by the B7.1 and B7.2 ligands on APCs to be important for T cell activation. The expression of CD28 was observed in 95% of human CD4$^+$ and in 50% of human CD8$^+$ T lymphocytes and in all the murine T cells. Engagement of the CD28 costimulatory domain together with TCR activation, showed increased T cell survival, proliferation and differentiation as well as IL-2 production (Lenschow, Walunas and Bluestone, 1996).
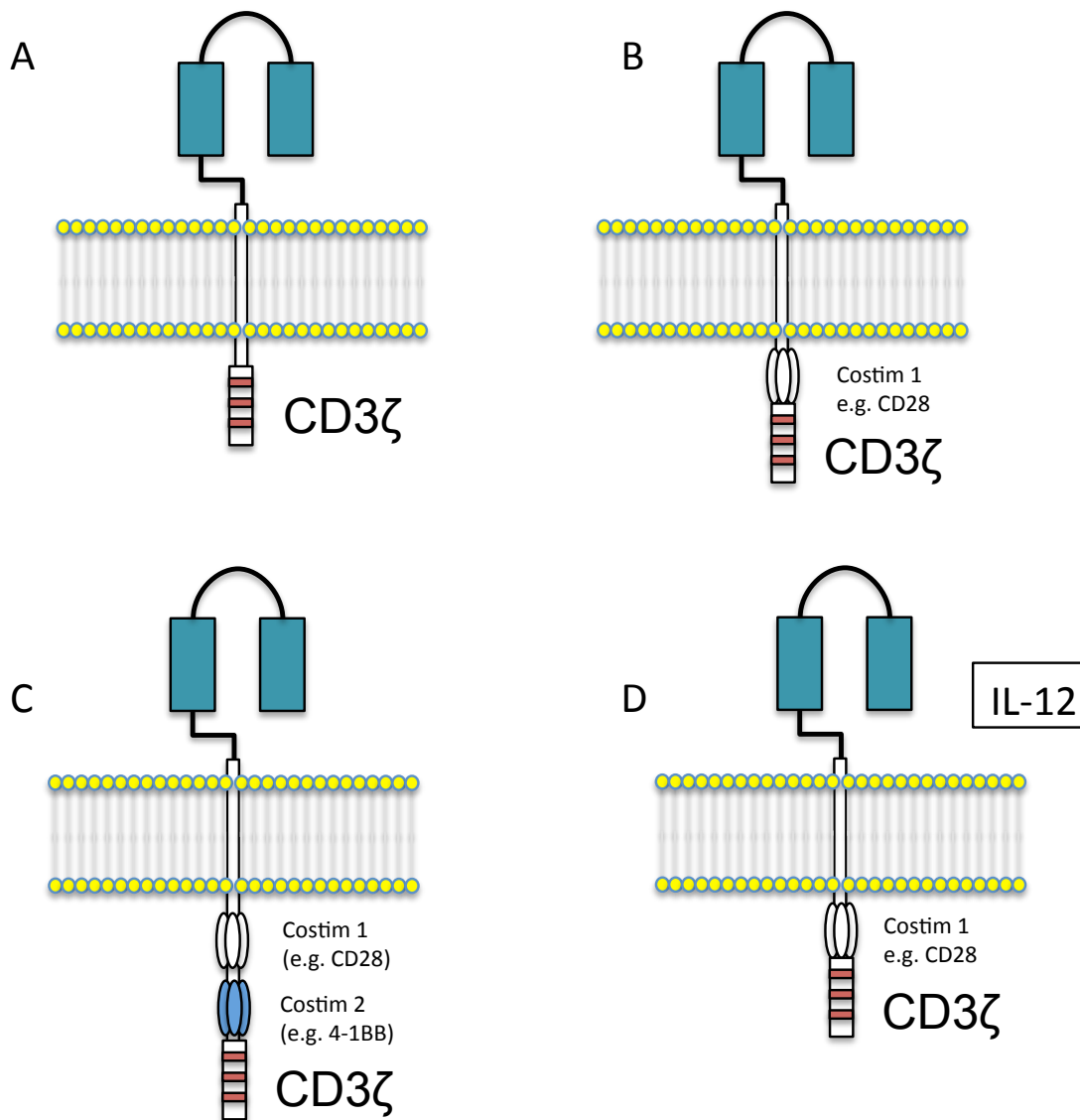
Figure 1.5 Schematic representation of four generation chimeric antigen receptors

A. First generation CAR, carrying only the CD3ζ. B. A costimulatory domain is introduced in the second-generation CAR (e.g. CD28, 4-1BB or OX40). C. In third generation CARs two stimulatory domains are included. D. The fourth generation of CARs is based on the second-generation constructs including gene cassettes for the production of cytokines such as IL-12. This generation of CAR T cells is also known by the name "T cell redirected for universal cytokine killing" (TRUCK) cells

According to the costimulatory theory and the observations on the effect of the costimulation mediated by CD28, in 1998 costimulatory domains were introduced also in CAR applications. Initially the CD28 domain was introduced as an independent construct named chimeric costimulatory receptor (CCR) and it could induce IL-2 production and prolong survival in primary human T cells.

Finney and colleagues were the first to introduce the costimulatory domain within the CD3ζ CAR construct. This second generation of CARs showed a greater production of IL-2 than CAR T cell only expressing CD3ζ (20-fold greater) (Finney *et al.*, 1998). Moreover, it was shown that the position of CD3ζ and CD28 within the receptor was important for cell expression.

Since the first introduction of the second generation its superiority was easily demonstrable and many *in vitro* studies showed a greater production of IL2, IFNγ and GMCSF when compared with the first generation (Hombach *et al.*, 2001; Haynes *et al.*, 2002; Maher *et al.*, 2002). Moreover, it has been demonstrated that CD28 domain addition to CAR constructs was able to upregulate the anti-apoptotic gene Bcl2 in an antigen-specific manner, promoting survival. Other costimulatory domains were tested. Hayes and colleagues demonstrated in animal models *in vivo* that the use of second generation CARs resulted in higher proliferation and cytokine production as well as in a more efficient tumour eradication than the older generation (Haynes *et al.*, 2002). It has been shown that few tumours express the costimulatory ligands and this reinforces the importance of costimulatory domains within the CAR.

CD28 costimulatory pathway is one of the most studied, but many others over the years have been discovered and not as well characterised. For what it may concern the CAR design, two main other costimulatory domains have been frequently employed: OX40 and 41BB (Imai *et al.*, 2004; Pulè *et al.*, 2005). Although many research groups are currently working on costimulation, it is still unclear if it is possible to identify a single optimal domain.

1.4.2 CAR as promising therapy for B cell malignancies

One of the most impressive applications of the CAR T cell technology is clearly the treatment of B cell malignancies (Figure 1.6). In particular, CD19 has been favoured for targeting these malignancies both using monoclonal antibodies and immunotherapy. CD19 is a marker, which can be found expressed on B cells at various stages (e.g. precursors, mature B cells or malignant B cells) (Uckun *et al.*, 1988). From the first application of CARs against CD19, this technology proved to be more effective for cancer treatment than monoclonal antibodies. The use of CAR T cells showed the possibility of eradicating the B-cell lineage to achieve regression in a lymphoma patient (Kochenderfer *et al.*, 2010). Further, it has been noted that the efficiency of the CARs was strongly associated with prior conditioning of the host. In other words, patients who were irradiated at the moment of the CAR T cell therapy responded consistently better to the treatment.

First trials employing CAR T cells were designed for treating Non-Hodgkin's lymphoma (NHL) such as chronic lymphocytic leukaemia (CLL) patients. Initially, first

generation CARs showed no clinical responses. A direct comparison between first and second generation of CAR T cells, using CD28 costimulatory domain, showed improved proliferation and persistence *in vivo* in the presence of the costimulation (Savoldo *et al.*, 2011). Although the second-generation CARs showed improvements, the clinical outcome was still poor. Indeed, after an initial stabilisation none of the patients showed signs of regression (Savoldo *et al.*, 2011). An improved clinical result was observed when second generation CAR T cells against CD19 were infused together with high doses of IL2 in CLL and lymphoma patients. In fact, out of 8 patients 5 showed a partial response and 1 patient showed complete response still ongoing after 15 months (Kochenderfer *et al.*, 2012). More recently, another clinical report showed that the use of a second generation CAR (19-BBz CAR) carrying the 4-1BB-costimulatory domain in chronic lymphocytic leukaemia (CLL) patients had an overall response of 57% (8 of 14) with 4 of the patients in complete remission and 4 in refractory remission (Porter *et al.*, 2015).

Nevertheless, the most impressive results of the same 19-BBz CAR were obtained employing this CD19 specific CAR for treatment of acute lymphoblastic leukaemia (B-ALL). In fact, in this trial 27 out of 30 patients treated showed a complete response. Moreover, 22 patients also showed no minimal residual disease. Consistently, most of these patients remained in remission over a follow up of 2-24 months (Maude *et al.*, 2014). A different CAR targeting CD19 (19-28z) showed almost equally positive results. On the other hand, the T cells expressing this car were showing a much lower persistence (days versus years of the 19-BBz CAR). Nevertheless, most patients treated with 19-28z CAR showed complete remission (CR) in this short timeframe

(Lee *et al.*, 2015). A more recent clinical trial showed increasing positive outcome for patients treated with 19-BBz CAR (Turtle *et al.*, 2016).

However, although the results of the most recent clinical trial were outstanding for the treatment of B-cell malignancies, it is important not to overlook the toxicity that can arise. The important infusions of activated T cells carry with them a high inflammatory response, which can have major side effects. Thus, patients may develop cytokine release syndrome (CRS) caused by an overwhelming amount of cytokines released in the blood stream from activated immune cells. The immediate consequences are reduced blood flow and low oxygen delivered to organs. The extent of the CRS usually correlates with a high tumour burden as well as high T cell doses. Symptoms for the patients who experience CRS may vary from mild fever to life-threating conditions such as multi-organ failure (Maude *et al.*, 2014; Lee *et al.*, 2015; Turtle *et al.*, 2016). During or after the resolution of CRS, neurotoxicity is commonly observed in patients, which can result in symptoms such as confusion, delirium or seizures. It is still unclear why patients experience neurotoxicity, and, although its transient and reversible nature, a patient died because of the strong neurotoxicity that developed (Turtle *et al.*, 2016).

Finally, due to the CD19 targeting strategies of the mentioned clinical trial, a common side effect was B cell aplasia. In fact, CARs targeting CD19 are not able to discriminate between precursors, mature or malignant B cells, depleting blindly the B-cell population. This condition of aplasia is maintained according to the persistence of the CAR T cells infused.

Step 1 Leukapheresis: leukocytes are separated by other blood's patient

Step 2 Elutriation: Enrichment for T cells by separating the cells by size

Step 3 T cell activation: T cells are stimulated with αCD3/αCD28 and IL-2

Step 4 T cell expansion: upon stimulation with IL-2 T cell can grow logarithmically in a bioreactor for a few weeks

Step 5 CAR T cell transduction: CAR DNA is transduced and integrated into the genome of T cells via retroviral/lentiviral infection

Step 6: T cells are concentrated and and cryopreserved

Step 7: T cells are infused into the patient

Figure 1.6 CAR T cell therapy in the clinic

The diagram represents the main steps for CAR T cell development in the clinic. After leukapheresis, T cells are separated by size and activated (Step 1-3). After stimulation T cells are expanded and transduced with the CAR construct (Step 4 and 5). T cells are either cryopreserved or re-infused into the patient (Step 6 and 7) adapted from (Levine *et al.*, 2017).

33

An indication of poor persistence is the reappearance of the host B cell population. This was used to monitor persistence during clinical trials. In figure it is schematically shown the typical protocol employed in the clinic for CAR T cell therapy.

1.4.3 Chimeric antigen receptor T cells against solid tumours and their endothelium

Clinical trials on CAR T cells have shed light on the potentiality of CARs in haematological diseases, but little is known in solid tumours. Most of the clinical trials studying the effect of CAR T cell therapy in solid tumours have not been evaluated yet. However, it is possible to delineate various critical points that can affect CAR functionality in this setting. Primarily, the choice of the epitope, the CAR structure and the doses of CAR T cell to infuse are the starting points for an efficient CAR. According to the type of tumour, it is necessary to identify specific targetable antigens. The identification of these antigens is without any doubt one of the most important issues to the generation of efficient CARs, due to their rarity (D'Aloia *et al.*, 2018). A specific splice variant for EGFR (EGFRvIII) has been shown to be a promising target due to its limited expression in glioma cells (Sampson *et al.*, 2008). Regardless of the target, each CAR T cell therapy should be evaluated in a specific manner.

Another fundamental aspect to consider in solid tumours is to evaluate all the possible physiological and functional barriers that might impede a correct delivery of CAR T cells to the tumour site. In particular, the extravasation, the tumour homing

and persistence in a hostile microenvironment are limiting factors for the functionality of CARs (D'Aloia *et al.*, 2018).

Targeting epitopes expressed by cancer cells raised a number of problems. An efficient infiltration of T cells within the tumour mass is difficult to obtain. Moreover, the tumour microenvironment proves to be strongly hostile towards T cells. In fact, hypoxia, acidic environment and low nutrients inhibit T cell proliferation and cytokines production. In addition, within the tumour mass due to the presence of tumour associated macrophages and neutrophils as well as regulatory T cells and myeloid derived suppressor cells, the concentration of immunosuppressive cytokines such as TGFβ, IL-10, IL-4 or prostaglandin-E2 suppress CAR T cell activity (Sakaguchi *et al.*, 2010). New strategies have been implemented to avoid the suppression of CAR T cells. In a preclinical model it has been demonstrated that it is possible to overcome the TGFβ action within the tumour microenvironment using tumour-specific cytotoxic T lymphocytes that are expressing a TGFβ dominant negative (Bollard *et al.*, 2018). Furthermore, "armored" CAR expressing IL12 have also been used to mitigate the hostile microenvironment, enhancing the innate immunity, and stimulating recruitment (Pegram *et al.*, 2015).

Finally, to avoid problems related to the barrier constituted by the endothelium and the hostile microenvironment, recent reports showed efforts to re-direct CAR T cells against the endothelium and not against epitopes expressed by the tumour. One of the most notable examples is the CAR designed to target the VEGFR-1 expressing cells, namely V-1 CAR. As previously mentioned, the VEGF/VEGFRs pathway has been

long exploited for anti-angiogenic therapy, but problems of resistance, due to compensatory pathway limited the efficacy of Bevacizumab in the clinic. The approach of using modified T cells overcomes the problem, selectively killing VEGFR1 expressing endothelial cells and not acting on one pathway. Wang and colleagues reported an inhibition in tumour formation and growth in a xenograft model in mice, mimicking the clinical protocol normally used for transferring of modified T cells (Wang *et al.*, 2013). Moreover, it is shown that V1- CAR T cells have a strong anti-angiogenic effect *in vitro*. Essentially targeting the tumour vasculature environment constitutes a strategy to disrupt newly formed vessels and impede tumour growth without the necessity for T cells to infiltrate the tumour.

1.5 C-type lectin domain group 14 family

C-type lectin-like domains (CTLDs) proteins belong to a large superfamily of proteins with diverse functions. In particular, 17 families of CTLDs proteins have been described so far. The group 14 family of CTLD contains CLEC14A, CD93, Thrombomodulin and Endosialin (CD248) and they all share similar domain architecture (Zelensky and Gready, 2005) (Figure 1.7). Each of these proteins from the N-terminal shows a signal-peptide, a CTLD domain with 8 conserved cysteine residues, a sushi domain (also known as control protein domain, CCP), various repeats of EGF-like domain, a variable region rich in proline, serine and threonine containing predicted sites for O-linked glycosylation (known as mucin-like domain) in the extracellular part of the protein. They all have a transmembrane domain and a short cytoplasmic tail.
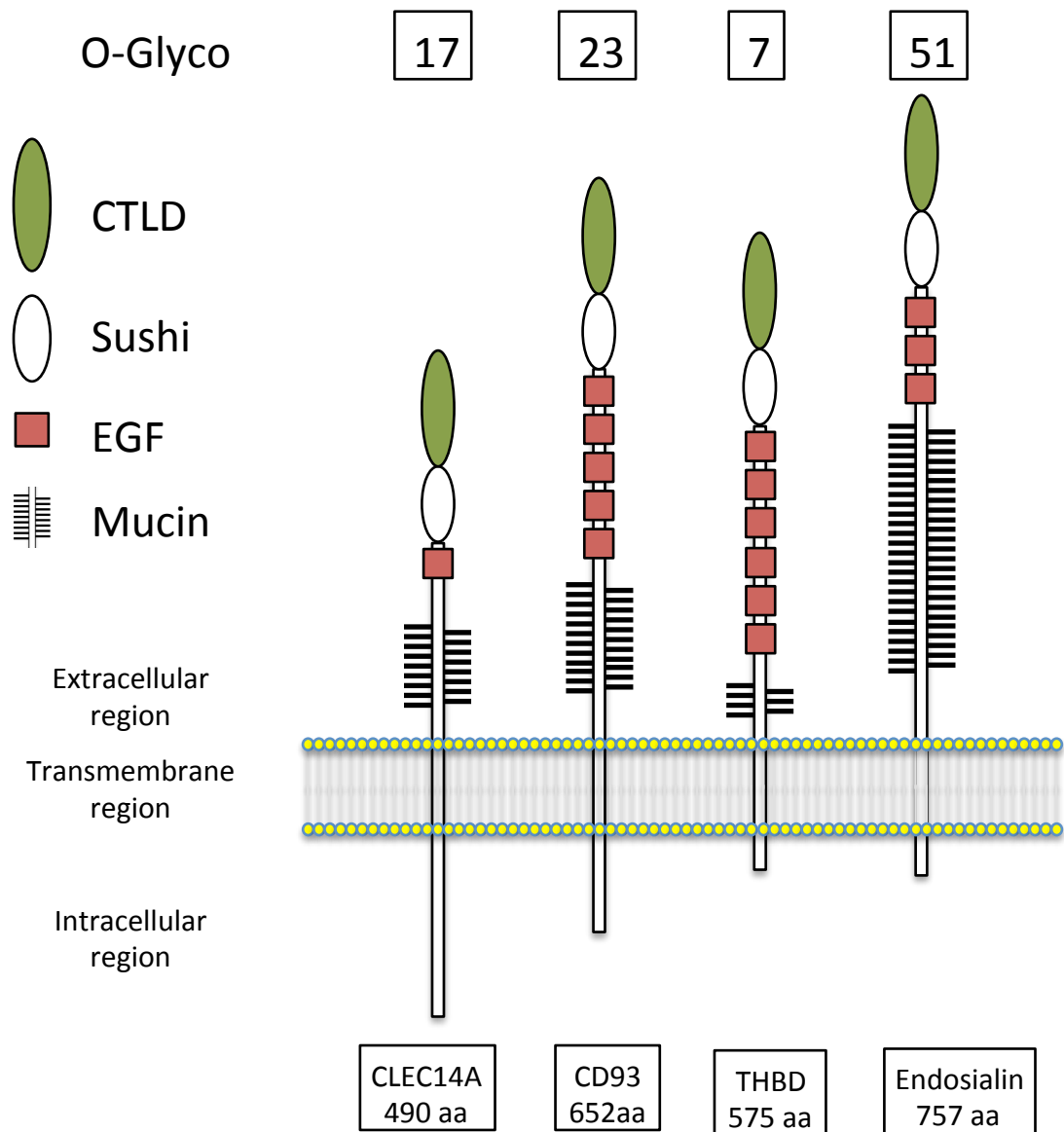
Figure 1.7 Schematic representation of the domain distribution of the C-type lectin domain family 14 members

The numbers at the top of each protein indicates the number the predicted O-glycosylations, represented within the mucin domain with black bars. The CTLD domain is represented in green, the sushi domain in white and the EGF-like domain repeats in red.

Interestingly, although the CTLD was thought to be a calcium dependent carbohydrate-binding domain, not all the CTLDs binds to calcium or carbohydrates. The characteristic structure of a CTLD domain entails a double-loop (loop-in-a-loop). In addition to the two conserved disulphide bridges, a set of hydrophobic and polar interactions stabilise this structure (Zelensky and Gready, 2005). The sushi domain generally presents sequence variation, but it is possible to identify various conserved residues, such as 4 conserved cysteine residues and a tryptophan residue. Structural studies confirmed that they are responsible for its tertiary structure (Norman *et al.*, 1991). As already mentioned, the repeats of EGF-like domains on each protein of the family 14 varies and, in fact, CLEC14A contains one, CD93 five, THBD six and Endosialin three. The dimension of these domains is of 30-40 amino acids. Within this region it is possible to identify six conserved cysteine residues that are responsible for 3 intramolecular disulphide bonds (Wouters *et al.*, 2005). Furthermore, the whole family shows a high level of glycosylation, which are concentrated within the mucin region. This domain normally associates with the structure of adhesion proteins, such as CD164 or selectins (Kansas, 1992; Doyonnas *et al.*, 2018). The structure of the mucin region is very rigid and extended due to many O-linked sugars and it is inaccessible to the action of proteases, protecting the proteins from degradation (Jentoft, 1990). Due to this heavy glycosylation all the proteins of the family 14 were shown to be much larger than their predicted size based on the sequence.

Finally, studies on the protein sequences of this family related CLEC14A to endosialin and CD93 with thrombomodulin (THBD). Moreover it appears that THBD and CD93

share a common ancestor (Harhausen *et al.*, 2010). For the purpose of this work, the focus will be on CD93 and CLEC14A and their role in endothelial cell biology.

1.6 CD93

Cluster of differentiation 93 (or CD93) is a 120kDa O-glycoprotein that for many years was known by the name C1qRp and it was initially thought to be the putative receptor for C1q, a complement molecule (Nepomuceno and Tenner, 1998). Although this theory was corroborated by the fact that C1q acted on endothelial cells in a receptor-mediated fashion, latter studies disproved the possibility that C1qRp (CD93) is the receptor for C1q (McGreal *et al.*, 2002). Furthermore, it was confirmed by expression cloning that C1qRp and CD93 were in fact the same protein (Steinberger *et al.*, 2002). The mouse homolog of the protein is known as AA4. Interestingly, the homology of CD93 across species (rat versus human and mouse) is 67 and 87%, indicating that this receptor might play an important biological role (Norsworthy *et al.*, 2004).

The expression of CD93 is detectable in a wide range of cell types: endothelial cells, neurons, monocytes, neutrophils, B cells, natural killer and naïve T cells as well as platelets and haematopoietic stem cells, but not fibroblasts (Nepomuceno and Tenner, 1998). Subsequently, it has been shown by *in situ* hybridization that CD93 is predominantly expressed in endothelial cells and pneumocytes. It is present abundantly on human circulating monocytes but not on tissue macrophages or dendritic cells, suggesting a tight regulation during embryogenesis and adult life. A

study in rat showed also expression of the homologous AA4 on natural killer cells, which are known to express type II lectins to prevent killing of "self" cells. It has been also suggested that AA4 might regulate both monocytes and NK-mediated innate immune responses (Dean *et al.*, 2000). Murine AA4 was also detected on primitive haemopoietic stem cells, which would support a possible role in angiogenesis (Norsworthy *et al.*, 2004).

Due to the structural homology with adhesion molecules such as selectin, a putative role in adhesion and leukocyte rolling was suggested. Furthermore, CD93 presents a cell-bound form and a soluble form, which is shed in activated cells, similarly for what is observed for L-selectin and CD44 as well as TNF-α (Petrenko, 1999; Harhausen *et al.*, 2010). The release and production of soluble CD93 appears to be mediated by metalloproteinases (MMPs) upon stimulus with proinflammatory cytokines (Bohlson *et al.*, 2005). The level of CD93 in the plasma has been correlated with coronary artery disease and acute myocardial infarction and it is increased in patients with rheumatoid arthritis (Mälarstig *et al.*, 2011; Youn *et al.*, 2014). It has been demonstrated that the shed form of CD93 is provided by both immune cells, due to inflammation, and non-haematopoietic cells, such as the endothelium (Bohlson *et al.*, 2005; Greenlee, Sullivan and Bohlson, 2009; Jeon *et al.*, 2010). Soluble CD93 was associated with monocyte inflammation and the phagocytosis of macrophages (Youn *et al.*, 2014).

Interestingly, as it was theorised, the O-glycosylation of the mucin-like domain of CD93 has been shown to prevent the shedding when it is expressed at the cell

surface. In fact, it has been observed that lack of this post-translational modification resulted in higher levels of soluble CD93. It has also been speculated that soluble CD93 might be an immature form of the protein (Park and Tenner, 2003). Therefore, the O-glycosylation modification might regulate the protein cleavage.

Various studies have proposed and demonstrated putative roles of CD93 in various contexts. It has been shown that CD93$^{-/-}$ mice do not present defects during development and were grown up to 1 year of age. It has been observed that upon stimulation with the inflammatory cytokine IL-1β, there were no defects in leukocyte adhesion and transmigration upon CD93 loss, indicating that CD93 might not be involved in cell-cell interaction during leukocyte migration in the experimental model analysed. Due to the complexity of the leukocyte rolling and transmigration, it is evaluated the possibility that other receptors with redundant functions might have been recruited. Finally, the most striking phenotype observed in the knockout mice was the impaired clearance of apoptotic cells in a peritonitis model (Norsworthy *et al.*, 2004).

Furthermore, in the same CD93$^{-/-}$ mouse it has been shown that the absence of CD93 reduces protection of ischemic damage in the brain. In fact, it has been demonstrated that CD93 protects neurons by reducing the neuroinflammatory response inhibiting the production of cytokines, such as CCL21. Consequently, the knockout mice constitutively presented a high level of CCL21 both before and after the treatment with LPS. Normally CCL21 is released by damaged neurons and it

stimulates the infiltration of leukocytes. Upon ischemic damage, CD93^{-/-} mice presented increased oedema and infarct volumes (Harhausen *et al.*, 2010).

A recent study showed that in patients with colorectal cancer the expression of CD93 was upregulated in the endothelial cells of blood vessels, whereas little expression was observed in the blood vessels of healthy tissue. Surprisingly, although the high levels of MMPs in CRC, a reduction in soluble CD93 has been observed. Interestingly, a particular SNP on the CD93 gene (rs2749817) correlated with disseminated cancer and increased risk of recurrence after surgery (Olsen *et al.*, 2015).

Due to its main expression in endothelial cells and tight regulation during development, it was suggested that CD93 might play an important role in angiogenesis (Petrenko, 1999). More recently, CD93 was identified as one of the "tumour angiogenesis signature" genes together with CLEC14A. Upon anti-VEGF treatment some of these genes were downregulated, including CD93 (Masiero *et al.*, 2013). This regulation was also independently confirmed by Genentech in tumour xenografts (Bais *et al.*, 2011). Interestingly, CD93 has been identified as one of the main upregulated genes in the vasculature of IV grade glioblastoma tumours (Dieterich *et al.*, 2012). In the same year, it has been shown that specifically the EGF-like domain of the soluble CD93 is able to induce proliferation, migration *in vitro* and angiogenesis *in vivo* through PI3K/Akt/eNos and ERK ½ signalling pathways (Kao *et al.*, 2012). To identify new mediators of angiogenesis, Orlandini and colleagues raised a monoclonal antibody by immunising mice with proliferating HUVEC. Further characterization led to the conclusion that the monoclonal antibody raised was

specific for the CTLD and sushi domains of CD93 and showed anti-angiogenic features both *in vitro* and *in vivo* (Orlandini *et al.*, 2014)*.* A subsequent study has identified upregulated protein levels of CD93 in the vasculature of glioblastoma and a correlation between this upregulation with poor survival of the patients (Langenkamp *et al.*, 2015). Furthermore, the reduction in tumour growth observed in glioma and fibrosarcoma mouse models was detectable only for female mice. This sex-dependent effect might be due to the previously described influence of sex hormones on endothelial cell biology, angiogenesis and blood vessel function (Langenkamp *et al.*, 2015). At the functional level, shRNA and siRNA mediated knockdown in HUVEC and HDMEC showed in independent studies a reduction in proliferation, migration, adhesion and sprout formation (Orlandini *et al.*, 2014; Langenkamp *et al.*, 2015). Further findings have shown the interaction and crosstalk between CD93 and the laminin binding protein dystroglycan (DG) and its importance for cell adhesion and migration in endothelial cells. This study has shown the importance of a specific Src-mediated phosphorylation on CD93 tyr628 upon interaction with β-DG when adhered to laminin. As a result of this phosphorylation, the recruitment and phosphorylation of the adapter protein Cbl was mediating cell adhesion and spreading (Galvagni *et al.*, 2016). Previously it has also been reported in monocytes and HUVEC that the juxtamembrane (JX) region of CD93 interacts with the ERM family protein moesin in the presence of phosphatidylinositol 4,5-bisphosphate (PIP2). The interaction of the JX domain stabilises moesin in the active conformation, interacting at the C-terminus with the cytoskeleton actin. Through this mechanism CD93 is able to co-ordinate events such as cytoskeletal rearrangement, adhesion and/or phagocytosis (Zhang *et al.*, 2005). Another

intracellular partner of the (JX) CD93 have been identified namely the GAIP interacting protein C-terminus (GIPC) (Bohlson *et al.*, 2005). It was speculated that GIPC and moesin are either in competition for the binding on CD93 or one depend on the binding of the other (Zhang *et al.*, 2005). Finally CD93 is involved in neovascular age-related macular degeneration and it was identified as a potential new target for choroidal neovascularization (Tosi *et al.*, 2017).

1.7 CLEC14A

CLEC14 A (or C-type lectin family 14 member A) is a transmembrane glycoprotein of 490 amino acids. Multiple reports have identified CLEC14A as a new endothelial specific gene either combining microarray analysis and data mining or, later, in *in silico* analyses (Ho *et al.*, 2003; Herbert *et al.*, 2008). Microarray analysis also found CLEC14A regulated during endothelial progenitor cells differentiation (Maeng *et al.*, 2009). An additional study confirmed at the RNA level that CLEC14A in multiple human tissues shows an endothelial specific expression. It has also been reported that CLEC14A is expressed at embryonic day 10.5 in mice embryo and in the vasculature of the retina at the post-natal day 12 (Rho *et al.*, 2011). CLEC14A was then identified as a tumour endothelial marker because its expression was associated with tumour endothelial cells and tumour vessels but virtually no expression in the healthy tissues was observed. Various tissues have been analysed and in particular CLEC14A was found upregulated in the tumour vessels of prostate, breast, kidney and thyroid by immunohistochemical staining (Mura *et al.*, 2012). Notably, CLEC14A staining in colorectal cancer showed poor expression. Another

study confirmed that at the RNA level, CLEC14A was upregulated in resected tumour tissues of non-small cell lung carcinoma (NSCLC) compared to adjacent non cancerous lung tissues (Pircher *et al.*, 2013). Analysing clinical data it appeared that the upregulation of CLEC14A in lung tumours was correlated with prolonged survival. Recently it has been reported that CLEC14A was upregulated in circulating CD109^{+} tumour endothelial cells in cancer patients (Mancuso *et al.*, 2014). Similarly to CD93, also CLEC14A was included in the top 20 genes of the proposed "tumour angiogenesis signature" from breast, renal and head and neck cancers (Masiero *et al.*, 2013). CLEC14A was identified, along with CD93, to be one of the protein upregulated during morphogenesis in a mass-spectrometry analysis of HUVEC cells in matrigel. Additionally, the upregulation of CLEC14A was found in blood vessels of two different spontaneous tumour models, pancreatic and ovarian (Zanivan *et al.*, 2013). Comparably to what was observed with CD93, CLEC14A was also downregulated in response to anti-VEGF therapy, supporting the pro-angiogenic role reported (Bais *et al.*, 2011).

Due to its limited expression to endothelial cells and the involvement of the other proteins of the family 14 in angiogenesis, Rho *et al*. have investigated the role of CLEC14A in angiogenesis. It has been reported that the CTLD of the protein was responsible for cell-cell interactions and that siRNA-mediated knockdown of CLEC14A reduced endothelial cell angiogenic activity in tube formation and wound healing assays (Rho *et al.*, 2011). Similar results have been independently confirmed by Mura and colleagues, who showed an inhibition of endothelial cells migration and tube formation in matrigel, both with a CLEC14A antisera and siRNA-mediated

knockdown (Mura *et al.*, 2012). Furthermore, CLEC14A gene has also been described to be upregulated by low shear stress. Reduced shear stress happens within misshaped vessels, which are usually a result of pathological angiogenesis. This corroborates the hypothesis that describes CLEC14A as tumour endothelial marker (TEM). It has been shown that applying 2 Pa laminar shear flow on HUVEC in culture reduced the expression of CLEC14A by more than 90% (Mura *et al.*, 2012).

To elucidate the possible role of the CTLD domain of CLEC14A in angiogenesis, Ki and colleagues generated by phage display cross-reacting anti-mouse/human CLEC14A[CTLD] antibodies. It has been demonstrated that these antibodies were able to inhibit cell migration and filopodia formation without affecting cell viability. Furthermore, a mechanism by which the binding on the CTLD impedes CTLD-CTLD interaction and causes internalisation of CLEC14A in HUVEC cells was suggested (Ki *et al.*, 2013). The effects of the CTLD domain of CLEC14A were found to be invalid by another study. In fact, it has been shown with that the absence of the CTLD domain impedes the localization at the cell membrane of the GFP-tagged protein used (Noy *et al.*, 2016). A recent report showed that the optimised version of the anti-CLEC14A[CTLD] antibody showed a strong anti-angiogenic effect in *in vitro* VEGF-dependent angiogenesis assays. The same results were confirmed in 4 different angiogenesis mouse models *in vivo*. Notably, it has been shown efficacy to inhibit angiogenesis in bevacizumab-resistant colorectal cancer cells (Kim *et al.*, 2018). Recently, HSP-70-1A was confirmed to interact with the CTLD of CLEC14A in HUVEC. This interaction has been shown to have importance for HSP-70-1A-mediated

angiogenesis by promoting CTLD mediated endothelial cell-cell contacts (Jang *et al.*, 2017).

CLEC14A was later demonstrated to have a role in sprouting angiogenesis both *in vitro* and *in vivo*. Furthermore, the loss of CLEC14A in mice resulted in a reduction in tumour growth, measured as volume and weight. Finally, it has been shown *in vitro* that the knockdown of CLEC14A reduced the number of cells at the tip position in a spheroid assay, suggesting the implication of CLEC14A in initiating the sprout and migration (Noy *et al.*, 2015). A more recent report showed a contrasting phenotype for the loss of CLEC14A in mice (CLEC14A$^{-/-}$). It has been shown that upon loss of CLEC14A mice presented excessive developmental angiogenesis and lymphangiogenesis, as well as pathological angiogenesis. It has been confirmed as in the previous study that CLEC14A knockout mice showed reduced tumour growth but it has been also observed earlier cancer-related death in subcutaneous tumour models. It has been proposed a mechanism by which CLEC14A interacts with VEGFR3 and indirectly regulates the expression and phosphorylation of VEGFR2. The loss of this interaction leads to impaired expression and phosphoactivation of VEGFR3 and the enhanced VEGFR2 expression, which results in increased vessel density and haemorrhages (Lee *et al.*, 2017). Although the tumour models employing CLEC14A knockout mice have provided similar results regarding tumour growth, the tumour microvasculature phenotypes and the sprouting phenotype were distinctly different in these reports (Noy *et al.*, 2015; Lee *et al.*, 2017). Further investigation is needed to clarify the differences observed in the two studies. Finally, according to the shedding mechanism of thrombomodulin, CLEC14A was found to be substrate of a rhomboid

protease. In particular, CLEC14A is specifically cleaved by RHBDL2. Further reports

indicate that soluble CLEC14A shows a role in regulating sprouting angiogenesis (Noy

et al., 2016).

1.8 Multimerin-2

Multimerin-2 is a high molecular weight protein (originally named EndoGlyx-1)

identified as the first endothelial specific protein, due to its restricted expression

pattern to normal and tumour blood vessels (Sanz-Moncasi *et al.*, 1994). It was

discovered because it was identified as the antigen of a monoclonal antibody (H572)

obtained immunizing mice with HUVEC. Multimerin-2 is an extracellular matrix

protein, which is expressed and secreted by endothelial cells and belongs to the

EMILIN family of glycoproteins together with multimerin-1, emilin 1 and 2

(Colombatti *et al.*, 2012). The EMILIN family of proteins is present only in

vertebrates. It is possible to identify in zebrafish two paralogues for each gene,

except for multimerin-1, which is absent (Mei and Gui, 2008). Furthermore, it is

possible to detect the same expression pattern for the paralogues mmrn2a and

mmrn2b of zebrafish as the expression observed in mouse (Milanetto *et al.*, 2008).

All the proteins in the family share a common structure, at the N-terminus they

present an EMI domain (with 7 cysteine residues regularly distributed) followed by a

long predicted coiled coil (CC) region of approximately 700 amino acids and at the C-

terminus a C1q domain. In between the CC and the C1q domain, MMRN2 presents

an highly charged region due to the presence of arginine, lysine, glutamate and

aspartate residues (Colombatti *et al.*, 2012). Furthermore, MMRN2 undergoes heavy

glycosylation and it has been predicted to have 11 sites for N-linked glycosylation and one site for O-linked glycosylation within the coiled coil domain. Further studies have confirmed that MMRN2 expression was restricted to endothelial cells based on both *in silico* and confirmed at the mRNA level with qRT-PCR in various different cell types (Herbert *et al.*, 2008). During development in mice MMRN2 is expressed in endothelial-specific manner and it is detectable in intersomitic and umbilical vessel at embryonic day 9.5. At embryonic day 14.5 it is possible to detect the expression of MMRN2 in blood vessels, spinal cord and heart (Leimeister *et al.*, 2002). Other proteomics studied identified MMRN2 as part of the secretome of HUVEC cells in static or oscillatory flow conditions (Tunica *et al.*, 2009; Burghoff and Schrader, 2011). It has been also identified as one of the most representative endothelial cell matrix protein and, along with other 127 proteins, they constitutes about the 90% of the whole HUVEC endothelial cell matrix (Zanivan *et al.*, 2013). An immunohistochemical (IHC) analysis confirmed the expression of MMRN2 (Endoglyx-1) confined in normal and tumor blood vessel endothelium, along with the "hot spots" of neoangiogenesis in melanoma section (Huber *et al.*, 2006). Furthermore, the extensive use of the monoclonal antibody H572 originally used for MMRN2 identification revealed its expression in blood vessels of both healthy thyroid or carcinomas (Koperek *et al.*, 2007). Taking advantage of the same antibody, it has been shown that MMRN2 is also expressed on the luminal side of the vessels and it can be found in tight juxtaposition with endothelial cells (Christian *et al.*, 2001). Not surprisingly, along with CLEC14A and CD93 also MMRN2 gene was identified as one of the "tumour angiogenesis signature" genes in renal and breast cancer (Masiero *et al.*, 2013). Similarly to what have been shown for CLEC14A, MMRN2 was found at

higher levels in the urines of low-grade bladder cancer patients (Ambrose *et al.*, 2015). Finally, it has been also reported that MMRN2 knockout mice are viable and display hypertension (Colombatti *et al.*, 2012). This might be due to the increased availability of VEGF-A in proximity of endothelial cells inducing proliferation and the formation of narrow vessels. Alternatively, the lack of this important extracellular matrix might reduce elasticity of the blood vessels.

1.8.1 MMRN2 biological roles and interactions

For many years from its discovery no functional studies on MMRN2 have been published. The first report on MMRN2 function suggests a possible role in regulating angiogenesis. Indeed, it has been shown that in presence of a VEGF-A stimulus *in vitro*, the concomitant presence of recombinant MMRN2 is able to greatly reduce processes such as cell migration, tube formation and sprouting, which are fundamental for angiogenesis. It has been reported that MMRN2 is able to directly bind VEGF-A impairing the phosphorylation of VEGFR2 and consequently the impaired phosphorylation of FAK (Lorenzon *et al.*, 2012). From this study it is possible to conclude that MMRN2 functions as an angiostatic molecule. A tumour mouse model, in which HT1080 cells stably transfected for overexpressing MMRN2 were injected in immunodeficient mice, has also supported these *in vitro* data. According to the model, MMRN2-overexpressing HT1080 tumours failed to form and vascularise, suggesting that MMRN2 was able to sequester VEGF-A from the environment, preventing the VEGF-A/VEGFR2 signalling. Furthermore, a more recent follow-up study clearly showed that the interaction between MMRN2 and VEGF-A

was strongly glycosylation-dependent. Impairing glycosylation of the recombinant MMRN2 strongly reduced but not completely abrogated the binding. It has been also shown that at a lower extent MMRN2 is also able to bind various related VEGF proteins, such as VEGF-C, VEGF-D and placental growth factor 1 (PlGF1) (Colladel *et al.*, 2016).

Although the angiostatic role of MMRN2 was extensively demonstrated, other studies have shown that MMRN2 can function as a mediator of angiogenesis and siRNA-mediated knockdown of MMRN2 impairs angiogenesis *in vitro* (Zanivan *et al.*, 2013; Noy *et al.*, 2015). These independent studies reported that upon MMRN2 siRNA knockdown sprouting as well as tube formation were impaired. Interestingly, Zanivan and colleagues identified MMRN2 as a binding partner of CLEC14A (Zanivan *et al.*, 2013). Independent findings supported the direct interaction between CLEC14A and MMRN2 (Noy *et al.*, 2016; Khan *et al.*, 2017). Functional characterization of the binding led to the conclusion that the interaction between CLEC14A and MMRN2 is important for mediating angiogenic stimuli. In fact, the disruption of CLEC14A/MMRN2 interaction by C4 (CRT4) blocking antibody, which binds CLEC14A in the same region as MMRN2, led to a reduction of tumour growth *in vivo* when C4 was injected in LLC tumour bearing mice. Interestingly, the phenotype observed in this model was recapitulating the phenotype observed in CLEC14A$^{-/-}$ mice (Noy *et al.*, 2015). It has also been hypothesized that the use of recombinant MMRN2 in Lorenzon *et al.* could support this model as it might not only sequester VEGF-A acting on VEGFR2 signalling but also disrupting the interaction between CLEC14A and MMRN2 present in the extracellular matrix (Lorenzon *et al.*,

2012; Noy *et al.*, 2015). Another finding supporting the possible use of MMRN2 as a decoy to block the binding is given by the experiment in which mouse MMRN2[495-678] fragment, which includes the binding site for CLEC14A but not the one for VEGF-A, expressed in LLC tumours subcutaneously injected in syngeneic mice led to a reduction in tumour growth (Colladel *et al.*, 2016; Khan *et al.*, 2017). Surprisingly, it has been also reported in the same study that CD93 is also able to bind MMRN2 and the binding site is the same as CLEC14A (Khan *et al.*, 2017). Moreover, MMRN2 is described as a bridge, which stabilises the interaction of HUVEC to fibroblasts (Figure 1.8). Indeed, CLEC14A and CD93 expressed on HUVEC bind to MMRN2 on the fragment 495-678, whereas CD248 expressed by fibroblast is able to bind MMRN2 in a different region (Khan *et al.*, 2017). The regions of binding are different from the one that is used to sequester VEGF-A, explaining in part why MMRN2 is described controversially as an angiostatic molecule or a pro-angiogenic molecule (Lorenzon *et al.*, 2012; Zanivan *et al.*, 2013; Noy *et al.*, 2015; Khan *et al.*, 2017). Subsequently, two different studies were published confirming the interaction of MMRN2 with CD93 and its importance for the angiogenic process. In particular, the first study focused on the interaction between CD93 and MMRN2 identifying the regions of CD93 that are involved in the binding with MMRN2 and in particular the residue F238 as key for the interaction (Galvagni *et al.*, 2017). Finally, it has been further confirmed that CD93 and MMRN2 interact and co-localise within the tumour endothelium. Furthermore, it has been proposed a model that defines MMRN2 as fundamental for the stabilization of CD93 at the migratory front as well as at the extremity of the filopodia. Notably, in absence of MMRN2 the cleavage of CD93 is strongly upregulated (Lugano, Dejana and Dimberg, 2018). The interaction between CD93
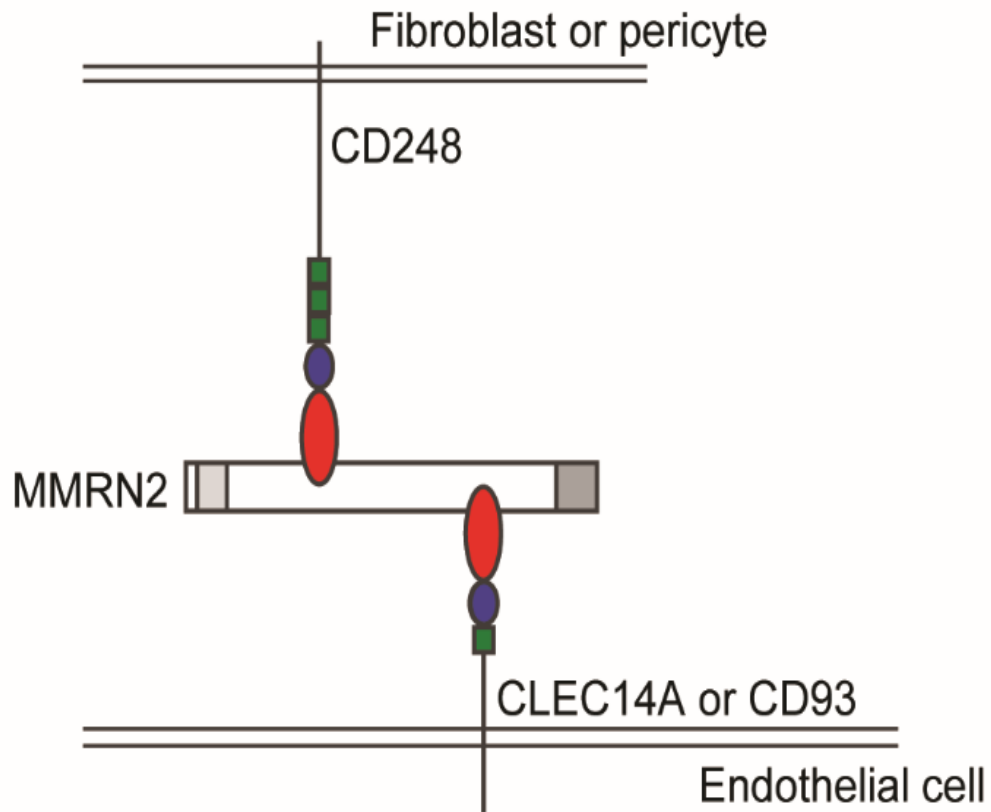
(adapted from Khan et al., 2017)

Figure 1.8 MMRN2 and the CTLD family 14

Schematic representation of the newly described MMRN2 interactions at the interface of Endothelial cell and either Fibroblast or Pericyte, by binding C-type lectin domain family 14 proteins (CLEC14, CD93 and CD248).

and MMRN2 is indispensable for the correct interaction and activation of integrin β1, regulating the fibronectin fibers deposition upon angiogenic stimuli (Lugano, Dejana and Dimberg, 2018). Data from high-grade (IV grade) human glioma samples confirmed that the interaction of CD93 and MMRN2 along with integrin β1 is necessary for the correct deposition of fibronectin. Implanted GL261 brain tumours in CD93$^{-/-}$ mice showed the lack of structure within the fibronectin fibrillary networks during angiogenesis. The phenotype recapitulates what has been shown *in vitro* assays.

1.9 Hypothesis and aims

CLEC14A and CD93 are two members of the C-type lectin domain family 14, which are both capable of interacting with the extracellular matrix protein MMRN2 (Zanivan *et al.*, 2013; Galvagni *et al.*, 2017; Khan *et al.*, 2017; Lugano, Dejana and Dimberg, 2018). Mapping the binding site on MMRN2 showed that CLEC14A and CD93 also share the same binding region (Khan *et al.*, 2017). Moreover, these two proteins have been reported to be involved in tumour angiogenesis and, interestingly, CLEC14A was also described as a tumour endothelial marker, because of its high expression on tumour endothelium compared to low expression on healthy endothelium.

Hypothesis 1: CLEC14A and CD93 have similar domain structure, binding partners and reported roles in angiogenesis. It is plausible that CLEC14A and CD93 are redundant proteins in angiogenesis, and lack of one can be compensated by the other.

Aim 1: To investigate the relative roles of CLEC14A and CD93 in their regulation of processes critical to angiogenesis.

Hypothesis 2: CLEC14A is a good target for developing anti-vascular targeting strategies. The MMRN2 binding fragment could be exploited to develop anti-tumour endothelial agents.

Aim 2: Exploit the tight binding of the MMRN2 fragment to CLEC14A in tumour endothelial targeting or blocking tumour angiogenesis by multiple approaches; engineered Chimeric Antigen Receptor (CAR) T cells, vaccination utilizing the CLEC14A and CD93 binding fragment mMMRN2$^{495-678}$-hFc and mMMRN2$^{495-678}$-Dianthin toxin conjugates.

CHAPTER 2: Material and Methods

2. Material and Methods

2.1 Reagents

2.1.1 Commonly used solutions

Phosphate Buffered Saline (PBS)	140 mM NaCl, 10 mM Na_2HPO_4, 2.7 mM KCl and 1.76 mM KH_2PO_4, pH 7.4
Phosphate Buffered Saline Tween (PBS-T)	140 mM NaCl, 10 mM Na_2HPO_4, 2.7 mM KCl and 1.76 mM KH_2PO_4, pH 7.4, 0.1% (v/v) TWEEN-20
Tris-acetate-EDTA (TAE)	40 mM Tris, 20mM acetic acid, 1 mM EDTA
Reducing 6x SDS-PAGE sample buffer	375 mM Tris-HCl pH 6.8, 6% (w/v) SDS, 48% (v/v) glycerol, 0.03% (w/v) bromophenol blue, 9% (v/v) β-mercaptoethanol
Non-reducing 6x SDS-PAGE sample buffer	375 mM Tris-HCl pH 6.8, 6% (w/v) SDS, 48% (v/v) glycerol, 0.03% (w/v) bromophenol blue
Stacking gel buffer	125 mM Tris-HCl pH 6.8, 0.1% (w/v) SDS
Resolving gel buffer	375 mM Tris-HCl pH 8.8, 0.1% (w/v) SDS
Running buffer SDS-PAGE	25 mM Tris, 250 mM glycine, 0.1% (w/v) SDS. pH 8.3
Transfer buffer Western blot	25 mM Tris, 187.2 mM glycine, 20% (v/v) methanol
NP40 Lysis Buffer	1% (v/v) NP40, 10 mM Tris pH7.5, 150 mM NaCl and 1 mM EDTA with complete protease inhibitor cocktail (Roche # 11836153001).
Stripping buffer	0.1 M sodium hydroxide (NaOH) or 62.5 mM Tris-HCl pH 6.8, 2% (w/v) SDS, 100 µM β-mercaptoethanol
Flow cytometry buffer	PBS with 0.2% (w/v) BSA and 0.02% (w/v) sodium azide
FACS buffer (MACS)	0.5-1% FCS or BSA and 1-2 mM EDTA in PBS
Phosphatase Inhibitor Cocktail	75 mM NaF, 15 mM Na_3VO_4, 150 mM Na β-glycero phosphate, 15 mM EDTA and 75 mM Na pyrophosphate
Blocking Buffer (IF)	PBS, 3% (w/v) BSA, 10% (v/v) FCS, 0.1% (v/v) TWEEN 20, 0.01% (w/v) sodium azide

Coating Buffer (IFNY ELISA)	0.1 M Na_2HPO_4, adjusted to pH 9 with 0.1 M NaH_2PO_4
Blocking Buffer (IFNY ELISA)	1% (w/v) BSA/PBS filtered and then Tween added (50 l/100ml)
Wash Buffer (IFNY ELISA)	PBS/0.05% (v/v) Tween (0.5 ml in 1 litre)
Stopping Buffer (IFNY ELISA)	1 M Phosphoric Acid
Equilibration Buffer (Protein A column)	20 mM Na_2HPO_4 pH 7.0
Elution Buffer (Protein A column	100 mM NaCitrate pH 3.0
Equilibration Buffer (Ni-NTA Column)	PBS with 0.5M NaCl and 10mM imidazole
Elution Buffer (Ni-NTA Column)	PBS with 0.5M NaCl and 250 mM imidazole
Regeneration Buffer (Ni-NTA column)	PBS with 0.5M NaCl
MACS Buffer	PBS with 0.5% (w/v) BSA and 2.5 mM Ethylenediaminetetraacetic acid

Table 2.1 Commonly used reagents and their composition

2.1.2 Primary Antibodies

Antibody	Manufacturer & Catalogue	Species raised in	Application (Concentration or dilution)
CLEC14A polyclonal	R&D (#AF4968)	Sheep	WB (0.1 µg/mL)
MMRN2 polyclonal	Abnova (#H00079812-B01P)	Mouse	WB (2 µg/mL) IF (4 µg/mL)
Polyhistidine tag monoclonal (CLONE AD1.1.10)	R&D (#MAB050)	Mouse	WB (1 µg/mL) ELISA (2 µg/mL)

α-Tubulin monoclonal (CLONE DM1A)	Sigma-Aldrich (#T6199)	Mouse	WB (0.5 µg/mL)
Human IgG Fc specific HRP conjugate	Sigma-Aldrich (#A0170)	Goat	WB (1:2500)
CD93 monoclonal (clone R139)	eBioscience (#14-0939-82)	Mouse	FC (20 µg/mL)
CD93 polyclonal	R&D (#AF2379)	Goat	WB (0.1 µg/mL)
CLEC14A monoclonal (clone CRT2)	N/A – produced in laboratory	Mouse	FC (20 µg/mL)
CLEC14A monoclonal (clone CRT4)	N/A – produced in laboratory	Mouse	FC (20 µg/mL)
EEA1	BD Biosciences	Mouse	IF (1.25 µg/mL)
GFP tag monoclonal (Clone 3E1)	Cancer Research UK	Mouse	WB (1:500)
Anti-mouse CD31 (Clone MEC 13.3)	BD Bioscience (#565629)	Rat	IF (1:200) (75 ng/mL)
Anti-human CD31 monoclonal (Clone JC70A)	Dako (#M0823)	Mouse	IHC (1.29 µg/mL)

Table 2.2 Primary antibodies

List of primary antibodies used, including the provider, the species in which they were raised and the concentrations for the specific applications: Immunofluorescence (IF), Immunohistochemistry (IHC) and western blot (WB).

2.1.3 Secondary Antibodies

Antibody	Manufacturer & Catalogue	Species raised in	Application (Concentration or dilution)
Anti-mouse alkaline phosphatase (AP)	Sigma-Aldrich (#A4656)	Goat	IHC (1:500)
Anti-mouse HRP	Dako (#P0447)	Goat	WB (1:5000) ELISA (1:5000)
Anti-rabbit HRP	GE Healthcare (#NA9340V)	Donkey	WB (1:5000)
Anti-goat HRP	Dako (#P0449)	Rabbit	WB (1:5000)
Anti-sheep HRP	R&D (#HAF016)	Donkey	WB (1:5000)
Anti-human HRP	R&D (#A0170)	Goat	WB (1:2000) ELISA (1:2500)
Anti-human IgG (H+L) Alexa633	Thermo Scientific (A-21091)	Goat	IF (2 µg/mL) FC (4 µg/mL)
Anti-mouse IgG (H+L) Alexa633	Thermo Scientific (A-21052)	Goat	IF (2 µg/mL) FC (4 µg/mL)
Anti-human IgG (H+L) Alexa488	Thermo Scientific (A-11013)	Goat	IF (2 µg/mL) FC (4 µg/mL)
Anti-mouse IgG (H+L) Alexa488	Thermo Scientific (A-11001)	Goat	IF (2 µg/mL) FC (4 µg/mL)
Anti-rat IgG (H+L) Alexa488	Thermo Scientific (A-11006)	Goat	IF (2 µg/mL) FC (4 µg/mL)
Anti-mouse IgG (H+L) Alexa647	Thermo Scientific (A-21235)	Goat	IF (2 µg/mL) FC (4 µg/mL)
Anti-human FITC	Sigma-Aldrich (#F9512)	Goat	FC (1:100) IF (1:500)

Table 2.3 Secondary antibodies

List of secondary antibodies used, including the provider, the species in which they were raised and the concentrations (or dilution) for the specific applications: Immunofluorescence (IF), Immunohistochemistry (IHC), western blot (WB) and enzyme-linked immunosorbent assay (ELISA).

2.1.4 Recombinant Proteins

Protein	Epitope Tags	Expression system	Application (concentration)
Human CLEC14A^{ECD}-hFc	Human IgG1 Fc	HEK293T	ELISA (0.1-10 µg/mL)
Mouse CLEC14A^{ECD}-hFc	Human IgG1 Fc	HEK293T	ELISA (0.1-10 µg/mL)
Human MMRN2$^{495-674}$-hFc	Human IgG1 Fc	HEK293T	FC (20 µg/mL)
Mouse MMRN2$^{495-678}$-hFc	Human IgG1 Fc	HEK293T	FC (20 µg/mL) Vaccine (50µg/mL) IF (5 µg/mL)
Mouse MMRN2$^{495-678}$-His	His tag	HEK293T	ELISA (10 µg/mL)

Table 2.4 Recombinant proteins

List of recombinant proteins produced, specifying the tag, the expression system and the concentration for each specific application: Flow cytometry (FC), immunofluorescence (IF), enzyme-linked immunosorbent assay (ELISA) and vaccination.

2.2 Molecular Biology

2.2.1 Oligonucleotides

Oligonucleotides were purchased from Eurogentec as a lyophilised powder. Upon arrival, they were dissolved in nuclease-free water to obtain a concentration of 100mM as a stock solution. They were stored at -20°C.

Name Oligonucleotides	Sequence
EGFPN1 **R**	CGTCGCCGTCCAGCTCGACCAG
EF1α Promoter **F**	TCAAGCCTCAGACAGTGGTTC
IRES **R**	CCTCACATTGCCAAAAGACG
T7 Promoter **F**	TAATACGACTCACTATAGGG
pET11d **F**	GAGATCTCGATCCCGCGAAA
pET11d **R**	GGTTCCGCGCACATTTCCC
pET11d **F 2**	GCGGCCACAGCATACACATT

Table 2.5 Sequencing primers

List of oligonucleotides used in sequencing reactions, displayed in the form 5'-3'.

N°	Name Oligonucleotides	Sequence
1	mMMRN2$^{495-678}$ for fusion with hFc (Gibson) **F**	ACTAGCCTCGAGGTTTAAACATGAGGCCAGCGCTTGCC
2	mMMRN2$^{495-678}$ for fusion with hFc (Gibson) **R**	GATGAAGAACCCAACTGTGGGTGCTGCTCC
3	hFc fragment for mMMRN2$^{495-678}$-hFc (Gibson) **F**	CACAGTTGGGTTCTTCATCGAGTGAG
4	hFc fragment for mMMRN2$^{495-678}$-hFc (Gibson) **R**	CTGCAGCCCGTAGTTTAAACTCATTTACCCGGAGACAG
5	mMMRN2$^{495-678}$-His (Gibson) **F**	ACTAGCCTCGAGGTTTAAACATGAGGCCAGCGCTTGCC
6	mMMRN2$^{495-678}$-His (Gibson) **R**	CTGCAGCCCGTAGTTTAAACTAGTGGTGGTGGTGGTGGTGCAACTGTGGGTGCTGCTCC
7	HisMMRN2$^{495-678}$ **F**	ACTTTAAGAAGGAGATATACCATGGGACACCACCACCACCACCACATGCAGAAGCTCTATTTAGACCTGGA
8	HisMMRN2$^{495-678}$ **R**	TGGCCGCGGCCATCGGCCGCGGGGGCTCCGA
9	Dianthin **F**	CCCGCGGCCGATGGCCGCGGCCACAGCATAC
10	Dianthin **R**	GAGGCCCTTTCGTCTTCAAGAATTCTTACTTCGGTCTACCTAAATACTTAAGGAGCCC
11	HisDianthin **F**	ACTTTAAGAAGGAGATATACCATGGGACATCATCATCATC
12	HisDianthin **R**	GCTTCTGCATCTTCGGTCTACCTAAATAC
13	MMRN2$^{495-678}$ **F**	TAGACCGAAGATGCAGAAGCTCTATTTAGACCTGGACGTCATCC

14	MMRN2$^{495-678}$ **R**	GAGGCCCTTTCGTCTTCAAGAATTCTTACGGCCGCGG GGGCTC
15	hMMRN2$^{495-674}$ for CAR construct **F**	GTTTCCATCTATGGCATCGATGCAGAAGCTCTATTTAG ACCTGGACGTCATCCGGGAGGG
16	hMMRN2$^{495-674}$ for CAR construct **R**	GATACATAACTTCAATTGCGGCCGCTGCCGGCCGCGG GGGCTC
17	mMMRN2$^{495-678}$ for CAR construct **F**	GTTTCCATCTATGGCATCGATGAGGCCAGCGCTTGCC
18	mMMRN2$^{495-678}$ for CAR construct **R**	GATACATAACTTCAATTGCGGCCGCTGCCAACTGTGG GTGCTG

Table 2.6 Oligonucleotides used for plasmid construction.

List of the respective forward (F) and reverse (R) oligonucleotide sequences for each amplification. The sequences are 5'-3'.

2.2.2 Plasmids

Plasmids were cloned using two different strategies: either digestion with restriction enzymes and ligation reactions or using the GIBSON assembly reaction kit (New England Biolabs).

Plasmid	Restriction sites	Number of the oligo (Ref. Table 2.6)
mMMRN2$^{495-678}$-hFc in pWPI	PmeI	1 /2 and 3/4
mMMRN2$^{495-678}$-His in pWPI	PmeI	5/6
HisMMRN2$^{495-678}$Dianthin in pET11d	NcoI and EcoRI	7/8 and 9/10
His Dianthin MMRN2$^{495-678}$ in pET11d	NcoI and EcoRI	11/12 and 13/14
hMMRN2 CAR in MP71	ClaI and NotI	15/16
mMMRN2 CAR in MP71	ClaI and NotI	17/18
hCLEC14A^{ECD}-hFc in pWPI	PmeI	N/A

(previously generated)		
mCLEC14A^{ECD}-hFc in pWPI (previously generated)	PmeI	N/A
hMMRN2$^{495-674}$ in pAvitag Kabir Khan, Thesis 2016)	AgeI and KpnI	N/A
hCLEC14A^{FL} in pEGFPN1 (Kabir Khan, Thesis 2016)	EcoRI	N/A
hCD93^{FL} in pEGFPN1 (Kabir Khan, Thesis 2016)	EcoRI	N/A
hCLEC14A^{C103S} in pEGFPN1 (Kabir Khan, Thesis 2016)	EcoRI	N/A
hCD93^{C104S} in pEGFPN1 (Kabir Khan, Thesis 2016)	EcoRI	N/A

Table 2.7 Plasmids

List of the plasmids generated and/or used, indicating the restriction sites used for the linearization of the vector and, when applicable, the oligonucleotides used in the amplification of the insert(s).
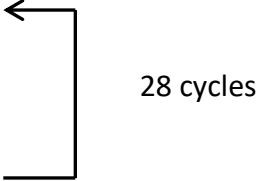
2.2.3 Polymerase chain reaction (PCR)

Polymerase chain reactions were assembled mixing the specific forward and reverse primers and the appropriate DNA template, either an IMAGE clone or a previously cloned plasmid. The matched primers used in these amplifications are listed in Table 2.6. The enzyme employed in this reaction was the proofreading DNA polymerase Phusion (New England Biolabs). The typical PCR mix was as it follows:

Template DNA	<250 ng
5X Phusion HF or GC Buffer	1X
10 mM dNTPs	200 µM
10 µM Forward Primer	0.5 µM

10μM Reverse Primer	0.5 μM
DMSO	3% (v/v)
Phusion Enzyme	1unit (50 μL reaction)
Nuclease-free Water	To 50 μL

PCR was carried out as follows, with annealing temperatures calculated according to the NEB Phusion annealing temperature calculation program.

Initial denaturation	98°C	30 Seconds
Denaturation	98°C	20 Seconds
Annealing	- - °C	30 Seconds
Extension	72°C	30 Seconds/Kb
Final extension	72°C	7 minutes

28 cycles

2.2.4 Restriction Enzyme digest

Restriction enzymes were selected appropriate to the cloning design and they were all from NEB. DNA digestions were according to the manufacturer's protocol and they were incubated for a minimum of 1 hour up to overnight incubation.

2.2.5 DNA agarose gel electrophoresis

Agarose gels were made dissolving by molecular biology grade agarose (Bioline) in TAE buffer with SYBR Safe DNA gel stain (Invitrogen). The standard percentage of gel used was 1% (w/v); higher percentages were used on occasion if an increased

resolution was needed. At each run, samples were mixed with 6x loading dye (Thermo scientific) and loaded into agarose gels along with Generuler 1kb DNA ladder (Thermo Scientific). After a run of 30 minutes at 100 V, gels were visualised using a UV transilluminator (SynGene).

2.2.6 DNA gel extraction

Agarose gels were also used to purify DNA of interest (e.g. digested DNA) for molecular biology purposes. After visualising the band with the UV transilluminator, the DNA was excised with a scalpel and extracted from the gel according to the protocols of the GeneJet gel purification kit (Thermo scientific).

2.2.7 Gibson cloning

The primers used to amplify the fragment of interest by PCR for each cloning experiment in the PCR reactions were designed using the NEBuilder tool on the NEB website. The amplicons were carrying homologous sequences at their ends to either the digested vector or to the other fragments. The homologues ends were at least of 18 nucleotides on each PCR product. All the Gibson reactions were assembled keeping at ratio of 1:3 linearised vector:Insert(s) and the 2x Gibson reaction master mix (New England Biolabs #E5510S). The reactions were incubated for 1 hour at 50°C; subsequently, they were cooled at 4°C and then transformed into competent *E. coli*.

2.2.8 Transformations

Transformations were carried out adding a plasmid or a Gibson reaction mix in 20 μL aliquots of competent bronze or gold efficiency DH5α *E. coli* (Bioline) thawed on ice. The mix was left incubating on ice for 30 minutes, heat-shocked at 42°C in a thermo-block for 30 seconds and incubated an additional 2 minutes on ice. Afterwards, 950 μL of SOC media was added and incubated at 37°C in a shaking incubator for at least 1 hour. Finally, the transformation mix was spread on pre-warmed LB agar plates containing the appropriate selection antibiotic and incubated at 37°C overnight.

2.2.9 Plasmid DNA isolation

Following transformation, single colonies were picked and inoculated into 5 ml (or larger volumes for a maxi prep) of LB media containing antibiotics, either Ampicillin 100 μg/ml or Kanamycin 50 μg/ml, appropriate to the resistance gene carried by the plasmid. These cultures were incubated approximately 16 hours in an orbital shaker (180 rpm) at 37°C. Cultures were centrifuged at maximum speed (13,000 rpm) and plasmid DNA was isolated according to the manufacturer's instruction for either GeneJET plasmid mini prep (Thermo Scientific) or maxi prep (Thermo Scientific) kits. DNA concentrations were measured by Nanodrop (Thermo Scientific) reading.

2.2.10 Sequencing

DNA was sequenced using Sanger sequencing performed by the Functional Genomics Service (University of Birmingham). Oligonucleotides for sequencing are listed in table 2.5.

2.2.11 RNA extraction

RNA was purified from HUVEC or HEK293T cells using the RNeasy Mini Kit (Qiagen), following the manufacturer's instructions. Briefly, a confluent well of a 6-well plate was harvested as described in section 2.3.1 and centrifuged at 1100 rpm for 5 minutes. The pellet was resuspended in 350 μL of RLT buffer with β-mercaptoethanol (1:100). An equal volume of 70% (v/v) ethanol was added to the lysate and mixed well by pipetting. The sample was then transferred into an RNeasy Mini spin column and centrifuged at maximum speed (13000 rpm) for 1 minute. The flow-through was discarded. In sequence, 700 μL of RW1 buffer and 2 times 500 μL of RPE buffer were added and centrifuged as previously for 1 minute, discarding the flow-through. Before the elution, each sample was then centrifuged empty at maximum speed for 1 minute to dry the membranes of the column. The spin columns were then transferred into a clean tube and RNA was eluted in 30-50 μL of RNase-free water at maximum speed for more than a minute. RNA was subsequently stored at -80°C.

2.2.12 Reverse Transcription

cDNA was obtained using the High Capacity cDNA Reverse Transcription Kit (Applied Biosystems), following the manufacturer's instructions. The following mix was assembled:

Component	Volume/Reaction
RNA template	2 µg in a total volume of 10 µL
10x RT Buffer	2 µL
25x dNTP Mix (100 mM)	0.8 µL
10x RT Random Primers	2.0 uL
MultiScribe Reverse Transcriptase	1.0 µL
RNase Inhibitor	1.0 µL
Nuclease-free H$_2$O	4.2 µL
Total Volume	**20 µL**

The mix was then loaded into a thermo mixer and kept at 25°C for 10 minutes, at 37°C for 2 hours and finally at 85°C for 5 minutes. Transcribed cDNA was then stored at -20°C.

2.2.13 qPCR

cDNA obtained from the reverse transcription was employed in qPCR reactions at 1/20 dilution. Probe based qPCR was done using the Roche universal probe library and the oligonucleotides were designed using the dedicated web tool. (https://lifescience.roche.com/en_it/brands/universal-probelibrary.html#assay-design-center). Alternatively, SyBRGreen was used.

Primers for qPCR	Sequence
Actin **F**	TCACCCACACTGTGCCCA TCTACGA
Actin **R**	CAGCGGAACCGCTCATTGCCAATGG
CLEC14A **F**	CTGGGACCGAGGTGAGTG
CLEC14A **R**	CGCGATGCAAGTAACTGAGA
CD93 **F**	GCCCCAGAATGCGGCAGACA
CD93 **R**	GCAGTCTGTCCCAGGTGTCGGA
MMRN2 **F**	AGGCTTCCAGTACTAGCCTCTCT
MMRN2 **R**	GGTAGGGGCACCAGTTACG

Table 2.8 Primers used in qPCR

Primers used in qPCR reactions displayed 5'-3'.

2.3 Cell Culture

Cell culture was carried out in sterile conditions in a laminar flow hood. Dulbecco's modified Eagle's medium (DMEM) (Sigma-Aldrich, Gillingham UK) was used to culture most of the adherent mammalian cell lines, with 10% (v/v) foetal calf serum (FCS) (GIBCO Life Technologies), 4 mM L-glutamine (Life Technologies), 100 U/ml penicillin and 100 μg/ml streptomycin (Life Technologies). Primary HUVEC cells were cultured in Endothelial Basal Medium-2 (EBM-2, Lonza), with all the growth factors included in the BulletKit (Lonza). Human T-cells were cultured in Iscove's modified Dulbecco's medium (IMDM) or Roswell Park Memorial Institute medium (RPMI) (Sigma) containing 10% (v/v) FCS, Interleukin 2 (100 IU/ml), 2mM L-Glutamine, Penicillin (100 IU/ml) and Streptomycin (100 μg/ml), named T cell medium (TCM). T-Cell ELISAs were performed in RPMI (Sigma) containing 10 (v/v) Fetal Bovine Serum (FBS), L-Glutamine 2mM, Streptomycin (100 mg/ml), Penicillin (100 IU/ml) and Interleukin 2 (50 IU/ml).

Cell Type	Cell source	Media
HEK293T	Human embryonic Kidney	cDMEM
Phoenix^TM Ampho Cell line (Virus for Human T cells)	Human embryonic kidney line transformed with adenovirus E1a and carrying a temperature sensitive T antigen co-selected with neomycin. They contain Gag-pol and an amphotropic envelop, specific for infection of mammalian cells	cDMEM

Phoenix™ Eco Cell line – (Virus for Mouse T cells)	Human embryonic kidney line transformed with adenovirus E1a and carrying a temperature sensitive T antigen co-selected with neomycin. They contains Gag-pol and an Ecotropic envelope, specific for infection of mouse and rat cells	cDMEM
HUVEC	Human umbilical vein endothelial cells (Lonza)	EBM-2 BulletKit
Human T cell	Adult peripheral blood mononuclear cells (PBMCs) from apheresis cones	TCM
Mouse T cell	Splenocytes from mice	TCM
Splenocytes	Isolated from immunised mice	cRPMI
NSO	Monoclonal antibody production unit	cRPMI

Table 2.9 List of cells and culture conditions

2.3.1 Cell release by exposure to trypsin

Media was removed and cells were washed with sterile PBS (Sigma). After the wash, cells were incubated with 1x Trypsin/EDTA (Gibco) at 37°C. Detached cells were collected in 10 ml of medium containing serum and centrifuged at 1100 rpm for 5 minutes.

2.3.2 HUVEC cell culture

Before thawing or detaching HUVECs (Lonza), new culture plates were covered and incubated at 37°C for 5min with 0.1% (w/v) porcine gelatin in PBS (Sigma). After removing the gelatine, $3x10^5$ cells were seeded in 10mL of the medium EBM-2 medium. Cells were cultured to passage 6 and used in assays at passage 3 or 4.

2.3.3 siRNA transfections

Small interfering RNA (siRNA) duplexes were either pre-designed by Life Technology website and then tested or based on published methods and ordered from Eurogentec. All duplexes were supplied at the stock concentration of 100 µM and stored in aliquots at -80°C.

Target gene and duplex number	Sequence	Supplier
CLEC14A D1	GAACAAGACAAUUCAGUAA	Eurogentec
CLEC14A D2	CAAUCAGGGUCGACGAGAA	Eurogentec
CD93 D1	CTGCGACAGCTTGTGCTTCAA	Eurogentec
CD93 D2	CCGGAACTCGTGCATCTCCAA	Eurogentec
MMRN2 D1	CUUACUAGCUCUUUGCAAA	Life technologies
MMRN2 D2	GAGACUUUCGAUCAGAUUA	Life technologies

Table 2.10 List of siRNA duplexes, sequences and suppliers

2.3.4 Transfection of siRNA duplexes to reduce gene expression

10^6 HUVEC cells were seeded on a gelatine-coated 10 cm plate. On the following day, duplexes were diluted to a working solution of 20 µM. For each gene to knockdown, 10 µL of diluted siRNA was added to 670 µL of optiMEM (Invitrogen #31985-047). 12 µL of RNAi MAX Lipofectamine (Invitrogen #13778-150) was added to 108 µL of optiMEM to give a final concentration of Lipofectamine of 0.3% (v/v). The two solutions were incubated at room temperature for 10 minutes, and then mixed, flicked and incubated for an additional 10 minutes. Cells were washed twice with PBS and cultured in 3.2 mL of optiMEM. At the end of the incubation, the 800 µL of Lipofectamine/siRNA solution was added to the cells. The final concentration of the siRNA in this mix was 50 nM. After 4 hours of incubation at 37°C, the medium was replaced with complete EMB2 medium without antibiotics. Cells were than used for experiments after 48h. The protocol was adjusted for either smaller or larger scales accordingly to the number of transfected cells needed.

2.3.5 PEI Plasmid transfections

Plasmids were transfected into HEK293T cells by use of polyethylenimine (PEI) (Sigma-Aldrich #408727), using 1:4 ratio of DNA:PEI.

The day before transfection, $3x10^6$ HEK293 cells were plated in a 10 cm plate in DMEM. On the day of transfection 9 µg of DNA were resuspended in 1 mL of optiMEM, flicked and supplemented with 12 µL PEI stock solution. The solution

DNA/PEI was gently vortexed and left for 10 min at room temperature. At the end of the incubation the solution was added to the HEK293T cells.

2.3.6 Lentiviral transduction

HEK293T cells were PEI transfected using 4.39 µg of transfer vector (target gene), 3.29 µg of packaging vector (PsPAX2) and 1.32 µg of envelope vector (PMD2G). The number of plates required for the transfection was calculated based on the amount of virus required for transducing the target cells. The cells were allowed to generate virus for 24 hours. The virus-containing medium was then supplemented with 0.8% (v/v) of 8 µg/mL Polybrene, filtered through a 0.45µm syringe filter, and concentrated in a Corning Spin-X UF concentrator that had a 5 kDa molecular weight cut off (Sigma-Aldrich #CLS431487). This was then added to 10^6 of target cells for 48 hours. Target genes were cloned into a pWPI plasmid, which contained an internal ribosome entry site (IRES), followed by a gene for GFP downstream of the cloning site. Constructs of this type allowed translation of the target and the GFP gene from a single mRNA. The presence of translation of the GFP allowed assessment of the transduction efficiency by flow cytometry. In cases where the transduction efficiency was low, the GFP positive population was isolated by FACS sorting, to obtain a purer population of cells expressing the target gene.

2.3.7 Fluorescence-activated cell sorting

Cells were detached, counted and resuspended at a concentration of $2x10^6$/mL in MACS buffer (0.5-1% (v/v) FCS or (w/v) BSA and 1-2 mM EDTA in PBS). Sorting was carried out by the Flow Cytometry and Sorting Facility of the University of Birmingham and a sterile GFP positive population was collected in 20% (v/v) FCS DMEM. Cells were then plated and amplified.

2.3.8 Matrigel assay

Matrigel (Corning® Matrigel® Growth Factor Reduced (GFR) Basement Membrane Matrix) was thawed overnight at 4°C on ice. PBS was used to wet the entire surface of each well of a 12-well plate and then aspirated. 70 μL of Matrigel was added to each well, and incubated at 37°C for 15 minutes to solidify. HUVEC cells were detached, counted and plated $1.4x10^5$ in each well. The plate was incubated for 24 hours at 37°C in the IncuCyte®. IncuCyte allowed monitoring of tube formation every 6 hours by taking pictures in 9 areas of each well. The number of meshes was calculated by the ImageJ plugin. "angiogenesis analyser". (http://image.bio.methods.free.fr/ImageJ/?Angiogenesis-Analyzer-for-ImageJ).

Meshes are areas enclosed by segments or master segments within the network form by endothelial cells on matrigel.

2.3.9 MTT assay

Proliferation was determined using a CellTiter 96® Non-radioactive Cell Proliferation Kit (Promega, G4000) according to the manufacturer's instructions. Briefly, HUVEC under different treatments were seeded sub-confluently in triplicate in 100 µL of EBM-2 and left for 24 hours at 37°C in the incubator. The following day, each well was supplemented with 15 µL of Dye solution and incubated for 4 hours at 37°C. Living cells convert the MTT tetrazolium component of the Dye solution into a formazan product, which results in colour formation. At the end of the incubation, 100 µL of stop solution were added and the absorbance at 570nm recorded on Bio-tek Synergy HT Multi-Detection Microplate Reader.

2.3.10 Chemotaxis assay

HUVEC cells were incubated in serum-free EBM2 medium for 1 hour. Meanwhile, sterile FluoroBloks HTS 24 Well Plate Cell Culture Insert with 8.0 µm High Density PET Membrane (Corning) were transferred to a 24-well plate and coated with 0.1% (w/v) gelatin in PBS for 30 minutes at 37°C. Cells were then detached, counted and seeded $3x10^4$ cells/well in 300 µl of serum-free media. Each insert was then placed in a well containing complete EBM-2 media and cells were left to migrate for 5 hours at 37°C. Inserts were washed gently with PBS and fixed in 4% (w/v) PFA. Membranes from each insert were then carefully cut out and mounted between two glass slides using DAPI mounting media. The lower part of the membrane was imaged at 10X magnification and nuclei were counted in 9 different fields of view.

2.3.11 Co-Culture Assay

3×10^4 human dermal fibroblasts were plated in each well of a 12 well plate in 1mL of complete DMEM. Four days later, the medium was replaced. On the same day HUVEC cells were transfected with siRNAs according to the protocol mentioned in 2.3.3. The following day 3×10^4 of HUVEC cells were plated in each well on top of the fibroblast monolayer in 1 mL of EMB-2 media. On the 7th and 9th day, medium was replaced and on the 11th day the tubules that HUVEC formed were immunostained.

Media was removed and the co-culture was washed with 1 mL of PBS and fixed with 1 mL of 70% (v/v) -20°C-cold ethanol for 30 minutes at room temperature. Ethanol was removed, the tubules were washed twice with PBS and incubated with anti-human CD31 (Dako, mouse monoclonal, clone JC70A) at 1.29 µg/mL diluted in 400 µL in 1% (w/v) BSA in PBS at 37°C for 40-60 minutes. The plate was washed gently 3 times with PBS and incubated with anti-mouse IgG (whole molecule)-Alkaline Phosphatase (goat polyclonal, Sigma A4656) diluted to 1:500 in 400 µL in 1% (w/v) BSA in PBS at 37°C for 40-60 minutes. Plates were washed 2 times with PBS and 3 times with water before incubating with 500 µL of SigmaFAST BCIP/NBT substrate (Sigma, B5655-25TAB) dissolved in H_2O. The reaction was finally stopped with 1ml of H_2O and the plates were left to dry in the dark at room temperature. Images were taken at 1.6x magnification using the MZ16 Leica microscope and analysed using the Angio Sys analysis software (TCS Cell Works).

2.3.12 Cell monolayer wound healing assay

HUVEC cells were plated in a 96-well plate (Essen BioScience) at 1×10^4 cells/well. The following day they were transfected with siRNA as described above 2.3.3. After 48 hours the monolayers of transfected HUVEC cells were scratch wounded using a 96-well plate scratcher (Essen BioScience). Plates were incubated in an Incucyte (Essen BioScience) and images were taken every 6 hours to document the closure of the wound. The area of closure was measured with ImageJ.

2.3.13 Human T cell culture

Human-T cells were obtained isolating from adult peripheral blood mononuclear cells (PBMCs) from apheresis cones (Blood Donor Centre), using lymphoprep (StemCell). Subsequently, cells were resuspended in T cell media (TCM) at a density of 1×10^6 cells/ml. PBMCs were activated by adding anti-CD3 (OKT3) (eBiosciences), anti-CD28 (Invitrogen) antibodies at a concentration of 30 ng/ml and IL2 (Sigma) at a concentration of 300 U/ml. Cells were stimulated for 48h before transduction and incubated at 37°C.

2.3.14 Mouse-T cell isolation and activation

Mice were housed at the Birmingham Biomedical Service Unit (University of Birmingham, UK). Mice 6 weeks old C57BL/6 were culled and the spleen dissected. A single cell suspension was prepared by smashing the spleen through a 70 μm

strainer. Cells were suspended in RPMI. To lyse red blood cells, 1x lysing buffer (BD Biosciences) was added in sterile water. Cells were washed and suspended in LCL at a final concentration of $3x10^6$ cells/ml. In order to stimulate T cell differentiation, Concanavalin A (Sigma) at a final concentration of 2 µg/mL and IL7 (eBiosciences) to a final concentration of 1 ng/ml were added to the culture. Cells were then incubated for 48 hours at 37°C.

2.3.15 Human T cell Transduction

Phoenix A (Ph. A) cells were seeded in T150 flasks at a final concentration of $1x10^7$ cells/flask in 10% FCS DMEM and incubated overnight at 37°C. Ph. A cells at a 60-80% confluence were transfected with 12µg of DNA carrying the CAR gene together with 12µg of pCl ampho plasmid in OptiMEM (Gibco) mixed with 120µl of FuGENE HD (Promega) in OptiMEM, according to manufacturer's instructions. The mix of DNA and Fugene was incubated for 45 minutes at room temperature. After adding 9 ml of 10% fresh DMEM without antibiotics to the Ph. A cells, the transfection reagents were added to the cultures. 24 hours later media was replaced with 21 ml of complete DMEM without antibiotics. Cells were incubated at 37°C for a further 24 hours. According to the number of T cells to be transduced, 6 well plates were coated with 30 µg/ml of retronectin for 3 hours at room temperature. After the removal of retronectin the wells received blocking buffer (PBS-2% BSA) for 30 min. Virus-containing medium was collected and centrifuged at 1500 rpm for 5 minutes to remove dead floating cells. This suspension was then distributed in the retronectin-coated wells and centrifuged in a pre-warmed centrifuge at 32°C for 2 hours. T cells
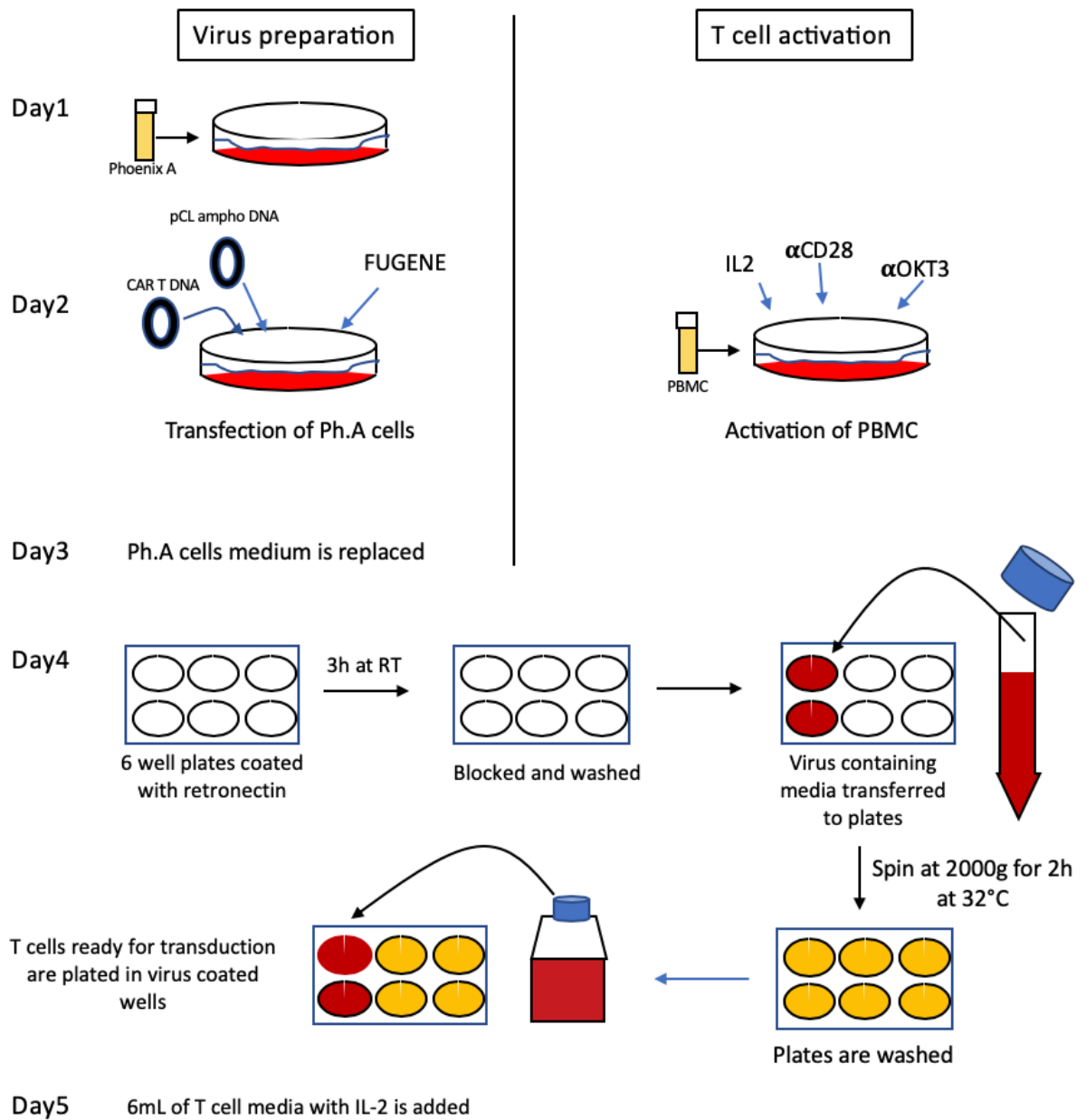
Figure 2.1 Retroviral transduction of human T cells

The figure represents the main steps to transduce T cells. First, Phoenix A (Ph.A) cells are cultured and transfected with both CAR T DNA and pCL ampho DNA, in order to produce active retroviral particles. Meanwhile on day 2, peripheral blood mononuclear cells are cultured and stimulated with IL2, anti-CD28 and anti-OKT3. On day 4, retronectin-coated plates are further incubated and coated with retrovirus-containing media. Finally, T cells are plated on top of the retrovirus.

were collected, counted and allowed to recover for 15-20 minutes at 37°C. After centrifugation, the virus was removed and wells were washed once with PBS (4 mL/well). T cells were plated $2x10^6$ cells/well, the plates were centrifuged at 1300 rpm for 5 minutes and incubated at 37°C. The following day, cells were supplemented with additional 6 ml of TCM and incubated at 37°C (Figure 2.1).

2.3.16 Mouse T cells Transduction

Mouse splenocyte transduction was performed with a similar protocol as described for human T cells in 2.3.14. Retrovirus was produced in Pheonix E cells, which were transduced using 12 μg of pCl Eco plasmid instead of pCL Ampho. The following steps were as described in 2.3.14. On the 5th day, cells were collected in a 50 mL tube and centrifuged at 1800 rpm for 5 minutes and resuspended in 25 mL of media. The cell suspension was layered onto 15 mL of ficoll histopaque and centrifuged at 1400 rpm for 30 minutes. Cells were gently aspirated from the interface of the gradient and placed in a 50 mL tube. Cells were washed 2 times with 50 mL of RPMI to remove ficoll. Cells were finally resuspended in TCM and counted or stained for transduction efficiency by Flow Cytometry analysis.

2.3.17 Human T cell transduction Efficiency

In order to verify the transduction efficiency of the human T cells flow cytometry was carried out. A small population of T cells was stained with the following antibodies: anti-human CD4 FITC (BD Biosciences, 555346), anti-human CD8 PE

(Abcam, ab134386), anti-human CD34 APC (Biolegend, 581) and a viability stain. The staining was performed on ice in the dark for 30 minutes and cells were washed with MACS buffer. Finally, T cells were resuspended in a total of 300 μL of MACS buffer and analysed on the LSRII (BD) flow cytometer. Transduced T cells were typically cryopreserved between their generation and their use in functional assays.

Antibodies for human T cells	Manufacturer	Concentration
Human CD4-FITC	BD Biosciences, 555346	1/8
Human CD8-PE	Abcam, ab134386	1/40
Human CD34-APC	Biolegend, 581	1/20

Table 2.11 List of antibodies for T cell transduction efficiency

2.3.18 Human T cell IFNγ ELISA

2.3.18.1 ELISA against recombinant antigen

In this assay, recombinant protein was used to activate the transduced T cells. Immunoabsorbent plates for ELISA were coated with both human or mouse recombinant CLEC14A ECD-hFc and hFc as a negative control. Each protein was tested in triplicates at different concentrations (10μg/μl, 1 μg/μl, 0.1 μg/μl) with hFc tested at 10 μg/μl. The plates were coated at room temperature overnight covered with transparent film. After washing the plates with PBS, T cells in ELISA media were plated at $2x10^5$ cells/well. Untransduced cells were used as a mock negative control.

Cells were incubated at 37°C for 16-24 hours. Supernatants containing INFγ were subsequently tested in the IFNγ ELISA protocol.

2.3.18.2 Cells expressing the antigen

In this type of assay, we used HUVEC cells (Lonza), which constitutively expressed both of the T cell targets CLEC14A and CD93, and HEK cells transfected with CLEC14A (full length and the non MMRN2 binding mutant CLEC14A^{C103S}) and CD93 (full length and the non MMRN2 binding mutant CD93^{C104S}). Target cells were seeded in tissue culture treated 96 well plates in TCM at 1×10^4 cells in 50 µl. T cells were seeded in TCM at 2×10^5 cells in 50 µl. Plates were centrifuged at 1400 rpm for 3 minutes and incubated for 16-24 hours at 37°C.

2.3.18.3 ELISA development

On the same day of seeding T cells with relevant targets (either recombinant proteins or cells expressing the antigen), Maxisorp plates (Nunc) were coated with anti-human IFNγ Ab diluted in coating buffer (0.75 µg/ml). The number of plates to coat was calculated based on the experiment size, including space for the standards. Plates were incubated overnight at 4 °C.

The following day media was flicked off and the plates received blocking buffer for 2 hours at room temperature. After incubation, the plates were washed four times and both the supernatants (50 µL/well) and the standards were added. Standards were added to a concentration of 2×10^4 pg/ml to 312 pg/ml in two-fold dilutions in

culture medium. Plates were incubated at room temperature for 3 hours and further washed 4 times with PBS/Tween. Biotinylated anti-IFNγ (Invitrogen) at 1/1333 dilution in blocking buffer was added to each well and the plate was incubated for 1 hour at RT and washed as previously. The plates were incubated one last time with extra-avidin peroxidase in blocking buffer at 1/1000 dilution, incubated 30 minutes and washed 8 times before developing. The ELISA signal was developed by adding 50 μl for 20 minutes of TMB substrate per well. The reaction was stopped with 1M phosphoric acid (50 μl/well) and the absorbance was read at 450nm with Bio-tek Synergy HT Multi-Detection Microplate Reader.

2.3.19 Chromium Release Experiment

T cell killing activity was measured performing a chromium release assay. Target cells were generated by transfecting HEK293T cells with the following constructs: CLEC14A^{FL}, CLEC14A^{C103S}, CD93^{FL} and CD93^{C104S}. In order to observe if the endogenous expression of the targets was able to trigger the killing activity of T cells, HUVEC cells were chosen as they express both CLEC14A and CD93. Target cells were released by exposure to trypsin, counted and pelleted at 1400rpm for 5 minutes. The supernatant was carefully removed, 10 μL (=50 μCi) of fresh ^{51}Cr was pipetted on top of the pellet and the tubes were flicked to resuspend the cells in the ^{51}Cr. In case the ^{51}Cr past its activity date or if high cell numbers were labelled, the amount of ^{51}Cr was increased accordingly. The cells incorporating the ^{51}Cr were incubated at 37°C for 2 hours and they were resuspended every half an hour. Meanwhile T cells were washed, counted and plated in 100 μL of media in V-bottom 96 well assay plates.

Plates were set up in order to include effector:target (E:T) ratio of 20:1, 10:1 and 5:1 and triplicates for each sample. For each target 3-6 replicates were also included with media alone and 3-6 replicates with 1% (v/v) SDS, necessary to calculate respectively spontaneous release and maximum lysis. At the end of the incubation, target cells were washed twice with 8 mL of media and centrifuged at 2000rpm for 3 minutes. They were diluted to a concentration of 2.5×10^4 cell/mL and 100 μL of each were plated out in V-bottomed 96-well assay plate containing the T cells. The plates were then centrifuged at 1400 rpm for 3 minutes and incubated at 37°C for 4-5 hours. At the end of the incubation 100 μL/well were harvested and transferred into LP2 tubes. The levels of ^{51}Cr were read by the Cobra 5010 gamma counter (Packard). The percentage of specific lysis was calculated with the following formula:

% specific lysis = ((release of test sample - spontaneous release)/(max release-spontaneous release)) * 100

2.4 Biochemistry

2.4.1 Cell Lysis

For cell lysis, cells were detached (either by treatment with trypsin or scraping) and pelleted. According to the cell type and the number of cells, they were resuspended in different amounts of lysis buffer NP40, usually 10 times the pellet volumes. The lysis buffer was supplemented with a protease inhibitor. After resuspending, cells were vortexed for 1 minute and incubated on ice for 30 minutes. The insoluble cellular debris was pelleted by centrifuging at maximum speed (13000 rpm) at 4°C

for 30 minutes and the lysate was transferred to a new microcentrifuge tube and stored at -20°C.

2.4.2 SDS PAGE and western blotting

Protein concentration was measured with BCA Protein Assay Kit (Thermo Scientific) according to manufacturer's instructions. Protein samples were separated by sodium dodecyl sulphate polyacrylamide gel electrophoresis (SDS-PAGE). SDS-PAGE gels were poured into XCell Surelock mini gel cassettes (Thermo Scientific) and run using XCell Surelock apparatus in SDS running buffer at 70mV through the stacking and 120 mV for the resolving gel. The stacking gel was composed of 15.8 mM Tris pH 6.8, 0.013% (v/v) SDS, 5% (w/v) polyacrylamide, 0.001% (v/v) TEMED. In the resolving gel, the percentage of polyacrylamide was variable (6-18%) according to the molecular weight of the proteins analysed whereas the remaining ingredients of the gel were at a fixed concentration of 97.5 After protein separation, wet transfer was performed onto PVDF membranes in transfer buffer for 2 hours at 30mV at 4°C in the cold room. After ensuring transfer with Ponceau S protein stain, PVDF membranes were blocked in 5% (w/v) milk in PBST for 1 hour at room temperature or 4°C overnight. Primary antibodies were resuspended at the working concentration (table 2.2) in PBST solution (3% (w/v) BSA and 0.001% (w/v) of sodium azide) and used to probe the PVDF membranes at the end of the blocking step at room temperature for 1 hour or at 4°C overnight. At the end of the incubation membranes were washed 5 times with PBST. The appropriate secondary antibodies conjugated with HRP were diluted as reported (table 2.3) and incubated with the membranes for

1 hour at room temperature. The blots were further washed as previously described and prepared to detect the presence of HRP conjugated antibodies by enhanced chemi-luminescence (ECL), using Amersham ECL western blotting detection reagent (GE Healthcare) and Amersham Hyperfilm X-ray film (GE Healthcare) according to the manufacturer's instructions.

2.4.3. Comparing the protein levels of endogenous CLEC14A and CD93 in HUVEC

A comparison of endogenous protein levels of CLEC14A and CD93 in HUVEC was achieved by western blotting.

HEK293T were transfected GFP-tagged construct of CLEC14A and CD93 cloned into pEGFPN1 vectors. Proteins were extracted from these transfected cells and alongside lysate from HUVEC they were used for SDS-PAGE and western blotting. In order to probe with different antibodies, three identical replicas of the same samples were run in the same gel and transferred onto a membrane. Subsequently, the membrane was cut and each replica was probed with a specific antibody. Western blot was performed as described in the previous paragraph (2.4.2).

The intensity values of CLEC14A-GFP bands obtained with the CLEC14A- or GFP-specific antibodies were compared with the intensity values of CD93-GFP bands obtained with CD93- and GFP-specific antibodies. Exploiting the CLEC14A-GFP and the CD93-GFP protein, and the GFP specific antibody allowed the calculation of the

relative efficacies of the CLEC14A- and CD93-specific antibodies and so enabled the relative expression levels of CLEC14A and CD93 in HUVEC to be determined.

2.4.4 ELISAs

2.4.4.1 Direct ELISA

Direct Enzyme-linked immunosorbent assay was employed in the detection of specific antibodies against h/mCLEC14A ECD-hFc in plasma. The plasma of vaccinated mice was tested against specific antigens. ELISA plates (NUNC MaxiSorp) were coated with the target protein (e.g. h/mCLEC14A ECD-hFc) in PBS at a concentration of 20-50 µg/mL at 4°C overnight. The wells were washed 3 times with PBS-T, blocked with 5% (w/v) BSA for 2 hours at room temperature and then washed again as before. The murine plasma or phage supernatant was incubated for 1 hour at room temperature. Wells were washed again 3 times, incubated with anti-myc antibody for 1 hour at room temperature and washed again. Before the last wash and to develop HRP signals, the anti-mouse HRP antibody was added for 1 hour at room temperature. The ready-to-use BM Chemi-luminescence ELISA Substrate (Roche) was added to the wells and left for 10 minutes in order for the colorimetric reaction to develop. The reaction was quenched with 2M sulphuric acid. The OD was read at 450nm.

2.4.4.2 In-cell ELISA

To assess recognition of an antigen expressed on cells, an in-cell ELISA was constructed. Two stable transduced lines of HEK293T expressing the full-length gene of hCLEC14A or the empty vector were generated. These cells were plated at 5×10^4 cells/well in 100 µL of complete DMEM media. On the following day, cells were fixed by adding 100 µL of 8% (w/v) paraformaldehyde (PFA), in order to have a final concentration of 4% (w/v) PFA, for 30 minutes at room temperature. Cells were then washed 3 times with PBS and then stored in PBS at 4°C for a maximum of a couple of weeks. On the day of the ELISA, the hybridoma supernatants were tested once against cells expressing the target and once against cells expressing the empty vector as negative control. From this point, the protocol was the same as described in 2.4.4.1.

2.4.5 Biotinylation of hCLEC14A-ECD-hFc

To generate a recombinant biotinylated hCLEC14A-ECD-hFc for Phage display panning purposes, the EZ-link NHS-SS-Biotin kit (Thermo) was employed. This kit allowed the reversible biotinylation of proteins on their free primary amines (-NH$_2$) such as lysine side chains or the amino termini. The biotinylation was performed according to the manufacturer's instructions at a ratio of 50:1 biotin to protein. Excess of free biotin was removed by buffer exchange using PD-10 desalting columns (GE Healthcare) according to manufacturer's instructions.

2.4.6 Alexafluor 488-conjugation to MMRN2$^{485-678}$-hFc

To obtain directly conjugated recombinant proteins, mMMRN2$^{485-678}$-hFc and hFc alone were conjugated to the fluorophore Alexa-Fluor 488 using anantibody labelling kit (Life Technology). The reaction with the dye is similar to the biotinylation reaction described in 2.4.4. The recombinant protein hFc and mMMRN2$^{485-678}$-hFc were conjugated according to the manufacturer's instruction.

2.5 Purification of proteins

2.5.1 Purification of Fc-tagged proteins

Fc-tagged proteins were expressed in the lentiviral vector pWPI. In order to produce these proteins, HEK293T cells were lentivirally transduced with these vectors and the stable cell lines, expressing and secreting (due to the presence of a signal peptide) these proteins, were generated. An exception was hMMRN2$^{495-674}$-hFc, which was cloned into the non-lentiviral expression vector pHL-Fc and, in order to produce this protein, cells were transiently transfected. Stable or transiently transfected cells were cultured in large dishes to reach confluence. At confluence, media was changed from complete DMEM to OptiMEM; it was then collected and replaced every two days over a period of 2-3 weeks. The collected medium was centrifuged, sterile filtered, supplemented with PMSF and EDTA, and stored at 4°C.

A protein A column was employed for the purification of Fc-tagged proteins. The column was washed with 5x the volume of the column with deionized water to

remove ethanol used for storage. The column was then equilibrated, running 5x the volume of the column with Na_2PO_4 pH 7.0. Once equilibrated, the protein containing optiMEM was run through the column in a loop, at a speed of 1mL per minute. Once all the media had run through the medium, pH of the column was lowered by running through NaCitrate pH 3.0, allowing the elution of the protein which was collected in 0.5 mL aliquots and neutralised with 0.2 mL of Tris pH 9.0. All the above-described steps were performed at 4°C. Eventually, in order to clean the column, the same steps were performed in reverse order allowing column storage in 20% EtOH at 4°C.

2.5.2 Purification of His-tagged proteins

The production and purification of His-tagged proteins were similar to that was done for Fc-tagged proteins. Sequentially the following were run through an Ni-NTA column: PBS, PBS 0.5 M NaCl, Protein containing OptiMEM, PBS 0.5 M NaCl 10 mM Imidazole (to wash non-specific binders) and PBS 0.5 M NaCl 250 mM Imidazole to elute proteins from the column.

2.6 Flow cytometry

2.6.1 Generic protocol for immunostaining cells

In order to detect the presence of a cell surface marker, such as CLEC14A or CD93, HUVEC were detached from the culture plates by scraping or by using cell dissociation buffer. Cells were stained on ice with 20 µg/mL of the antibody of

interest or recombinant proteins for an hour. After washing with an excess of Flow Cytometer buffer, cells were incubated with secondary antibodies (1:100) chosen accordingly to the species of the primary antibody and the conjugated fluorophore for 1 hour on ice in the dark. In all incubation steps cells were resuspended in Flow cytometer buffer. Samples were analysed either on a FACSCalibur Machine (BD Biosciences) or a Cyan ADP (Beckman Coulter). Data were analysed using FlowJo 10.2 (v3.05470).

2.6.2 Cell cycle

48 hours after transfection with siRNA (2.3.3), HUVEC were collected, including possible cells floating in the media. Cells were then pelleted at 1500 rpm for 3 minutes and resuspended in 3 mL of ice-cold PBS. Cells were fixed with 100% ethanol (at -20°C) added dropwise while vortexing gently. Following the addition of 100% ethanol cells were incubated at -20°C for at least one hour, centrifuged at 1500 rpm for 5 min and the ethanol removed. Cells were washed twice in ice-cold PBS. After washing, cells were incubated on a rocker for 15 minutes with ice-cold PBS with 0.25% Triton X-100. The PBS-Triton was carefully removed and cells were resuspended in 470 μL of PBS, transferred into a FACS tube and incubated with 5 μL of 0.1 mg/mL RNAse A and 25 μL of 50 μg/mL propidium iodide for at least 30 min in the dark on ice. Samples were analysed by at flow cytometer Cyan (Beckman counter) and data were analysed using FlowJo 10.2 (v3.05470).

2.6.3 Lentiviral transduction efficiency analysis

HEK293T cells lentivirally transduced with GFP constructs were detached, resuspended in Flow cytometer buffer (Table 2.1) and green fluorescence was directly detected by Flow cytometer analysis.

2.7 Cell and tissue staining

2.7.1 Immunofluorescent staining of cultured cells

2.7.1.1 Preparation of coverslips

Coverslips were sterilised with 1M HCl for 10 minutes at room temperature. Before storage, they were washed 5 times with sterile ddH$_2$O and then transferred to 70% (v/v) ethanol. Before use, they were washed with sterile PBS and then moved into a 6 well dish and coated with 0.1% (w/v) gelatin in PBS.

2.7.1.2 IF protocol

HUVEC were plated in 6-well dishes containing coverslips. Once reached the desired confluency, coverslips were washed 3 times with sterile PBS and incubated with 4% (w/v) PFA in PBS for 10 minutes at room temperature. After fixation, coverslips were washed 3 times with PBS and incubated with 50 mM NH$_4$Cl in PBS for 10 minutes at room temperature. Before the incubation with blocking buffer (Table 2.1) for 1 hour at room temperature cells were washed 3 times as previously described. Primary and secondary antibodies were diluted into blocking buffer and incubated 1 hour at

room temperature and, at the end of each incubation, cells were washed 3 times with PBS. Coverslips were mounted face down onto 5.5 µL ProLong Gold Antifade reagent with DAPI. They were left overnight at room temperature in the dark and the following day the edges of the coverslips were sealed with clear nail polish and stored at -20°C. Images were taken on a Zeiss LSM 780 Confocal microscope.

2.7.1.3 MMRN2$^{495-678}$-hFc internalisation experiment

HUVEC cells were plated in 6 well plates containing sterile coverslips. On the day of the experiment, cells were sparse on the plate and incubated for at least 30 minutes with pre-warmed serum-free media. The stimulation of each time point was performed using 5 µg/mL of either MMRN2$^{495-678}$-hFc or hFc alone as the negative control. At the end of the stimulation the cells were fixed with 4% (w/v) PFA for 10 minutes after 3 washes in ice-cold PBS. Then the standard protocol for IF described previously in the paragraph 2.7.1.2 was used. In order to detect the possible presence of MMRN2-hFc cells were stained with Alexa 633 anti-hFc. Moreover, endosome staining was achieved using an antibody against the early endosomes antigen 1 (EEA1) (BD Biosciences), which is a known marker for endosomes (Mu *et al.*, 1995).

Finally, the coverslips were mounted using the ProLong Gold Antifade Mountant with DAPI. Pictures were taken on the Zeiss LSM 780 Confocal microscope.

2.7.2 CD31 Immunofluorescent staining of frozen murine tumour tissues

Sections of frozen murine tumour tissues were fixed by immersion in acetone for 10 minutes at -20°C. The slides were washed 3 times with PBS and then mounted into a Sequenza slide rack with a Shandon cover plate. Sections were blocked with 2.5% (v/v) horse serum in PBS for 30 minutes at 23°C. CD31 monoclonal (Biolegend, Clone MEC13.3) antibody was diluted to 10 μg/mL (1/50) in sterile PBS and 100 μL of diluted antibody was added to each slide and incubated for 1 hour at 23°C. The slides were washed 3 times with PBS and incubated with chicken anti rat-alexafluor488 antibody (Life Technologies, A21470) at concentration of 10 μL/mL (1/200) in sterile PBS for 1 hour at 23°C. Before mounting the slides with Prolong Gold antifade reagent with DAPI, tissues were washed 3 times with PBS and once with deionised water. Slides were stored at -20°C in the dark. Images were taken with a Leica DM6000 fluorescent microscope.

2.8 In vivo experiments

All the in vivo experiments were performed at the University of Birmingham animal facility (BioMedical Service Unit, BMSU) under the Project License of Prof. Roy Bicknell (PPL70 8704).

2.8.1 Hybridoma antibody production

The generation of monoclonal antibodies to CLEC14A was performed in collaboration with the monoclonal antibody production unit of the University of Birmingham with the help of Dr. Margaret Goodall.

2.8.1.1 Immunisation protocol

The protocol of immunisation was similar to the one used from Cancer Research Technology (CRT). The mouse version of the extracellular domain of CLEC14A was expressed fused with a human Fc fragment, in order to elicit the immune response. Three mice were immunised subcutaneously at the base of the tail with 50 μg of the antigen thoroughly resuspended in complete Freund's Adjuvant (CFA). The following boosts were every two weeks. The first boost was an intraperitoneal (IP) injection of the same amount of protein in PBS. The second boost was performed similarly as the first immunisation, injecting subcutaneously 50 μg of protein but using incomplete Freund's Adjuvant (IFA). The serum was tested by in In-cell ELISA and, if the titre was sufficiently high to see a response at $1/10^4$ dilution, the last boost was given IP injection and three days later the fusion was performed.

2.8.1.2 Fusion protocol

Mice were culled and the spleen was removed and placed in a petri dish. Holes were created using the needle of a syringe and RPMI was used to gently flush cells out of

the spleen. In order to obtain a complete single cell suspension, the rest of the spleen was gently flushed through a 40 μm strainer. Both spleen cells and mouse myeloma cells NSO were washed 3 times with serum-free RPMI in order to eliminate any trace of serum, that is known to interfere with polyethylene glycol (PEG). The splenocytes isolated were counted and pooled in a 1:5 ratio (myeloma:splenocyte) with the myeloma cells in a sterile glass tube with a round bottom. Cells were then centrifuged and the supernatant was aspirated carefully. Cells were resuspended in 1 mL of PEG added with a plastic Pasteur pipette gently while stirring. The same operation was repeated while supplementing the PEG solution of cells with 1 mL of warm RPMI reducing the concentration of PEG. This was repeated 1 mL at a time up to 20 mL. After allowing cells to rest for 5 minutes, the process was continued up to 50 mL. Cells were centrifuged at 1700 rpm for 7 minutes and the supernatant was aspirated. The hybridomas were resuspended in 50 mL of RPMI 20% (v/v) FCS in a T75 flask. Cells were then resuspended and plated in 96-well plates in 150 μL of RPMI 15% (v/v) FCS. On the following day, 2x hypoxanthine-aminopterin-thymidine (HAT) media was added to the plates in order to select the hybridomas between myeloma cells and splenocytes.

2.8.2 Tumour vaccination experiment against MMRN2[495-678]

Mice were immunised subcutaneously every 2 weeks with 50 μg of the protein fused with hFc fragment. Purified hFc was injected in the control group. The first immunisation was in complete Freud's adjuvant whereas the second and third immunisations were in incomplete Freud's adjuvant. Before each immunisation,

blood samples were collected in order to check the antibody titre. One last immunisation was performed intraperitoneal in PBS. Two weeks after the last immunisation, 2×10^{6} LLC cells were injected and every 2 days measurements of the tumours were made with a calliper.

CHAPTER 3: Investigating the interaction of Multimerin-2 (MMRN2) with CD93 and CLEC14A

3. Investigating the interaction of Multimerin-2 (MMRN2) with CD93 and CLEC14A

3.1 Introduction

Angiogenesis is a highly regulated and complex process by which new vessels are generated from existing ones. In angiogenesis endothelial cells undergo multiple changes. Firstly, they have to escape quiescence, developing a proliferative phenotype. Then, in order to respond to pro-angiogenic stimuli, they have to migrate and transmigrate, remodelling the environment and the extracellular matrix. Finally, undergoing tubulogenesis to form functional vessels. Thus, angiogenesis may be divided into four main steps: (I) vascular sprouting, (II) tubule morphogenesis, (III) adaptation to tissue needs and (IV) vessel stabilisation. Different proteins regulate these steps although some may be involved in several. In addition, other cell types collaborate with endothelial cells during angiogenesis, for example a key role is played by pericytes (Carmeliet and Jain, 2011). As there is no gold standard assay *in vitro* to evaluate the involvement of a protein in each step, multiple *in vitro* assays are usually used. *In vivo* assays can give a comprehensive overview of angiogenesis, but it is not possible to appreciate the contribution of an individual protein to each step (Irvin *et al.*, 2014).

CLEC14A and CD93 are C-type lectin domain proteins that both belong to the family-14. CLEC14A has been shown to be a tumour endothelial marker, which means that it is upregulated in the vasculature in different tumour types, but it is virtually absent

within the vasculature of healthy tissues (Mura *et al.*, 2012). Knockdown of CLEC14A led to reduced endothelial cell migration and tube formation (Rho *et al.*, 2011; Mura *et al.*, 2012). Moreover the ectopic expression of CLEC14A resulted in increased filopodia in Hela and human embryonic kidney 293 cells, showing a polarization at the plasma membrane of CLEC14A (Mura *et al.*, 2012). Likewise CD93 is also involved in angiogenesis. Endothelial knockdown of CD93 showed impairment in cell-cell and cell-matrix contacts, migration and tubular morphogenesis. CD93 binds to dystroglycan and binding was important for those activities (Orlandini *et al.*, 2014; Langenkamp *et al.*, 2015; Galvagni *et al.*, 2016). More recently MMRN2, an extracellular matrix protein also involved in angiogenesis (Zanivan *et al.*, 2013; Noy *et al.*, 2015; Colladel *et al.*, 2016), was shown to be a ligand of both CLEC14A and CD93 (Khan *et al.*, 2017).

Altogether these data suggest that CLEC14A and CD93 are redundant receptors for MMRN2 and the interaction of all three proteins is relevant to their angiogenic roles. Therefore, the aim of this work was to evaluate the effect of the double knockdown compared to the singles knockdowns in various in vitro assays using HUVEC cells.

3.2 Validation of siRNA and antibodies for CLEC14A, CD93 and MMRN2

Two duplexes targeting each gene (CLEC14A, CD93 and MMRN2) were tested in knockdown experiments. The knockdowns were assessed at the RNA level via qPCR and at the protein level via western blot. HUVEC cells were transfected with each of the siRNA independently and after 48 hours proteins were extracted and subjected
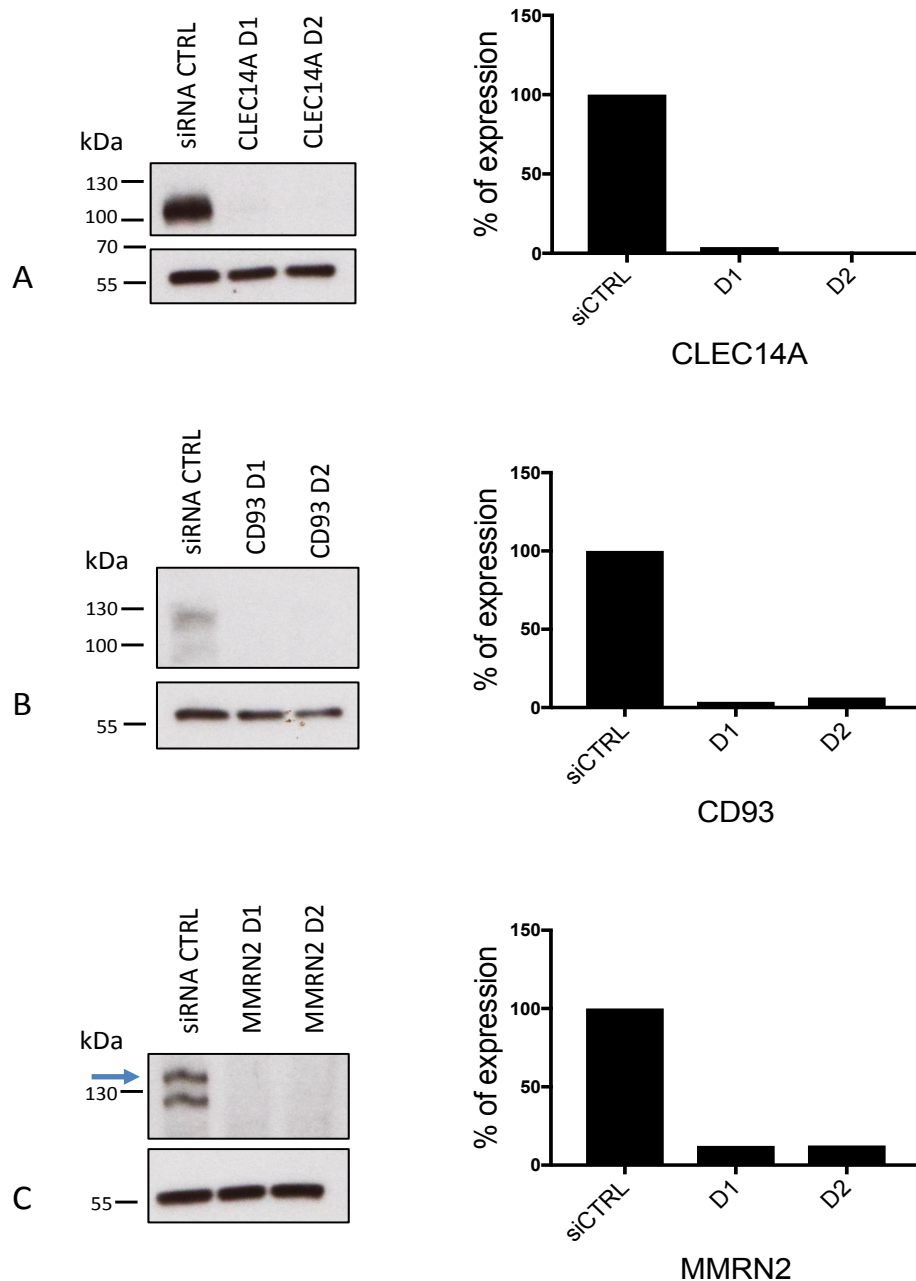
Figure 3.1 Validation of siRNA and antibodies for CLEC14A, CD93 and MMRN2

To validate the siRNAs, HUVEC cells were transfected with siCTRL and the respective duplexes for MMRN2, CLEC14A and CD93. After 48 hours, lysates from transfected cells were prepared and subjected to western blot. The upper part of the blot was developed probing with CLEC14A, CD93 or MMRN2 antibody, and the lower part with α-tubulin control. The blot shows the knockdown experiment A for CLEC14A, B. for CD93 and C. for MMRN2. The graphs on the right side of the figure show the densitometry analysis, normalising the value of each protein band to the corresponding band for α-tubulin. Blue arrows indicate the specific bands in case of ambiguity. The data is expressed as a percentage. n=1
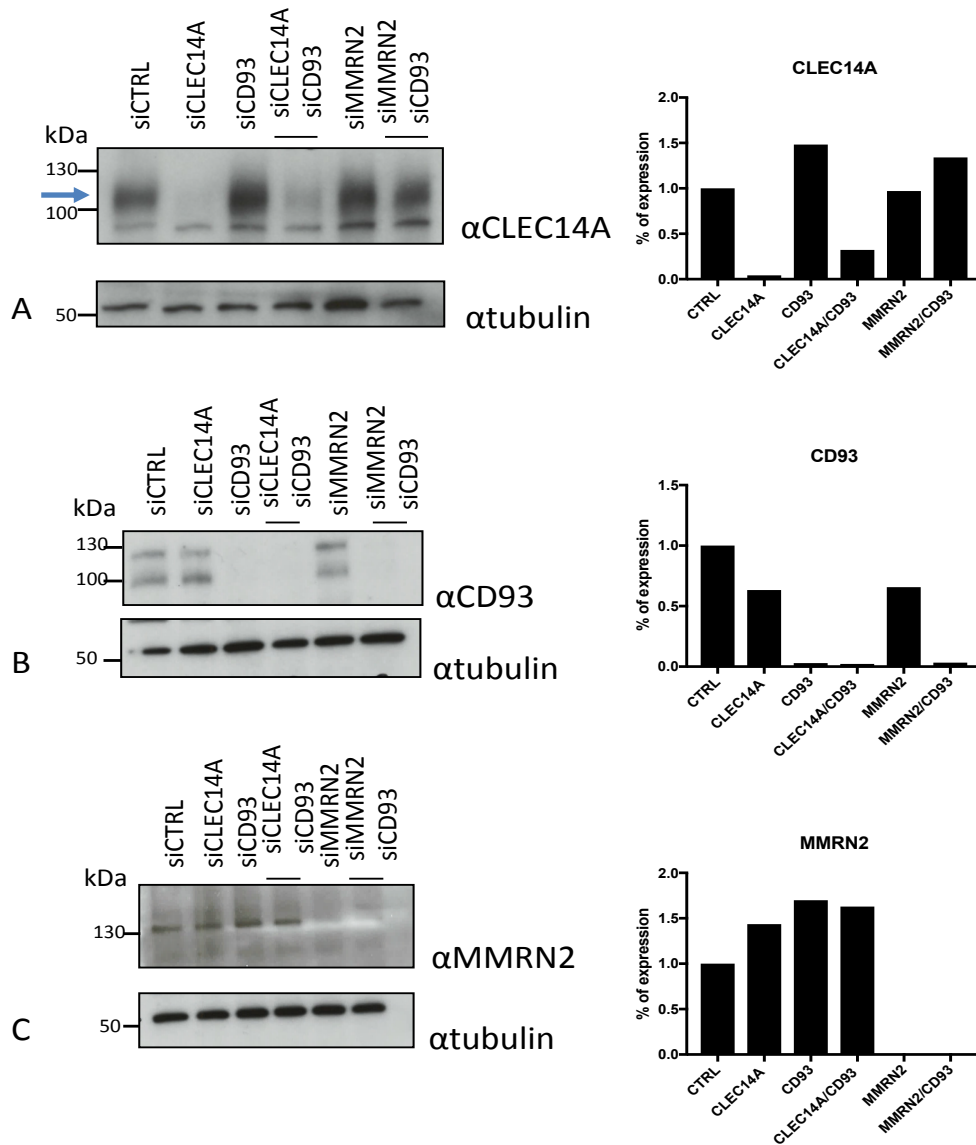
Figure 3.2 siRNA double knockdowns of CD93/CLEC14A and CD93/MMRN2

To investigate the possibility of obtaining a double silencing of these proteins in HUVEC cells, cells were transfected with the different siRNAs (alone or in combination). Lysates after 48 hours were prepared and subjected to western blot. A. The blot shows the protein levels of CLEC14A in the various combinations of KD. B and C show the levels of CD93 and MMRN2. Each of the blots shows α-tubulin as housekeeping gene in the lower part of each blot. The same samples were loaded in three independent gels and blotted for one of the proteins. This result confirmed the possibility of obtaining a successful double knockdown. The graphs on the right side of the figure show the densitometry analysis, normalising the value of each protein band to the corresponding band for α-tubulin. The data is expressed as a percentage. The same analysis also was repeated for each transfection to ensure that cells used later in functional assay were knocked down successfully. Blue arrows indicate the specific bands in case of ambiguity n=5

to western blot, probing with commercial polyclonal antibodies for each of the proteins.

Blots showed bands at 100-120 kDa for CLEC14A and CD93 and at 135 kDa for MMRN2. Although CLEC14A and CD93 amino acids predicted molecular weights are 50 kDa and 68 kDa (Uniprot), the actual bands were shown at much higher molecular weights, due to the fact they are both highly glycosylated. Knockdown reduced (almost 100%) for all three proteins and with both of the duplexes (D1 and D2) (Figure 3.1). This confirmed that both the antibodies used and the duplexes were specific for their targets. A similar experiment was performed to show the knockdown of two genes at the same time. Based on the strong effect of CD93 in some preliminary functional assays, the double knockdown of CD93-CLEC14A and CD93-MMRN2 was attempted. As shown in Figure 3.2 it was possible to achieve double knockdowns for each combination. These combined knockdown cells were then studied in functional assays. The effect of the siRNAs was also checked at the mRNA level by qPCR for CLEC14A, CD93 and MMRN2 in collaboration with Dr Peter Hewett. HUVEC cells were collected at 24 and 48 hours after transfection and the cDNA from these cells was subjected to qPCR. The result showed a strong reduction in the mRNA of CD93 and CLEC14A, both at 24 hours and at 48 hours. Data for the 48-hour experiment are shown in figure 3.3.
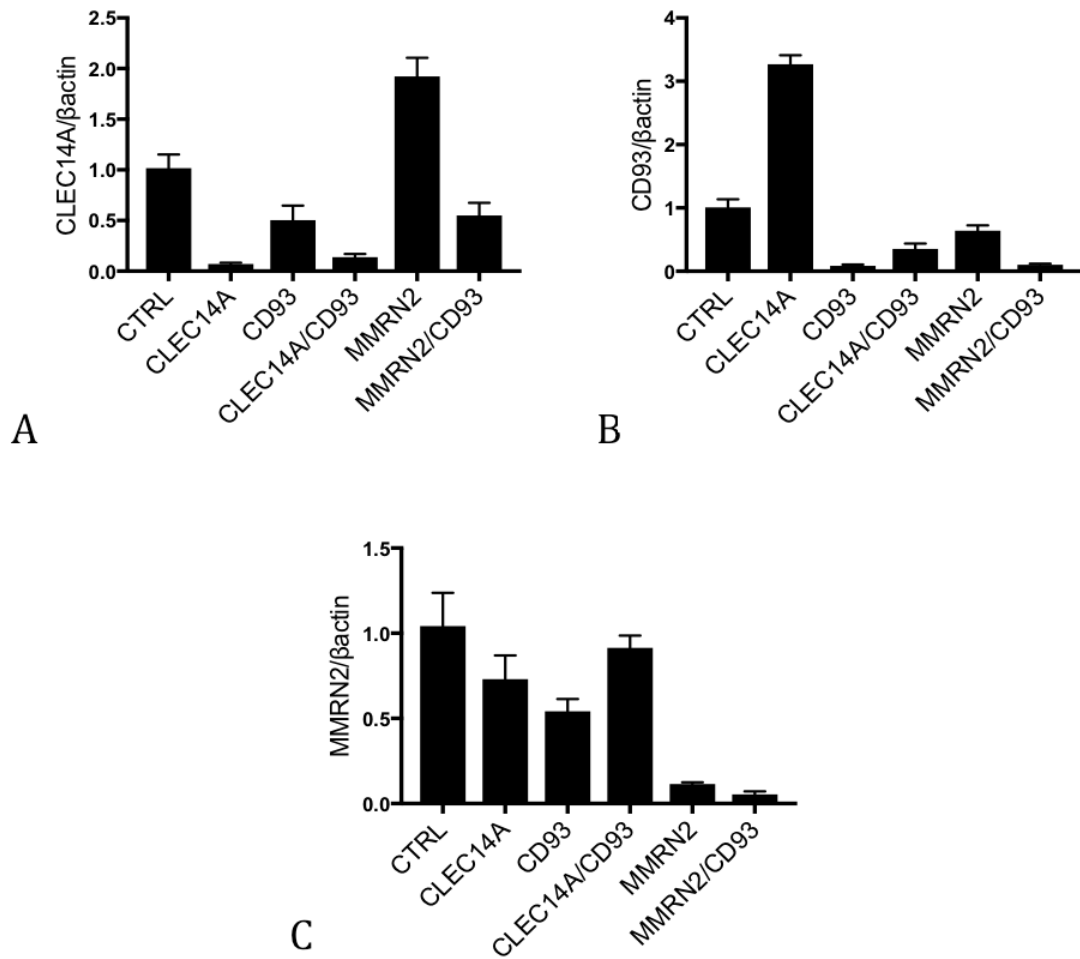
Figure 3.3 qPCR result of knockdowns 48h after transfection

To investigate whether the knockdown was confirmed at the mRNA level, HUVEC cells transfected with CTRL, CLEC14A, CD93 and MMRN2 siRNAs (alone or in combination) were collected after 48hours. From these populations mRNA was extracted, retrotranscribed and subjected to qPCR analysis. Probes employed in this experiment were designed for Sybergreen analysis. The expression levels were normalised for the levels of β-actin. A. The bar graph shows the gene expression of CLEC14A in each knockdown population tested. B and C The graphs represent the expression level of CD93 and MMRN2 respectively. Data are expressed as fold change. The data represent the mean of 3 technical replicates ± SEM. n=1

3.3 Knockdown of CLEC14A, CD93 and MMRN2 does not inhibit proliferation or block cell cycle checkpoints in HUVEC

Proliferation was examined using an MTT assay. HUVEC were transfected with the previously validated siRNAs duplexed and proliferation was measured based on the conversion of tetrazolium into a formazan dye. This showed that there is a subtle but not significant reduction in proliferation after transfection. Reduction was observed to a greater extent on CLEC14/CD93 and MMRN2 knockdown, whereas only slightly on MMRN2/CD93 and CD93 knockdown. No observable changes compared to controls were found on CLEC14A knockdown (Figure 3.4). Although there are no obvious effects on cell proliferation 24 hours after transfection, there might be observable differences at later time points. The inclusion of siRNA for cyclin D1 as positive control could give a better indication whether the absence of a phenotype is due to the short time point rather than the actual consequence of the knockdown.
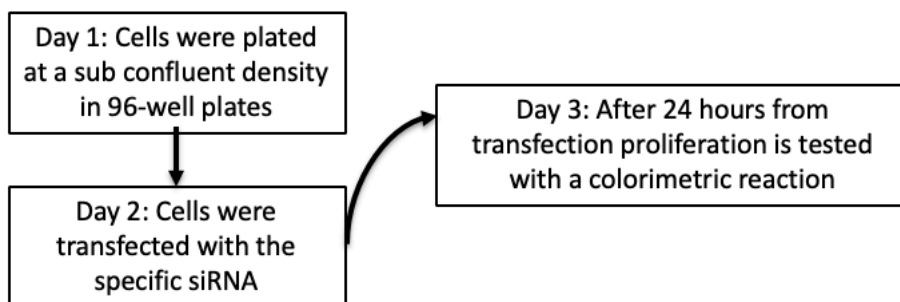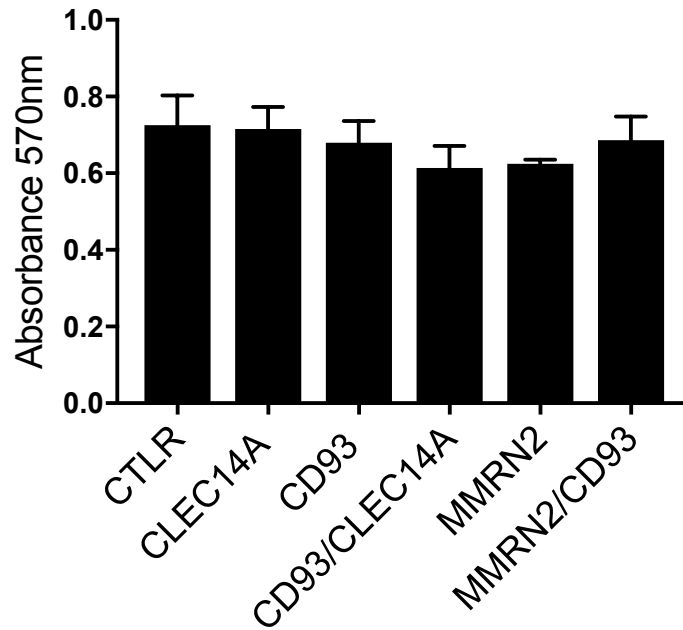
Figure 3.4 The knockdown of CLEC14A, CD93 and MMRN2 has no effect on HUVEC proliferation

An equal number of HUVEC cell was cultured in a wells of a 96-well plate and in situ transfected with different siRNA. After 24 hours, a tetrazolium solution was added to the cells and incubated. Absorbance of the colorimetric reaction was read at 570nm. In the lower part of the graph the timeline of the experiment. This experiment showed no significant difference in the proliferation rate on knockdown. n=3 (Duplex 2 for each gene was used once), *$p<0.05$ versus Negative Control (Tukey's test). The graphs show mean ± SEM.

HUVEC cells 48 hour after transfection were stained with Propidium Iodide (PI) and the content of DNA was measured with a flow cytometer. This experiment showed the percentage of cells in specific phases of the cell cycle: subG0, G0/G1, S, G2/M. The result confirmed no effect of the knockdowns on the cell cycle. There is an accumulation of cells in subG0 if transfected with CD93 siRNA (12.23% more than control). The combination of CD93 siRNA with either CLEC14A (26%) or MMRN2 (36.4%) shows a further increase in the percentage of cells in subG0 compared to the control (6.77%). This effect might be explained by the cytotoxicity of the siRNAs used. The percentages in subG0 of the cells upon knockdown of CLEC14A and MMRN2 are comparable to the negative control. MMRN2/CD93 showed an 8% reduction of cells in the S phase and a 15% increase of cells in G0/G1. No great differences were found across the other knockdowns regarding the percentage of cells undergoing the S and G2/M phase. A notable reduction of the cells in the G0 phase was observed upon double knockdown of CLEC14A/CD93 and MMRN2/CD93 (Figure 3.5).

It was concluded that CLEC14A, CD93 and MMRN2 do not play a role in HUVEC proliferation or the cell cycle under these culture conditions.

A

111
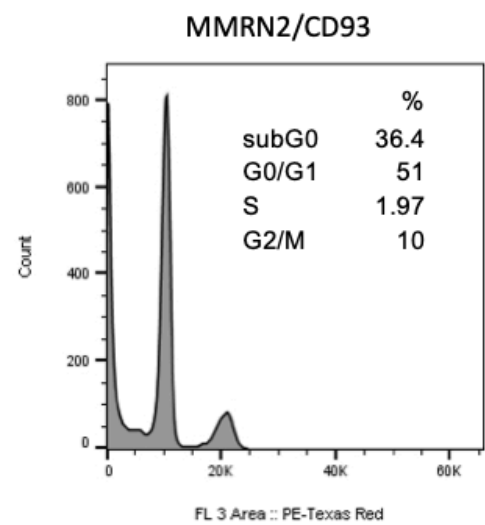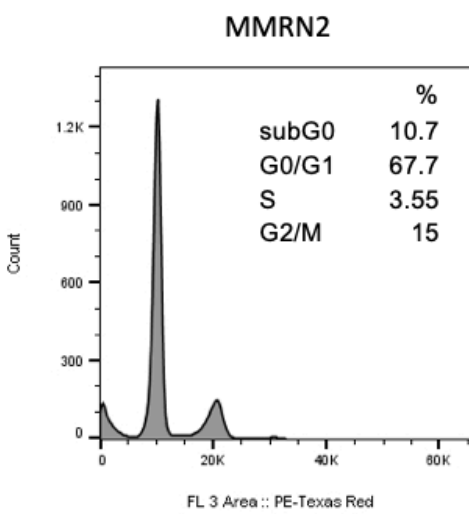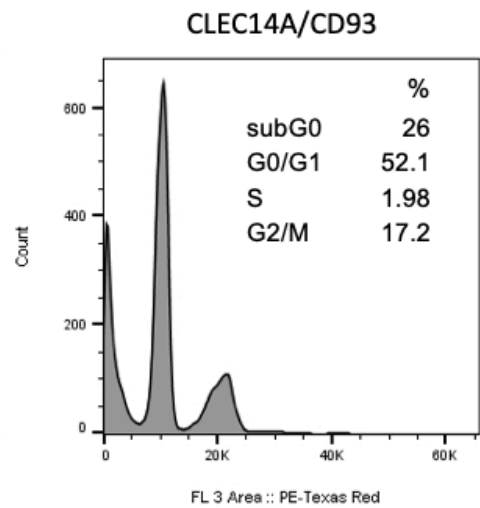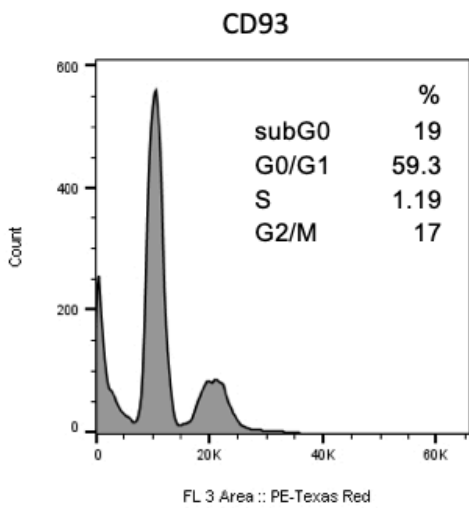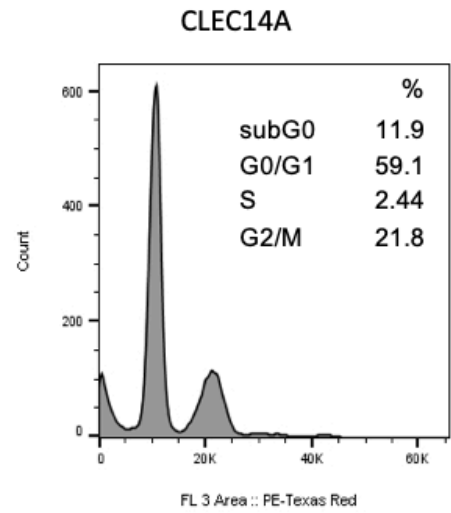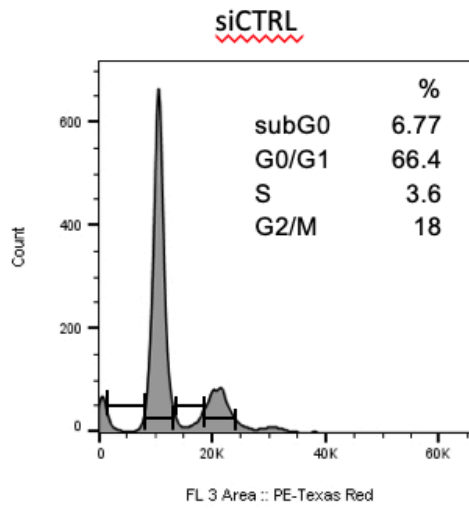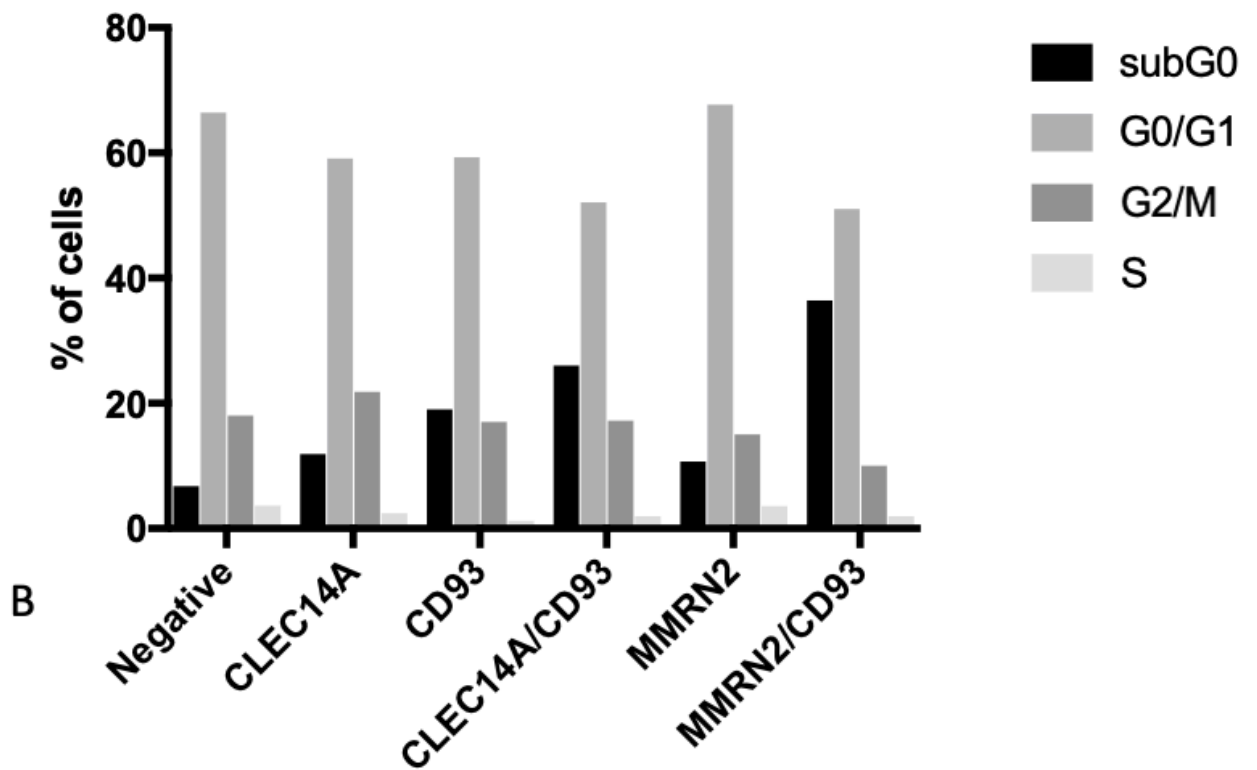
Figure 3.5 The knockdown of CLEC14A, CD93 and MMRN2 does not change the cell cycle in HUVEC

siRNA transfected HUVEC were ethanol fixed, permeabilized and stained with propidium iodide (PI) for 30 minutes in the dark. Cell cycle data were collected by flow cytometry. Equal gating was employed in each of the condition. Example of the gating strategy used is shown in the NegCTRL. A. The flow cytometer histograms show the distribution of the cells in the characteristic G0/G1, S, G2/M division. B The graph summarizes the percentage of cells in each stage of the cell cycle. The experiment shows no blockade of the HUVEC cell cycle upon knockdown but increased cell death upon CD93 knockdown either alone or in combination. n=1.

3.4 siRNA knockdown of CD93 reduces tube formation in a Matrigel assay in a CLEC14A and MMRN2 independent manner.

Matrigel is a secreted gelatinous protein mixture obtained from Engelbreth-Holm-Swarm (EHS) mouse sarcoma cells, containing different extracellular matrix proteins and growth factors and sold commercially. It is known that endothelial cells such as HUVEC plated on Matrigel undergo a morphological differentiation into capillary-like structures (Kubota *et al.*, 1988). This process was recognised to mimic the way by which endothelial cells form capillaries in vivo, hence it has been extensively used as model for tube-formation.

Briefly, 1.4×10^5 HUVEC cells were plated onto solidified Matrigel and the tube formation was monitored every 6 hours in the incucyte over 24 hours. An incucyte incubator was used to record 9 fields of view per test condition. The number of meshes was then analysed. The most significant differences in their phenotype were shown after 6 and 12 hours. At 18 and 24 hours the phenotypes are similar and significant as the previous timepoints, but the differences are slightly reduced. The experiment showed that upon CLEC14A and MMRN2 knockdown alone there was a non-significant increase in tube formation compared to the HUVEC cells transfected with a negative control siRNA. Whereas, silencing CD93 alone or in combination with CLEC14A and MMRN2 showed a strong and significant reduction in tube formation both at 6 and 12 hour time points compared with the control. Interestingly, there was no significant difference between silencing both CD93 and CLEC14A compared to the knockdown of CD93 alone.

Negative CTRL   CLEC14A   CD93   CLEC14A/CD93

6h

12h

MMRN2   MMRN2/CD93

6h

12h
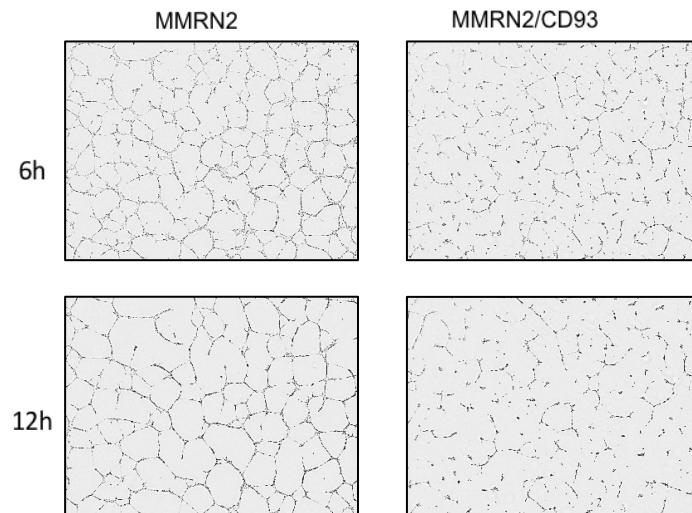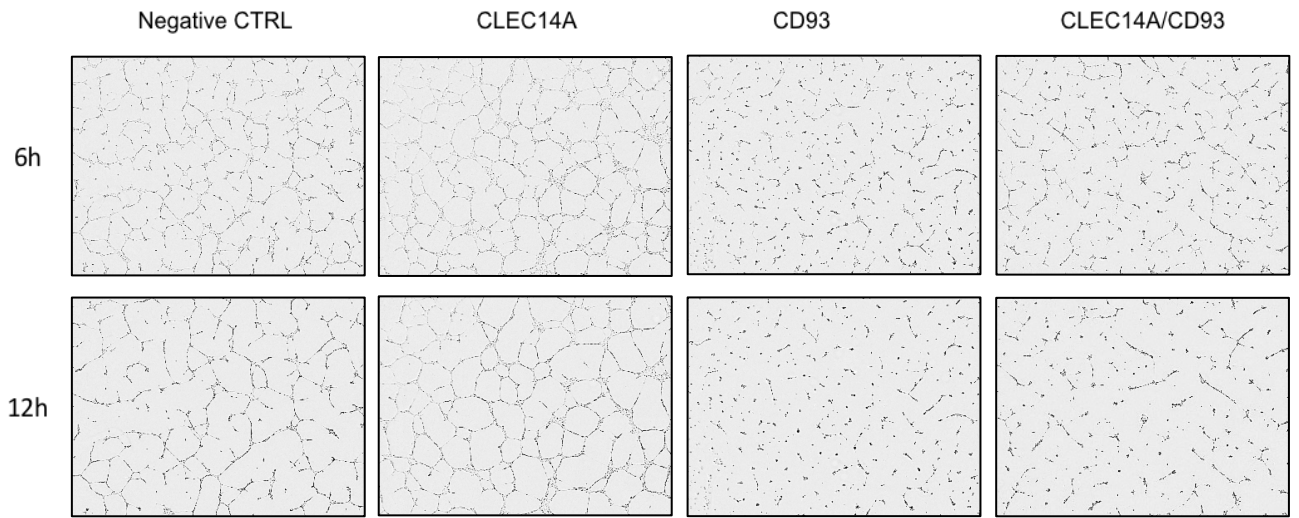
A
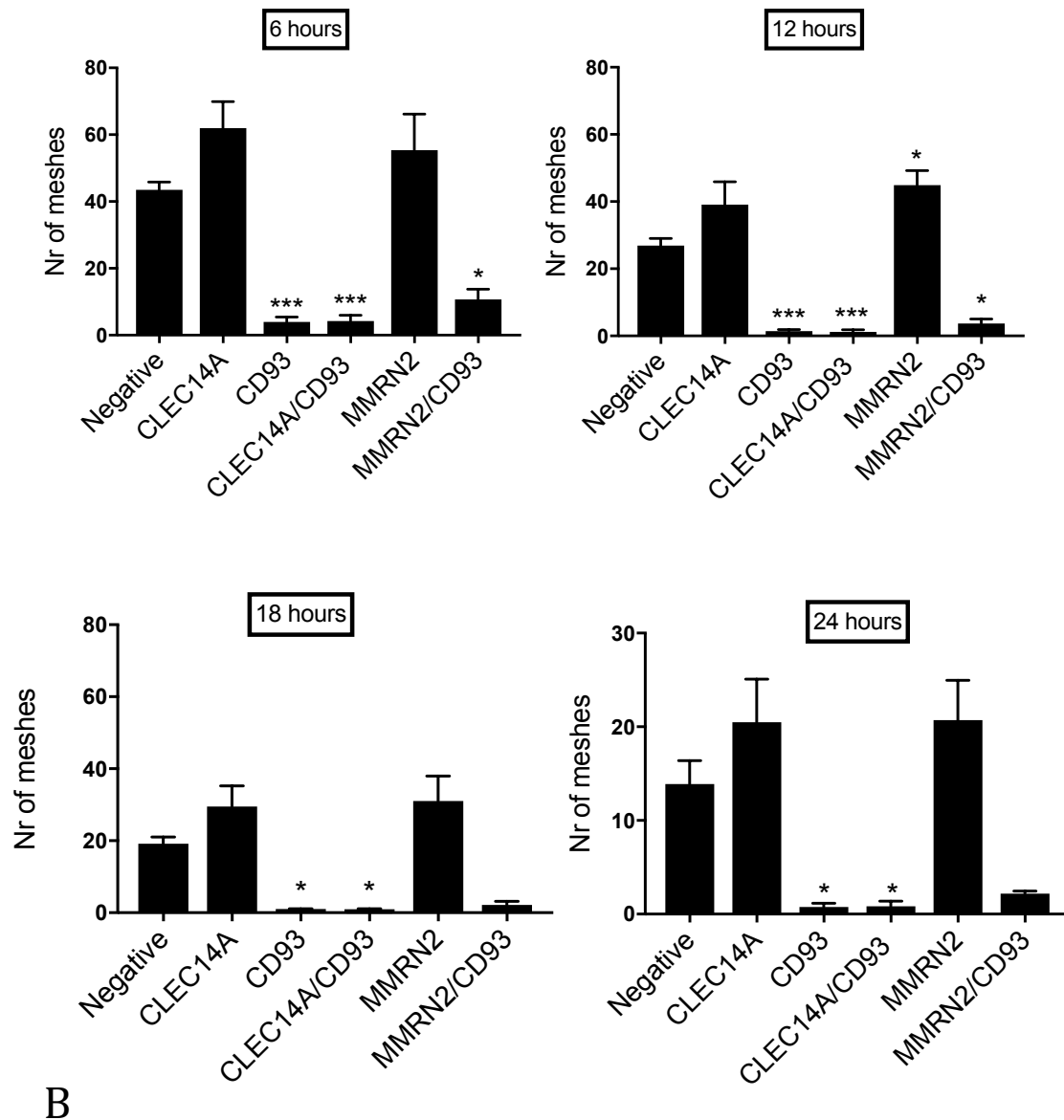
Figure 3.6 CD93 siRNA knockdown reduces tube formation in Matrigel assay in a CLEC14A and MMRN2 independent manner

HUVEC cells were transfected and after 48 hours they were seeded on Matrigel. Tube formation was monitored every 6 hours over 24 hours using an Incucyte. For each sample and time point, nine fields of view were taken. Pictures were analysed using the "angiogenesis analyser" plug-in for ImageJ. The number of meshes was considered as main parameter for the quantification. The most significant effects were observed at 6 and 12 hours. A. Representative pictures of the tube formation at 6h and 12h time points. CD93 significantly reduces tube formation and upon double KD with CLEC14A and MMRN2 the level was the same as the single CD93 knockdown. At 12 hours MMRN2 knockdown showed a significant increase in tube formation. B. The graphs represent the quantification on the number of meshes. n=5 (Duplex 2 for each gene was used twice), *$p < 0.05$ versus Negative Control (Tukey's test). The graphs show mean ± SEM

The combined knockdown of CD93 and MMRN2 showed a trend towards rescue of the control phenotype compared to CD93 knockdown alone. This effect was, however, minimal as there was a significant reduction of the CD93/MMRN2 knockdown compared with the negative control. The experiment was repeated 5 times with independent cultures of commercial HUVEC (Lonza), resulting in comparable outcomes each time (Figure 3.6).

3.5 CD93 knockdown reduced tube formation in co-culture assays

The Matrigel assay is very phenotype sensitive. Due to its short time course and the large amount of mouse ECM proteins included in the Matrigel, the results obtained with this assay are often confirmed in a more physiological setting with a co-culture assay. In fact, HUVEC in co-culture with fibroblasts form significantly more heterogeneous tubules, including both short and long interconnecting tubules. In contrast, the tubules in Matrigel assays are relatively short and homogeneous (Donovan *et al.*, 2001).

Briefly, HUVEC cells after knockdown were seeded on top of a confluent monolayer of fibroblasts and cultured for a further 6 days, replacing media every other day. At the end of the experiment, the network of tubules was stained with an anti-CD31 monoclonal antibody and imaged. Interestingly, HUVEC silenced for CD93 struggled to adhere to plastic when re-plated, whereas they were properly adhering to the fibroblast monolayer. The use of an inducible shRNA system could provide a valid alternative in order not to overlook late effects of the knockdowns. This co-culture

experiment demonstrated that upon silencing of CLEC14A and MMRN2 HUVEC cells showed no impairment in network formation. Following CLEC14A knockdown, the network formed in a similar fashion to the negative control; in contrast, MMRN2 knocked down cells showed a slight increase in network formation. CD93 silenced cells were significantly impaired in tube formation and the total tubule length was half of that in the negative control. A similar but milder phenotype was seen in double knockdowns of CD93/CLEC14A and CD93/MMRN2. Thus, CD93/CLEC14A double knockdown showed a 25% reduction in the total tubule length compared to controls. In contrast the CD93/MMRN2 double knockdown showed a significantly reduced network similar to the CD93 knockdown alone where the total tubule length was a half of that in controls (Figure 3.7).
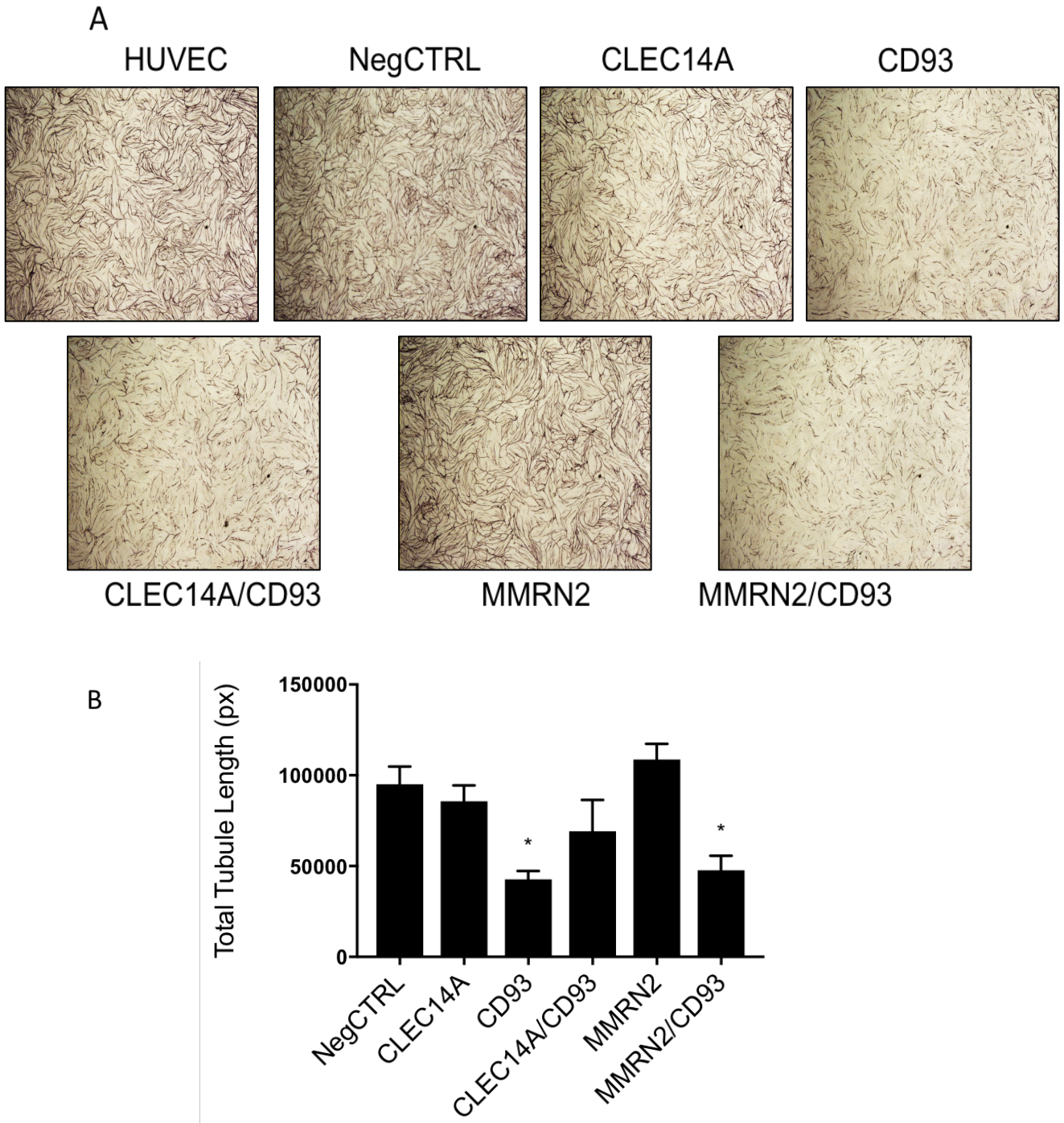
Figure 3.7 CD93 knockdown reduced the tube formation in co-culture assays

As previously, HUVEC cells were transfected with siRNAs. 24 hours after transfection cells were seeded on top of a monolayer of fibroblasts and cultured for a further 6 days. On the last day, cells were fixed and stained for CD31. Networks were imaged and analysed with Angio Sys analysis software (TCS Cell Works). The total tubule length was plotted. A Representative images of the tube formation. B The graph shows a significant reduction of the tubule length upon CD93 knockdown versus the negative control. n=5 (Duplex 2 for each gene was used once), *p<0.05 versus negative control ANOVA. The graphs show mean ± SEM.

118
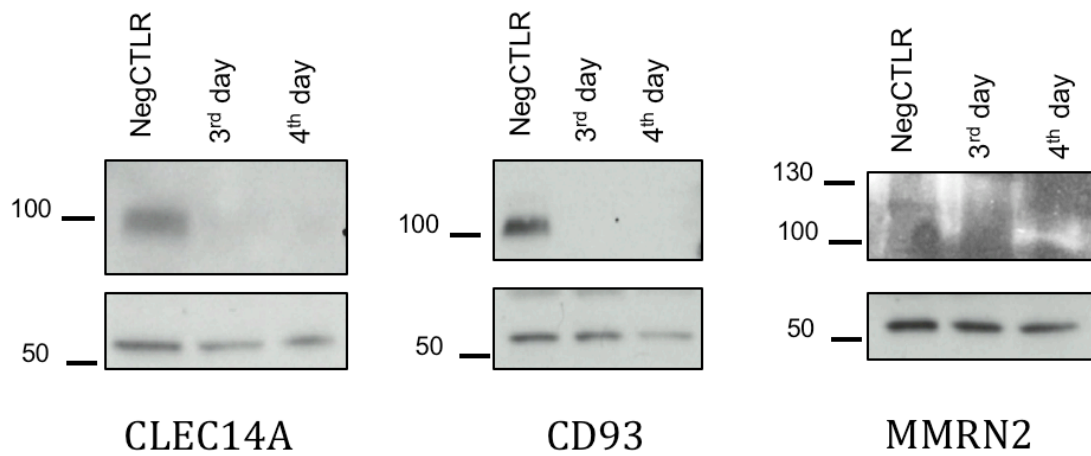
Figure 3.8 Knockdown timecourse in HUVEC

A timecourse on HUVEC was performed in order to ensure that each knockdown was effective for more than 48 hours. HUVEC cells were transfected with siRNA and collected on the third and fourth day after transfection. Lysates were prepared and subjected to western blot. In the upper parts of the blot, the membranes were incubated with the specific antibodies (CLEC14A, CD93 and MMRN2), in the lower part they were incubated with anti α-tubulin. The blots confirm a complete knockdown up to the fourth day after transfection for CLEC14A, CD93 and MMRN2.

As this assay takes 6 days, protein knockdown was examined by western blot 3 and 4 days after transfection. The blots confirmed knockdowns for at least 4 days following transfection. Protein knockdown for at least 4 days was considered sufficient to observe a phenotypic change if present in this assay (Figure 3.8).

3.6 MMRN2 and CD93 play opposing roles in cell migration

To further investigate the possible role of MMRN2 and CD93 in cell migration, a scratch wound assay was employed. The scratch wound assay is a simple and reproducible assay, which does not require specific chemoattractant or gradient chambers. It allows observing the migration process in two dimensions of a sheet of cells in response to a wound (Cory, 2011).

A
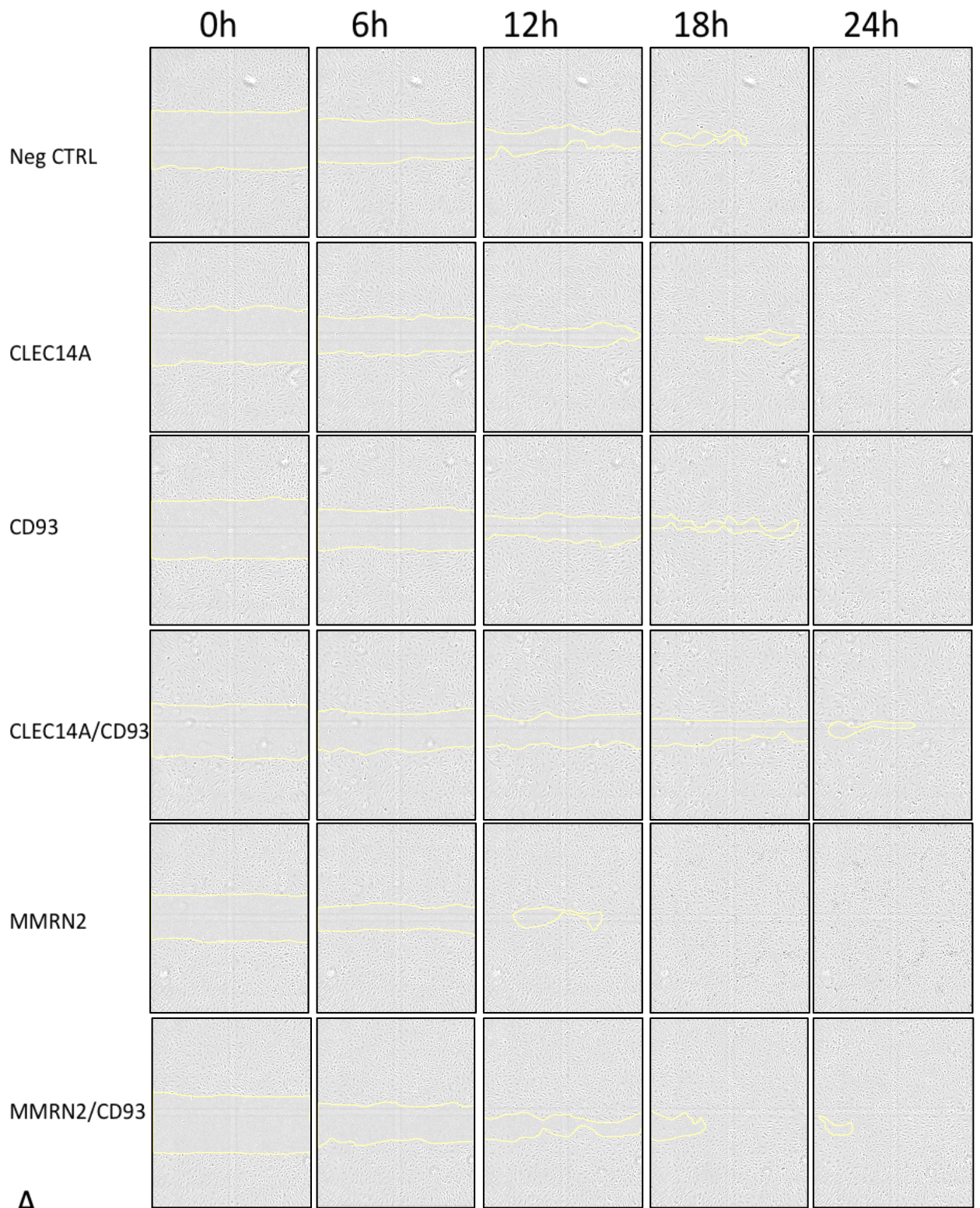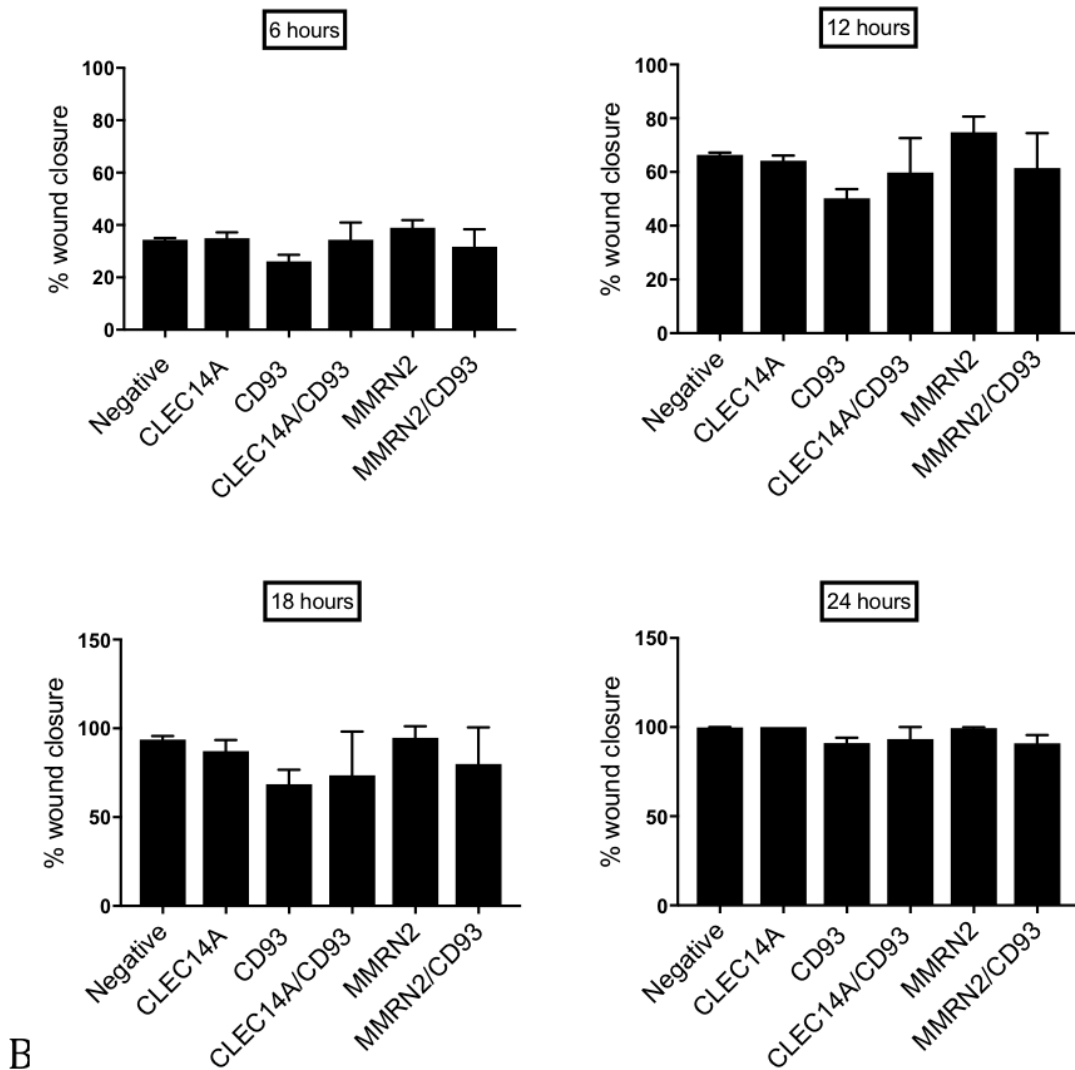
Figure 3.9 MMRN2 and CD93 play an opposite role in cell migration in a scratch wound assay

HUVEC cells were plated in wells of a 96-well plates and in-situ transfected. Once they reached confluence 48 hours post-transfection a scratch was made. The cells were cultured for an additional 24 hours. The closure of the scratch was monitored, and images were taken every 6 hours using the Incucyte. Images were then analysed manually with imageJ. A. Representative images over the 24 hours from the moment of the scratch (0h). B. Quantification of the percentage of wound closure at the different time points. At 18 and 24 hours a non-significant retardation in the wound closure upon CD93 knockdowns (alone or in combination) was observable. Overall no significant effect was detected. n=3 (Duplex 2 for each gene was used once), *$p<0.05$ versus Negative Control. (Dunnett's Test). The graphs show mean ± SEM

Cells were seeded into 96 well plates and then transfected with different siRNAs. Cells were transfected in the well, rather than plating transfected cells, because upon CD93 knockdown cells showed a defective adhesion. This effect of CD93 knockdown has been reported (Langenkamp *et al.*, 2015) and they showed a significant retardation in the wound closure.

Briefly, 48 hours after transfection the monolayer was scratched using a WoundMaker (Essenbioscience). Using the Incucyte, pictures were taken at 6-hour intervals. Knockdown of CLEC14A cells had no effect on cell migration. The absence of MMRN2 showed a trend to enhanced migration and the wound closed faster than controls. In contrast, silencing CD93 alone or in combination with the silencing of CLEC14A or MMRN2 showed reduced migration. The greatest differences were observed at 12 and 18 hours. At 24 hours it was possible to see a closure of the wound in most cases, except for the ones where CD93 was silenced, which showed an open wound (Figure 3.9). Although the CD93 data did not reach significance it is in agreement with the literature (Langenkamp *et al.*, 2015).

3.7 CD93 knockdown significantly inhibited transmigration, whereas in contrast MMRN2 knockdown stimulated transmigration by HUVEC

The transwell migration assay assesses the ability of cells to directionally respond to different stimuli such as a chemo-attract gradient. Briefly, after starvation, 3×10^4 cells were plated on a gelatin-coated FluoroBlok 8.0 μm transwells in serum free media. In the bottom chamber growth factors and serum containing EBM2 media

were placed and cells were left for 5 hours. Transmigrated cells were then stained with DAPI and imaged. Finally, cells were manually counted with imageJ. In order to obtain reduced variability in the experiment, pictures of different areas of the membrane were taken. The sum of all the cells counted was considered the total number of cells transmigrated. The nuclei are imaged as larger grey dots in figure 3.10 (some indicated by blue arrows), whereas the white smaller uniform dots are the pores of the membranes. The calculation was performed uniformly for each condition.

Overall this experiment showed different effects for the knockdowns analysed. CLEC14A knockdown had no effect on cell transmigration. MMRN2 knockdown showed a significantly increased transmigration. CD93 knockdown showed a significantly decreased transmigration. CLEC14A/CD93 and MMRN2/CD93 double knockdown cells transmigrated in a similar fashion to CD93 knockdown alone. This experiment was repeated 3 times, using different cultures of commercial HUVEC cells transfected independently and showing comparable results (Figure 3.10).

3.8 Relative expression of CLEC14A and CD93 in HUVEC cells

CLEC14 and CD93 are proteins of the C-type lectin domain family 14, are both expressed in HUVEC cells and share the same binding site on MMRN2. We investigated their comparative expression in HUVEC cells in culture by western blot. Lysates of HEK293T cells overexpressing either CLEC14A-GFP or CD93-GFP were prepared along with a lysate from HUVEC cells. Equal amounts of the lysates were

used for western blotting with GFP, CLEC14A and CD93 antibodies. Blots were developed with Odyssey Imager and quantified with the software ImageStudioLite. In order to calculate relative expression, the relative amounts of GFP fusion protein in the lysates was obtained and used to work out the relative efficiencies of the two antibodies within the same GFP lysates. Finally, this value was used to normalise the expression of CLEC14A and CD93 in the HUVEC lysates and the result was expressed as fold change compared to the expression of CLEC14A in HUVEC cells. This showed that under these culture conditions, CD93 is expressed 10 times more than CLEC14A (Figure 3.11).
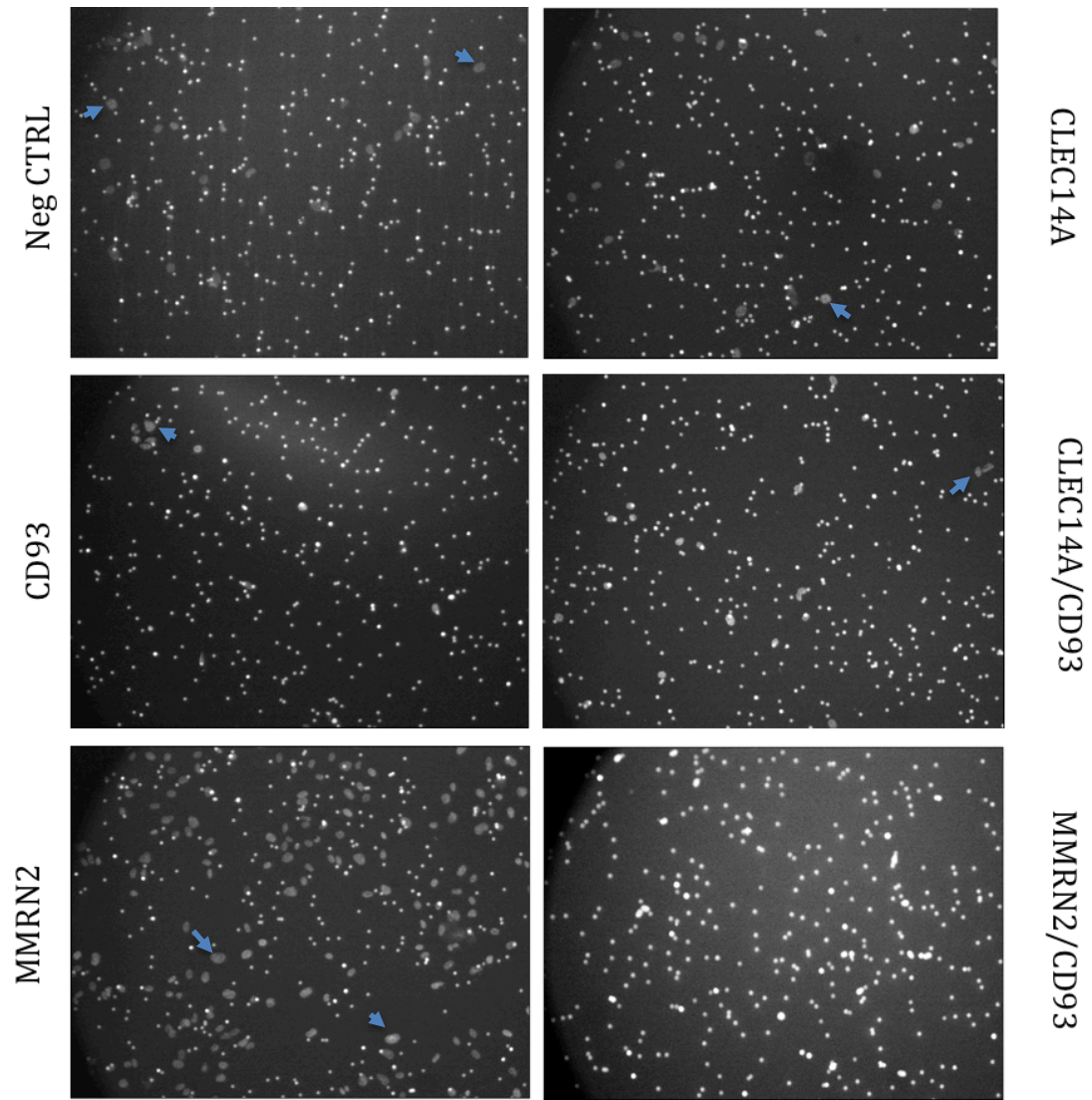
Transswell migration
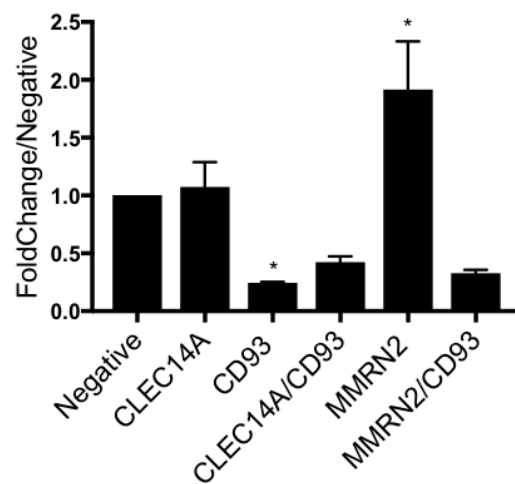
(Legend on the next page)

Figure 3.10 CD93 knockdown strongly impaired transmigration, whereas MMRN2 knockdown stimulated transmigration in HUVEC

Cells were transfected as for the previous functional assay. Before the assay, cells were incubated in starvation M199 medium, without growth factors, calcium and magnesium. After starvation, in the same medium HUVEC were plated in the transwell, whereas in the bottom chamber complete EBM2 was placed. Cells were left migrating for 5 hours at 37°C. At the end of the transmigration, the lower part of the chamber was fixed and stained with DAPI. Nuclei (some indicated by the blue arrows) were manually counted. The images are one representative of 3 experiments. The graph expresses the transmigration data as fold change versus the negative control of the total cells transmigrated. The experiment showed a significant reduction in transmigration in absence of CD93 and significant increase in transmigration in absence of MMRN2. n=3 (Duplex 2 for each gene was used once) *$p<0.05$ versus negative control ANOVA (Dunnet's test). The graph shows mean ± SEM.
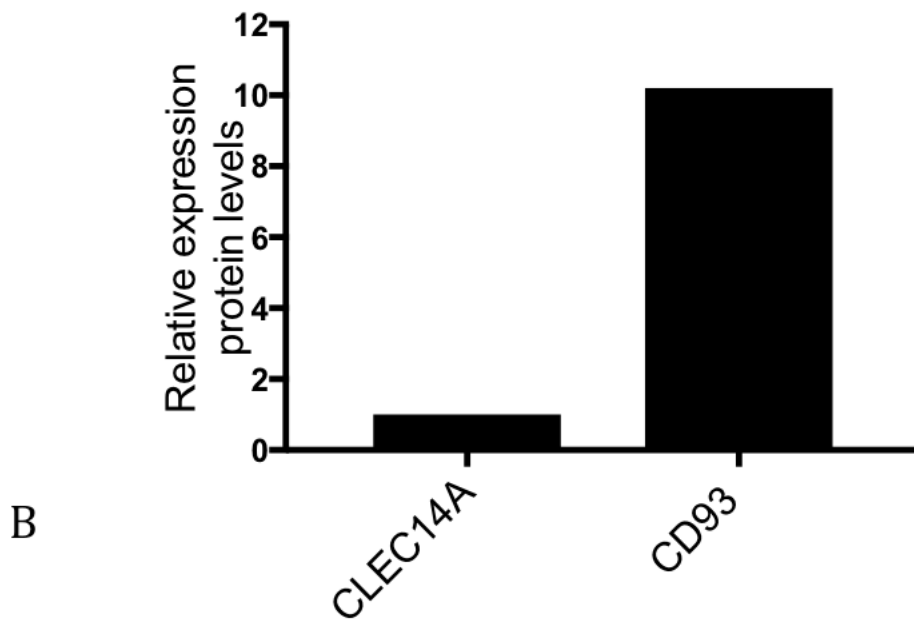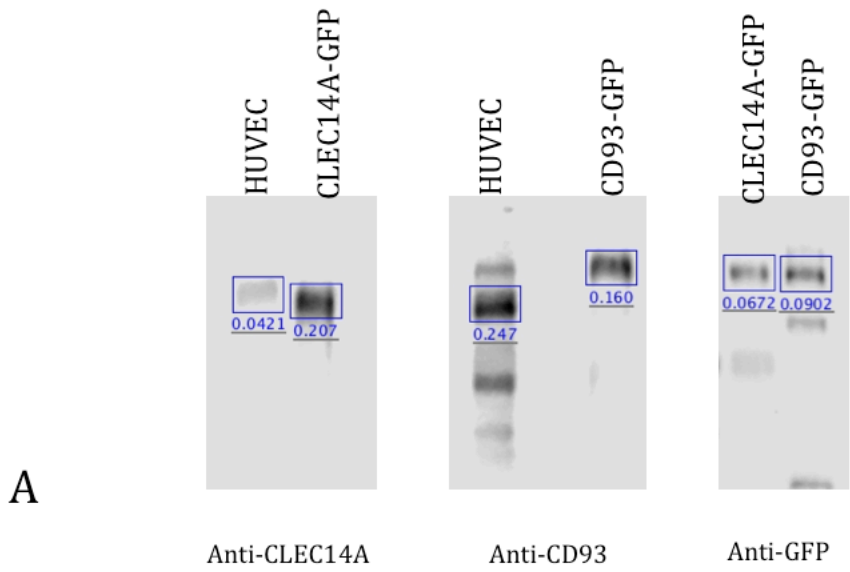
Figure 3.11 Relative expression of CLEC14A and CD93 in HUVEC cells

A. HEK293T were transfected with plasmids encoding CLEC14A-GFP, CD93-GFP and lysates were prepared. These and HUVEC lysates were subjected to western blot with respective antibodies and the reaction was developed using an Odyssey machine. With the dedicated software ImageStudio lite the bands were quantified. B the chart shows calculated relative CLEC14A and CD93 protein levels in HUVEC expressed as fold change/CLEC14A.

3.9 Discussion

CD93 knockdown showed a clear Matrigel phenotype. For this reason, the double knockdowns of CLEC14A/CD93 and MMRN2/CD93 were also studied. First, the efficacy of the duplexes was assessed by western blot. Both single and double knockdowns were successful at the mRNA and protein level. The efficacy of the duplexes chosen to knockdown CD93 was originally described in a previous report (Langenkamp *et al.*, 2015). In the course of this work, the potential co-regulation of CLEC14A, CD93 and MMRN2 has not been investigated. A recent report suggests that the knockdown of MMRN2 is affecting the protein expression of CD93, due to loss of stability (Lugano, Dejana and Dimberg, 2018). Further analyses would be necessary to confirm this regulation and to investigate the regulation of expression of CLEC14A and MMRN2 upon the different knockdowns. Once the efficacy of the knockdowns was confirmed, it has been evaluated whether the transfection of HUVEC with the different duplexes was affecting HUVEC proliferation and progression of the cell cycle. An MTT assay showed that there is no significant effect of knockdown on proliferation of HUVEC. No effect on proliferation for CD93 knockdown in HDMEC has been reported previously (Langenkamp *et al.*, 2015).

It has been reported in the literature a role of CD93 in cell cycle and the silencing of CD93 in acute myeloid leukaemia cells led to an increased number of quiescent cells (Iwasaki *et al.*, 2015). However, in HUVEC the analysis of the cell cycle performed has shown no changes. Interestingly, it is shown that on CD93 knockdown HUVEC do not become quiescent, as has been reported in AML cells.

Although single knockdowns of CLEC14A, CD93 or MMRN2 have been reported, double knockdowns have not. In agreement with previous literature, the single knockdown of CD93 strongly inhibited the tube formation in endothelial cells (Langenkamp *et al.*, 2015). This was also observed when the silencing of CD93 occurred in combination with CLEC14A or MMRN2. Surprisingly, this experiment failed to reproduce what has been previously reported for CLEC14A (Rho *et al.*, 2011; Mura *et al.*, 2012). In fact, the result showed that upon CLEC14A knockdown not only no reduction in tube formation was observed but also that the effect was a consistent, but not significant, increase in the number of meshes. Although Mura and colleagues reported a strong reduction in tube formation, this effect has been observed only at 0h (the moment when the cells are seeded) but not at 12 and 24 hours. At the latter time points in fact, when a proper phenotype is actually observable, the figure shows a strong increment in tube formation upon siRNA-mediated knockdown of CLEC14A when compared to the control. Due to discrepancies between the discussion and the figures, it is unclear whether these findings are relevant to support either one or the other phenotype observed (Mura *et al.*, 2012). An explanation for the differences observed with the another report that showed CLEC14A as a pro-angiogenic molecule (Rho *et al.*, 2011) might be the presence of VEGF in the medium. In the experiment performed in this work cells were incubated with EMB2 media containing different growth factors, including VEGF, whereas Rho and colleagues used a basic M199 media containing only basic FGF. The strong pro-angiogenic signalling of VEGF might have overcome the absence of CLEC14A acting on different pathways. Over the past few years contrasting

reports have been published reporting different roles of CLEC14A in angiogenesis also *in vivo* (Noy *et al.*, 2015; Lee *et al.*, 2017). It is possible to speculate that the role of CLEC14A might be context dependent and according to what interactions are involved different signalling pathways might be activated downstream. To note, the double knockdown CLEC14A/CD93 clearly showed a strong reduction in tube formation, comparable to what observed for CD93 alone, suggesting that CLEC14A did not rescue or strengthen the CD93 phenotype. Similarly, it was observed when CD93 was silenced along with MMRN2, indicating that CD93 is necessary. In agreement with the published role of MMRN2 as an angiostatic protein, which sequesters VEGFA molecule, the absence of MMRN2 in tube formation led to a significant increase of the number of meshes (Lorenzon *et al.*, 2012). These findings are in contrast with other publications which advocate for MMRN2 angiogenic properties (Zanivan *et al.*, 2013; Noy *et al.*, 2015). The results here obtained on Matrigel were also supported by a co-culture assay with fibroblasts. In this more physiological assay, upon CLEC14A knockdown the network formation showed a slight impairment when compared to the control, corroborating the possibility that CLEC14A phenotype might vary based on different environmental conditions. The time-course of the knockdown confirmed at the protein level that the during the co-culture experiments the silencing was effective up to the 4th day after transfection, indicating that any phenotype observed was due to the siRNA transfection. It is possible to assume that even if the expression of each protein would be restored in the last two days of the experiment that the phenotype would still be appreciable.

CD93 was shown to be an important mediator of tube formation, and also HUVEC migration and chemotaxis. Upon CD93 knockdown both HUVEC migration was retarded and chemotaxis was strongly impaired in a transwell experiment. This confirms what has been published (Langenkamp *et al.*, 2015; Galvagni *et al.*, 2016). Interestingly, neither the dual knockdown with CLEC14A or MMRN2 rescued or aggravated the phenotype. A recently proposed mechanism showed that the presence of MMRN2 is necessary for the stabilization of CD93 and its correct localization at the front of the migration (Lugano, Dejana and Dimberg, 2018). Based on this mechanism it was a surprise that the absence of both CD93 and MMRN2 did not recapitulate the phenotype of the single MMRN2 knockdown. This might be explained by the fact that in absence of MMRN2, CD93 shedding is strongly upregulated releasing CD93 in its soluble form. It has been reported that soluble CD93 stimulates angiogenesis *in vitro* and *in vivo* (Kao *et al.*, 2012). For this reason, it is plausible that an increased soluble CD93 within the medium stimulated the angiogenic phenotype observed upon MMRN2 knockdown.

Furthermore, it has been also reported that MMRN2 can function as a VEGF-A trap, impeding the VEGF/VEGFR2 signalling pathway (Lorenzon *et al.*, 2012). The absence of MMRN2 strongly increases the availability of VEGF-A within the medium, leading to a stronger angiogenic phenotype. The interaction between CLEC14A and MMRN2 was proven to be important for angiogenesis and its disruption led to a reduction in angiogenesis both *in vitro* and *in vivo* (Noy *et al.*, 2015). It is reasonable to speculate that in absence of either CLEC14A or MMRN2 the resulting phenotype would show less angiogenesis. Based on these results, it is possible to conclude that due to the

different interactions with which MMRN2 is implicated are predominant in this specific setting than the one signalling through the interaction MMRN2/CLEC14A. Moreover, this might in part explained by the fact that CD93 is 10 times more expressed than CLEC14A in HUVEC cells. Due to their relative levels, it is not possible to exclude that these two proteins might have the same role and, for this reason, the effects upon loss of CLEC14A are much less evident in HUVEC *in vitro*. It is important to note that the band of CLEC14A-GFP in HEK293T cells was expected to run at a higher molecular weight than endogenous CLEC14A in HUVEC cells. This behaviour was also previously reported by Khan et *al.*, in far western experiments employing the same construct. A plausible explanation might be an impairment or a different glycosylation pattern expressing this construct in HEK293T, compared to endogenous CLEC14A in HUVEC. To confirm this, the same construct could be used to transfect HUVEC and verify by Western if CLEC14A GFP runs at a higher molecular weight than in HEK293T.

Here we present the first comparison of CLEC14A and CD93 function. These data suggest that CD93 is a much stronger mediator of angiogenesis than CLEC14A and this effect is CLEC14A and MMRN2 independent. In fact, the double knockdowns showed no aggravated or rescued phenotype, compared to CD93 alone. Interestingly the role of MMRN2 has been shown to be both pro- and anti-angiogenic (Lorenzon *et al.*, 2012; Zanivan *et al.*, 2013; Noy *et al.*, 2015; Colladel *et al.*, 2016; Khan *et al.*, 2017). The results in our setting reveal a more angiostatic phenotype, although it is clear that MMRN2 phenotype depends on a subtle balance. Little or no effects have been observed in these experiments when CLEC14A was knockdown.

CHAPTER 4: Development of novel approaches targeting CLEC14A

4. Development of novel approaches targeting CLEC14A

4.1 Introduction

The interaction of MMRN2 and CLEC14A has been shown to be important for tumour progression and that its disruption inhibited tumour growth and angiogenesis (Noy *et al.*, 2015). The kinetics and structural studies of the binding between CLEC14A and MMRN2 have shown that it is a tight and stable interaction (Khan *et al.*, 2017). Moreover, Khan and colleagues identified, employing deletion mutants of MMRN2 in Far western blots that a minimal region of MMRN2 still bound. Due to its antibody-like binding affinity the MMRN2 fragment was particularly appealing for possible therapeutic uses. In addition, mouse MMRN2$^{495-678}$-mFc expressing cancer cells injected subcutaneously in syngeneic mice showed a reduction in tumour growth compared to the mFc expressing counterpart (Khan *et al.*, 2017). For these reasons and the fact that CLEC14A was a characterised tumour endothelial marker (Mura *et al.*, 2012), it was decided to further investigate the properties of the recombinant protein mouse MMRN2$^{495-678}$ and to elaborate different strategies to exploit this fragment in targeting specifically tumour endothelium.

Targeted toxins are a group of therapeutics employed in cancer research to specifically kill cancer cells and avoid the possible side effects of non-specific cancer therapies. Targeted toxins work due to two functional parts: the toxic component, which causes cytotoxicity, and a targeting ligand, which directs the complex to the target. For example, there are studies showing the efficiency of ligands conjugated

to Dianthin from *Dianthus caryophyllus L*. (Von Mallinckrodt *et al.*, 2014; Bhargava *et al.*, 2017).   Dianthin is an enzyme, which is able to mediate the cleavage of a particular bond in the 28S RNA of mammalian cells. This cleavage releases an adenine residue, impeding the binding of the eukaryotic elongation factors, resulting in the arrest of protein synthesis. This block of synthesis eventually leads to apoptosis and cell death. In order to act appropriately as a toxin, dianthin needs to be released in the cytosol. This means that the fusion partner of dianthin within the fusion complex should be internalized.

The aim of this chapter was to produce a stable recombinant MMRN2 fragment retaining the binding properties to CLEC14A that could be employed in different approaches targeting tumour endothelium via the interaction with CLEC14A.

4.2 Recombinant protein expression of human MMRN2$^{495\text{-}674}$ and mouse MMRN2$^{495\text{-}678}$

Previous work has identified the region of MMRN2 that binds to CLEC14A and CD93 (Zanivan *et al.*, 2013; Noy *et al.*, 2015; Galvagni *et al.*, 2017; Khan *et al.*, 2017). By constructing a series of deletion constructs, far western blot confirmed that this region lies between amino acids 495 and 678 in mouse and 495 and 674 in the human. The minimal binding region was found in a even smaller fragment, but this proved to be unstable. So, the MMRN2$^{495\text{-}674}$ fragment incorporating the binding region was studied instead. It is of interest that homology across vertebrate species of this region was high, showing that it was strongly conserved during evolution. In

this study, the mouse version was also produced with 4 additional amino acids: MMRN2$^{495-678}$. The fact that CLEC14A and CD93 shared the same binding site and that the binding was occurring with high affinity was suggestive of biological significance (Khan *et al.*, 2017). For these reasons it was decided to investigate further the properties of this peptide and to attempt to exploit it for therapeutic purposes.

In this work different variants of the peptide have been generated. Initially a mouse Fc-tagged version was designed. MMRN2$^{495-678}$ was cloned in a lentiviral pWPI vector using a PmeI restriction site. The signal peptide of CLEC14A was added at the N-terminus, and the human fragment crystallisable region (Fc) sequence was added at the C-terminus. The use of the lentiviral vector enabled the generation of a HEK293T cell line stably expressing MMRN2$^{495-678}$. The fragment was secreted from the cells due to the signal peptide and purified using the Fc fragment on a protein A column. In order to verify the correct secretion of the peptide a small amount of the medium was incubated with protein A beads and expression checked by gel electrophoresis and Coomassie staining (not shown). As the production/purification process was working efficiently, a larger scale preparation was carried out. The purity of the mouse fragment was analysed on a protein gel by Coomassie staining (Figure 4.1 A). The most concentrated aliquots, as measured by nanodrop, were also tested on western blot by detecting the human Fc fragment (Figure 4.1 B). This fragment was then studied in *in vitro* assays.
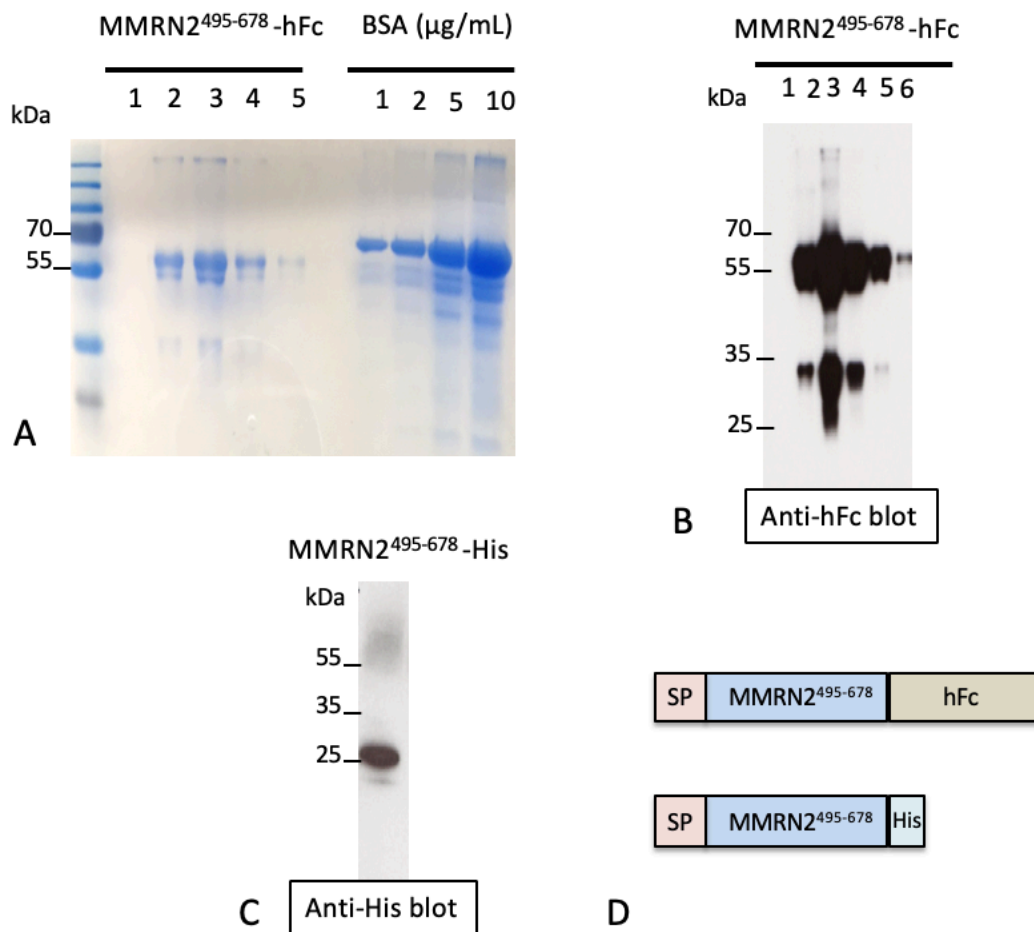
Figure 4.1 Production and purification of the hFc- and His-tagged recombinant mouse MMRN2[495-678]

In order to study the properties of the fragment, two tagged version of MMRN2[495-678] were produced. The constructs were designed to allow the production in mammalian cells and for the fragment to be released in the medium. MMRN2[495-678] was purified from media either on protein A columns (hFc-tagged version) or on Ni-NTA columns (His-tagged version). A. Protein gel stained with Coomassie blue to detect impurities after protein A column purification of MMRN2[495-678]. In each lane an equal volume of different aliquots of recombinant was loaded. BSA standard concentrations were used as control. B. The anti-hFc blot shows the accessibility of the hFc tag on the recombinant protein. C. Anti-his blot shows the accessibility of the His-tagged version of MMRN2[495-678]. MMRN2[485-678] was stable and the tag was accessible for purification and detection by western blot. D. Diagram of the fusion protein cloned and produced. From N-terminus, signal peptide (SP), the mouse MMRN2 fragment (495-678) and either an hFc-tag or an his-tag.
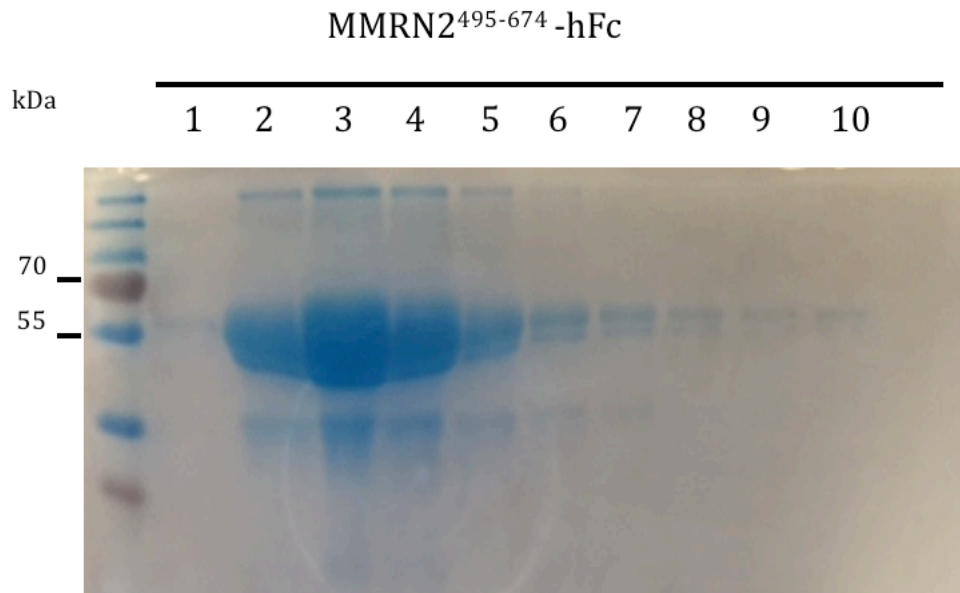
Figure 4.2 Production of hFc-tagged human MMRN2$^{495\text{-}674}$

Similarly to what was performed for the mouse version of the fragment, human MMRN2$^{495\text{-}674}$ was designed to be produced in mammalian cells (HEK293T) and released in the supernatant. The protein-containing media was collected and protein A columns were used for the purification. The figure shows a protein gel stained with Coomassie blue, in which different aliquots of purified MMRN2$^{495\text{-}674}$ were loaded at the same volume, showing the different stages of the elution phase. The numbers from 1 to 10 indicate the order of collection of the different fractions during purification.

In the course of the project, an immunisation experiment using the mouse MMRN2$^{495-678}$-hFc in mice was performed. For this reason, there was also a need for an identical fragment but with a different tag in order to monitor the response of the mice to MMRN2$^{495-678}$-hFc immunisation. For this purpose, the fragment was cloned into the same vector pWPI with the same signal peptide at the N-terminus but with a 6 histidine (His) tag at the C-terminus. The purity of the fragment was examined by SDS PAGE with Coomassie staining (not shown) and the His-tag was detected by western blot, using an anti-His antibody (Figure 4.1 C). Both the hFc and His tagged mouse fragments were produced efficiently and obtained at high purity with a yield in the range of 5-10 mg for each batch.

The human version of the fragment was also produced. MMRN2$^{495-674}$ was previously cloned into the pHL-Fc expression vector (Kabir Khan). This vector had a signal peptide and the hFc sequence, using the AgeI and KpnI restriction site, it was possible to clone in frame the sequence with the signal peptide at the N-terminus and the hFc at the C- terminus. In contrast to pWPI, pHL-Fc is not a lentiviral vector. Thus, the peptide was produced by transient transfection in this instance.

Purification was efficient and Coomassie blue stained SDS PAGE analysis showed few contaminants (Figure 4.2), yielding around 0.5-1 mg for each batch.

4.3 Peptides human MMRN2$^{495-674}$ and mouse MMRN2$^{495-678}$ bind CLEC14A transfected HEK293T and HUVEC cells

CLEC14A was previously validated as a tumour endothelial marker. Expression on the tumour vasculature is thought to be due to reduced shear stress. In other words, it would be possible to target CLEC14A in order to deplete tumour endothelium, resulting in starvation of the tumour and blockage of tumour growth (Mura *et al.*, 2012; Noy *et al.*, 2015). As MMRN2 binds at high affinity to CLEC14A and CD93 (Khan *et al.*, 2017), the fragment minimal stable (mouse) MMRN2$^{495-678}$-hFc fragment that bound to CLEC14A expressing cells was investigated.

To test whether the recombinant MMRN2$^{495-678}$-hFc fragment bound to CLEC14A was confirmed by FACS. It was important to determine whether or not the mouse MMRN2$^{495-678}$-hFc fragment could bind to human cells and *in vivo* experiments in mice. Due to difficulties in its production, the human MMRN2$^{495-674}$-hFc was used only in selected experiments to confirm the results obtained with the mouse counterpart.

HEK293T overexpressing CLEC14A full length or HUVEC that express both CLEC14A and CD93 endogenously, were incubated one hour with MMRN2$^{495-678}$-hFc. Control cells were incubated with a commercially available recombinant human Fc tag. Binding was confirmed with a fluorescent Alexa488 secondary antibody against the human Fc tag. Both control and MMRN2$^{495-678}$-hFc cells were then analysed by flow cytometry.

HEK293T cells overexpressing human CLEC14A full length were examined. The CRT2 monoclonal antibody was used as positive control. A reproducible increase in fluorescence was detected in cells incubated with the mouse MMRN2$^{495-678}$-hFc compared to the negative control incubated with hFc only. The increased fluorescence was comparable to that obtained with the CRT2 antibody (Figure 4.3).
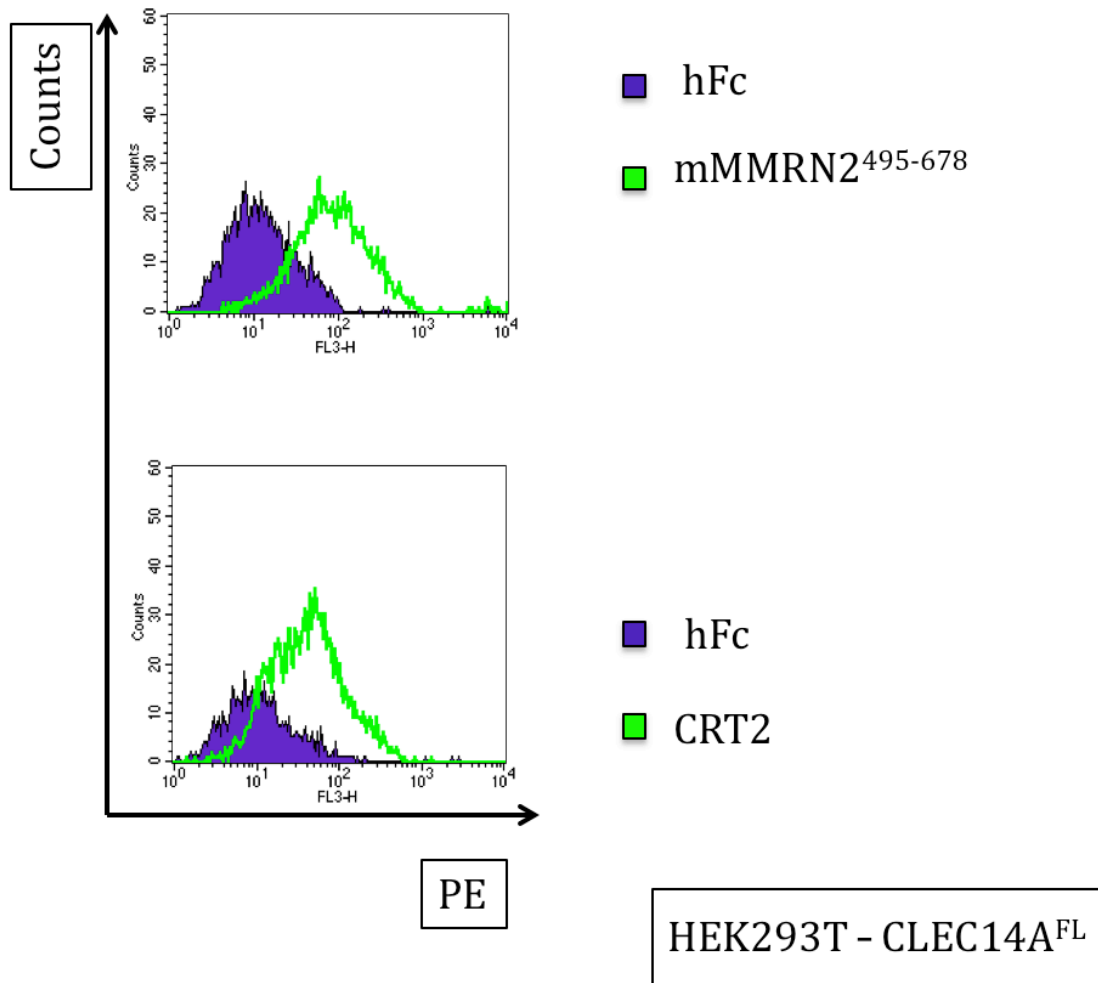
Figure 4.3 FACS analysis of the binding capacity of MMRN2$^{495\text{-}678}$ to CLEC14A transfected HEK293T cell

In order to see if the recombinant mouse fragment retained the binding properties of the full-length MMRN2 FACS was performed. Firstly, HEK293T cells were transfected with a construct coding for the full-length CLEC14A. 24 hours post-transfection, HEK293T cells were collected and stained with either hFc, CRT2 (monoclonal antibody for CLEC14A) or MMRN2$^{495\text{-}678}$-hFc. After incubation, each was stained with anti-hFc PE and cells were analysed by flow cytometry. The upper part of the figure, the flow cytometry histograms show an appreciable binding of MMRN2$^{495\text{-}678}$ to HEK293T expressing CLEC14A^{FL}. In the lower part binding of CRT2 is used as positive control. The experiment shows that MMRN2$^{495\text{-}678}$ binds to CLEC14A overexpressed on the cell surface and as does the antibody CRT2. The experiment was repeated 3 times.

This showed that recombinant MMRN2$^{495\text{-}678}$-hFc retained affinity towards CLEC14A and that there was cross-reactivity between mouse MMRN2$^{495\text{-}678}$ and human CLEC14A. The tertiary structure of this region was presumably not impaired, as the loss of the 3D structure of a protein is usually fundamental for the protein-protein interaction.

We next investigated binding to endogenous CLEC14A. Previous studies showed that CLEC14A is expressed endogenously in HUVEC (Rho *et al.*, 2011; Mura *et al.*, 2012). In a similar fashion both mouse MMRN2$^{495\text{-}678}$-hFc and human MMRN2$^{495\text{-}674}$-hFc showed an increment of fluorescence at the flow cytometer when compared with the hFc alone. Moreover, these shifts were comparable indicating a similar behaviour towards the target.

Both employing MMRN2$^{495\text{-}678}$-hFc and MMRN2$^{495\text{-}674}$-hFc it was possible to detect a consistent binding to HUVEC compared to hFc alone (Figure 4.4).

It has been shown that the MMRN2 binding site on CLEC14A is in the same region as the binding site of the CRT4 antibody (Noy *et al.*, 2015). In order to further evaluate the activity of the recombinant MMRN2 fragment, a blocking experiment was performed. Cells were first blocked with IgG, CRT4 or CRT2. CRT2 was used as negative control, because it has been shown to bind a different epitope to MMRN2 and CRT4. Therefore, blocking with CRT2 was expected to have no reduction of recombinant MMRN2 binding and no shift of the fluorescence. When cells were first
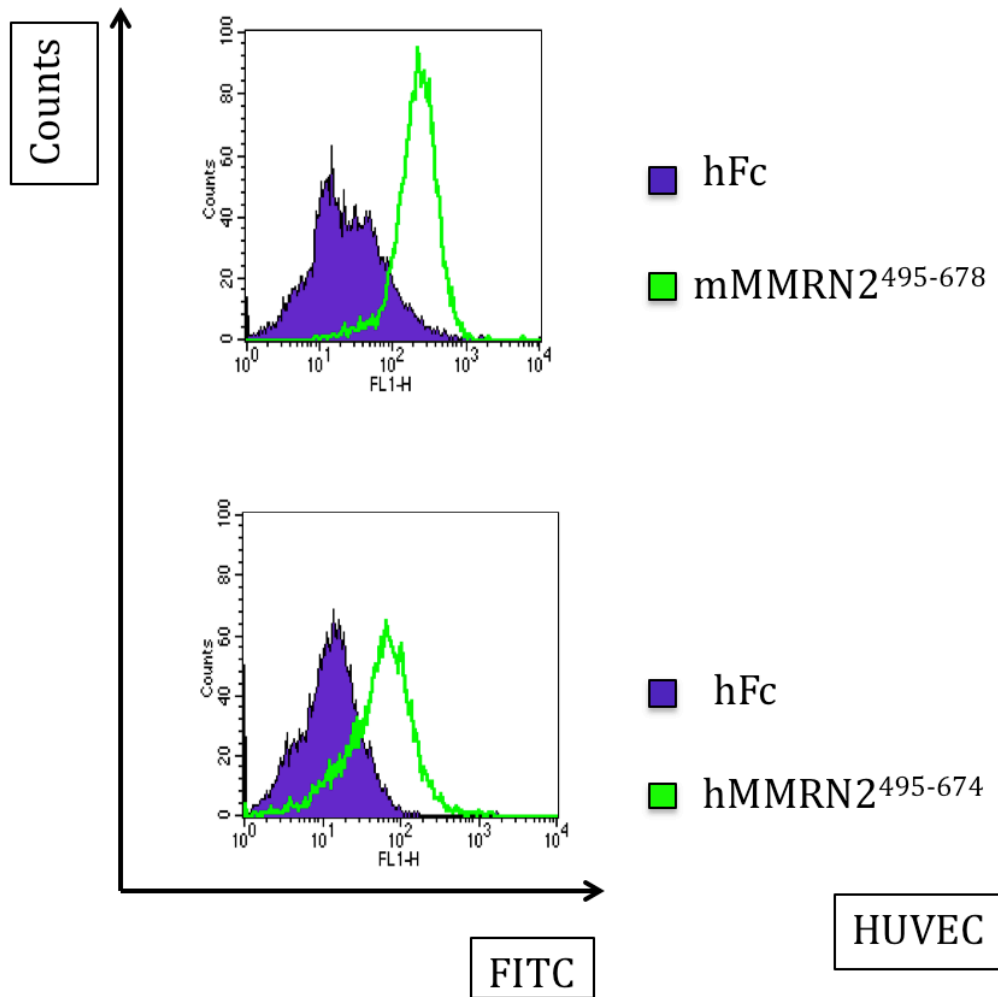
Figure 4.4 Testing the binding capacity of mouse MMRN2$^{495-678}$-hFc and human MMRN2$^{495-674}$-hFc in HUVEC

To assess if both human and mouse recombinant fragments are able to bind to HUVEC, which express MMRN2 binding CLEC14A and CD93 at a physiological level, FACS analysis was performed. HUVEC were incubated with the two versions of the fragment or hFc as negative control. As secondary antibody an anti-hFc FITC was used. Stained cells were analysed by flow cytometry. The experiment demonstrated that both the mouse (upper graph) and the human (lower graph) version of MMRN2 fragment were able to bind HUVEC. The experiment was repeated 3 times with similar results.

Figure 4.5 CRT4 and MMRN2$^{495\text{-}678}$ bind to the same region of CLEC14A

To confirm previously published data in which it was demonstrated that CRT4 and MMRN2 are binding on the same CLEC14A site. HUVEC cells were blocked with either IgG, CRT2 and CRT4 antibodies. It is known that CRT4 binds the same site on CLEC14A than MMRN2, whereas CRT2 bind an alternative site. Cells were washed and incubated with either mouse MMRN2$^{495\text{-}678}$-hFc or recombinant hFc alone. The loss of mouse MMRN2 binding when HUVEC were blocked with CRT4 but not with CRT2 or IgG. The experiment was repeated 3 times with similar results.

blocked with CRT4, the shift corresponding to MMRN2$^{495-678}$-hFc binding was lost, indicating that CRT4 was blocking all the binding sites for MMRN2$^{495-678}$ (Figure 4.5).

4.4 Vaccination against the mouse MMRN2$^{495-678}$-hFc fragment in mice

Previous studies have shown examples of vaccination in mice against at least two different tumour endothelial markers (Zhuang *et al.*, 2015; Ferguson *et al.*, 2016). Vaccination resulted in a reduction in tumour growth by generating an antibody response against the antigen used. In both cases the extracellular portion of a mouse protein was fused with a hFc. This method showed an antibody response to hFc, also breaking tolerance against the mouse portion of the chimeric protein (Zhuang *et al.*, 2015; Ferguson *et al.*, 2016). For this reason, we decided to examine the response to a chimeric mouse MMRN2 fragment human Fc protein (Figure 4.6).

4.4.1 Antibody response to mouse immunisation with MMRN2$^{495-678}$-hFc

The mouse MMRN2 fragment was examined as a vaccine. C57BL/6 mice were injected with 50µg of protein (either MMRN2$^{495-678}$-hFc or hFc) mixed with complete Freund's adjuvant (CFA) at day 0. Mice were boosted twice with the same amount of protein in incomplete Freund's adjuvant (IFA) every two weeks. The ratio between the protein and the adjuvant was 1:1 (v/v) and mixed to form an emulsion. Each boost was injected subcutaneously. A final boost was given in PBS with an intraperitoneal injection (IP) (Figure 4.7). In order to test the immune response, before each immunisation, 50µL of blood was collected from each mouse and the
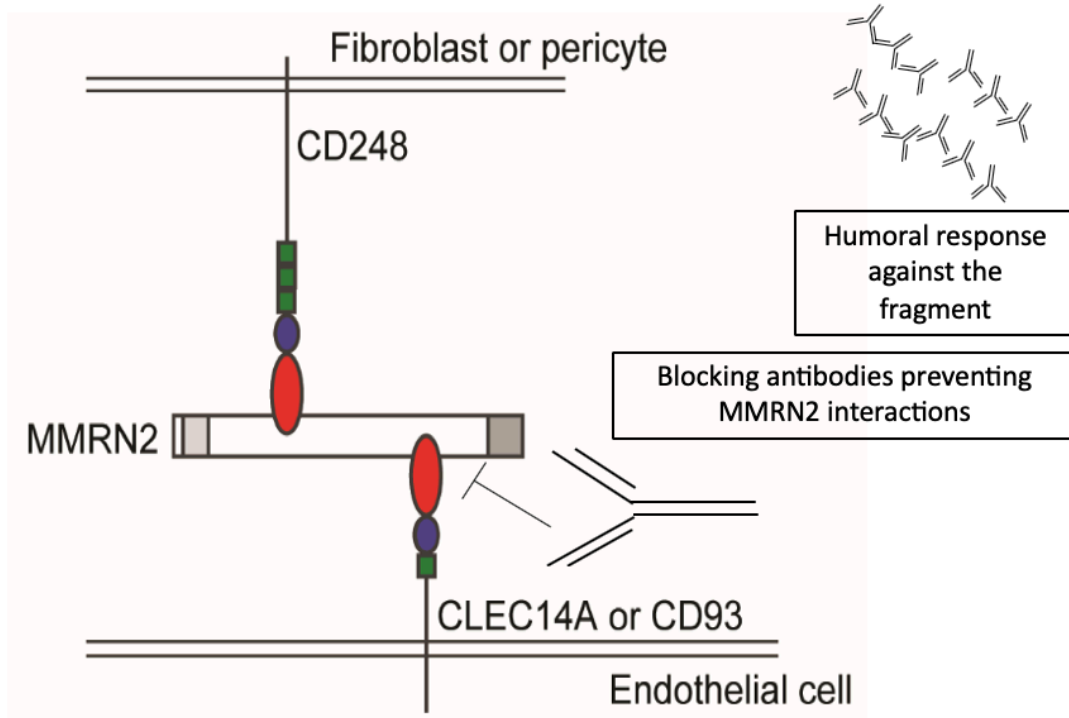
Figure 4.6 Schematic diagram of the MMRN2495-678-hFc vaccine approach

Representation of the MMRN2 interactions with CLEC14A and CD93 and the expected immune response disrupting these interactions. The generation of blocking antibodies upon immunisation with the binding MMRN2 fragment are expecting to disrupt the interaction between MMRN2-CLEC14A and MMRN2-CD93, impairing angiogenesis and leading to a reduction of tumour growth in an LLC subcutaneous tumour model.

Bleed
Day 0

Bleed
Day 14

Bleed
Day 28

Bleed
Day 43

End of the experiment
Day 13 after implantation

2 weeks later

S.C. CFA
Day 1

S.C. IFA
Day 15

S.C. IFA
Day 29

IP PBS
Day 44

LLC Tumour
Implantation
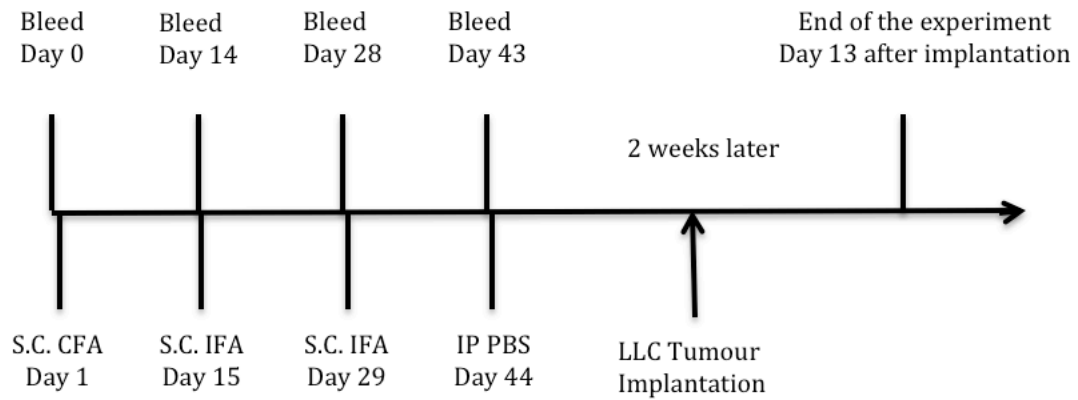
Figure 4.7 Schematic representation of the immunization strategy

On day 1, 15, and 29 mice were subcutaneously injected (SC) with the antigen in either complete or incomplete Freund's adjuvant (CFA or IFA). Before each injection, mice were bled to monitor the possible immune response. Following immunisation, Lewis Lung Carcinomas cells were implanted subcutaneously and tumour growth and weight were monitored. Due to ulcers at the injection site in some of the mice, the experiment was ended 13 days after tumour implantation.

Last bleed

**CTRL Cohort
hFc immunisation**

- ●— hFc response
- ■— mMMRN2 response

**Treated Cohort
mMMRN2-hFc immunisation**

- ●— hFc response
- ■— mMMRN2 response

A

B

150

Average response mMMRN2 - mMMRN2 cohort

C

1:10^2 dilution
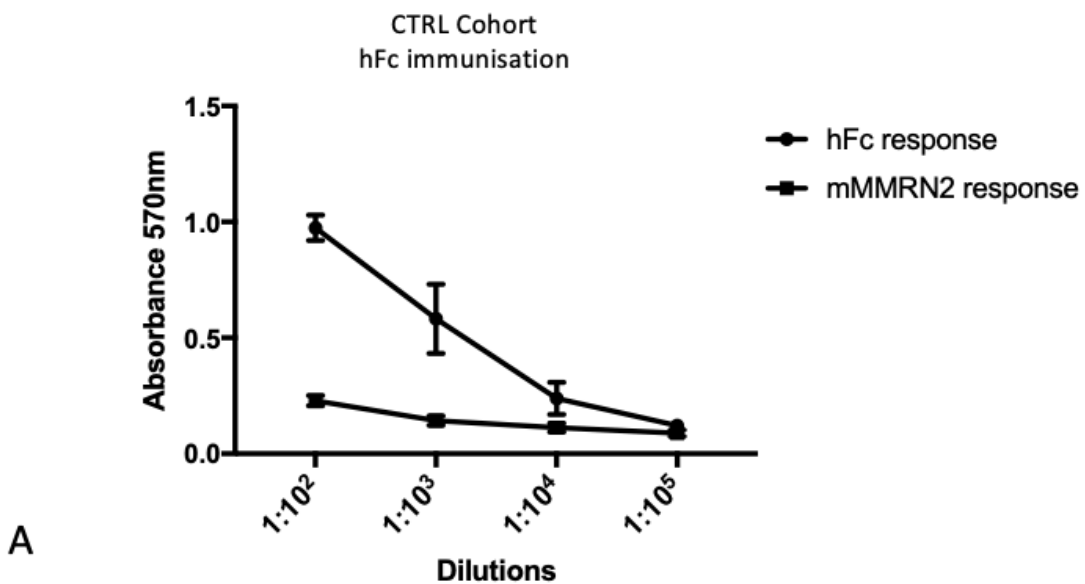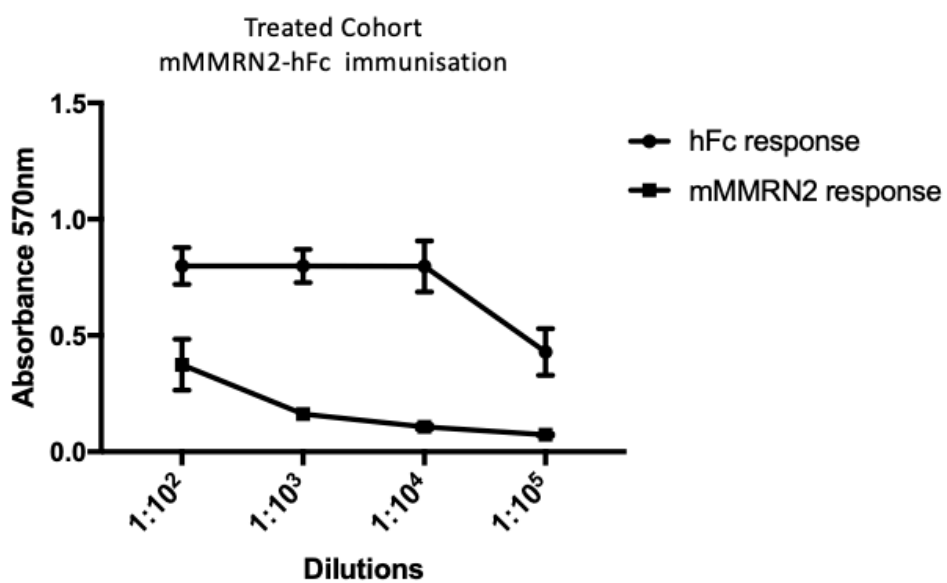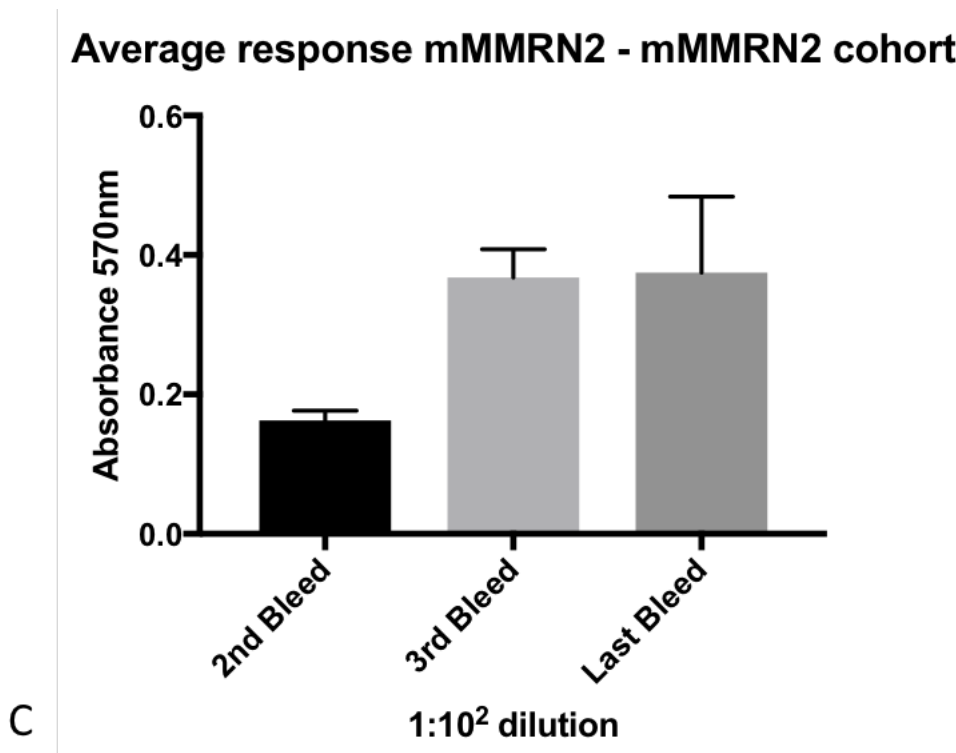
Figure 4.8 Humoral response upon mMMRN2$^{495-678}$-hFc and hFc immunisation

To monitor the immune response after subcutaneous immunisation, blood from the mice was collected and the serum was tested against mMMRN2$^{495-678}$-His in ELISA assay. A The graph shows the humoral response after the last bleed in the hFc control group at different dilution against both hFc and mMMRN2$^{495-678}$. There is a strong response to hFc but a very weak response towards mMMRN2. B. The graph shows the response of the mMMRN2$^{495-678}$-hFc group. There is a strong response to hFc; whereas there is little, if any, response against mMMRN2. C. Average response against mMMRN2 in mMMRN2 cohort for the last three bleeds. (n=9 ± SEM)

serum was tested in ELISA at different dilutions (from $1:10^2$-$1:10^5$). In order to detect the response to MMRN2$^{495\text{-}678}$ and not to the hFc tag (that was the most immunogenic portion of the antigen), an ELISA screening was performed against MMRN2$^{495\text{-}678}$-His. As shown by the last bleed, there was a strong response to hFc both in the control group and in the MMRN2$^{495\text{-}678}$-hFc. The response to MMRN2$^{495\text{-}678}$ was absent in mice immunised against hFc (Figure 4.8 A). It was possible to see a small increase in the response to MMRN2 along the last three immunisations in the mice immunised against the fragment (Figure 4.8 B). Nevertheless, if in the last bleed the response towards the fragment of the treated group was compared with the response of the control group it was clear that the immunisation using the mouse MMRN2$^{495\text{-}678}$-hFc was weak (Figure 4.8).

4.4.2 Effects of the vaccination on tumour growth in a LLC mouse model

Although the vaccination response to the MMRN2$^{495\text{-}678}$ fragment was much weaker than published studies on ROBO4 and GRIN2D, Lewis Lung Carcinoma (LLC) cells were implanted in vaccinated mice. 10^6 LLC cells were injected subcutaneously in both control and treated mice. Tumour size was monitored. The experiment was terminated 13 days after tumour implantation, due to the formation of ulcers at the injection site (Figure 4.9). Tumour volumes were measured using a calliper and the volume was calculated using the following formula V= $\pi\times[d^2\times D]/6$, where d is the minor tumour axis and D is the major tumour axis. Additionally, after all tumour-bearing mice were culled and tumours excised, the wet weight of each tumour was recorded. No observable differences were found in tumour growth between the
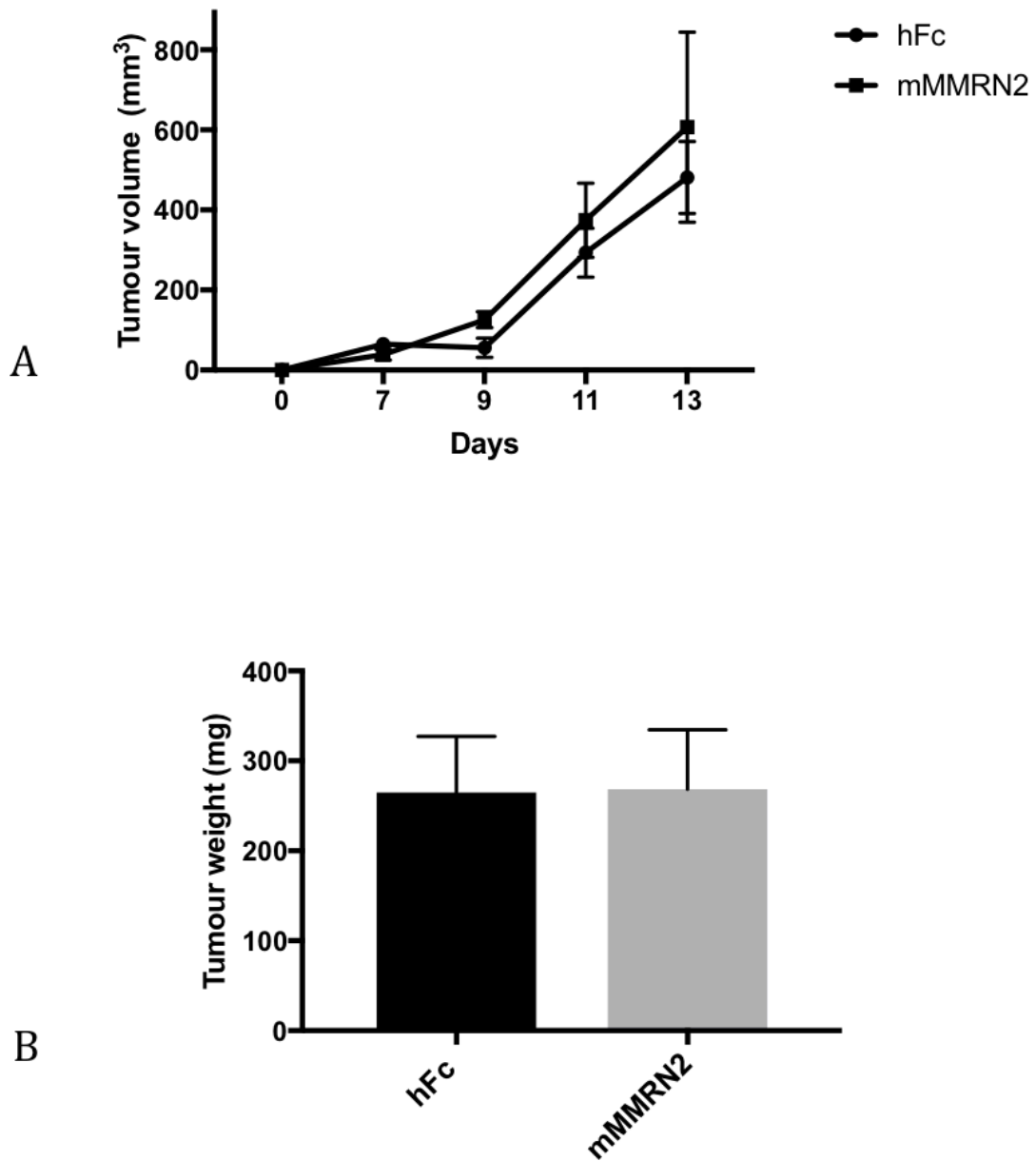
Figure 4.9 Effects of mMMRN2[495-678]-hFc immunisation on tumour growth and burden

After tumour implantation, tumours were measured using a caliper and, at the end of the experiment, were dissected out and weighed. A. the graph shows the kinetic of growth of the tumours in mice immunised with mMMRN2 versus the ones immunised with hFc. B. The bar chart shows the mean weight of the tumours between the two experimental groups. The experiment showed no observable differences in tumour growth or burden. (n=9 ± SEM).

MMRN2$^{495-678}$ vaccinated mice and hFc control (Figure 4.9 A). Moreover, the average tumour weight of the treated mice was consistent with the average tumour weight of the control group (Figure 4.9 B). In conclusion, the mild immune response obtained against MMRN2$^{495-678}$ did not affect tumour growth in the LLC tumour model compared with the control group.

4.5 Internalisation of the multimerin fragments

Overviewing all the different possibilities to exploit mouse MMRN2$^{495-678}$ binding with the TEM CLEC14A, the option to conjugate the fragment with toxins in order to target the tumour vasculature was considered. It was decided to opt for the use of targeted anti-tumour toxins, such as dianthin.

Due to their mechanism of action of the toxins chosen it was important to check whether the recombinant fragment of MMRN2 could also be internalized. There was evidence from unpublished data that the binding of CLEC14A was inducing internalization of the CRT antibodies (Lodhia, PhD Thesis 2017). Internalisation of the mouse MMRN2$^{495-678}$-hFc was investigated in HUVEC.

Firstly, cells were starved with serum-free media for 30 minutes. The protein was added to a final concentration of 5µg/mL and incubated for different times. After incubation cells were fixed in 4% PFA and stained. Recombinant hFc was used as negative control. Different time points were chosen according to the ones used for the antibody internalization study: 70, 90 and 120 minutes. The slides were stained

	DAPI	Endosomes	Anti-hFc	Merge	

hFC

70'

90'

120'

MMRN2$^{495-678}$

70'

90'

120'

A

DAPI

Endosome EEA1

α-hFc

Merge
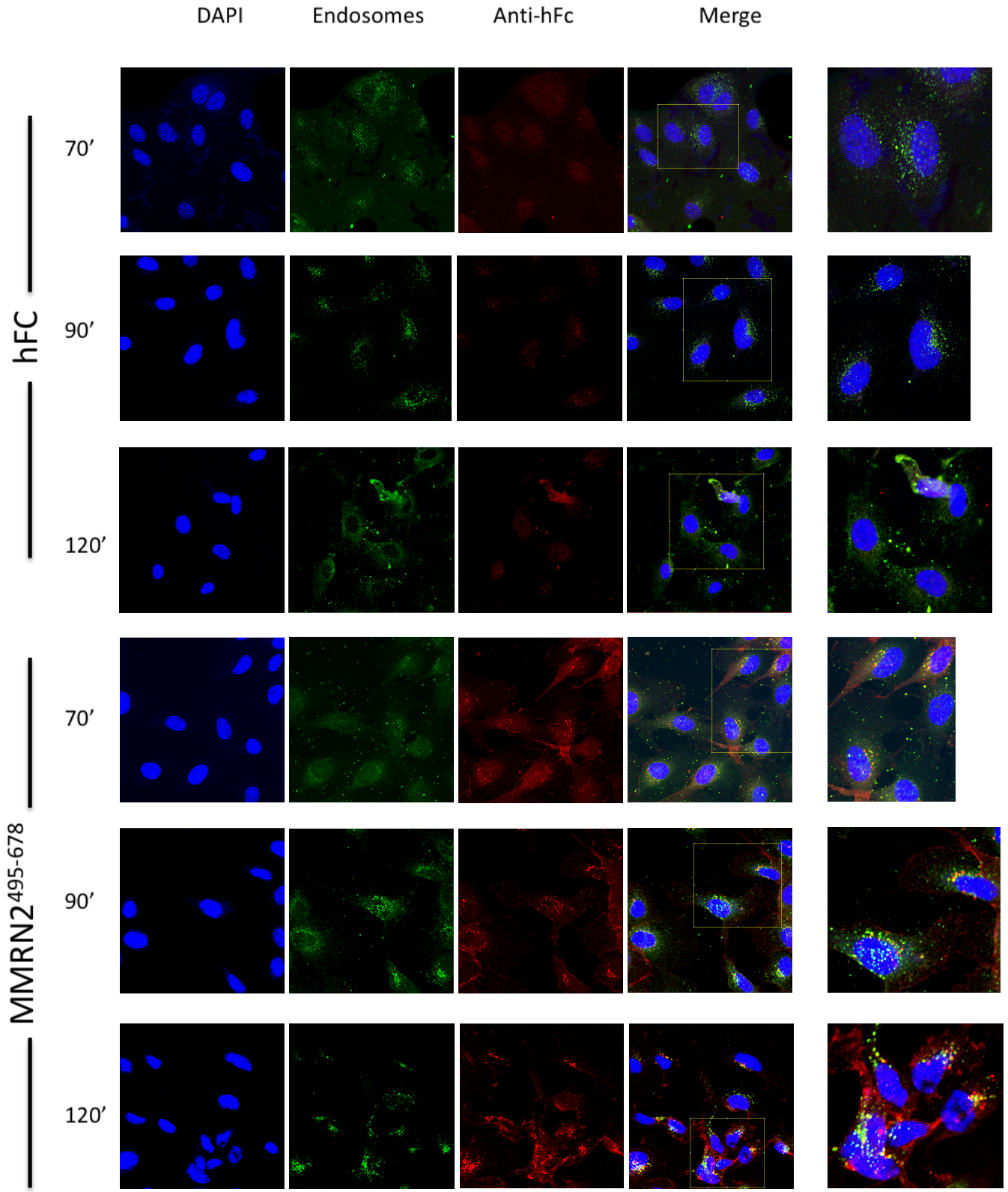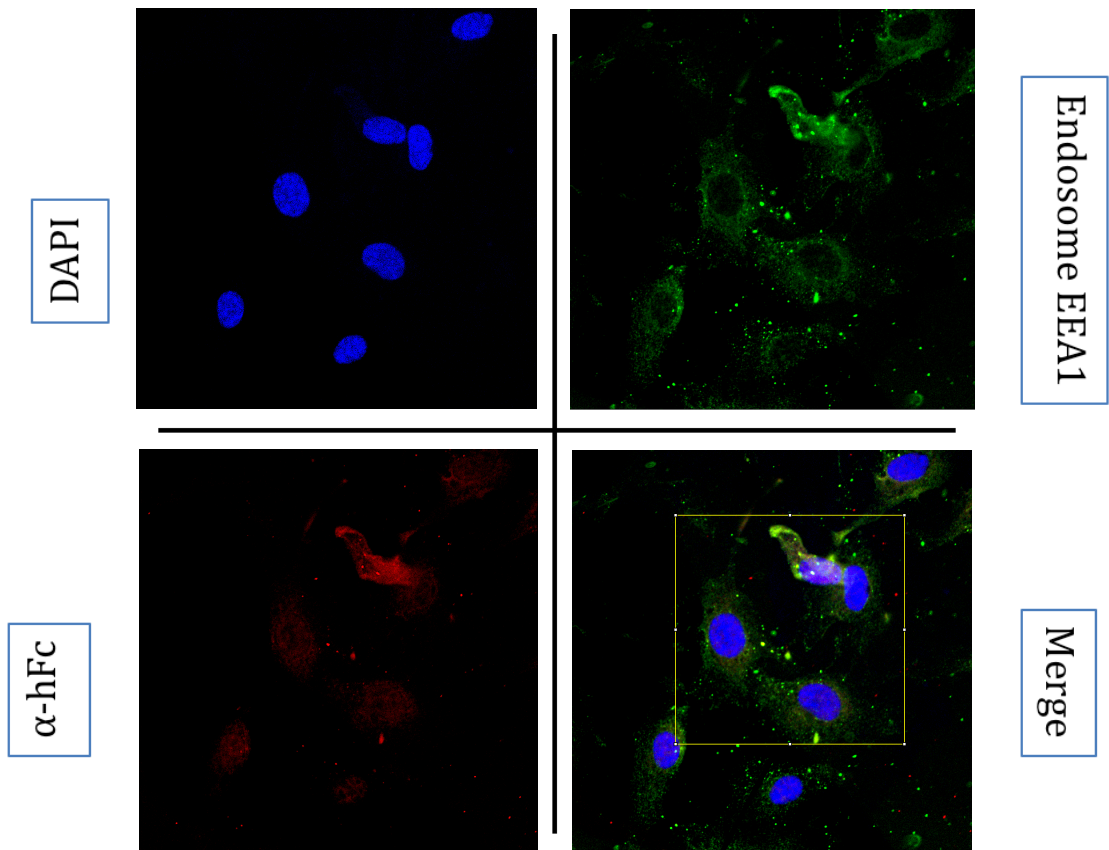
hFc control
Staining
120'

B

156
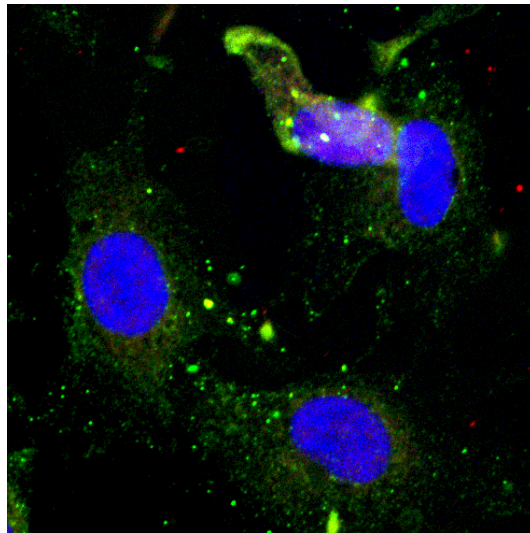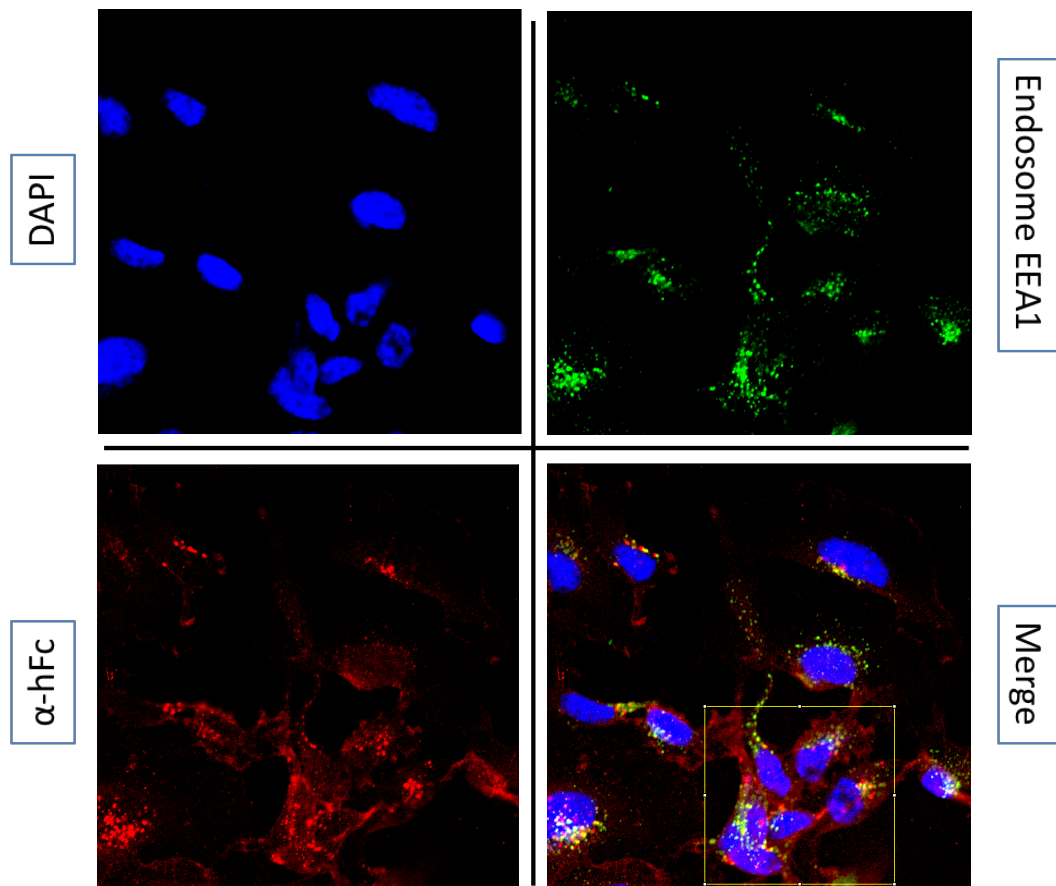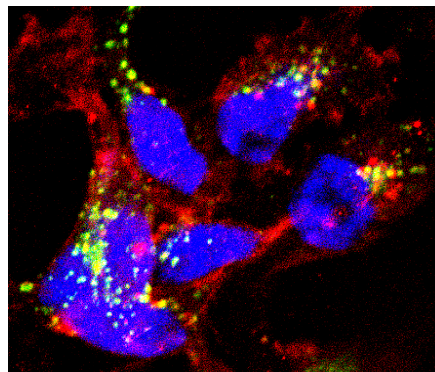
Figure 4.10 mMMRN2$^{495-678}$-hFc internalisation in HUVEC cells

To examine if the mMMRN2$^{495-678}$-hFc fragment behaves as CRT antibodies, which are internalised, an internalisation experiment was carried out. Either the fragment or hFc were incubated with HUVEC cells and at the end of each timepoint cells were fixed and stained (DAPI, α-hFc and EEA1). Cells were imaged by confocal microscopy. This experiment showed mMMRN2 internalised at the earliest timepoint (70'), but signal is absent in the same channel for cells treated with hFc only. A Shows images at each time point for both mMMRN2 and hFC treated cells. B The images show the hFc treated HUVEC at 120' (zoomed in) C. The images show the mMMRN2-hFc treated HUVEC at 120' (zoomed in). The experiment was repeated 3 times with similar results (n=3).

with anti-hFc for hFc/MMRN2$^{495-678}$-hFc, anti-EEA1 (early endosome antigen 1) for endosomes and DAPI for nuclei.

Overall, it was possible to see a positive staining for mMMRN2-hFc starting from the 70' time point. Consistently, the staining was positive in the following time points at 90 and 120 minutes. Interestingly, only part of the staining was co-localising with the endosome staining suggesting that the internalization of the fragment could be mediated by endosomes. The presence of MMRN2 was also seen in the cytosol, which is important when conjugated with Dianthin to obtain the cytotoxic effect of the inhibitor. This was also correlating with the previous unpublished findings on the internalization of CRT3 and CRT4. There was no signal in the hFc channel for HUVEC treated with hFc only, indicating that the signal observed with MMRN2-hFc was specific. In fact, there was no signal detectable in hFc treated HUVEC at any time point considered (Figure 4.10).

4.6 Generation of targeted toxins ^{His}MMRN2$^{495-678}$-Dianthin and ^{His}Dianthin-MMRN2$^{495-678}$

Based on the internalization experiment, MMRN2$^{495-678}$ was a good candidate to generate a targeted toxin able to selectively deplete CLEC14A expressing cells. In order to generate this new possible therapeutic tool different types of toxins were taken into consideration. We evaluated two different types of toxins: the ribosome inactivating protein saporin-2 and the antiviral protein DAP-30, dianthin. Both of them are Ribosomes-Inactivating Proteins (RIPs) and work as N-glycosylases.
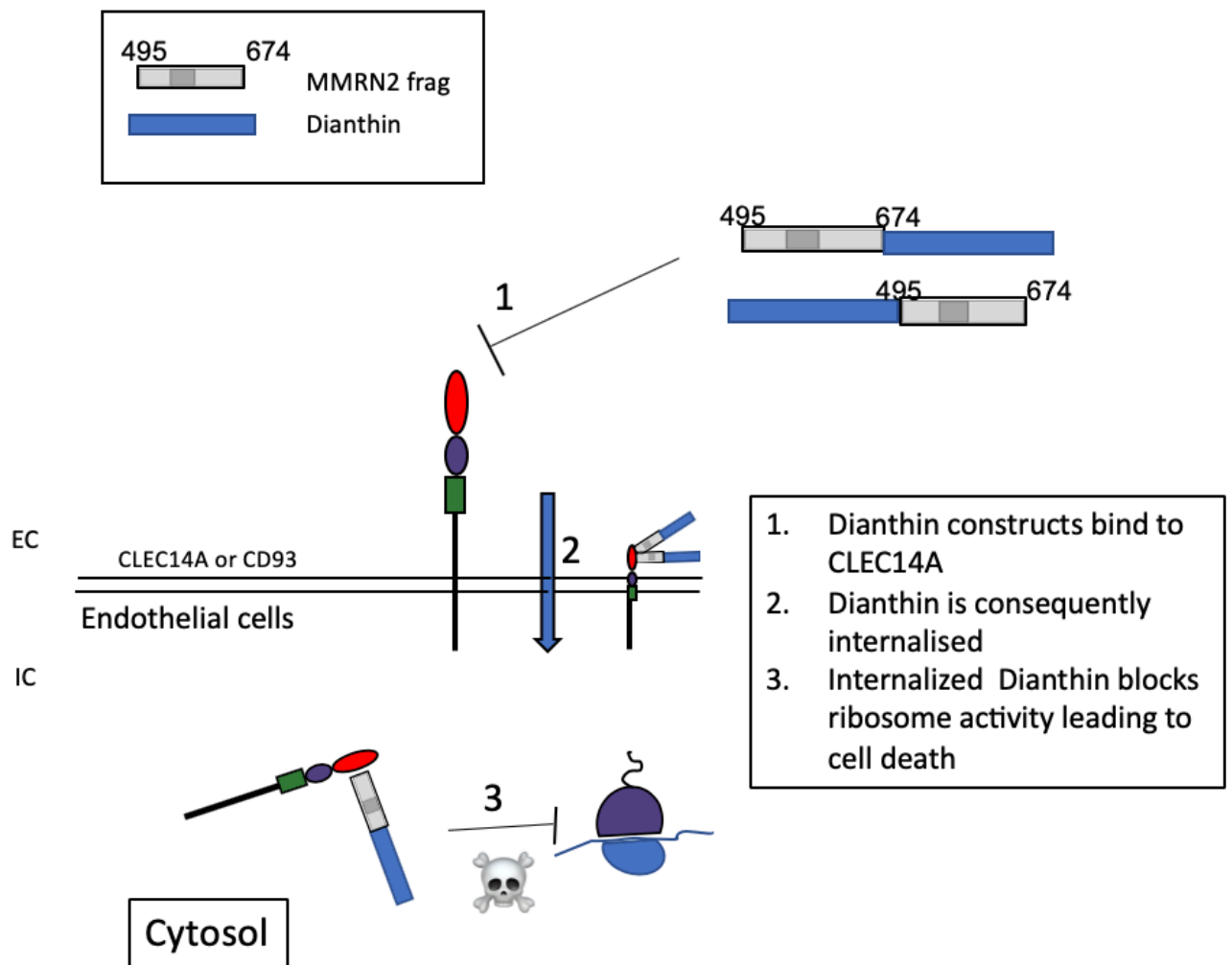
Figure 4.11 MMRN2-dianthin toxin rationale

Based on the fact that MMRN2495-678 is internalised upon binding in HUVEC, MMRN2-dianthin toxin is expected to bind to CLEC14A and being internalised (1 & 2). The presence of these recombinant toxins within the cytoplasm is expected to block the ribosome activity leading to cell death (3).

They belong to the type 1 RIPs, which lack a natural cell-binding domain and, for this reason, they constitute the perfect candidates for targeted toxins. According to a published study, which compares two targeted toxins ([His]Saporin-EGF and [His]Dianthin-EGF), the differences in saporin and dianthin were minimal (Gilabert-Oriol *et al.*, 2013). They showed the same cytotoxic activity measured in real time. The identity of the two toxins moieties aligned was 80% and the similarity was 90%. The main difference between the two constructs was at the expression level after purification. They showed that [His]Saporin-EGF was produced at significant lower levels than the dianthin counterpart. It has been shown, that three main structural differences, one at the N-terminus, one at the C-terminus and the presence of a gap in saporin, which is replaced by an extra amino acid in dianthin, were impairing the production of saporin. These sites made saporin more accessible to the action of bacterial proteases. Some of the fusion proteins were losing the His-tag when cleaved at the N-terminus, affecting the purification, and other proteins were cleaved at the C-terminus of the toxin portion, resulting in a truncated form (Gilabert-Oriol *et al.*, 2013). For all these reasons, it was decided to proceed only with the cloning of the targeted toxin, using dianthin as toxic moiety (Figure 4.11).

The group of Prof. Fuchs provided us with a pET11d vector, carrying the gene of dianthin. In order to clone a functional targeted toxin, two different approaches were designed: [His]MMRN2$^{495-678}$-Dianthin and [His]Dianthin-MMRN2$^{495-678}$. Both of the approaches were attempted, as it was not known whether the presence of the Dianthin portion in the recombinant protein at the N-terminus or at the C-terminus could affect the correct folding of MMRN2$^{495-678}$ and its binding to CLEC14A, or its
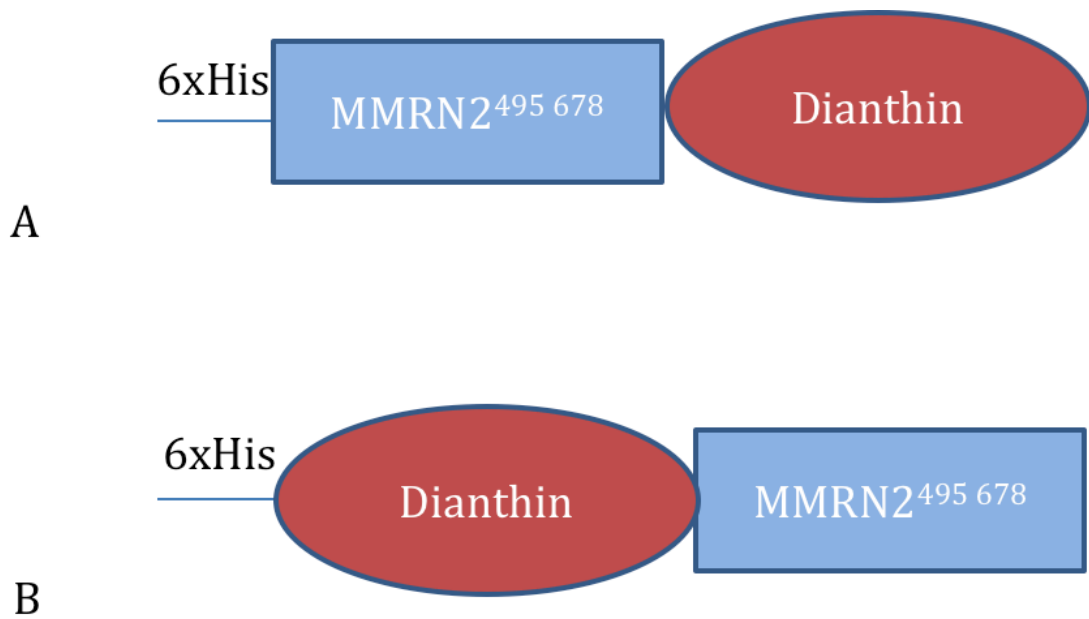
Figure 4.12 Diagrams of MMRN2$^{495\text{-}678}$ dianthin constructs

As MMRN2$^{495\text{-}678}$ is internalised, two different dianthin constructs were designed and constructed in order to test if MMRN2$^{495\text{-}678}$ was a good candidate for conjugation with this type of toxin (ribosome inactivating proteins). Indeed in order to function, dianthin should be delivered within the cytoplasm of the cell, but mammals do not express natural receptors for dianthin. A fusion protein with an internalised ligand would be an ideal construct to target specific cell types. The figure shows either an N-terminus (A) or a C-terminus (B) MMRN2 fusion protein with an his tag for purification and study.

effect on the accessibility of the His-tag for purification purposes. Similarly, for both the designs, the pET11d empty vector was digested using NcoI and EcoRI restriction sites. The dianthin and the MMRN2$^{495-678}$ fragments were amplified with primers by PCR, incorporating a His-tag at the N-terminus at each construct. Moreover, each fragment was carrying homologous regions of at least 18 nucleotides at each end. Gibson cloning kit was used to ligate the multiple DNA fragments cloning. As result it was possible to generate both of the targeted constructs planned (Figure 4.12).

4.7 Discussion

The latest studies underlined the importance of a newly discovered interaction between MMRN2 with either CLEC14A or CD93. In particular the interaction between CLEC14A and MMRN2 has been recently characterized and the minimal binding fragment of MMRN2 has been identified (Zanivan *et al.*, 2013; Khan *et al.*, 2017). Furthermore, it has been shown that the disruption of CLEC14A and MMRN2 interaction leads to a strong reduction in sprouting *in vitro* and tumour growth and angiogenesis *in vivo* (Noy *et al.*, 2015). Interestingly, the overexpression in LLC tumours of the mouse MMRN2$^{495-678}$-mFc fragment showed significant reduction in tumour growth *in vivo* (Khan *et al.*, 2017). The fact that the interaction between CLEC14A and MMRN2 happens with high affinity and the fact that CLEC14A has been identified as a tumour endothelial marker (Mura *et al.*, 2012) prompted efforts in trying to exploit the recombinant MMRN2 to specifically target the tumour endothelium.

This study mainly focused on the use of the mouse MMRN2$^{495-678}$-hFc because it proved to be cross-reacting between human and mouse CLEC14A. The cross-reactivity of the mouse fragment towards human and mouse CD93 has not been investigated. Mouse MMRN2$^{495-678}$-hFc retained the binding capability for both HEK293T overexpressing CLEC14A and HUVEC, which express CLEC14A at the endogenous level along with CD93. The binding was repeated and confirmed with the human form of the fragment in HUVEC. Interestingly, it was also possible to corroborate previously published findings that showed CRT4 antibody binding to the same region of CLEC14A as MMRN2. HUVEC incubated with CRT4 but not CRT2 and IgG showed an inhibition of the binding of mouse MMRN2$^{495-678}$-hFc. The same experiment was repeated with the human MMRN2$^{495-674}$-hFc counterpart but in this case CRT4 was unable to block HUVEC (Appendix 1). It is not surprising that the CRT4 would not block the human MMRN2$^{495-674}$-hFc binding, because it is known that, although CLEC14A binding sites are not accessible, CD93 is still available for the binding. The most likely explanation is that mouse MMRN2$^{495-678}$-hFc is able to cross-react only with mouse and human CLEC14A, whereas it is not able to bind the human CD93. In order to confirm this possibility an experiment in which human CD93 is overexpressed in HEK293T cells and blocked with CRT4 before binding of mouse MMRN2$^{495-678}$-hFc should be performed.

Due to the characteristics of this recombinant protein and previous published reports, mouse MMRN2$^{495-678}$-hFc was employed in a vaccination experiment in mice. It has been reported that the injection of a human Fc-tagged mouse recombinant protein was able to raise an immune response mainly against the hFc

163

tag but also with the fragment of the peptide adjacent the hFc tag. The protocol of vaccination was based on what was reported in previous studies for GRIND2D and ROBO4 (Zhuang *et al.*, 2015; Ferguson *et al.*, 2016). The aim of GRIND2D and ROBO4 vaccination was to raise an immune response against proteins that are recognized to be tumour endothelial markers. Conversely, immunizing against the MMRN2 fragment was aiming to exploit the immune system to generate antibodies able to block the interactions of MMRN2$^{495-678}$ with CLEC14A or CD93 (Figure 4.6). Mouse MMRN2$^{495-678}$-hFc was not able to induce a strong immune response. Interestingly, the published reports only showed the immune response at the serum dilution 1:10 (v/v), which is fairly concentrated, when determining the titer of the humoral response. In this study the minimal immune response investigated was 1:10^2 (v/v) up to a dilution of 1:10^5. According to the ELISA results, the response towards mMMRN2$^{495-678}$-hFc was minimal, whereas the response to hFc both in the treated group and the control was strong. Consequently, it is not surprising that tumour weight and tumour growth were similar to the ones measured in the control group. It is still unclear if, even though the dilution at which they could observe a response for ROBO4 and GRIND2D was 1:10 (v/v), the response was actually detectable at increasing dilutions (e.g. 1/10$^{4-5}$) (Zhuang *et al.*, 2015; Ferguson *et al.*, 2016). It is doubtless that each recombinant fusion protein has a specific immunogenicity and raises a different degree of response. It is possible to conclude that the immunization with mouse MMRN2$^{495-678}$-hFc does not raise a strong immune response against the fragment and its ubiquitous expression might be a reason. Even though the protocol implemented was not able to induce a proper titer against MMRN2 fragment, the literature supports the theory that a vaccination response

against MMRN2$^{495\text{-}678}$-hFc might have two strong consequences: the first would be blocking MMRN2-CLEC14A interaction (Noy *et al.*, 2015) and second blocking the recently described MMRN2-CD93 interaction (Lugano, Dejana and Dimberg, 2018). Both of the interactions have been reported to be important for tumour angiogenesis.

Finally, because CLEC14A was identified as a tumour endothelial marker, the possibility of using the fragment conjugated with a toxin to target tumour endothelium was explored. Therefore, it has been decided to generate a fusion protein, MMRN2$^{495\text{-}678}$-Dianthin. As previously mentioned, dianthin is a plant toxin, which is able to block the ribosome activity during translation if released in the cytosol. As human cells do not naturally express receptors for dianthin, a fusion partner that is internalized should be used to create an active toxin. For this reason, we investigated whether mouse MMRN2$^{495\text{-}678}$-hFc was internalized, as previously observed for the CRT monoclonal antibodies against CLEC14A by Puja Lodhia (Thesis, 2017). The specific staining of MMRN2$^{495\text{-}678}$-hFc was partly co-localising with the EEA-1 staining (endosomes marker), indicating that MMRN2 might be internalized through the endosome pathway and subsequently released in the cytosol. Further experiments would be necessary in order to confirm whether the endosomes are actually involved (Figure 4.11). Moreover, it would be interesting to understand if the internalization is depending only on the binding of the fragment with CLEC14A and not also due to CD93. It is possible to speculate, due to the mechanism observed with the internalization of the CRT antibodies, that the binding to CLEC14A is at least in part involved. For therapeutic purposes, the internalization should be preferably

only CLEC14A-dependent to avoid toxicity on off-target cell types that express CD93, because its expression is not tumour endothelial specific. Consequently, it would be extremely appealing to confirm whether mouse MMRN2$^{495-678}$ is able to cross react only with human CLEC14A and not with human CD93.

Due to lack of time to complete this part of the project, two recombinant toxin-fusion proteins (^{His}MMRN2$^{495-678}$-Dianthin and ^{His}Dianthin-MMRN2$^{495-678}$) were designed and cloned, in order to identify the best construct to further study *in vitro* on HUVEC cells and eventually *in vivo.*

CHAPTER 5: A ligand-based chimeric antigen receptor

5. A ligand-based chimeric antigen receptor

5.1 Introduction

Chimeric antigen receptor (CAR) T cells are a promising new approach for cancer treatment and over the last few years many clinical trials of them have been initiated. Four generations of CAR T cell have been developed, introducing more co-stimulatory signals. This is to improve survival and activation of the T cells upon recognition of their target. Aside from the presence of the co-stimulatory signals, a fundamental part of these chimeric receptors is the single chain variable fragment (ScFv), which is responsible for the specificity to the T cells (Pettitt *et al.*, 2018). ScFv comprises a variable light and a variable heavy chain joined together by a linker. The molecular weight of an ScFv is around 25 kDa (Ahmad *et al.*, 2012).

Due to its strong binding with CLEC14A (Khan *et al.*, 2017) and its molecular weight, MMRN2$^{495-674}$ behaviour was comparable to the one of an ScFv and various applications were taken into account in order to exploit it for therapeutic purposes, due to its CLEC14A binding properties. One of the most innovative methods attempted was the generation of a fragment-based Chimeric Antigen Receptor (CAR).

5.2 Construction of a ligand-based chimeric antigen receptor

This work was in collaboration with the Dr Steve Lee in the Institute of Immunity and Infection, University of Birmingham. A second generation CAR T cell plasmid (MP71) was provided by Dr Lee, which included a CD3ζ and a CD28 co-stimulatory domain
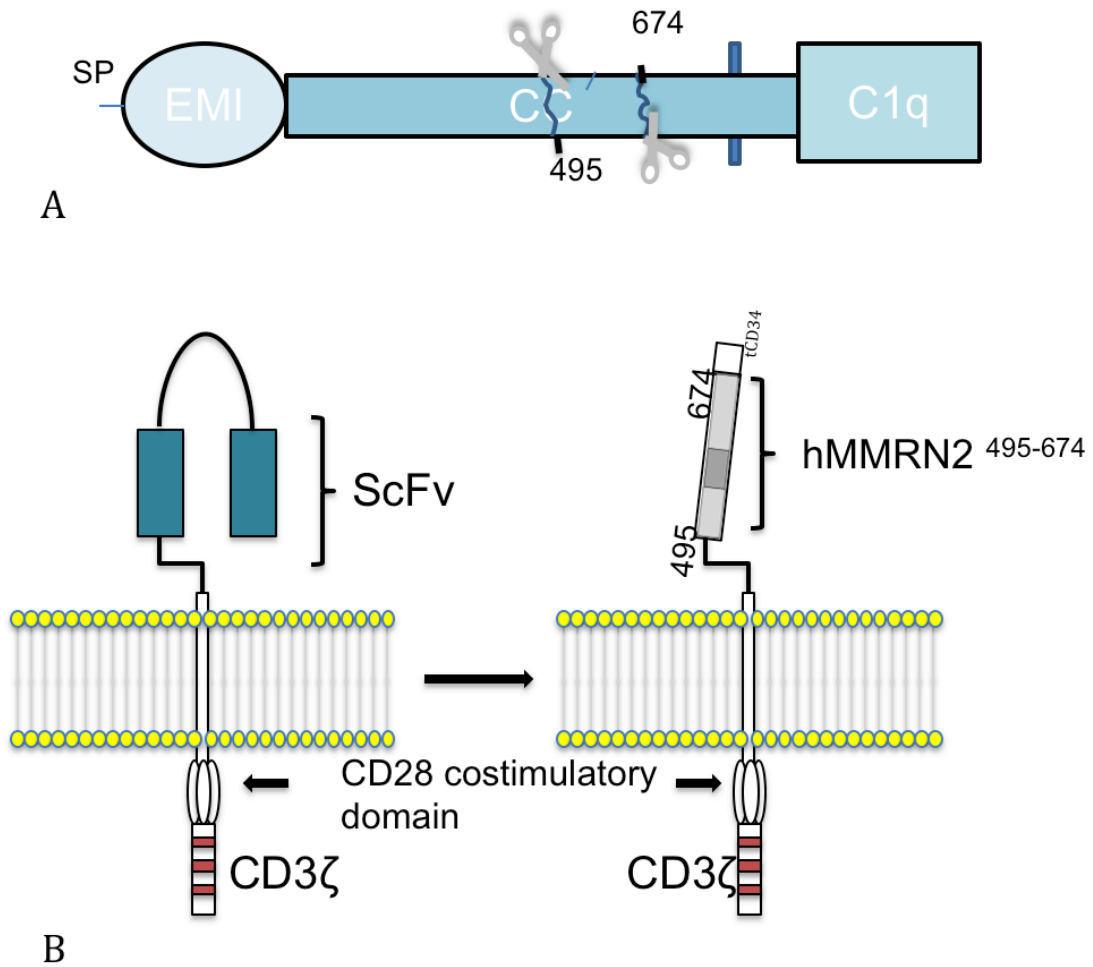
Figure 5.1 Schematic diagram representing the ligand-based chimeric antigen receptor strategy

A. Schematic representation of the various domains of hMMRN2 and the position of the fragment 495-674 within the coiled-coil domain. B. Figure showing the difference between a conventional ScFv-based CAR (on the left) and the MMRN2$^{495-674}$-based CAR (on the right) constructed in order to target the tumour endothelial marker CLEC14A.

(Engels *et al.*, 2003). Currently there are more advanced chimeric antigen receptors in use, described as 'third' and 'fourth' generation. In these new generations of CAR further intracellular domains have been added to the second-generation structure of the CAR, in order to improve cytokine production and the killing activity. Due to the common use in the literature of second generation CAR T cells, which are the most studied so far, it has been decided here to use this construct instead of the newer generations.

As demonstrated in the previous chapter, both MMRN2$^{495-674}$ and MMRN2$^{495-678}$ were able to bind CLEC14A expressed on the cell surface. Because of this, it was decided to clone both the human MMRN2$^{495-674}$ and the mouse MMRN2$^{495-678}$ version of the CAR. To do so, the human and the mouse version of the fragment were amplified by PCR with homologous endings to the vector. These fragments were separately inserted in frame in to the MP71 vector, instead of a single chain antibody (scFv) normally employed in the generation of CAR T cells (Figure 5.1B). The plasmid constructs are shown schematically in Figure 5.2.

These constructs were then used to produce a retrovirus carrying the genetic information for the specific CAR: either the mouse or human MMRN2 fragment. Peripheral blood mononuclear cells (PBMCs) were activated with anti-OKT3 (anti-CD3), anti-CD28 and IL-2. After two days, activated T cells were retro-transduced with the retrovirus either carrying the genetic information for the CAR constructs or no DNA as mock. Each of the following experiments will compare mock control, MMRN2$^{495-674}$ (or human MMRN2) and MMRN2$^{495-678}$ (or mouse MMRN2) CAR T
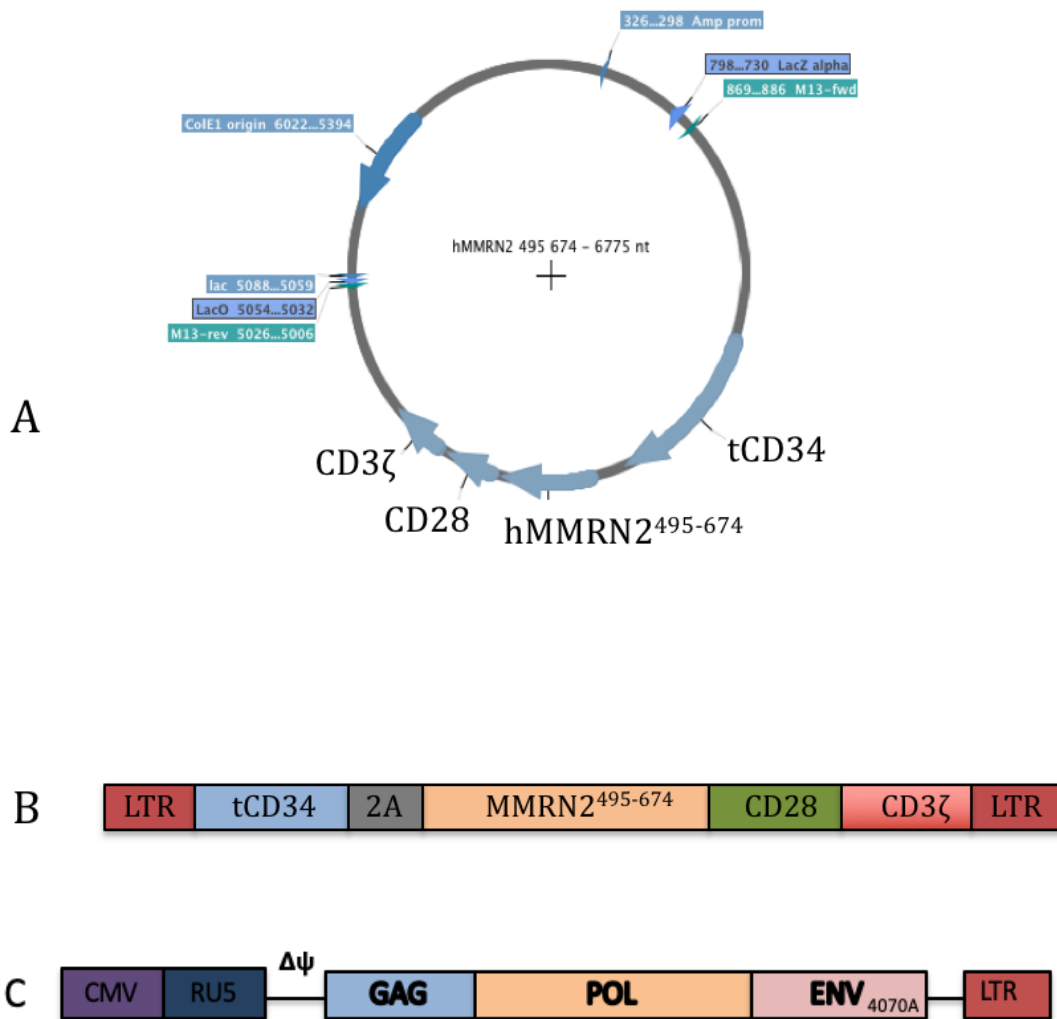
Figure 5.2 Plasmid map of the ligand-based CAR generated

A. Plasmid map of the human MMRN[495-674] CAR T cells, indicating the main domains of the chimeric antigen receptor. A similar map would schematically represent the plasmid of the mouse version. B. A linear representation of the DNA construct is shown. It contains an N-terminus and a C-terminus Long Terminal Repeats (LTR) domains, a truncated form of CD34 as extracellular tag, a peptide 2A linker, the gene of MMRN2[495-674] and the two signalling domains CD28 and CD3ζ. C. A linear representation of pCL ampho, including the Envelope gene 4070A, as well as GAG and POL genes, under a cytomegalovirus promoter.

cells. The results shown in this chapter were obtained with one transduction. The same experiment was repeated with PBMCs obtained from different donors and independently transduced. The same pattern of reactivity was observed across multiple transductions confirming the activity of the CAR.

5.3 MMRN2$^{495-674}$ CAR modified T cells activate on contact with the recombinant CLEC14A antigen as shown by IFNγ ELISAs

Once the T cells were activated and transduced with the CAR as previously described (2.3.13/14), the transduction efficiency was measured by flow cytometry. The four human PBMCs plasmapheresis cones transduced were analysed before the functional experiments. The transduction efficiency shows the percentage of the cells that are transduced and expressing the CAR gene in the population.

There are two main differences to be taken into account when comparing different repeats: the intrinsic donor variability and, in particular, the transduction efficiency. Presumably, two donors transduced with the same CAR and at the same transduction efficiency will show little, if any, variations in activation. More relevant to be considered is the transduction efficiency levels of the different donors. In fact, two or more donors transduced with the same CAR construct at different efficiencies would show different levels of activation. The extent of the IFNγ production is correlated with the efficiency of transduction, because in each experiment the same number of cells from the total population is plated. For this reason, it has been decided not to pool the data and simply evaluate the pattern of response.
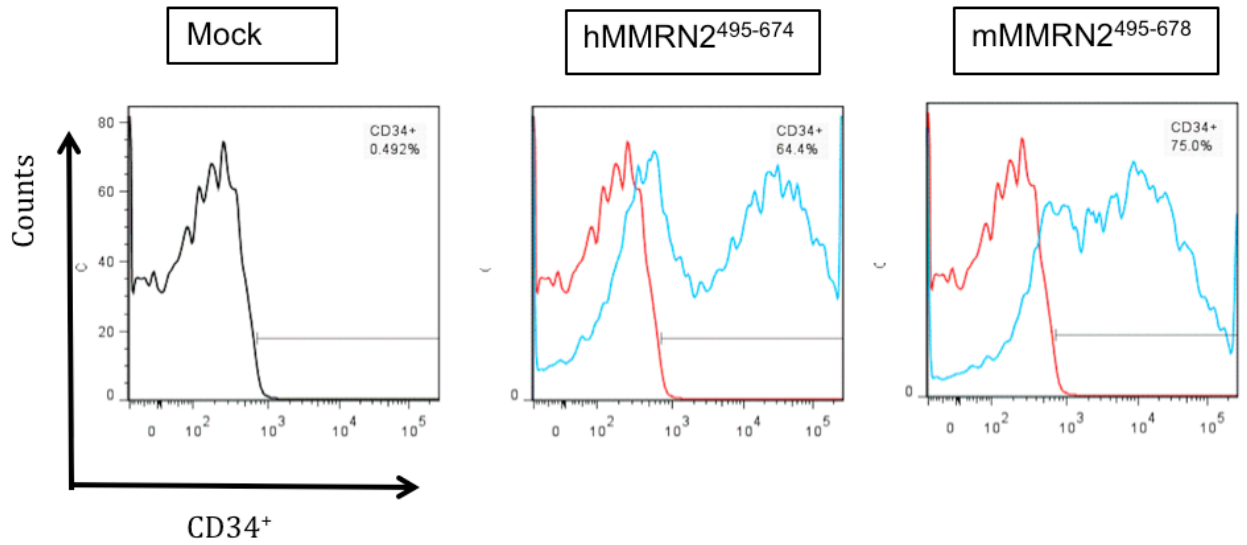
Figure 5.3 Determination of the transduction efficiency

Following activation, human PBMCs were transduced with either hMMRN2[495-674], mMMRN2[495-678] CAR or no DNA for mock cells. Flow cytometry analysis was performed gating for a viability marker and a selecting the lymphocyte population. In addition, viable lymphocytes were analysed for the expression of a truncated form of CD34, which is employed as tag of the CAR surface expression. Finally, the CD34 gate was set using the mock/transduced cells. This is a representative analysis performed on one of the four donors. Similar staining and gating were applied to each transduction.

Four different donors were employed and showed different transduction efficiencies in the following experiments.

With respect to the donor shown, the transduction efficiency was relatively high for both CARs and similar between each other; human MMRN2 CAR T cells were transduced at 64.4%, whereas the mouse MMRN2 CAR T cells were transduced at 75.5% (Figure 5.3).

Recombinant human and mouse CLEC14A^{ECD}-hFc were produced in HEK293T and purified on protein A columns. The sequences of either human or mouse CLEC14A^{ECD}-hFc were cloned into the pWPI vector with the CLEC14A signal peptide at the N-terminus. These constructs were transfected together with the packaging and envelope vectors into HEK293T cells. The virus containing supernatant from this transfection was then used to transduce HEK293T according to the protocol described in 2.3.5. In this way it was possible to obtain a cell line stably expressing and secreting the recombinant proteins. The efficiency of the purification was analysed by a protein gel stained with Coomassie blue (Figure 5.4A). Moreover, the availability of the hFc-tag was checked via western blot, using the anti-hFc antibody (Figure 5.4B).

The recombinant CLEC14A and hFc control were then coated on a NUNC-immuno 96 well plate. After coating, both mock, hMMRN2and mMMRN2 CAR T cells were seeded in technical triplicates. The following day, the INFγ containing media was tested in the IFNγ ELISA as described in 2.3.16.1.
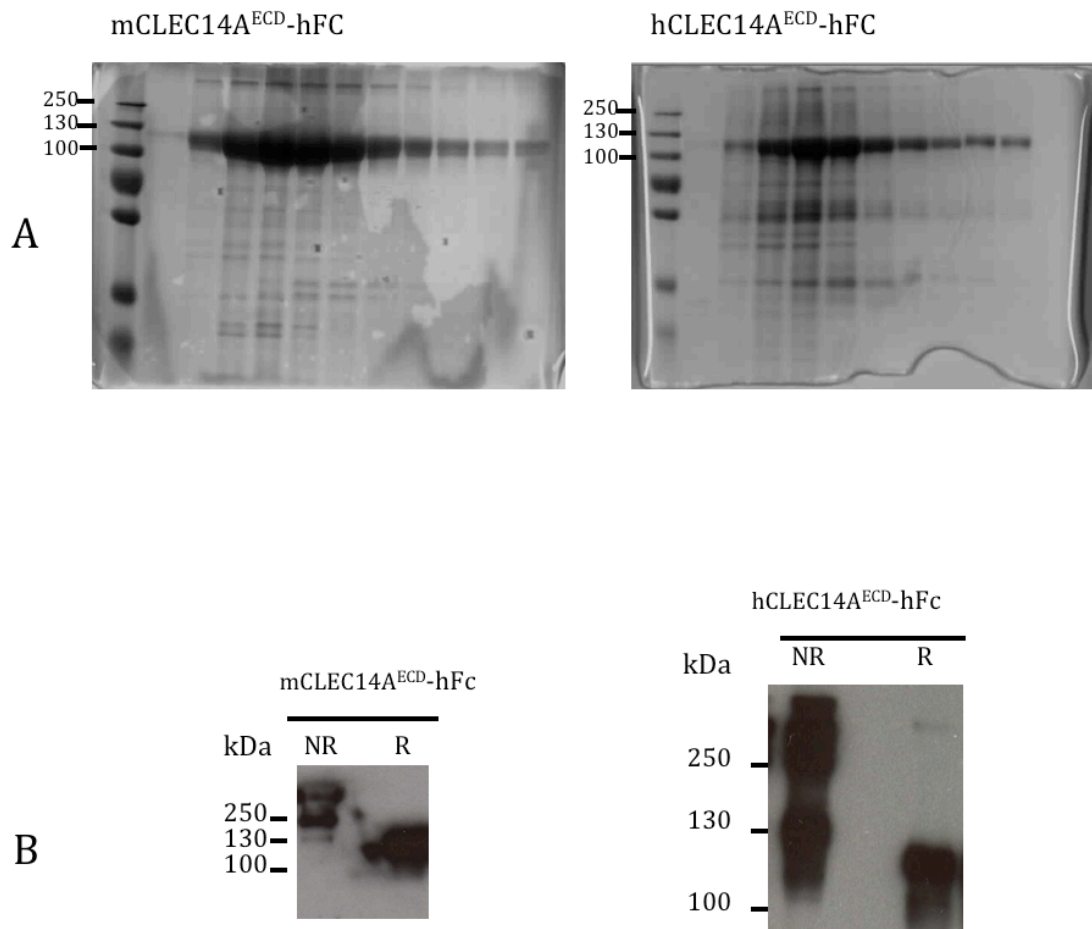
Figure 5.4 Expression and purification of mouse and human CLEC14A^{ECD}-hFc

A. Protein gel and Coomassie staining of both mouse and human CLEC14A aliquots after protein A purification. The same volume was loaded from each aliquot showing clearly the beginning and the end of the elution phase. The proteins are seen to be more than 90% pure. B. Western blots detecting the purified proteins either in non-reducing (NR) or (R) reducing conditions with a anti-hFc HRP antibody. It was possible to detect the protein in both conditions, showing the accessibility of the hFc tag within the recombinant protein.
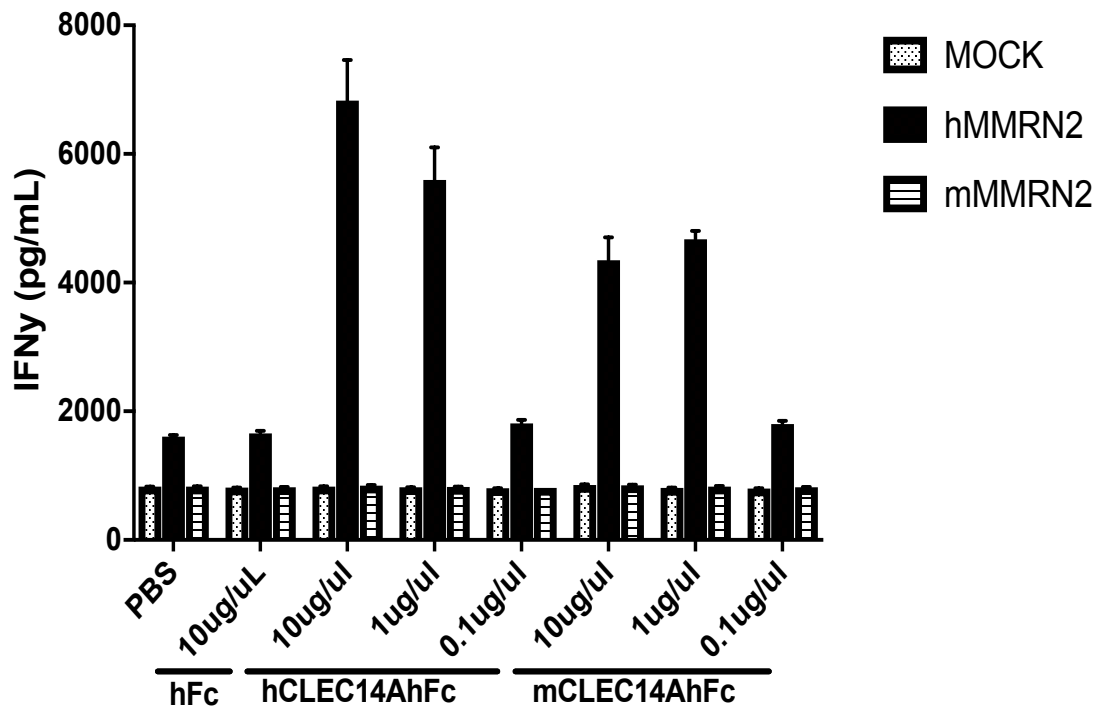
Figure 5.5 MMRN2$^{495\text{-}674}$ T cells activate on contact with the recombinant antigens in IFNγ ELISAs

To normalise the transduction, human and mouse MMRN2 CAR T cells were matched by diluting with mock cells the population with the highest transduction efficiency. The same number of cells was then incubated with recombinant human and mouse CLEC14A-hFc and hFc as control at decreasing concentrations. The medium was finally tested in ELISA for INFγ production. The figure represents the INFγ response of the mock, hMMRN2 and mMMRN2 CAR T cells after stimulation with purified recombinant proteins. The graph shows the results of one donor of the four tested obtaining similar results. The bars represent the average of 3 technical replicates ± SEM.

The mMMRN2 CAR was unresponsive to both mouse and human CLEC14A^{ECD}-hFc as its INFγ levels were the same as those exposed to mock CAR T cells. In contrast, the hMMRN2 CAR was responsive to both mouse and human CLEC14A^{ECD}-hFc but not to hFc alone. This indicated that T cells expressing the human version of the fragment as a CAR were able to recognise and to be activated by target antigen. The INFγ produced in the presence of CLEC14A-ECD-hFc was greater than with recombinant hFc control. Further, this experiment showed that hMMRN2 CAR was able to cross-activate with both the human and the mouse antigen. The response was dose dependent and comparable for the two species. Only in presence of 10 μg/μL of purified antigen, the response of the CAR to mouse CLEC14A^{ECD}-hFc was lower than the response to human CLEC14A^{ECD}-hFc. The baseline response of the hMMRN2$^{495-674}$ CAR T cells was consistently greater than the mock or the mouse version, indicating that the expression of this CAR in T cells causes a constitutive basal activation. Finally, the response of the CARs to hFc was comparable to the one obtained in wells containing PBS only, showing that these CARs were not affected by the presence of the hFc tag of the recombinant CLEC14A^{ECD} (Figure 5.5). This result was confirmed by transfecting different donors with the same CAR constructs. The extent of the IFNγ response was different because of the different levels of transduction, but the same pattern of response was observed.

5.4 Human MMRN2$^{495-674}$ T cells are responsive to CLEC14A and CD93 expressing cells in IFNγ ELISAs

Antigen activation of the human CAR prompted further study. The CAR T cells were next challenged in an in-cell INFγ ELISA. In order to have a more comprehensive understanding of the specificity of these CARs, a variety of targets were employed. HEK293T do not express any of the possible targets of MMRN2 CAR: CLEC14A or CD93. So, it was possible to use them as negative control to investigate the overexpression of the full-length version of the targets and their mutant versions. HEK293T were PEI transfected with the constructs of CLEC14A and CD93 full-length both cloned into pEGFPN1. It has been reported that the two cysteine residues in the long loop region of CLEC14A, conserved also on CD93, are important for the binding to MMRN2 due to the formation of disulphide bonds (Khan *et al.*, 2017). The mutation of these cysteine residues (CLEC14A^{C103S} and CLEC14A^{C138S}) to a serine residue, which is the most similar amino acid to cysteine that lacks the ability to form disulphide bonds, resulted in the loss of the binding.

Similarly, this was also observed with the CD93^{C104S} and CD93^{C138S} mutants (Khan *et al.*, 2017). These mutants, cloned in the same vector of the full-length constructs pEGFPN1, were also used to generate transiently transfected HEK293T cell lines. It was expected that upon cysteine mutation, the human MMRN2$^{495-674}$ CART cell was not able to bind properly to the targets and activate the T cells, so these mutants were used as negative control. In the plan of the study only the CLEC14A^{C103S} and CD93^{C104S} mutants were used. The transfected HEK293T cell lines together with
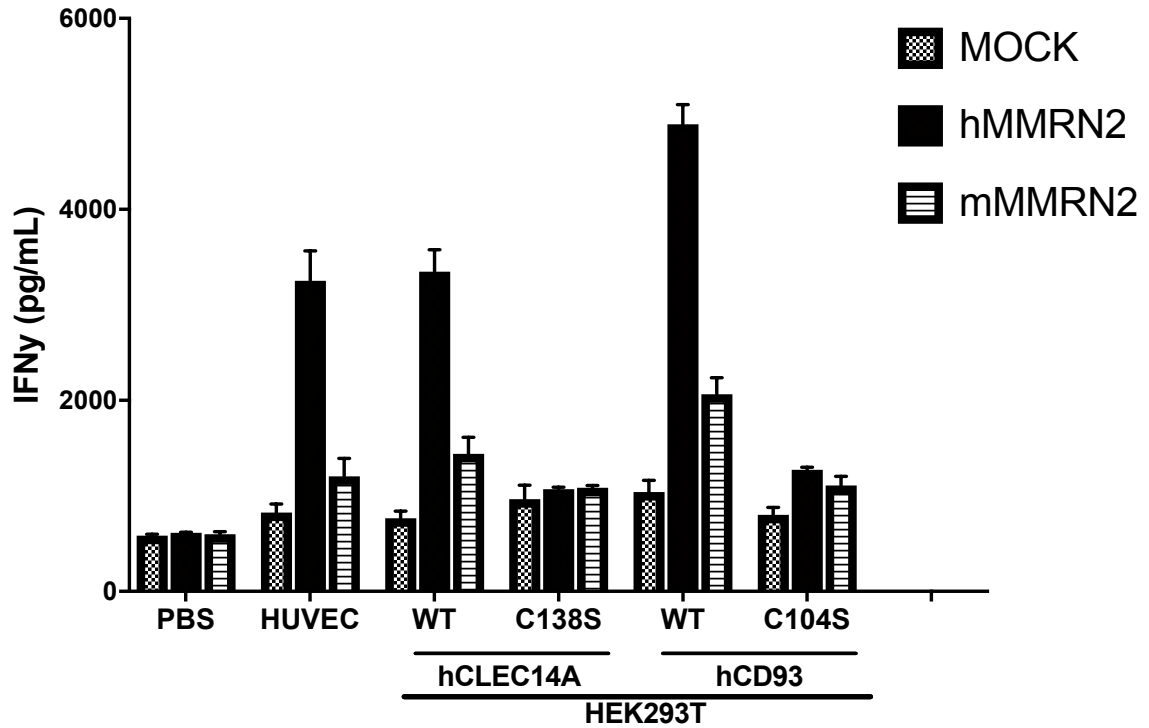
Figure 5.6 MMRN2$^{495\text{-}674}$ T cells are responsive to CLEC14A and CD93 expressing cells in IFNγ ELISAs

HEK293T were transfected with CLEC14A and CD93 (either WT or mutant). After 24 hours, together with HUVEC, which express both CLEC14A and CD93 endogenously, transfected HEK293T were seeded with the T cells (E:T=20:1). After overnight incubation, the supernatant was tested in ELISA for IFNγ production. This figure shows the response of the different CARs tested (mock, hMMRN2 and mMMRN2) to targets expressed on cells. The graph shows the results of one donor of the four tested obtaining similar results. The bars represent the average of 3 technical replicates ± SEM.

HUVEC, that express both CLEC14A and CD93 endogenously, were tested as targets of the previously described CARs.

The transfected HEK293T cells and HUVEC were placed in co-culture with mock, hMMRN2 and mMMRN2 CAR modified T cells overnight. IFNγ containing supernatants were then analysed as described in 2.3.16.1.

As previously for the purified antigen IFNγ ELISA, mMMRN2 CAR T cells were not responsive to the antigens, showing that this CAR was not able to recognise the target, leading to comparable IFNγ levels of the untransduced T cells of the mock. Moreover, it was possible to observe a basal activation across all the CAR T cells towards each target, because the levels of INFγ were slightly higher than the one detected with PBS only. In contrast human as opposed to mouse was responsive to the targets. This strong response towards HEK293T overexpressing CLEC14A^{FL} and CD93^{FL} was seen. Moreover, as expected hMMRN2$^{495-674}$ was not activated upon contact with the mutated targets CLEC14A^{C103S} and CD93^{C104S}. The IFNγ levels were comparable to the mock and the non-responsive mMMRN2 CAR against the same conditions. Human MMRN2 CAR showed a strong activation when in co-culture with HUVEC. The concentration of INFγ in the medium was comparable to the one detected with this CAR in co-culture with HEK293T cells expressing CD93 (Figure 5.6).

5.5 MMRN2$^{495-674}$ CAR modified T cells are cytotoxic to HUVEC in culture

The action of CAR T cells *in vivo* is mainly cytotoxic. After recognition and binding of the target, the T cells activate and eventually kill the cells expressing the target. An important prerequisite to study CAR T cells in vivo is to show cell killing *in vitro.* It is then known that the CAR is functional and you can look for a therapeutic effect *in vivo*. A reliable assay to measure the cytotoxicity of T cells is the Chromium (Cr^{51}) release assay.

The chromium release assay was set up with the same target cells employed in the cell ELISA. Target cells were incubated with Cr^{51} for cell loading. Once the Cr^{51} was incorporated, the target cells were co-cultured with the CAR T cells at different Effector:Target (E:T) ratios (20:1, 10:1, 5:1). Cells were co-cultured for 5 hours and, then, the Cr^{51} containing medium was analysed by a gamma counter. Each combination of co-culture was seeded in triplicates. Moreover, for each target cell spontaneous (untreated cells) and maximum lysis (cells treated with 1% SDS) were measured in order for the counter to calculate the ratio of each sample according to the formula in paragraph 2.3.19.

According to previous experiments, mMMRN2 CAR T cells did not show any killing activity towards the targets. In fact, the levels of chromium registered were comparable with the mock. On the other hand, hMMRN2 CAR showed strong killing activity in HUVEC when compared with the mock (Figure 5.7). The experiment was performed testing the killing activity of all the 4 transduced donors available. The

results of the first attempt across the different donors were not entirely consistent. This was probably due to the fact that the donors not shown were having a lower transduction and all the T cells used had spent a long time in culture. The same experiment was performed a second time. The results of this second attempt were not taken into consideration due to the maximum release values registered, which were not suitable for a correct calculation of the ratio.
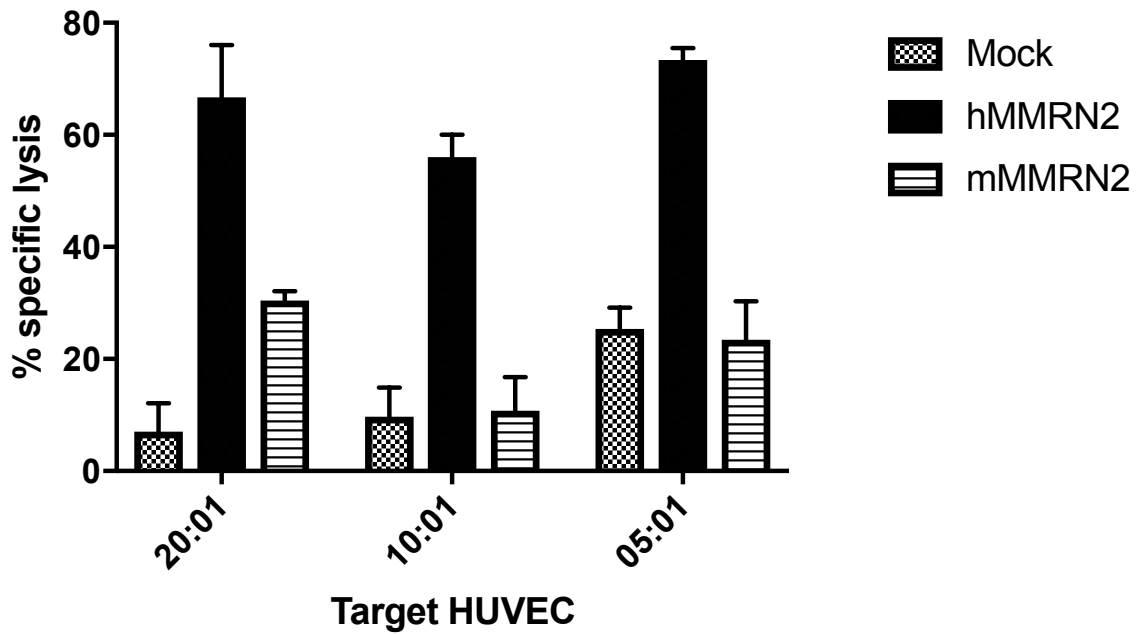
Figure 5.7 MMRN2$^{495-674}$ T cells display cytotoxic activity towards HUVEC

Target cells (HUVEC) were labelled with 50μCi of fresh ^{51}Cr. After staining, these cells were cultured with CAR T cells at different E:T ratios (20:01, 10:01 and 05:01). At the end of the incubation, radioactive containing media resulting from the T cell mediated lysis was collected and read at the scintillator. The graph shows the killing activity of the different CAR T cells against HUVEC. The graph shows the results of one donor of the four tested. The bars represent the average of 3 technical replicates ± SEM.

5.6 Discussion

Current in cancer research aims to identify new therapeutic approaches, which are more effective and less invasive for the patient than conventional treatment with chemo- or radio-therapeutic agents. Over the past few years, chimeric antigen receptor (CAR) T cell therapy has been demonstrated to improve patient survival in B cell malignancies' clinical trials (Kochenderfer *et al.*, 2010, 2012; Maude *et al.*, 2014; Lee *et al.*, 2015; Porter *et al.*, 2015). Regular CAR constructs employ a single chain antibody (ScFv) to drive the specificity. Here we present an alternative method to generate a CAR, which utilize a receptor/ligand binding. This is a comparatively unexplored approach and, in fact, only two previous examples of ligand/receptor CAR T cells have been published, a NKG2D based and an ErBb based CAR (Parente-Pereira *et al.*, 2013; Sentman and Meehan, 2014). These two attempts were focused on targeting tumour cells, whereas the CARs generated in this work are aiming to target tumour endothelial cells. Due to its strong interaction with CLEC14A, a reported tumour endothelial marker (Mura *et al.*, 2012; Zanivan *et al.*, 2013), MMRN2$^{495-674}$ was a putative candidate for targeted therapy development.

Both human MMRN2$^{495-674}$ and mouse MMRN2$^{495-678}$ chimeric antigen receptors have been generated. We evaluated the functionality of the CAR *in vitro*. Initially, specifically the ability of T cells transduced with the MMRN2 CARs to be activated on the purified antigen, mouse and human CLEC14A^{ECD}-hFc. Upon activation T cells secrete IFNγ that is measured in the culture media. Human MMRN2 CAR T cells showed strong levels of IFNγ upon recognition with both human and mouse

1. CAR T cell binding to target cells
2. CAR T cell activation and IFNɣ production
3. Cytotoxic activity towards target cells

MMRN2 CAR T cell

hMMRN2 495-674

IFNɣ IFNɣ
IFNɣ

CLEC14A or CD93

Endothelial cells
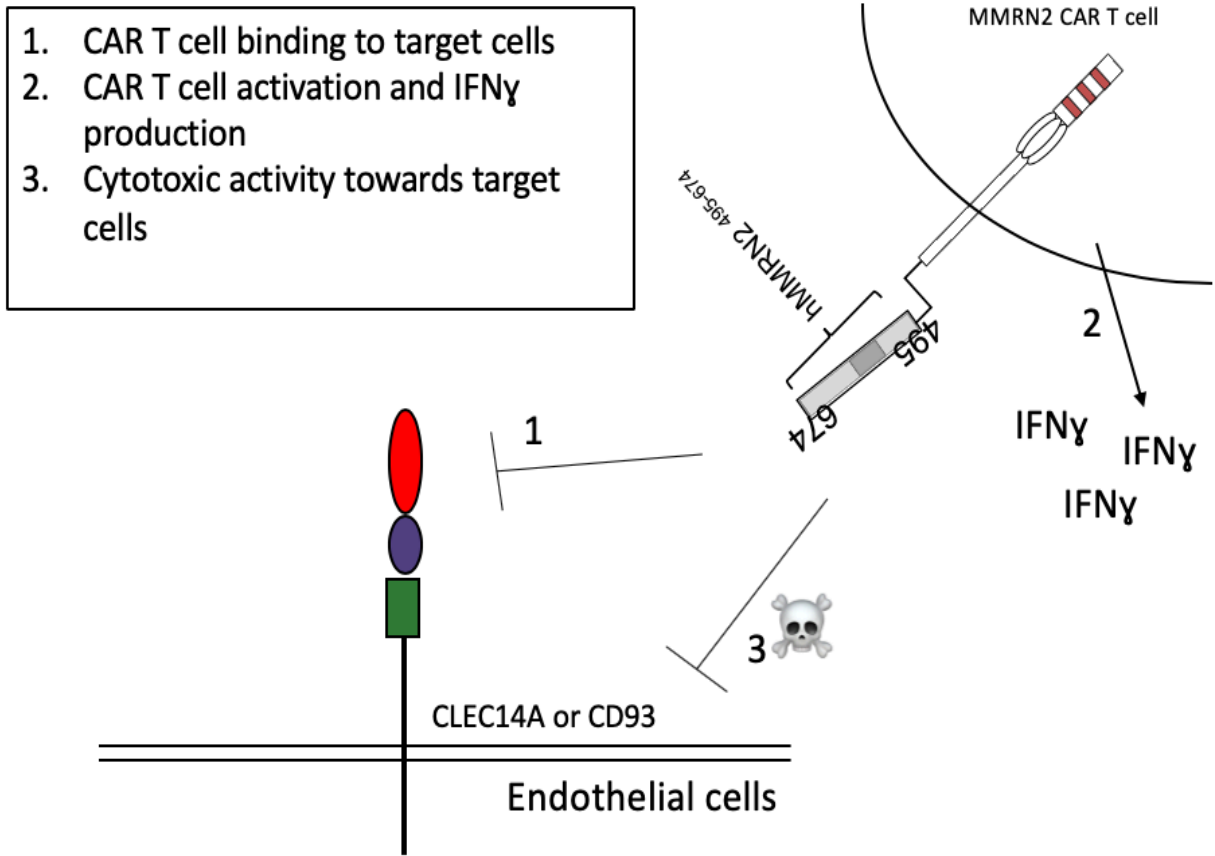
Figure 5.8 Schematic representation of hMMRN2 CAR T activation.

T cells expressing the chimeric antigen receptor based on the MMRN2 fragment recognise the targets, CLEC14A and CD93 expressing cells. Upon binding, T cells activate and produce IFNɣ. After activation, T cells exert their killing activity by the action of granzymes and perforins.

recombinant CLEC14A. The cross-reactivity of the CAR is important for future studies in pre-clinical and clinical settings. This result indicates that hMMRN2 CAR T cells are able to selectively recognise the target and activate. According to the hypothesized specificity of the binding, CAR T cells were unable to activate when HEK293T were expressing the mutated forms of CLEC14A and CD93. The response pattern was consistent across all the donors. The levels of IFNγ were variable, due to their different transduction efficiency. Conversely, mMMRN2 CAR T cells show no activity. As the recombinant mMMRN2$^{495-678}$-hFc was retaining the binding properties towards both human and mouse CLEC14A, it is possible to speculate that the confirmation of mMMRN2 within the CAR construct was either not folding correctly or presenting a different pattern of glycosylation, losing its binding capability. Further investigations are needed to assess why this CAR is unable to bind to its target. Interestingly, hMMRN2 showed great efficiency of binding both to HEK293T overexpressing CLEC14A and CD93, and HUVEC that express both of the targets physiologically. Finally, it was shown that hMMRN2 CAR T cells were able to activate in response to HUVEC cells and kill them, in a chromium release experiment (Figure 5.8). In this experiment it is not possible to appreciate a dose-dependent killing activity. This is probably due to the fact that at this E:T ratios the killing activity resulted in the saturation of these signals. Employing less T cells per target cells would allow to appreciate a dose dependent effect. If these preliminary data are confirmed, this would open the possibility of testing this specific CAR in a pre-clinical tumour model in mice. It would be important to assess whether hMMRN2 is able to cross-react with mCD93. This interaction would be critical to evaluate the off-target toxicity of the CAR in preclinical models, because CD93 expression is not limited to

tumour endothelium. Finally, if the levels of toxicity were acceptable, the effects on tumour growth can be evaluated. Targeting solid tumours with CAR T cells has been demonstrated to be challenging when compared with what observed in haematological cancers. Theoretically, targeting the tumour endothelium should be an effective way to employ CAR T cell therapy to treat solid tumours. In fact, hMMRN2 CAR transduced T cells would not necessarily need to penetrate the tumour to be effective. This would allow them to avoid the strong immunosuppressive environment driven by hypoxia and, among others, regulatory T cells.

Here we present an example of a functional CAR T cell based on a ligand. So far, only a couple of examples for this type of approach have been reported. This work supports the possibility of exploiting known interactions to generate new chimeric antigen receptors for immunotherapy. In particular, it shows the generation of a possible therapeutic use based on hMMRN2 fragment in order to deplete the tumour endothelial compartment because of the expression of CLEC14A.

CHAPTER 6: General discussion

Chapter 6: General discussion

6.1 Introduction

The success of anti-angiogenic drugs in preclinical studies did not translate in clinical trials. In fact, they have failed to improve overall survival of patients (Kerbel, 2008). This type of therapy can result in acquired resistance due to alternative angiogenic pathways taking over, due to tumour cells secreting other angiogenic factors other than VEGF. Vascular targeting might represent an alternative strategy to potentially combat acquired resistance, as tumour vessels themselves will be targeted rather than the actual angiogenic process of blood vessel formation. By targeting changes in the tumour blood vessels it is less likely that acquired resistance will occur as the endothelial cells expressing such markers will be more genetically stable, more homogeneous and less able to give rise to tumour endothelial cells that do not express certain tumour endothelial markers. For all these reasons, new, more effective targets for anti-vascular therapies for cancer are urgently needed.

The recently described CLEC14A interacts with the extracellular matrix protein MMRN2 (Zanivan *et al.*, 2013) and actively promotes angiogenesis. The antibody mediated disruption of the CLEC14A/MMRN2 interaction led to a reduction in tumour growth in a LLC tumour model (Noy *et al.*, 2015). This was further confirmed by disrupting the interaction by expressing the binding fragment of MMRN2 (MMRN2$^{495-678}$) in mouse LLC tumour cells injected subcutaneously (Khan *et al.*, 2017). *In vitro* studies also demonstrated that upon loss of CLEC14A in HUVEC, pro-angiogenic activities such as tube formation and cell migration were impaired (Rho

et al., 2011; Mura *et al.*, 2012). The closely related CD93 is also involved in angiogenesis and has been shown to interact with MMRN2 (Galvagni *et al.*, 2017; Khan *et al.*, 2017; Lugano, Dejana and Dimberg, 2018). The region responsible for the interaction between MMRN2 and CD93 is the same as for CLEC14A, falling between amino acids 495 and 674 of MMRN2. These reports suggest that CLEC14A and CD93 may be involved in the same signalling pathway or play a redundant role in angiogenesis.

As the CLEC14A, CD93/MMRN2 interactions appear to be important in angiogenesis, the interaction was exploited as a mean to generate new cancer therapies.

6.2 CLEC14A and CD93: possible redundancy

No study has yet compared the function of both CLEC14A and CD93 in angiogenesis. The first aim of this work was to explore whether the loss of function of CLEC14A or CD93 in angiogenesis was redundant, or whether the loss of both proteins had an additive effect on components of angiogenesis, such as tube formation, migration or membrane transmigration. The double knockdown of MMRN2 and CD93 was also studied to verify whether the phenotype observed in the single knockdown was mediated by the presence of MMRN2.

In chapter 3 it was shown that CD93 is involved in angiogenesis and has an independent function from CLEC14A. This conclusion was supported by the fact that with CLEC14A knockdown there was no effect on tube formation (both in Matrigel

and in a co-culture assay with fibroblasts), migration or membrane transmigration. In contrast, CD93 knockdown showed a significant reduction in network formation and transmigration. CD93 knockdown also showed an observable retardation in a wound healing assay (at 24 hours the wound was not closed), supporting what has been previously shown (Langenkamp *et al.*, 2015). The strong phenotype observed on CD93 knockdown seems to be independent from CLEC14A and MMRN2, because upon double knockdown there was no phenotypic change. In the double knockdowns the phenotype was the same as the CD93 single knockdowns. It is interesting to note that upon single knockdown of MMRN2, there is a significant increase in tube formation on Matrigel and in transmigration, but this effect was lost completely when the knockdown was coupled with CD93 knockdown.

Measurement of the relative expression of CLEC14A and CD93 showed that CD93 is expressed around 10 times more than CLEC14A in HUVEC in cultures. It is plausible that CLEC14A has the same role as CD93, but due to its low level of expression *in vitro* there is little effect on knockdown.

This work supports the angiostatic role of MMRN2 reported by Lorenzon and colleagues (Lorenzon *et al.*, 2012). According to these reports, the reduction of MMRN2 increases the availability of VEGFA, because MMRN2 is able to directly bind VEGFA sequestering it from the environment. MMRN2 has also been described as a scaffold at the interface between endothelial cells and pericytes, orchestrating various different proteins, underling the complexity of its interactions (Khan *et al.*, 2017).

In the frame of this work, it would be interesting to analyse the CLEC14A/MMRN2 double knockdown phenotype, which has not been investigated yet, to test whether the phenotype observed for MMRN2 knockdowns were lost or exacerbated upon knockdown of CLEC14A, or vice versa. Furthermore, it would be interesting to employ an anti-VEGF antibody upon MMRN2 knockdown, to see if it is possible to reverse the phenotype observed and to conclude if the effect observed is mediated by an increased VEGF-A availability. For future studies it would be also interesting to investigate if these proteins are co-regulated or if they regulate the expression of other key proteins involved in angiogenesis. qPCR analysis has shown a regulation at the RNA level of VE-cadherin and VEGFR3 upon loss of CLEC14A. Further studies *in vitro* together with a few recent reports may shed light on the mechanism by which CD93 and potentially CLEC14A mediates angiogenesis and what the role MMRN2 plays in this signalling pathway. As the respective knockout mice are all viable, the generation of double and potentially triple knockout mice offer the potential to confirm the *in vitro* data in *in vivo* angiogenesis and tumour models.

6.3 Exploiting the MMRN2 binding fragment for anti-angiogenic and anti-tumour therapies

A second aim of this work was to exploit our knowledge regarding the interaction between CLEC14A and MMRN2 in order to generate therapeutic tools for anti-vascular and anti-angiogenic therapy. Previously, Khan and colleagues had used far western blot to identify a minimal binding fragment of MMRN2, namely MMRN2[495-]

[678], which retains the avidity capability towards CLEC14A and CD93. This work has explored the possibilities of using a recombinant MMRN2$^{495-678}$-hFc fragment as a vaccine and alternatively the generation of a drug conjugate.

Two previous reports from our laboratory described the vaccination against the TEM's Robo4 and GRIN2D (Zhuang *et al.*, 2015; Ferguson *et al.*, 2016). In a similar vein we attempted to vaccinate against the MMRN2 fragment. This should disrupt the interaction between MMRN2 and CLEC14A blocking tumour angiogenesis. However, in practise our vaccination attempts failed, this could be due to the inability to break tolerance and generate antibodies towards the MMRN2 self-protein. Future strategies could employ using a stronger adjuvant as a fusion protein such as the C-terminal fragment of tetanus toxoid (TT) instead of the human Fc protein. The TT fragment was successfully used to generate a vaccination response against TEM1 (Facciponte *et al.*, 2014).

There have been numerous successful attempts in using antibody drug conjugates (ADCs) described in the literature, such as those targeting Endosialin or CD276 (Capone *et al.*, 2017; Seaman *et al.*, 2017). Here we present an analogous approach, which exploits a binding fragment rather than an actual antibody. It was shown that mouse MMRN2$^{495-678}$ is internalised in HUVEC and this makes it the perfect fusion partner for toxins like dianthin, which need to be released within the cytosol. Our results showing the internalisation of MMRN2$^{495-678}$ confirmed unpublished data from our lab that demonstrated the internalisation of monoclonal antibodies to CLEC14A (Puja Lodhia PhD Thesis 2016). The use of the fragment would have a

double effect, targeting CLEC14A expressing cells (specifically the tumour compartment), but also disrupting the interaction between CLEC14A and MMRN2 as previously shown when expressed by transfected tumour cells (Khan *et al.*, 2017). Future study will be necessary to test the actual toxin *in vitro* in HUVEC. It is also plausible, if CD93 mediates also the internalisation of the target, that the effect of the toxin will be stronger on endothelial cells than the one observed with monoclonal antibodies specific for CLEC14A. *In vivo* studies will be necessary to determine whether the fragment binding CD93 will have cytotoxic consequences.

Finally, the last and most innovative approach was the generation of a fragment-based Chimeric Antigen Receptor T cell. Here we demonstrate the functionality of T cells expressing this CAR *in vitro.* Further confirmation of the activity of this CAR in cytotoxic assay is needed.

hMMRN2 CAR represents the third example of chimeric antigen receptors based on ligands in the literature (Parente-Pereira *et al.*, 2013; Sentman and Meehan, 2014). These reports are the proof of principle that ligand-based CARs are a feasible option and open the possibility of creating functional immunotherapy strategies even in absence of specific monoclonal antibodies, taking advantage of possible information on natural ligands. Furthermore, these ligand-based CARs might have multiple specificity like hMMRN2 or the previously described T1E28z CAR by Parente-Pereira *et al.,* 20013, making them more powerful tools for immunotherapy. Theoretically, it would also be possible to generate chimeric antigen receptors based on ligands of

specific isoforms of protein known to promote tumorigenesis. The generation of antibodies with such specificity might not be easily achievable.

It is possible to speculate that the targeting of the endothelium using modified T cells might present advantages such as avoiding resistance and necessity of penetrating the tumour mass, but also limitations. In fact, immune cells to reach the tumour site usually extravasate from the blood stream. Selectively targeting tumour vessels might reduce the number of modified T cells as well as of other immune cell types recruited at the tumour sites. Dedicated *in vivo* studies are necessary confirm what the effects of this therapy are in tumour models.

APPENDIX

Figure A1 MMRN2$^{495-674}$ is able to bind CD93 on HUVEC

HUVEC cells were blocked with either IgG, CRT2 and CRT4 antibodies. It is known that CRT4 binds the same site on CLEC14A than MMRN2, whereas CRT2 bind an alternative site. Cells were washed and incubated with either human MMRN2$^{495-674}$-hFc or recombinant hFc alone. CRT4 is not able to block MMRN2 binding in HUVEC, suggesting that the fragment is able to bind CD93 on HUVEC. The experiment was repeated 3 times with similar results.

REFERENCES

Aday, S., Zoldan, J., Besnier, M., Carreto, L., Saif, J., Fernandes, R., Santos, T., Bernardino, L., Langer, R., Emanueli, C. and Ferreira, L. (2017) 'Synthetic microparticles conjugated with VEGF165improve the survival of endothelial progenitor cells via microRNA-17 inhibition', *Nature Communications*. Springer US, 8(1). doi: 10.1038/s41467-017-00746-7.

Ahmad, Z. A., Yeap, S. K., Ali, A. M., Ho, W. Y., Alitheen, N. B. M. and Hamid, M. (2012) 'ScFv antibody: Principles and clinical application', *Clinical and Developmental Immunology*, 2012. doi: 10.1155/2012/980250.

Ambrose, S., Gordon, N., Goldsmith, J., Wei, W., Zeegers, M., James, N., Knowles, M., Bryan, R. and Ward, D. (2015) 'Use of Aleuria alantia Lectin Affinity Chromatography to Enrich Candidate Biomarkers from the Urine of Patients with Bladder Cancer', *Proteomes*, 3(3), pp. 266–282. doi: 10.3390/proteomes3030266.

Bais, C., Singh, M., Kaminker, J. and Brauer, M. (2011) 'Biological markers for monitoring patient response to vegf antagonists', *U.S. Patent*, 20,110,117.

Bhargava, C., Dürkop, H., Zhao, X., Weng, A., Melzig, M. F. and Fuchs, H. (2017) 'Targeted dianthin is a powerful toxin to treat pancreatic carcinoma when applied in combination with the glycosylated triterpene SO1861', *Molecular Oncology*, 11(11), pp. 1527–1543. doi: 10.1002/1878-0261.12115.

Bjarnegard, M. (2004) 'Endothelium-specific ablation of PDGFB leads to pericyte loss and glomerular, cardiac and placental abnormalities', *Development*, 131(8), pp. 1847–1857. doi: 10.1242/dev.01080.

Bohlson, S. S., Silva, R., Fonseca, M. I. and Tenner, A. J. (2005) 'CD93 Is Rapidly Shed from the Surface of Human Myeloid Cells and the Soluble Form Is Detected in Human Plasma', *The Journal of Immunology*, 175(2), pp. 1239–1247. doi: 10.4049/jimmunol.175.2.1239.

Bollard, C. M., Ro, C., Calonge, M. J., Huls, M. H., Wagner, H., Massague, J., Brenner, M. K., Heslop, H. E. and Rooney, C. M. (2018) 'Adapting a transforming growth factor β – related tumor protection strategy to enhance antitumor immunity', Blood 2002 99:3179-3187; doi: https://doi.org/10.1182/blood.V99.9.31798.

Bretscher, P. and Cohn, M. (1970) 'A Theory of Self-Nonself Discrimination', 169(1964) *Science* 11 Sep 1970: Vol. 169, Issue 3950, pp. 1042-1049 DOI: 10.1126/science.169.3950.1042.

Burghoff, S. and Schrader, J. (2011) 'Secretome of human endothelial cells under shear stress', *Journal of Proteome Research*, 10(3), pp. 1160–1169. doi: 10.1021/pr100937a.

Capone, E., Piccolo, E., Fichera, I., Ciufici, P. and Barcaroli, D. (2017) 'Generation of a novel Antibody-Drug Conjugate targeting endosialin : potent and durable antitumor response in sarcoma', *Oncotarget* 8(36), pp. 1–10. doi: 10.18632/oncotarget.19499.

Carmeliet, P. (2003) 'Angiogenesis in health and disease', *Nature Medicine*, 9(6), pp. 653–660. doi: 10.1038/nm0603-653.

Carmeliet, P. and Jain, R. K. (2011) 'Molecular mechanisms and clinical applications of angiogenesis', *Nature*, 473(7347), pp. 298–307. doi: 10.1038/nature10144.

Carter, P. J. and Senter, P. D. (2008) 'Antibody-Drug Conjugates for Cancer Therapy', *The Cancer Journal*, 14(3), pp. 154–169. doi: 10.1097/PPO.0b013e318172d704.

Casanovas, O., Hicklin, D. J., Bergers, G. and Hanahan, D. (2005) 'Drug resistance by evasion of antiangiogenic targeting of VEGF signaling in late-stage pancreatic islet tumors', *Cancer Cell*, 8(4), pp. 299–309. doi: 10.1016/j.ccr.2005.09.005.

Christian, S., Ahorn, H., Novatchkoval, M., Garin-Chesa, P., Park, J. E., Weber, G., Eisenhaber, F., Rettig, W. J. and Lenter, M. C. (2001) 'Molecular Cloning and

Characterization of EndoGlyx-1, an EMILIN-like Multisubunit Glycoprotein of Vascular Endothelium', *Journal of Biological Chemistry*, 276(51), pp. 48588–48595. doi: 10.1074/jbc.M106152200.

Colladel, R., Pellicani, R., Andreuzzi, E., Paulitti, A., Tarticchio, G., Todaro, F., Colombatti, A. and Mongiat, M. (2016) 'MULTIMERIN2 binds VEGF-A primarily via the carbohydrate chains exerting an angiostatic function and impairing tumor growth.', *Oncotarget*, 7(2), pp. 2022–2037. doi: 10.18632/oncotarget.6515.

Colombatti, A., Spessotto, P., Doliana, R., Mongiat, M., Bressan, G. M. and Esposito, G. (2012) 'The EMILIN/multimerin family', *Frontiers in Immunology*, 2(JAN), pp. 1–13. doi: 10.3389/fimmu.2011.00093.

Compagni, A., Wilgenbus, P., Impagnatiello, M. A., Cotten, M. and Christofori, G. (2000) 'Fibroblast growth factors are required for efficient tumor angiogenesis', *Cancer Research*, 60(24), pp. 7163–7169.

Cory, G. (2011) 'Scratch-Wound Assay', in *Methods in molecular biology (Clifton, N.J.)*, pp. 25–30. doi: 10.1007/978-1-61779-207-6_2.

Coulson, A., Levy, A., Coulson, A. and Levy, A. (2014) 'Monoclonal Antibodies in Cancer Therapy : Mechanisms , Successes and Limitations Los Anticuerpos Monoclonales en el Tratamiento del Cáncer : Mecanismos , Éxitos y Limitaciones', 63(6), pp. 650–654. doi: 10.7727/wimj.2013.241.

D'Aloia, M. M., Zizzari, I. G., Sacchetti, B., Pierelli, L. and Alimandi, M. (2018) 'CAR-T cells: The long and winding road to solid tumors review-article', *Cell Death and Disease*. Springer US, 9(3). doi: 10.1038/s41419-018-0278-6.

Dean, Y. D., McGreal, E. P., Akatsu, H. and Gasque, P. (2000) 'Molecular and cellular properties of the rat AA4 antigen, a C-type lectin-like receptor with structural homology to thrombomodulin', *Journal of Biological Chemistry*, 275(44), pp. 34382–

34392. doi: 10.1074/jbc.M006229200.

Diamantis, N. and Banerji, U. (2016) 'Antibody-drug conjugates - An emerging class of cancer treatment', *British Journal of Cancer*. Nature Publishing Group, 114(4), pp. 362–367. doi: 10.1038/bjc.2015.435.

Dieterich, L. C., Mellberg, S., Langenkamp, E., Zhang, L., Zieba, A., Salom, H., Teichert, M., Huang, H., Edqvist, P., Kraus, T., Augustin, H. G., Olofsson, T., Larsson, E., Ola, S., Molema, G., Pont, F. and Dimberg, A. (2012) 'Transcriptional profiling of human glioblastoma vessels indicates a key role of VEGF-A and TGF β 2 in vascular abnormalization', *J Pathol*. 2012 Nov;228(3):378-90. doi: 10.1002/path.4072. Epub 2012 Aug 31.

Donnem, T., Reynolds, A. R., Kuczynski, E. A., Gatter, K., Vermeulen, P. B., Kerbel, R. S., Harris, A. L. and Pezzella, F. (2018) 'Non-angiogenic tumours and their influence on cancer biology', *Nature Reviews Cancer*, 18(5), pp. 323–336. doi: 10.1038/nrc.2018.14.

Donovan, D., Brown, N. J., Bishop, E. T. and Lewis, C. E. (2001) 'Comparison of three in vitro human "angiogenesis" assays with capillaries formed in vivo.', *Angiogenesis*, 4(2), pp. 113–21.

Doyonnas, R., Chan, J. Y., Butler, L. H., Lee-prudhoe, J. E., Zannettino, A. C. W., Simmons, P. J., Bühring, H., Levesque, J., Watt, S. M., Lee-prudhoe, J. E., Zannettino, A. C. W. and Simmons, P. J. (2018) 'CD164 Monoclonal Antibodies That Block Hemopoietic Progenitor Cell Adhesion and Proliferation Interact with the First Mucin Domain of the CD164 Receptor'. doi: 10.4049/jimmunol.165.2.840.

Duan, C. L., Hou, G. H., Liu, Y. P., Liang, T., Song, J., Han, J. K. and Zhang, C. (2014) 'Tumor vascular homing endgolin-targeted radioimmunotherapy in hepatocellular carcinoma', *Tumor Biology*, 35(12), pp. 12205–12215. doi: 10.1007/s13277-014-2529-1.

Dunn, G. P., Bruce, A. T., Ikeda, H., Old, L. J. and Schreiber, R. D. (2002) 'Cancer immunoediting : from immuno- surveillance to tumor escape', 3(11), pp. 991–998. DOI: 10.1038/ni1102-991.

Ebos, J. M. L., Lee, C. R., Cruz-Munoz, W., Bjarnason, G. A., Christensen, J. G. and Kerbel, R. S. (2009) 'Accelerated Metastasis after Short-Term Treatment with a Potent Inhibitor of Tumor Angiogenesis', *Cancer Cell*. Elsevier Ltd, 15(3), pp. 232–239. doi: 10.1016/j.ccr.2009.01.021.

Engels, B., Cam, H., Schüler, T., Indraccolo, S., Gladow, M., Baum, C., Blankenstein, T. and Uckert, W. (2003) 'Retroviral Vectors for High-Level Transgene Expression in T Lymphocytes', *Human Gene Therapy*, 14(12), pp. 1155–1168. doi: 10.1089/104303403322167993.

Facciponte, J. G., Ugel, S., Sanctis, F. De, Li, C., Wang, L., Nair, G., Sehgal, S., Raj, A., Matthaiou, E., Coukos, G. and Facciabene, A. (2014) 'Tumor endothelial marker 1 – specific DNA vaccination targets tumor vasculature', 124(4), pp. 1497–1511. doi: 10.1172/JCI67382DS1.

Ferguson, H. J. M., Wragg, J. W., Ward, S., Heath, V. L., Ismail, T. and Bicknell, R. (2016) 'Glutamate dependent NMDA receptor 2D is a novel angiogenic tumour endothelial marker in colorectal cancer', *Oncotarget*, 7(15), pp. 20440–20454. doi: 10.18632/oncotarget.7812.

Finney, H. M., Lawson, A. D., Bebbington, C. R. and Weir, A. N. (1998) 'Chimeric receptors providing both primary and costimulatory signaling in T cells from a single gene product.', *Journal of immunology*, 161(6), pp. 2791–2797. doi: 10.4049/jimmunol.172.1.104.

Folkman, J. (1971) 'Tumor angiogenesis: therapeutic implications.', *The New England journal of medicine*, 285(21), pp. 1182–1186. doi: 10.1056/NEJM197111182852108.

Francia, G., Cruz-munoz, W., Man, S., Xu, P. and Kerbel, R. S. (2011) 'Mouse models of advanced spontaneous metastasis for experimental therapeutics, *Nat Rev Cancer*. 2011 Feb;11(2):135-41. doi: 10.1038/nrc3001.

Galvagni, F., Nardi, F., Maida, M., Bernardini, G., Vannuccini, S., Petraglia, F., Santucci, A. and Orlandini, M. (2016) 'CD93 and dystroglycan cooperation in human endothelial cell adhesion and migration adhesion and migration.', *Oncotarget*, 7(9). doi: 10.18632/oncotarget.7136.

Galvagni, F., Nardi, F., Spiga, O., Trezza, A., Tarticchio, G., Pellicani, R., Andreuzzi, E., Caldi, E., Toti, P., Tosi, G. M., Santucci, A., Iozzo, R. V., Mongiat, M. and Orlandini, M. (2017) 'Dissecting the CD93-Multimerin 2 interaction involved in cell adhesion and migration of the activated endothelium', *Matrix Biology*. Elsevier B.V., 64, pp. 112–127. doi: 10.1016/j.matbio.2017.08.003.

Gavilondo, J. V., Hernández-Bernal, F., Ayala-Ávila, M., de la Torre, A. V., de la Torre, J., Morera-Díaz, Y., Bequet-Romero, M., Sánchez, J., Valenzuela, C. M., Martín, Y., Selman-Housein, K. H., Garabito, A. and Lazo, O. C. (2014) 'Specific active immunotherapy with a VEGF vaccine in patients with advanced solid tumors. Results of the CENTAURO antigen dose escalation phase I clinical trial', *Vaccine*, 32(19), pp. 2241–2250. doi: 10.1016/j.vaccine.2013.11.102.

Gerber, H.-P., Senter, P. D. and Grewal, I. S. (2009) 'Antibody drug-conjugates targeting the tumor vasculature', *mAbs*, 1(3), pp. 247–253. doi: 10.4161/mabs.1.3.8515.

Gerhardt, H., Golding, M., Fruttiger, M., Ruhrberg, C., Lundkvist, A., Abramsson, A., Jeltsch, M., Mitchell, C., Alitalo, K., Shima, D. and Betsholtz, C. (2003) 'VEGF guides angiogenic sprouting utilizing endothelial tip cell filopodia', *Journal of Cell Biology*, 161(6), pp. 1163–1177. doi: 10.1083/jcb.200302047.

Gilabert-Oriol, R., Thakur, M., Weise, C., Dernedde, J., Von Mallinckrodt, B., Fuchs, H.

and Weng, A. (2013) 'Small structural differences of targeted anti-tumor toxins result in strong variation of protein expression', *Protein Expression and Purification*. Elsevier Inc., 91(1), pp. 54–60. doi: 10.1016/j.pep.2013.07.004.

Goel, S., Wong, A. H. and Jain, R. K. (2012) 'Vascular Normalization as a Therapeutic Strategy', *Cold Spring Harb Perspect Med*, 2, pp. 1–24. doi: 10.1101/cshperspect.a006486.

Greenlee, M. C., Sullivan, S. A. and Bohlson, S. S. (2009) 'Detection and characterization of soluble CD93 released during inflammation.', *Inflammation research : official journal of the European Histamine Research Society ... [et al.]*, 58(12), pp. 909–19. doi: 10.1007/s00011-009-0064-0.

Gross, G., Waks, T. and Eshhar, Z. (1989) 'Expression of immunoglobulin-T-cell receptor chimeric molecules as functional receptors with antibody-type specificity.', *Proceedings of the National Academy of Sciences*, 86(24), pp. 10024–10028. doi: 10.1073/pnas.86.24.10024.

Hanahan, D. and Weinberg, R. A. (2000) 'The hallmarks of cancer.', *Cell*, 100(1), pp. 57–70. doi: 10.1007/s00262-010-0968-0.

Hanahan, D. and Weinberg, R. A. (2011) 'Hallmarks of cancer: The next generation', *Cell*. Elsevier Inc., 144(5), pp. 646–674. doi: 10.1016/j.cell.2011.02.013.

Harhausen, D., Prinz, V., Ziegler, G., Gertz, K., Endres, M., Lehrach, H., Gasque, P., Botto, M., Stahel, P. F., Dirnagl, U., Nietfeld, W. and Trendelenburg, G. (2010) 'CD93/AA4.1: A Novel Regulator of Inflammation in Murine Focal Cerebral Ischemia', *The Journal of Immunology*, 184(11), pp. 6407–6417. doi: 10.4049/jimmunol.0902342.

Haynes, N. M., Trapani, J. A., Teng, M. W. L., Jackson, J. T., Cerruti, L., Jane, S. M., Kershaw, M. H., Smyth, M. J. and Darcy, P. K. (2002) 'Single-chain antigen recognition

receptors that costimulate potent rejection of established experimental tumors', *Blood*, 100(9), pp. 3155–3163. doi: 10.1182/blood-2002-04-1041.

Hellström, M., Phng, L. K., Hofmann, J. J., Wallgard, E., Coultas, L., Lindblom, P., Alva, J., Nilsson, A. K., Karlsson, L., Gaiano, N., Yoon, K., Rossant, J., Iruela-Arispe, M. L., Kalén, M., Gerhardt, H. and Betsholtz, C. (2007) 'Dll4 signalling through Notch1 regulates formation of tip cells during angiogenesis', *Nature*, 445(7129), pp. 776–780. doi: 10.1038/nature05571.

Hemmerle, T., Probst, P., Giovannoni, L., Green, A. J., Meyer, T. and Neri, D. (2013) 'The antibody-based targeted delivery of TNF in combination with doxorubicin eradicates sarcomas in mice and confers protective immunity', *British Journal of Cancer*. Nature Publishing Group, 109(5), pp. 1206–1213. doi: 10.1038/bjc.2013.421.

Herbert, J. M. J., Stekel, D., Sanderson, S., Heath, V. L. and Bicknell, R. (2008) 'A novel method of differential gene expression analysis using multiple cDNA libraries applied to the identification of tumour endothelial genes', *BMC Genomics*, 9, pp. 1–21. doi: 10.1186/1471-2164-9-153.

Ho, M., Yang, E., Matcuk, G., Deng, D., Sampas, N., Tsalenko, A., Tabibiazar, R., Zhang, Y., Chen, M., Talbi, S., Ho, Y. D., Wang, J., Tsao, P. S., Ben-Dor, A., Yakhini, Z., Bruhn, L. and Quertermous, T. (2003) 'Identification of endothelial cell genes by combined database mining and microarray analysis', *Physiological Genomics*, 13(3), pp. 249–262. doi: 10.1152/physiolgenomics.00186.2002.

Holmgren, L., O'reilly, M. S. and Folkman, J. (1995) 'Dormancy of micrometastases: Balanced proliferation and apoptosis in the presence of angiogenesis suppression', *Nature Medicine*, 1(2), pp. 149–153. doi: 10.1038/nm0295-149.

Hombach, A., Wieczarkowiecz, A., Marquardt, T., Heuser, C., Usai, L., Pohl, C., Seliger, B. and Abken, H. (2001) 'Tumor-Specific T Cell Activation by Recombinant Immunoreceptors: CD3 Signaling and CD28 Costimulation Are Simultaneously

Required for Efficient IL-2 Secretion and Can Be Integrated Into One Combined CD28/CD3 Signaling Receptor Molecule', *The Journal of Immunology*, 167(11), pp. 6123–6131. doi: 10.4049/jimmunol.167.11.6123.

Huber, M. A., Kraut, N., Schweifer, N., Dolznig, H., Peter, R. U., Schubert, R. D., Scharffetter-Kochanek, K., Pehamberger, H. and Garin-Chesa, P. (2006) 'Expression of stromal cell markers in distinct compartments of human skin cancers', *Journal of Cutaneous Pathology*, 33(2), pp. 145–155. doi: 10.1111/j.0303-6987.2006.00446.x.

Huminiecki, L. and Bicknell, R. (2000) 'In silico cloning of novel endothelial-specific genes', *Genome Research*, 10(11), pp. 1796–1806. doi: 10.1101/gr.150700.

Hurwitz, H., Fehrenbacher, L., Novotny, W., Cartwright, T., Hainsworth, J., Heim, W., Berlin, J., Baron, A., Griffing, S., Holmgren, E., Ferrara, N., Fyfe, G., Rogers, B., Ross, R. and Kabbinavar, F. (2004) 'Bevacizumab plus Irinotecan, Fluorouracil, and Leucovorin for Metastatic Colorectal Cancer', *New England Journal of Medicine*, 350(23), pp. 2335–2342. doi: 10.1056/NEJMoa032691.

Ichim, T. E., Li, S., Ma, H., Yurova, Y. V., Szymanski, J. S., Patel, A. N., Kesari, S., Min, W. P. and Wagner, S. C. (2015) 'Induction of tumor inhibitory anti-angiogenic response through immunization with interferon Gamma primed placental endothelial cells: ValloVax™', *Journal of Translational Medicine*, 13(1), pp. 1–9. doi: 10.1186/s12967-015-0441-0.

Imai, C., Mihara, K., Andreansky, M., Nicholson, I. C., Pui, C. H., Geiger, T. L. and Campana, D. (2004) 'Chimeric receptors with 4-1BB signaling capacity provoke potent cytotoxicity against acute lymphoblastic leukemia', *Leukemia*, 18(4), pp. 676–684. doi: 10.1038/sj.leu.2403302.

Irvin, M. W., Zijlstra, A., Wikswo, J. P. and Pozzi, A. (2014) 'Techniques and assays for the study of angiogenesis', *Experimental Biology and Medicine*, 239(11), pp. 1476–1488. doi: 10.1177/1535370214529386.

Iwasaki, M., Liedtke, M., Gentles, A. J. and Cleary, M. L. (2015) 'CD93 Marks a Non-Quiescent Human Leukemia Stem Cell Population and Is Required for Development of MLL-Rearranged Acute Myeloid Leukemia', *Cell Stem Cell*. Elsevier Ltd, 17(4), pp. 412–421. doi: 10.1016/j.stem.2015.08.008.

Jakobsson, L., Franco, C. A., Bentley, K., Collins, R. T., Ponsioen, B., Aspalter, I. M., Rosewell, I., Busse, M., Thurston, G., Medvinsky, A., Schulte-Merker, S. and Gerhardt, H. (2010) 'Endothelial cells dynamically compete for the tip cell position during angiogenic sprouting', *Nature Cell Biology*. Nature Publishing Group, 12(10), pp. 943–953. doi: 10.1038/ncb2103.

Jang, J., Kim, M. R., Kim, T. K., Lee, W. R., Kim, J. H., Heo, K. and Lee, S. (2017) 'CLEC14a-HSP70-1A interaction regulates HSP70-1A-induced angiogenesis', *Scientific Reports*, 7(1), pp. 1–12. doi: 10.1038/s41598-017-11118-y.

Jentoft, N. (1990) 'interest, these biological roles have been shown to apply only to a few gly- coproteins. This article will focus on', pp. 291–294.

Jeon, J.-W., Jung, J.-G., Shin, E.-C., Choi, H. I., Kim, H. Y., Cho, M.-L., Kim, S.-W., Jang, Y.-S., Sohn, M.-H., Moon, J.-H., Cho, Y.-H., Hoe, K.-L., Seo, Y.-S. and Park, Y. W. (2010) 'Soluble CD93 Induces Differentiation of Monocytes and Enhances TLR Responses', *The Journal of Immunology*, 185(8), pp. 4921–4927. doi: 10.4049/jimmunol.0904011.

Kansas, G. S. (1992) 'Structure and function of h l e c t i n', pp. 287–293.

Kao, Y., Jiang, S., Pan, W., Wang, K., Chen, P., Wei, J., Chen, W., Chang, B., Shi, G. and Wu, H. (2012) 'The Epidermal Growth Factor-like Domain of CD93 Is a Potent Angiogenic Factor', 7(12), pp. 1–11. doi: 10.1371/journal.pone.0051647.

Kerbel, R. S. (2008) 'Tumor angiogenesis', *New England Journal of Medicine*, 358(19). doi: 10.1056/NEJMra0706596.

Kerbel, R. S., Guerin, E., Francia, G., Xu, P., Lee, C. R., Ebos, J. M. L. and Man, S. (2013) 'Preclinical recapitulation of antiangiogenic drug clinical efficacies using models of early or late stage breast cancer metastatis', *Breast*. Elsevier Ltd, 22(S2), pp. S57–S65. doi: 10.1016/j.breast.2013.07.011.

Khan, K. A., Naylor, A. J., Khan, A., Noy, P. J., Mambretti, M., Lodhia, P., Athwal, J., Korzystka, A., Buckley, C. D., Willcox, B. E., Mohammed, F. and Bicknell, R. (2017) 'Multimerin-2 is a ligand for group 14 family C-type lectins CLEC14A, CD93 and CD248 spanning the endothelial pericyte interface', *Oncogene*. Nature Publishing Group, 36(44), pp. 6097–6108. doi: 10.1038/onc.2017.214.

Ki, M. K., Jeoung, M. H., Choi, J. R., Rho, S. S., Kwon, Y. G., Shim, H., Chung, J., Hong, H. J., Song, B. D. and Lee, S. (2013) 'Human antibodies targeting the C-type lectin-like domain of the tumor endothelial cell marker clec14a regulate angiogenic properties in vitro', *Oncogene*, 32(48), pp. 5449–5457. doi: 10.1038/onc.2013.156.

Kim, R. (2007) 'Cancer Immunoediting: From Immune Surveillance to Immune Escape', in *Cancer Immunotherapy*, pp. 9–27. doi: 10.1016/B978-012372551-6/50066-3.

Kim, T. K., Park, C. S., Jang, J., Kim, M. R., Na, H. J., Lee, K., Kim, H. J., Heo, K., Yoo, B. C., Kim, Y. M., Lee, J. W., Kim, S. J., Kim, E. S., Kim, D. Y., Cha, K., Lee, T. G. and Lee, S. (2018) 'Inhibition of VEGF-dependent angiogenesis and tumor angiogenesis by an optimized antibody targeting CLEC14a', *Molecular Oncology*, 12(3), pp. 356–372. doi: 10.1002/1878-0261.12169.

Kochenderfer, J. N., Dudley, M. E., Feldman, S. A., Wilson, W. H., Spaner, D. E., Maric, I., Stetler-stevenson, M., Phan, G. Q., Hughes, M. S., Sherry, R. M., Yang, J. C., Kammula, U. S., Devillier, L., Carpenter, R., Nathan, D. N., Morgan, R. A., Laurencot, C., Rosenberg, S. A., Kochenderfer, J. N., Dudley, M. E., Feldman, S. A., Wilson, W. H., Spaner, D. E., Maric, I., Stetler-stevenson, M., Phan, G. Q., Hughes, M. S., Sherry, R. M., Yang, J. C., Kammula, U. S., Devillier, L., Carpenter, R., Nathan, D. N., Morgan, R.

A., Laurencot, C. and Rosenberg, S. A. (2012) 'cytokine-associated toxicity in a clinical trial of anti-CD19 Plenary paper B-cell depletion and remissions of malignancy along with cytokine-associated toxicity in a clinical trial of anti-CD19 chimeric-antigen-receptor – transduced T cells', 119(12), pp. 2709–2720. doi: 10.1182/blood-2011-10-384388.

Kochenderfer, J. N., Wilson, W. H., Janik, J. E., Dudley, M. E., Feldman, S. a, Maric, I., Raffeld, M., Nathan, D. N., Brock, J., Morgan, R. a, Rosenberg, S. a, Stetler-stevenson, M. and Lanier, B. J. (2010) 'Eradication of B-lineage cells and regression of lymphoma in a patient treated with autologous T cells genetically engineered to recognize Brief report Eradication of B-lineage cells and regression of lymphoma in a patient treated with autologous T cells', 116(20), pp. 4099–4102. doi: 10.1182/blood-2010-04-281931.

Konerding, M. A., Fait, E. and Gaumann, A. (2001) '3D microvascular architecture of pre-cancerous lesions and invasive carcinomas of the colon', *British Journal of Cancer*, 84(10), pp. 1354–1362. doi: 10.1054/bjoc.2001.1809.

Koperek, O., Scheuba, C., Puri, C., Birner, P., Haslinger, C., Rettig, W., Niederle, B., Kaserer, K. and Chesa, P. G. (2007) 'Molecular characterization of the desmoplastic tumor stroma in medullary thyroid carcinoma', *International Journal of Oncology*, 31(1), pp. 59–67.

Kubota, Y., Kleinman, H. K., Martin, G. R. and Lawley, T. J. (1988) 'Role of laminin and basement membrane in the morphological differentiation of human endothelial cells into capillary-like structures.', *The Journal of cell biology*. Rockefeller University Press, 107(4), pp. 1589–98. doi: 10.1083/JCB.107.4.1589.

Kuczynski, E. A. and Kerbel, R. S. (2016) 'Implications of vessel co-option in sorafenib-resistant hepatocellular carcinoma', *Chinese journal of cancer*. BioMed Central, 35(1), p. 97. doi: 10.1186/s40880-016-0162-7.

Langenkamp, E., Zhang, L., Lugano, R., Huang, H., Elhassan, T. E. A., Georganaki, M., Bazzar, W., Lööf, J., Trendelenburg, G., Essand, M., Pontén, F., Smits, A. and Dimberg, A. (2015) 'Elevated expression of the C-Type Lectin CD93 in the glioblastoma vasculature regulates cytoskeletal rearrangements that enhance vessel function and reduce host survival', *Cancer Research*, 75(21), pp. 4504–4516. doi: 10.1158/0008-5472.CAN-14-3636.

Lee, D. W., Kochenderfer, J. N., Stetler-Stevenson, M., Cui, Y. K., Delbrook, C., Feldman, S. A., Fry, T. J., Orentas, R., Sabatino, M., Shah, N. N., Steinberg, S. M., Stroncek, D., Tschernia, N., Yuan, C., Zhang, H., Zhang, L., Rosenberg, S. A., Wayne, A. S. and Mackall, C. L. (2015) 'T cells expressing CD19 chimeric antigen receptors for acute lymphoblastic leukaemia in children and young adults: A phase 1 dose-escalation trial', *The Lancet*. Elsevier Ltd, 385(9967), pp. 517–528. doi: 10.1016/S0140-6736(14)61403-3.

Lee, S., Rho, S. S., Park, H., Park, J. A., Kim, J., Lee, I. K., Koh, G. Y., Mochizuki, N., Kim, Y. M. and Kwon, Y. G. (2017) 'Carbohydrate-binding protein CLEC14A regulates VEGFR-2- and VEGFR-3-dependent signals during angiogenesis and lymphangiogenesis', *Journal of Clinical Investigation*, 127(2), pp. 457–471. doi: 10.1172/JCI85145.

Leimeister, C., Steidl, C., Schumacher, N., Erhard, S. and Gessler, M. (2002) 'D evelopm ental Expression and Biochem ical Characterization of Emu Family Members', 218, pp. 204–218 *Developmental Biology* **249,** 204–218 (2002) doi:10.1006/dbio.2002.0764 .

Leite de Oliveira, R., Deschoemaeker, S., Henze, A. T., Debackere, K., Finisguerra, V., Takeda, Y., Roncal, C., Dettori, D., Tack, E., Jönsson, Y., Veschini, L., Peeters, A., Anisimov, A., Hofmann, M., Alitalo, K., Baes, M., D'hooge, J., Carmeliet, P. and Mazzone, M. (2012) 'Gene-Targeting of Phd2 Improves Tumor Response to Chemotherapy and Prevents Side-Toxicity', *Cancer Cell*, 22(2), pp. 263–277. doi: 10.1016/j.ccr.2012.06.028.

Lenschow, D. J., Walunas, T. L. and Bluestone, J. A. (1996) 'CD28/B7 SYSTEM OF T CELL COSTIMULATION', *Annual Review of Immunology*, 14(1), pp. 233–258. doi: 10.1146/annurev.immunol.14.1.233.

Levine, B. L., Miskin, J., Wonnacott, K. and Keir, C. (2017) 'Global Manufacturing of CAR T Cell Therapy', *Molecular Therapy - Methods and Clinical Development*. Elsevier Ltd., 4(March), pp. 92–101. doi: 10.1016/j.omtm.2016.12.006.

Li, G., Guo, J., Shen, B., Yadav, D. B. and Mark, X. (2018) 'Mechanisms of Acquired Resistance to Trastuzumab Emtansine in Breast Cancer Cells', (650). doi: 10.1158/1535-7163.MCT-17-0296.

Lorenzon, E., Colladel, R., Andreuzzi, E., Marastoni, S., Todaro, F., Schiappacassi, M., Ligresti, G., Colombatti, A. and Mongiat, M. (2012) 'MULTIMERIN2 impairs tumor angiogenesis and growth by interfering with VEGF-A/VEGFR2 pathway', *Oncogene*. Nature Publishing Group, 31(26), pp. 3136–3147. doi: 10.1038/onc.2011.487.

Lu, K. V., Chang, J. P., Parachoniak, C. A., Pandika, M. M., Aghi, M. K., Meyronet, D., Isachenko, N., Fouse, S. D., Phillips, J. J., Cheresh, D. A., Park, M. and Bergers, G. (2012) 'VEGF Inhibits Tumor Cell Invasion and Mesenchymal Transition through a MET/VEGFR2 Complex', *Cancer Cell*, 22(1), pp. 21–35. doi: 10.1016/j.ccr.2012.05.037.

Lugano, R., Dejana, E. and Dimberg, A. (2018) 'CD93 promotes integrin- b 1 activation and fibronectin fibrillogenesis during tumor angiogenesis' *J Clin Invest.* 2018;128(8):3280-3297. https://doi.org/10.1172/JCI97459.

Maeng, Y., Choi, H., Kwon, J., Park, Y., Choi, K., Min, J., Kim, Y., Suh, P., Kang, K., Won, M., Kim, Y. and Kwon, Y. (2009) 'Endothelial progenitor cell homing: prominent role of the IGF2-IGF2R-PLCb2 axis', 113(1), pp. 233–244. doi: 10.1182/blood-2008-06-162891.The.

Maher, J., Brentjens, R. J., Gunset, G., Rivière, I. and Sadelain, M. (2002) 'Human T-lymphocyte cytotoxicity and proliferation directed by a single chimeric TCRζ/CD28 receptor', *Nature Biotechnology*, 20(1), pp. 70–75. doi: 10.1038/nbt0102-70.

Mälarstig, A., Silveira, A., Wågsäter, D., Öhrvik, J., Bäcklund, A., Samnegård, A., Khademi, M., Hellenius, M. L., Leander, K., Olsson, T., Uhlén, M., de Faire, U., Eriksson, P. and Hamsten, A. (2011) 'Plasma CD93 concentration is a potential novel biomarker for coronary artery disease', *Journal of Internal Medicine*, 270(3), pp. 229–236. doi: 10.1111/j.1365-2796.2011.02364.x.

Von Mallinckrodt, B., Thakur, M., Weng, A., Gilabert-Oriol, R., Dürkop, H., Brenner, W., Lukas, M., Beindorff, N., Melzig, M. F. and Fuchs, H. (2014) 'Dianthin-EGF is an effective tumor targeted toxin in combination with saponins in a xenograft model for colon carcinoma', *Future Oncology*. doi: 10.2217/fon.14.164.

Mancuso, P., Calleri, A., Gregato, G., Labanca, V., Quarna, J., Antoniotti, P., Cuppini, L., Finocchiaro, G., Eoli, M., Rosti, V. and Bertolini, F. (2014) 'A subpopulation of circulating endothelial cells express CD109 and is enriched in the blood of cancer patients', *PLoS ONE*, 9(12), pp. 1–16. doi: 10.1371/journal.pone.0114713.

Masiero, M., Simões, F. C., Han, H. D., Snell, C., Peterkin, T., Bridges, E., Mangala, L. S., Wu, S. Y.-Y., Pradeep, S., Li, D., Han, C., Dalton, H., Lopez-Berestein, G., Tuynman, J. B., Mortensen, N. and Buffa, M. (2013) 'A Core Human Primary Tumor Angiogenesis Signature Identifies the Endothelial Orphan Receptor ELTD1 as a Key Regulator of Angiogenesis', pp. 229–241. doi:http://dx.doi.org/10.1016/j.ccr.2013.06.004.

Maude, S. L., Frey, N., Shaw, P. A., Aplenc, R., Barrett, D. M., Bunin, N. J., Chew, A., Gonzalez, V. E., Zheng, Z., Lacey, S. F., Mahnke, Y. D., Melenhorst, J. J., Rheingold, S. R., Shen, A., Teachey, D. T., Levine, B. L., June, C. H., Porter, D. L. and Grupp, S. A. (2014) 'Chimeric Antigen Receptor T Cells for Sustained Remissions in Leukemia', *New England Journal of Medicine*, 371(16), pp. 1507–1517. doi:

10.1056/NEJMoa1407222.

Mazzone, M., Dettori, D., Leite de Oliveira, R., Loges, S., Schmidt, T., Jonckx, B., Tian, Y. M., Lanahan, A. A., Pollard, P., Ruiz de Almodovar, C., De Smet, F., Vinckier, S., Aragonés, J., Debackere, K., Luttun, A., Wyns, S., Jordan, B., Pisacane, A., Gallez, B., Lampugnani, M. G., Dejana, E., Simons, M., Ratcliffe, P., Maxwell, P. and Carmeliet, P. (2009) 'Heterozygous Deficiency of PHD2 Restores Tumor Oxygenation and Inhibits Metastasis via Endothelial Normalization', *Cell*, 136(5), pp. 839–851. doi: 10.1016/j.cell.2009.01.020.

McGreal, E. P., Ikewaki, N., Akatsu, H., Morgan, B. P. and Gasque, P. (2002) 'Human C1qRp Is Identical with CD93 and the mNI-11 Antigen But Does Not Bind C1q', *The Journal of Immunology*, 168(10), pp. 5222–5232. doi: 10.4049/jimmunol.168.10.5222.

Mei, J. and Gui, J. (2008) 'Bioinformatic identification of genes encoding C1q-domain- containing proteins in zebrafish', *Journal of Genetics and Genomics*, 35(1), pp. 17–24. doi: 16/S1673-8527(08)60003-X.

Mesri, M., Birse, C., Heidbrink, J., McKinnon, K., Brand, E., Bermingham, C. L., Feild, B., FitzHugh, W., He, T., Ruben, S. and Moore, P. A. (2013) 'Identification and characterization of angiogenesis targets through proteomic profiling of endothelial cells in human cancer tissues', *PLoS ONE*, 8(11). doi: 10.1371/journal.pone.0078885.

Milanetto, M., Tiso, N., Braghetta, P., Volpin, D., Argenton, F. and Bonaldo, P. (2008) 'Emilin genes are duplicated and dynamically expressed during zebrafish embryonic development', *Developmental Dynamics*, 237(1), pp. 222–232. doi: 10.1002/dvdy.21402.

Mu, F. T., Callaghan, J. M., Steele-Mortimer, O., Stenmark, H., Parton, R. G., Campbell, P. L., McCluskey, J., Yeo, J. P., Tock, E. P. C. and Toh, B. H. (1995) 'EEA1, an early endosome-associated protein.', *Journal of Biological Chemistry*, pp. 13503–

13511. doi: 10.1074/jbc.270.22.13503.

Mura, M., Swain, R. K., Zhuang, X., Vorschmitt, H., Reynolds, G., Durant, S., Beesley, J. F. J., Herbert, J. M. J., Sheldon, H., Andre, M., Sanderson, S., Glen, K., Luu, N. T., McGettrick, H. M., Antczak, P., Falciani, F., Nash, G. B., Nagy, Z. S. and Bicknell, R. (2012) 'Identification and angiogenic role of the novel tumor endothelial marker CLEC14A', *Oncogene*. Nature Publishing Group, 31(3), pp. 293–305. doi: 10.1038/onc.2011.233.

Nepomuceno, R. R. and Tenner, a J. (1998) 'C1qRP, the C1q receptor that enhances phagocytosis, is detected specifically in human cells of myeloid lineage, endothelial cells, and platelets.', *Journal of immunology (Baltimore, Md. : 1950)*, 160(4), pp. 1929–1935.

Neri, D. and Bicknell, R. (2010) 'The Discovery and Characterisation of Tumour Endothelial Markers', in *Vascular Disruptive Agents for the Treatment of Cancer*. New York, NY: Springer New York, pp. 31–48. doi: 10.1007/978-1-4419-6609-4_2.

Norman, D. G., Barlow, P. N., Baron, M., Day, A. J. and Sim, R. B. (1991) 'Three-dimensional Structure of a Complement Module in Solution Control Protein', pp. 717–725.

Norsworthy, P. J., Fossati-Jimack, L., Cortes-Hernandez, J., Taylor, P. R., Bygrave, A. E., Thompson, R. D., Nourshargh, S., Walport, M. J. and Botto, M. (2004) 'Murine CD93 (C1qRp) Contributes to the Removal of Apoptotic Cells In Vivo but Is Not Required for C1q-Mediated Enhancement of Phagocytosis', *The Journal of Immunology*, 172(6), pp. 3406–3414. doi: 10.4049/jimmunol.172.6.3406.

Noy, P. J., Lodhia, P., Khan, K., Zhuang, X., Ward, D. G., Verissimo, A. R., Bacon, A. and Bicknell, R. (2015) 'Blocking CLEC14A-MMRN2 binding inhibits sprouting angiogenesis and tumour growth', *Oncogene*. Nature Publishing Group, 34(47), pp. 5821–5831. doi: 10.1038/onc.2015.34.

Noy, P. J., Swain, R. K., Khan, K., Lodhia, P. and Bicknell, R. (2016) 'Sprouting angiogenesis is regulated by shedding of the C-type lectin family 14, member A (CLEC14A) ectodomain, catalyzed by rhomboid-like 2 protein (RHBDL2)', *FASEB Journal*, 30(6), pp. 2311–2323. doi: 10.1096/fj.201500122R.

Oh, P., Li, Y., Yu, J., Durr, E., Krasinska, K. M., Carver, L. A., Testa, J. E. and Schnitzer, J. E. (2004) 'Subtractive proteomic mapping of the endothelial surface in lung and solid tumours for tissue-specific therapy', *Nature*, 429(6992), pp. 629–635. doi: 10.1038/nature02580.

Oliner, J., Min, H., Leal, J., Yu, D., Rao, S., You, E., Tang, X., Kim, H., Meyer, S., Han, S. J., Hawkins, N., Rosenfeld, R., Davy, E., Graham, K., Jacobsen, F., Stevenson, S., Ho, J., Chen, Q., Hartmann, T., Michaels, M., Kelley, M., Li, L., Sitney, K., Martin, F., Sun, J. R., Zhang, N., Lu, J., Estrada, J., Kumar, R., Coxon, A., Kaufman, S., Pretorius, J., Scully, S., Cattley, R., Payton, M., Coats, S., Nguyen, L., Desilva, B., Ndifor, A., Hayward, I., Radinsky, R., Boone, T. and Kendall, R. (2004) 'Suppression of angiogenesis and tumor growth by selective inhibition of angiopoietin-2', *Cancer Cell*, 6(5), pp. 507–516. doi: 10.1016/j.ccr.2004.09.030.

Olsen, R. S., Lindh, M., Vorkapic, E., Andersson, R. E., Zar, N., Löfgren, S., Dimberg, J., Matussek, A. and Wågsäter, D. (2015) 'CD93 gene polymorphism is associated with disseminated colorectal cancer', *International Journal of Colorectal Disease*, 30(7), pp. 883–890. doi: 10.1007/s00384-015-2247-1.

Orlandini, M., Galvagni, F., Bardelli, M., Rocchigiani, M., Lentucci, C., Anselmi, F., Zippo, A., Bini, L. and Oliviero, S. (2014) 'The characterization of a novel monoclonal antibody against CD93 unveils a new antiangiogenic target.', *Oncotarget*, 5(9), pp. 2750–2760. doi: 10.18632/oncotarget.1887.

Pàez-Ribes, M., Allen, E., Hudock, J., Takeda, T., Okuyama, H., Viñals, F., Inoue, M., Bergers, G., Hanahan, D. and Casanovas, O. (2009) 'Antiangiogenic Therapy Elicits Malignant Progression of Tumors to Increased Local Invasion and Distant

Metastasis', *Cancer Cell*, 15(3), pp. 220–231. doi: 10.1016/j.ccr.2009.01.027.

Papetti, M. and Herman, I. M. (2002) 'Mechanisms of normal and tumor-derived angiogenesis', *AJP: Cell Physiology*, 282(5), pp. C947–C970. doi: 10.1152/ajpcell.00389.2001.

Parangi, S., O'Reilly, M., Christofori, G., Holmgren, L., Grosfeld, J., Folkman, J. and Hanahan, D. (1996) 'Antiangiogenic therapy of transgenic mice impairs de novo tumor growth', *Proceedings of the National Academy of Sciences*, 93(5), pp. 2002–2007. doi: 10.1073/pnas.93.5.2002.

Parente-Pereira, A. C., Whilding, L. M., Brewig, N., van der Stegen, S. J. C., Davies, D. M., Wilkie, S., van Schalkwyk, M. C. I., Ghaem-Maghami, S. and Maher, J. (2013) 'Synergistic Chemoimmunotherapy of Epithelial Ovarian Cancer Using ErbB-Retargeted T Cells Combined with Carboplatin', *The Journal of Immunology*, 191(5), pp. 2437–2445. doi: 10.4049/jimmunol.1301119.

Park, M. and Tenner, A. J. (2003) 'Cell surface expression of C1qRp/CD93 is stabilized by O-glycosylation', *Journal of Cellular Physiology*, 196(3), pp. 512–522. doi: 10.1002/jcp.10332.

Pegram, H. J., Park, J. H., Brentjens, R. J., Centre, M. S. C., Centre, M. S. C., Program, C. and Centre, M. S. C. (2015) 'HHS Public Access', 20(2), pp. 127–133. doi: 10.1097/PPO.0000000000000034.CD28z.

Petrenko, O. (1999) 'The molecular characterization of the fetal stem-cell marker AA4', *Immunity*, 10, pp. 691–700. DOI:https://doi.org/10.1016/S1074-7613(00)80068-0.

Pettitt, D., Arshad, Z., Smith, J., Stanic, T., Holländer, G. and Brindley, D. (2018) 'CAR-T Cells: A Systematic Review and Mixed Methods Analysis of the Clinical Trial Landscape', *Molecular Therapy*. Elsevier Ltd., 26(2), pp. 342–353. doi:

10.1016/j.ymthe.2017.10.019.

Pircher, A., Fiegl, M., Untergasser, G., Heidegger, I., Medinger, M., Kern, J. and Hilbe, W. (2013) 'Favorable prognosis of operable non-small cell lung cancer (NSCLC) patients harboring an increased expression of tumor endothelial markers (TEMs)', *Lung Cancer*, 81(2), pp. 252–258. doi: 10.1016/j.lungcan.2013.04.014.

Poli, G. L., Bianchi, C., Virotta, G., Bettini, A., Moretti, R., Trachsel, E., Elia, G., Giovannoni, L., Neri, D. and Bruno, A. (2013) 'Radretumab Radioimmunotherapy in Patients with Brain Metastasis: A 124I-L19SIP Dosimetric PET Study', *Cancer Immunology Research*, 1(2), pp. 134–143. doi: 10.1158/2326-6066.CIR-13-0007.

Porter, D. L., Hwang, W.-T., Frey, N. V., Lacey, S. F., Shaw, P. A., Loren, A. W., Bagg, A., Marcucci, K. T., Shen, A., Gonzalez, V., Ambrose, D., Grupp, S. A., Chew, A., Zheng, Z., Milone, M. C., Levine, B. L., Melenhorst, J. J. and June, C. H. (2015) 'Chimeric antigen receptor T cells persist and induce sustained remissions in relapsed refractory chronic lymphocytic leukemia', *Science Translational Medicine*, 7(303), p. 303ra139-303ra139. doi: 10.1126/scitranslmed.aac5415.

Pulè, M. A., Straathof, K. C., Dotti, G., Heslop, H. E., Rooney, C. M. and Brenner, M. K. (2005) 'A chimeric T cell antigen receptor that augments cytokine release and supports clonal expansion of primary human T cells', *Molecular Therapy*, 12(5), pp. 933–941. doi: 10.1016/j.ymthe.2005.04.016.

Raphael, I., Nalawade, S., Eagar, T. N. and Forsthuber, T. G. (2015) 'T cell subsets and their signature cytokines in autoimmune and inflammatory diseases', *Cytokine*. Elsevier Ltd, 74(1), pp. 5–17. doi: 10.1016/j.cyto.2014.09.011.

Rho, S.-S., Choi, H.-J., Min, J.-K., Lee, H.-W., Park, H., Park, H., Kim, Y.-M. and Kwon, Y.-G. (2011) 'Clec14a is specifically expressed in endothelial cells and mediates cell to cell adhesion', *Biochemical and Biophysical Research Communications*, 404(1). doi: 10.1016/j.bbrc.2010.11.075.

Rigamonti, N., Kadioglu, E., Keklikoglou, I., Rmili, C. W., Leow, C. C. and de Palma, M. (2014) 'Role of angiopoietin-2 in adaptive tumor resistance to VEGF signaling blockade', *Cell Reports*, 8(3), pp. 696–706. doi: 10.1016/j.celrep.2014.06.059.

Roskoski, R. (2007) 'Sunitinib: A VEGF and PDGF receptor protein kinase and angiogenesis inhibitor', *Biochemical and Biophysical Research Communications*, 356(2), pp. 323–328. doi: 10.1016/j.bbrc.2007.02.156.

Rubenstein, J. L., Kim, J., Ozawa, T., Zhang, M., Westphal, M., Deen, D. F. and Shuman, M. A. (2000) 'Anti-VEGF Antibody Treatment of Glioblastoma Prolongs Survival But Results in Increased Vascular Cooption', *Neoplasia*, 2(4), pp. 306–314. doi: 10.1038/sj.neo.7900102.

Sakaguchi, S., Miyara, M., Costantino, C. M. and Hafler, D. A. (2010) 'FOXP3 + regulatory T cells in the human immune system', *Nature Publishing Group*. Nature Publishing Group, 10(7), pp. 490–500. doi: 10.1038/nri2785.

Sampson, J. H., Archer, G. E., Mitchell, D. A., Heimberger, A. B. and Bigner, D. D. (2008) 'Tumor-specific immunotherapy targeting the EGFRvIII mutation in patients with malignant glioma', *Seminars in Immunology*, 20(5), pp. 267–275. doi: 10.1016/j.smim.2008.04.001.

Sanz-Moncasi, M. P., Garin-Chesa, P., Stockert, E., Jaffe, E. A., Old, L. J. and Rettig, W. J. (1994) 'Identification of a high molecular weight endothelial cell surface glycoprotein, endoGlyx-1, in normal and tumor blood vessels', *Lab Invest*, 71(3), pp. 366–373.

Savoldo, B., Ramos, C. A., Liu, E., Mims, M. P., Keating, M. J., Carrum, G., Kamble, R. T., Bollard, C. M., Gee, A. P., Mei, Z., Liu, H., Grilley, B., Rooney, C. M., Heslop, H. E., Brenner, M. K. and Dotti, G. (2011) 'CD28 costimulation improves expansion and persistence of chimeric antigen receptor – modified T cells in lymphoma patients', *The Journal of Clinical Investigation*, 121(5), pp. 1822–1826. doi:

10.1172/JCI46110DS1.

Schreiber, R. D., Old, L. J. and Smyth, M. J. (2011) 'Cancer Immunoediting: Integrating Immunity's Roles in Cancer Suppression and Promotion', *Science*, 331(6024), pp. 1565–1570. doi: 10.1126/science.1203486.

Seaman, S., Zhu, Z., Saha, S., Zhang, X. M., Yang, M. Y., Hilton, M. B., Morris, K., Szot, C., Morris, H., Swing, D. A., Tessarollo, L., Smith, S. W., Degrado, S., Borkin, D., Jain, N., Scheiermann, J., Feng, Y., Wang, Y., Li, J., Welsch, D., DeCrescenzo, G., Chaudhary, A., Zudaire, E., Klarmann, K. D., Keller, J. R., Dimitrov, D. S. and St. Croix, B. (2017) 'Eradication of Tumors through Simultaneous Ablation of CD276/B7-H3-Positive Tumor Cells and Tumor Vasculature', *Cancer Cell*. Elsevier Inc., 31(4), p. 501–515.e8. doi: 10.1016/j.ccell.2017.03.005.

Sentman, C. L. and Meehan, K. R. (2014) 'NKG2D CARs as Cell Therapy for Cancer', *The Cancer Journal*, 20(2), pp. 156–159. doi: 10.1097/PPO.0000000000000029.

Sharkey, R. M. and Goldenberg, D. M. (2008) 'Use of antibodies and immunoconjugates for the therapy of more accessible cancers', *Advanced Drug Delivery Reviews*, 60(12), pp. 1407–1420. doi: 10.1016/j.addr.2008.04.011.

St Croix, B., Rago, C., Velculescu, V., Traverso, G., Romans, K. E., Montgomery, E., Lal, A., Riggins, G. J., Lengauer, C., Vogelstein, B. and Kinzler, K. W. (2000) 'Genes expressed in human tumor endothelium.', *Science (New York, N.Y.)*, 289(5482), pp. 1197–202. doi: 10.1126/science.289.5482.1197.

Steinberger, P., Szekeres, A., Wille, S., Stöckl, J., Selenko, N., Prager, E., Staffler, G., Madic, O., Stockinger, H. and Knapp, W. (2002) 'Identification of human CD93 as the phagocytic C1q receptor (C1qRp) by expression cloning.', *Journal of leukocyte biology*, 71(1), pp. 133–40. https://doi.org/10.1189/jlb.71.1.133

Teicher, B. A. (1996) 'A systems approach to cancer therapy', *Cancer and Metastasis*

Reviews, 15(2), pp. 247–272. doi: 10.1007/BF00437479.

Tosi, G. M., Caldi, E., Parolini, B., Toti, P., Neri, G., Nardi, F., Traversi, C., Cevenini, G., Marigliani, D., Nuti, E., Bacci, T., Galvagni, F. and Orlandini, M. (2017) 'CD93 as a Potential Target in Neovascular Age-Related Macular Degeneration', *Journal of Cellular Physiology*, 232(7), pp. 1767–1773. doi: 10.1002/jcp.25689.

Tunica, D. G., Yin, X., Sidibe, A., Stegemann, C., Nissum, M., Zeng, L., Brunet, M. and Mayr, M. (2009) 'Proteomic analysis of the secretome of human umbilical vein endothelial cells using a combination of free-flow electrophoresis and nanoflow LC-MS/MS', *Proteomics*, 9(21), pp. 4991–4996. doi: 10.1002/pmic.200900065.

Turtle, C. J., Hanafi, L.-A., Berger, C., Hudecek, M., Pender, B., Robinson, E., Hawkins, R., Chaney, C., Cherian, S., Chen, X., Soma, L., Wood, B., Li, D., Heimfeld, S., Riddell, S. R. and Maloney, D. G. (2016) 'Immunotherapy of non-Hodgkins lymphoma with a defined ratio of CD8+ and CD4+ CD19-specific chimeric antigen receptor-modified T cells', *Science Translational Medicine*, 8(355), p. 355ra116-355ra116. doi: 10.1126/scitranslmed.aaf8621.

Uckun, F., Fauci, S., Wick, R. and Myers, E. (1988) 'on Expression', 71(1), pp. 13–29.

Vrisekoop, N., Monteiro, J. P., Mandl, J. N. and Germain, R. N. (2014) 'Revisiting thymic positive selection and the mature T cell repertoire for antigen', *Immunity*, 41(2), pp. 181–190. doi: 10.1016/j.immuni.2014.07.007.

Wagner, S. C., Riordan, N. H., Ichim, T. E., Szymanski, J., Ma, H., Perez, J. A., Lopez, J., Plata-Munoz, J. J., Silva, F., Patel, A. N. and Kesari, S. (2016) 'Safety of targeting tumor endothelial cell antigens', *Journal of Translational Medicine*. BioMed Central, 14(1), pp. 1–12. doi: 10.1186/s12967-016-0842-8.

Wang, L., Park, H., Chhim, S., Ding, Y., Jiang, W., Queen, C. and Kim, K. J. (2012) 'A novel monoclonal antibody to fibroblast growth factor 2 effectively inhibits growth of hepatocellular carcinoma xenografts.', *Molecular cancer therapeutics*, 11(4), pp.

864–72. doi: 10.1158/1535-7163.MCT-11-0813.

Wang, W., Ma, Y., Li, J., Shi, H. S., Wang, L. Q., Guo, F. C., Zhang, J., Li, D., Mo, B. H., Wen, F., Liu, T., Liu, Y. T., Wang, Y. S. and Wei, Y. Q. (2013) 'Specificity redirection by CAR with human VEGFR-1 affinity endows T lymphocytes with tumor-killing ability and anti-angiogenic potency', *Gene Therapy*, 20(10), pp. 970–978. doi: 10.1038/gt.2013.19.

Wilhelm, S. M., Adnane, L., Newell, P., Villanueva, A., Llovet, J. M. and Lynch, M. (2008) 'Preclinical overview of sorafenib, a multikinase inhibitor that targets both Raf and VEGF and PDGF receptor tyrosine kinase signaling', *Molecular Cancer Therapeutics*, 7(10), pp. 3129–3140. doi: 10.1158/1535-7163.MCT-08-0013.

Wouters, M. A., Rigoutsos, I., Chu, C. K., Feng, L. L., Sparrow, D. B. and Dunwoodie, S. L. (2005) 'Evolution of distinct EGF domains with specific functions'. doi: 10.1110/ps.041207005.naling.

Wragg, J., Finnity, J. P., Anderson, J. A., Ferguson, H. J. M., Porfiri, E., Bhatt, R. I., Murray, P. G., Heath, V. L. and Bicknell, R. (2016) 'MCAM and LAMA4 are highly enriched in tumor blood vessels of renal cell carcinoma and predict patient outcome', *Cancer Research*, 76(8), pp. 2314–2326. doi: 10.1158/0008-5472.CAN-15-1364.

Wragg, J. W., Heath, V. L. and Bicknell, R. (2017) 'Sunitinib treatment enhances metastasis of innately drug-resistant breast tumors', *Cancer Research*, 77(4), pp. 1008–1020. doi: 10.1158/0008-5472.CAN-16-1982.

Wyder, L., Vitaliti, A., Schneider, H., Hebbard, L. W., Moritz, D. R., Wittmer, M., Ajmo, M. and Klemenz, R. (2000) 'Blood Vessels Increased Expression of H/T-Cadherin in Tumor-penetrating Increased Expression of H/T-Cadherin in Tumor-penetrating Blood Vessels 1', *Cancer Res [CANCER RESEARCH*, 60(60), pp. 4682–4688.

Xiangbao, Y., Linquan, W., Mingwen, H., Fan, Z., Kai, W., Xin, Y., Kaiyang, W. and Huaqun, F. (2014) 'Humanized anti-VEGFR-2 ScFv-As2O3-stealth nanoparticles, an antibody conjugate with potent and selective anti-hepatocellular carcinoma activity', *Biomedicine and Pharmacotherapy*. Elsevier Masson SAS, 68(5), pp. 597–602. doi: 10.1016/j.biopha.2014.04.006.

Youn, J.-C., Yu, H. T., Jeon, J.-W., Lee, H. S., Jang, Y., Park, Y. W., Park, Y.-B., Shin, E.-C. and Ha, J.-W. (2014) 'Soluble CD93 Levels in Patients with Acute Myocardial Infarction and Its Implication on Clinical Outcome', *PLoS ONE*, 9(5), p. e96538. doi: 10.1371/journal.pone.0096538.

Zanivan, S., Maione, F., Hein, M. Y., Hernández-Fernaud, J. R., Ostasiewicz, P., Giraudo, E. and Mann, M. (2013) 'SILAC-Based Proteomics of Human Primary Endothelial Cell Morphogenesis Unveils Tumor Angiogenic Markers', *Molecular & Cellular Proteomics*, 12(12), pp. 3599–3611. doi: 10.1074/mcp.M113.031344.

Zelensky, A. N. and Gready, J. E. (2005) 'The C-type lectin-like domain superfamily', 272, pp. 6179–6217. doi: 10.1111/j.1742-4658.2005.05031.x.

Zhang, M., Suzanne, S., Dy, M. and Tenner, A. J. (2005) 'Modulated interaction of the ERM protein , moesin , with CD 93', pp. 63–73. doi: 10.1111/j.1365-2567.2005.02120.x.

Zhuang, X., Ahmed, F., Zhang, Y., Ferguson, H. J., Steele, J. C., Steven, N. M., Nagy, Z., Heath, V. L., Toellner, K. M. and Bicknell, R. (2015) 'Robo4 vaccines induce antibodies that retard tumor growth', *Angiogenesis*, 18(1), pp. 83–95. doi: 10.1007/s10456-014-9448-z.

Zhuang, X., Herbert, J. M. J., Lodhia, P., Bradford, J., Turner, A. M., Newby, P. M., Thickett, D., Naidu, U., Blakey, D., Barry, S., Cross, D. A. E. and Bicknell, R. (2015) 'Identification of novel vascular targets in lung cancer', *British Journal of Cancer*. Nature Publishing Group, 112(3), pp. 485–494. doi: 10.1038/bjc.2014.626.